eman ta zabal zazu

Universidad del País Vasco

Euskal Herriko Unibertsitatea

Doctoral Thesis

LEARNING AND MEMORY IMPROVEMENT MEDIATED BY CB_1 CANNABINOID RECEPTORS IN ANIMAL MODELS OF CHOLINERGIC DYSFUNCTION

Marta Moreno Rodríguez

2018

Marta Moreno received a grant from Fundación Jesús de Gangoiti Barrera for a period of one year beginning in January 2014. This work was supported by the Departments of Industry and Education from the Basque Government (KK-2017/14 Elkartek and IT975-16 Consolidated research group grants). Technical and human support provided by General Research Services SGiker [University of the Basque Country (UPV/EHU), Ministry of Economy and Competitiveness (MINECO), Basque Government, European Regional Development Fund (ERDF) and European Social Fund (ESF)] is gratefully acknowledged.

A mi gente ...

Este trabajo ha sido realizado en el Departamento de Farmacología de la Universidad del País Vasco y quisiera agradecer a todas las personas que lo han hecho posible.

En primer lugar, quiero dar las gracias a mi director de tesis Dr. Rafael Rodríguez Puertas por abrirme las puertas de su laboratorio, por confiar en mí, por guiarme y aconsejarme durante el desarrollo de este trabajo, por darme todos los recursos necesarios para mi formación y por liderar este excelente grupo de investigación. Gracias Rafa por cada momento dedicado a mi aprendizaje y desarrollo como investigadora.

También quiero agradecer enormemente a mis compañeros de laboratorio, ellos han conseguido durante estos años que cada día ir a trabajar se convierta en algo divertido. Al Dr. Iván Manuel por estar siempre a mi rescate, por todos esos cafés con risas que hemos compartido y por convertirte en un ejemplo al que seguir. A la Dra. Laura Lombardero por prestarme su ayuda siempre que la he necesitado y por llenar el laboratorio con energía y buen rollo. A la Dra. Estibaliz González de San Román por mostrarme que con dedicación y esfuerzo se puede llegar lejos. A la Dra. María Dolores Fernández por darme siempre su consejo y apoyo, por regalarme esos ratos de después de comer que han forjado una preciosa amistad. Al Dr. Alberto Llorente por facilitarme su ayuda siempre con optimismo, por todos los buenos consejos y toda la ayuda brindada en esos interminables días de experimentación. Por último, a mi compañero Jonatan, gracias por ofrecerte siempre a ayudarme, por todas esas palmeras compartidas, por esas largas charlas de viernes tarde y por esas risas tontas en los días largos. Este trabajo lleva un poco de cada uno de vosotros.

Me gustaría también agradecer a todas aquellas personas con las que he compartido el día a día en la facultad como son los compañeros del departamento, donde la hora de comer servía para desconectar y olvidarse del estrés del trabajo. No me gustaría olvidarme de todas aquellas personas que han pasado por el laboratorio y han contribuido de alguna manera a la realización de este trabajo, como son los técnicos de laboratorio, los estudiantes de master y los estudiantes de grado. También me gustaría agradecer a mis compañeros del laboratorio investigación de la enfermedad de Alzheimer del Barrow Neurological Institute, especialmente a Elliott Mufson y a Sylvia Pérez por toda la ayuda que me han proporcionado durante mi estancia.

Tengo que agradecer también a todos mis amigos, que gracias a los buenos momentos pasados han conseguido que el camino sea más llevadero. Especialmente a Idoia, Alesk, Rubén y Oscar por sacarme siempre una sonrisa y a Toñito por estar siempre que te he necesitado, gracias por esas largas charlas de teléfono donde arreglábamos el mundo.

Finalmente me gustaría agradecer a mi familia, a mis padres por todo el apoyo y compresión, por todos los ánimos que me habéis dado, os lo debo todo. A mi hermano y a mis tíos y primos que gracias a su apoyo me he creído capaz de hacer cualquier cosa. Por último, debo agradecer a Rubén, mi compañero de vida, gracias por despejarme los días oscuros y por hacerme sonreír en los días tristes. Sobre todo, gracias por toda la paciencia que has tenido en esta etapa, has sabido llevarme de la mano y levantarme cuando me tropezaba.

INDEX

INTRODUCTION

1. Cholinergic system

The endogenous neurotransmitter acetylcholine (ACh) was discovered by Henry Hallett Dale in 1914, and its existence was later confirmed by Otto Loewi. It is present in both the **central nervous system** (CNS) and the **peripheral nervous system** (PNS). In CNS cholinergic signaling is the basis of neuronal circuit of cognitive functions and behaviors, including attention, learning, memory and motivation. In PNS it is the responsible of the neuromuscular transmission between motor nerves and skeletal muscles. During learning and memory formation, activation of **muscarinic acetylcholine receptors** (mAChRs) alters the activation state of different groups of neurons. ACh is composed by **choline** (Ch) and acetyl co-enzyme A (Acetyl-CoA) and synthetized by **choline acetyltransferase** (ChAT) enzyme in the cholinergic neurons. Once released, ACh binds to and activates cholinergic receptors. **Acetylcholinesterase** (AChE) rapidly hydrolyzes ACh in Ch and acetate in the synapse. Finally, Ch is uptaken into the axon terminal through the high affinity choline transporter and is used to synthesize more ACh (Figure 1) (Stedman and Stedman, 1937; Barker et al., 1972).

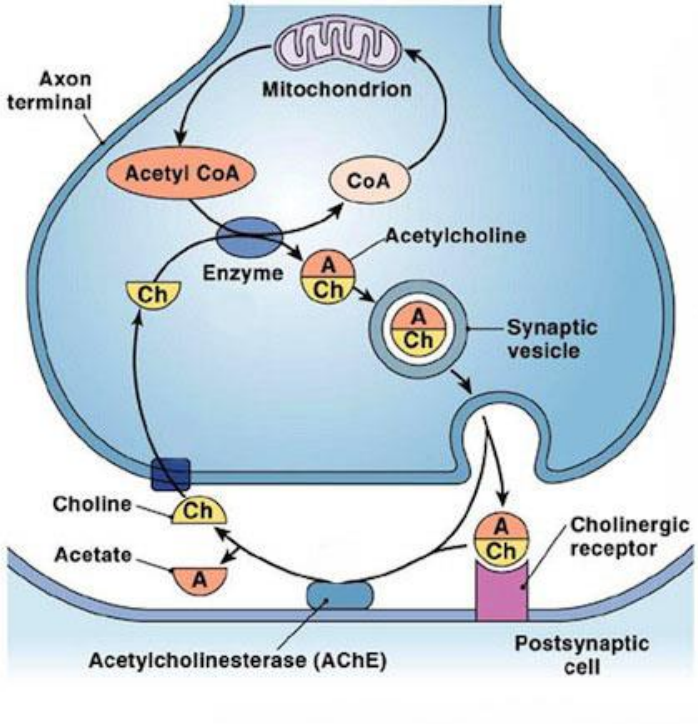

Figure 1. Schematic representation of a cholinergic synapse. The endogenous ligand, ACh is synthesized in cholinergic neurons by the enzyme ChAT (named in the picture as Enzyme). Copyright © 2007 Pearson Education, Inc., publishing as Benjamin Cummings.

1.1. Acetylcholine metabolism

Ch is an essential nutrient present in many foods and a variety of diets that can satisfy the need for this nutrient. Acetyl-CoA represents a key node in its metabolism due to its presence in many metabolic pathways. High amounts of nucleocytosolic acetyl-CoA indicate a "growth" or "fed" state and promote its utilization for lipid synthesis and histone acetylation (Shatalin et al., 1999). In the other hand, Ch has been shown to exert neuroprotective effects in both animal and human studies. High Ch levels intake during the perinatal period is neuroprotective in a variety of animal models of neuronal dysfunction, including that resulting from aging (Meck and Williams, 1997; Meck and Williams, 2003; Meck et al., 2008). Besides, Ch is a precursor for the biosynthesis of sphingomyelins, as well as of phosphatidylcholines, the most abundant phospholipid of eukaryotic membranes and is also found in selected prokaryotes. This reaction is carried out by CDP-choline cycle, and its alteration can affect the distribution of lipid-related metabolites (Fagone and Jackowski, 2013). The synthesis of ACh critically depends on the levels of Ch, and when the levels decrease, membrane phospholipids could provide an alternative source from which Ch can be synthesized *de novo* (Millington and Wurtman, 1982). As previously mentioned ChAT enzyme synthetizes ACh from Ch and acetyl CoA, and its activity can be acutely regulated by neuronal perturbations, such as depolarization and Ca^{2+} influx, that release ACh and increase delivery of the precursor Ch into the nerve terminal by sodium-coupled Ch transporter. ChAT is a phenotypic marker of cholinergic neurons and a decreased activity is consistently found in several neurological disorders including **Alzheimer's disease** (AD) (Lopez, O. L. and DeKosky, 2031).

Other pathway to obtain Ch is through the activity of AChE. It is strategically located in cholinergic and non-cholinergic neurons close to the post-synaptic receptors in order to ensure a quick inactivation of ACh. The importance of AChE in mammals is illustrated by the effect of abrupt blockade of AChE catalytic activity. Then inhibition of AChE leads to excessive ACh levels at neuromuscular synapses, continued activation of ACh receptors, subsequent receptor inactivation, respiratory and/or cardiac dysfunction and death (Haywood et al., 1999). Therapeutically, controlled application of AChE inhibitors is used to increase synaptic levels of ACh in diseases that impair ACh neurotransmission, such as AD and Parkinson's disease (Zemek et al., 2014). When AChE broke ACh to Ch and acetate, Ch is then immediately uptaken by the sodium-dependent high affinity Ch uptake system located in the presynaptic membrane. There are two Ch transporter systems, one with high affinity for Ch and the other with low affinity. The high affinity Ch transporter is an integral membrane protein with 13 transmembrane (TM) segments, which belongs to the Na+/glucose co-transporter family, and which captures Ch for the synthesis of ACh (Haga, 1971; Okuda and Haga, 2003). The second reuptake system captures Ch

with very low affinity, displays its maximum capacity of transportation independently of Na+, and does not use Ch in the synthesis of ACh.

1.2. Central cholinergic signaling

The acetylcholine receptors are divided into metabotropic muscarinic receptors and ionotropic nicotinic receptors.

Muscarinic acetylcholine receptors subtypes

mAChR are a family of seven-transmembrane (TM) domain receptors and belong to the guanine nucleotide-binding protein coupled receptor (GPCR) superfamily. There are five subtypes of mAChR which mediate multiple actions of ACh in the CNS and the periphery. All five subtypes of mAChR are expressed in the CNS and are thought to play a relevant role in the signaling mechanism for learning and memory processes, REM sleep, attention, control of movement and thermoregulation.

M_1 and M_2 mAChR subtypes were the first to be cloned (Kubo et al., 1986), followed by the cloning of the M_3, M_4 and M_5 genes (Bonner et al., 1987), which confirmed that the mAChR are glycoproteins which belong to the superfamily of GPCR (Hulme, 1990; Hulme et al., 1990). The chromosomal localization of the human mAChR genes are as follows: M_1, 11q12–13; M_2, 7q35–36; M_3, 1q43–44; M_4, 11p12–11.2; M_5, 15q26. The amino acid composition of the human mAChR subtypes ranges from 460 amino acids for M_1, 466 for M_2, 589 for M_3, 479 for M_4, to 532 for M_5. Primary sequence alignment reveals that the individual subtypes share approximately 145 invariant amino acid residues and show between 89% and 98% common amino acid identity in various mammalian species (Wess, 1993). Within the TM segments, there is 63% common identity in all mAChR subtypes, but it is even higher among the M_1, M_3, and M_5, and between the M_2 and M_4 subtypes.

In addition, the preferential coupling of M_1, M_3 and M_5 subtypes is to $G_{\alpha q/11}$ proteins that activate phospholipase C (PLC). PLC hydrolyzes phosphatidylinositol 4,5-bisphosphate (PIP2) to diacyl glycerol (DAG) and inositol trisphosphate (IP3), which act as intracellular secondary messengers. DAG activates protein kinase C (PKC) and IP3 contributes to the phosphorylation of some proteins and the mobilization of intracellular Ca^{2+}.

M_2 and M_4 mAChR subtypes are preferentially coupled to $G_{\alpha i/o}$ proteins, whose activation mainly inhibits the cAMP dependent pathway by inhibiting adenylate cyclase activity, which decreases the activity of cAMP-dependent protein kinases (Caulfield and Birdsall, 1998).

Distribution of mAChR

M_1 mAChR mRNA transcript is mainly localized in the cerebral cortex, hippocampus, thalamus, caudate-putamen, amygdala, olfactory bulb, olfactory tubercle and dentate gyrus, whereas M_2 mAChR mRNA is more abundantly detected in the basal forebrain, caudate-putamen, hippocampus, hypothalamus, amygdala and pontine nuclei (Buckley et al., 1988). At the cellular level, M_1 mAChR-immunoreactivity is restricted to neuronal bodies and neurites, which is consistent with its role as the major postsynaptic mAChR subtype. In the basal forebrain, M_2 mAChR is expressed at high levels in the BFCN, which suggests that M_2 mAChR can act as an autoreceptor. However, M_2 mAChR is also present in non-cholinergic cortical and subcortical structures, thus providing evidence that this subtype may presynaptically modulate the release of ACh and other neurotransmitters and may also operate postsynaptically (Levey et al., 1991; Levey, Edmunds, Koliatsos, Wiley and Heilman, 1995). Quantitative autoradiographic experiments reveal the highest levels of M_1 mAChR in the hippocampus, nucleus accumbens and caudate-putamen. M_2 mAChR labeling is observed in the occipital region of the cerebral cortex, the dorsal region of the caudate, the olfactory tubercle, the nucleus accumbens, the superficial layers of the superior and inferior colliculi, the pontine and parabrachial nuclei, the motor trigeminal and the facial nuclei in the brainstem, and some labeling is also present in the cerebellum. In general, these findings are consistent with previous studies (Mash and Potter, 1986; Levey et al., 1991), but not with *in situ* experiments that failed to find M_2 mRNA in the cortex and striatum (Buckley et al., 1988; Vilaro et al., 1994). M_3 mRNA transcription occurs in the olfactory tubercle, cerebral cortex, hippocampus, thalamus, caudate-putamen, and amygdala, whereas M_4 mRNA is highest in the olfactory bulb, olfactory tubercle, hippocampus, and striatum ((Buckley et al., 1988; Caulfield, 1993), which is consistent with the quantitative autoradiographic results obtained by Flynn et al. (1997), and with those of immunohistochemical studies carried out by Levey et al. (1991). M_5 mRNA has been detected in the substantia nigra pars compacta (Weiner et al., 1990). M_5 mAChR binding is observed in the most external layers of the cortex, in the caudate-putamen, nucleus accumbens, CA1 and CA2 hippocampal regions and in the polymorphic layer of the dentate gyrus (Reever et al., 1997).

Muscarinic ligands

These receptors share a similar amino acid sequence in their trans-membrane domains (63%), which align to form a pore, in which acetylcholine binds to a conserved set of residues forming the orthosteric site. The high homology at the orthosteric sites has historically presented a major challenge in the search for receptor subtype specific ligands (Heinrich et al., 2009). Below we refer to current ligands for each type of receptor (Table 1).

Table 1. Specific and non-specific ligands for the five muscarinic receptor subtypes. Alexander et al., (2017). The Concise Guide to PHARMACOLOGY 2017/18: G protein-coupled receptors. *Br J Pharmacol.* 174 Suppl 1: S17-S129.

M_1	
Agonist	pilocarpine (Partial agonist), carbachol, bethanechol
antagonist	otenzepad,umeclidinium, propantheline, AE9C90CB, tiotropium, 4-DAMP,dicyclomine, atropine , scopolamine , trihexyphenidyl, tripitramine, UH-AH 37, oxybutynin, tolterodine, pirenzepine, darifenacin, solifenacin, AFDX384, AQ-RA 741, muscarinic toxin 3, methoctramine, himbacine, glycopyrrolate
Selective antagonists	biperiden, VU0255035, guanylpirenzepine
Allosteric modulators	benzoquinazolinone 12 (Positive), BQCA (Positive) , KT 5720 (Positive), brucine (Positive), muscarinic toxin 7 (Negative) , VU0090157 (Positive), VU0029767 (Positive)
Labelled ligands	[^{3}H]QNB (Antagonist), Cy3B-telenzepine (Antagonist), [^{3}H]N-methyl scopolamine (Antagonist), Alexa-488-telenzepine (Antagonist), [^{3}H]pirenzepine (Antagonist), [^{3}H](+)telenzepine (Antagonist), BODIPY pirenzepine (Antagonist), [^{11}C]butylthio-TZTP (Agonist), [^{18}F](R,R)-quinuclidinyl-4-fluoromethyl-benzilate (Antagonist), [^{11}C]xanomeline (Agonist)
M_2	
Agonist	bethanechol
antagonist	biperiden, tiotropium, umeclidinium, propantheline, AE9C90CB, atropine, tolterodine (Inverse agonist), AQ-RA 741, 4-DAMP, AFDX384, himbacine, oxybutynin, methoctramine, UH-AH 37, darifenacin (Inverse agonist), solifenacin, otenzepad, pirenzepine, VU0255035, muscarinic toxin 3, guanylpirenzepine, muscarinic toxin 7, glycopyrrolate (Full agonist)
Selective antagonists	tripitramine
Allosteric modulators	C7/3-phth (Negative), W-84 (Negative), alcuronium (Negative), gallamine (Negative), LY2119620 (Positive), LY2033298 (Positive)
Labelled ligands	[^{3}H]QNB (Antagonist), [^{3}H]tiotropium (Antagonist), [^{3}H]N-methyl scopolamine (Antagonist), [^{3}H]acetylcholine (Agonist), [^{3}H]oxotremorine-M (Agonist), [^{3}H]dimethyl-W84 (Allosteric modulator, Positive), Cy3B-telenzepine (Antagonist), Alexa-488-telenzepine (Antagonist), [^{18}F]FP-TZTP (Agonist)

M_3	
Agonist	pilocarpine (Partial agonist), bethanechol, carbachol
antagonist	biperiden ,tiotropium ,umeclidinium, propantheline ,AE9C90CB, clidinium, ipratropium, atropine, 4-DAMP, dicyclomine, darifenacin, oxybutynin, tolterodine, UH-AH 37, solifenacin, tropicamide, AQ-RA 741, AFDX384, himbacine, tripitramine, pirenzepine, methoctramine, guanylpirenzepine, otenzepad, VU0255035, muscarini, toxin 3, muscarinic toxin 7, aclidinium, glycopyrrolate
Allosteric modulators	WIN 62,577 (Positive), N-chloromethyl-brucine (Positive)
Labelled ligands	[^{3}H]tiotropium (Antagonist), [^{3}H]QNB (Antagonist), [^{3}H]N-methyl scopolamine (Antagonist),[^{3}H]darifenacin (Antagonist)
M_4	
Agonist	pilocarpine (Partial agonist), carbachol, bethanechol
antagonist	biperiden, otenzepad, umeclidinium, AE9C90CB, 4-DAMP, oxybutynin, tolterodine, UH-AH 37, himbacine, AFDX384, AQ-RA 741, tripitramine, darifenacin, pirenzepine, methoctramine, solifenacin, guanylpirenzepine, VU0255035, muscarinic toxin 7, glycopyrrolate
Allosteric modulators	LY2119620 (Positive), thiochrome (Positive), muscarinic toxin 3 (Negative), VU0152100 (Positive), VU0152099 (Positive), LY2033298 (Positive)
Labelled ligands	[^{3}H]QNB (Antagonist), [^{3}H]N-methyl scopolamine (Antagonist), [^{3}H]acetylcholine (Agonist)
M_5	
Agonist	pilocarpine (Partial agonist), carbachol
antagonist	biperiden, guanylpirenzepine, umeclidinium, AE9C90CB, 4-DAMP, tolterodine, UH-AH 37, darifenacin, oxybutynin, tripitramine, solifenacin, pirenzepine, AQ-RA 741, methoctramine, AFDX384, muscarinic toxin 3, himbacine, otenzepad, muscarinic toxin 7, glycopyrrolate
Selective antagonists	ML381
Allosteric modulators	ML380
Labelled ligands	[^{3}H]QNB (Antagonist), [^{3}H]N-methyl scopolamine (Antagonist)

Nicotinic acetylcholine receptors

Nicotinic acetylcholine receptors (nAChRs) are ligand-gated ion channels, sensitive to activation by nicotine and whose activity is induced in the micro- to submicrosecond range. They can be divided into two types; muscle receptors, which are found at the skeletal neuromuscular junction where they mediate neuromuscular transmission, and neuronal receptors, which are found throughout the peripheral and central nervous systems where they are involved in fast synaptic transmission (Gotti and Clementi, 2004).

nAChRs are pentameric structures that are made up of combinations of individual subunits closely related to an extended family of cDNAs that in mammals encode 16 structurally homologous subunits with primary structural identity. All subunits have the following: 1) an extracellular large NH_2-terminal domain of ~200 amino acids; 2) three TM domains; 3) a cytoplasmic loop of variable size and an amino acid sequence; and 4) a fourth TM domain with a relatively short and variable extracellular COOH-terminal sequence (Lukas et al., 1999). Neuronal nAChRs can be homopentamers or heteropentamers composed of different subunits of

α2, α3, α4, α5, α6, α7, α9, and α10; and 3 non-α subunits (termed β2, β3, and β4), which have been cloned from neuronal tissues (Gotti and Clementi, 2004). The receptor channel is also permeable to selected ions such as Na^+, K^+, Ca^{2+} and Mg^{2+}

nAChRs can be located at the cell soma, dendrites, preterminal axon regions, axon terminals and myelinated axons (Albuquerque et al., 2009). Binding experiments in human brain have been performed by using [^{3}H]-nicotine, [^{3}H]-cytisine, [^{3}H]-methylcarbamylcholine and, in a few cases, [^{125}I]α-bungarotoxin. Nicotine labels all nAChRs; cytisine labels those containing the α3, α4 and β2 or β4 subunits; α-bungarotoxin labels α7 receptors. [^{3}H]-nicotine and [^{3}H]-cytisine binding studies show the highest density of nAChR in the periacqueductal grey matter, putamen, substantia nigra pars compacta, dentate gyrus of hippocampus, thalamus and dorsal raphe, and moderate densities in the cortex, claustrum, cingulated gyrus, hippocampal pyramidal and molecular layers, subiculum, tegmentum, nbM, parahippocampal area, cerebellum and substantia nigra pars reticulata. [^{125}I]α-bungarotoxin binding studies show high density in the sympathetic ganglia; moderate density in the hippocampal granular layer, subiculum, cerebellum, cortex, medial and lateral geniculate and reticular thalamic nucleus; and low density in the stratum lacunosum molecular, entorhinal cortex and cerebellum (Gotti et al., 1997). The distribution of nAChR has also been analyzed in the human CNS by using in situ hybridization and PET and these techniques have reported a similar distribution to that described using binding studies (Rubboli et al., 1994).

1.3. Central cholinergic system

The central cholinergic system is believed to be involved in the control of many physiological functions and is an important pharmacological target for numerous neurological pathologies. There are two major groups of cholinergic neurons. The first is the basal forebrain, composed by medial septum nuclei (MS), vertical (VDB) and horizontal (HDB) limb nuclei of diagonal band of Broca and the nucleus basalis magnocellularis (B) called in humans nucleus basalis of Meynert, one of the first area to be degenerated in AD. The second major group of cholinergic neurons is found in the brainstem (excluding the neurons found in cranial nerve motor nuclei), in the region of the pedunculopontine tegmental nucleus (PPTg) and laterodorsal pontine tegmentum (Mesulam et al., 1983a). Basal forebrain cholinergic neurons innervate neocortical, juxtacortical (cingulate cortex) and allocortical sites (hippocampus, basolateral amygdala, and olfactory bulb). Brainstem cholinergic neurons (PPTg neurons) principally innervate to the thalamus (Figure 2).

The cortical mantle, the amygdaloid complex, the hippocampal formation, the olfactory bulb and the thalamic nuclei receive their cholinergic innervation principally from cholinergic projection neurons of the basal forebrain and upper brainstem. The cholinergic system in the brain of mammals is subdivided into 8 "major sectors" named Ch1 to Ch8 (Mesulam, et al., 1983b; Mesulam, 1990). The cholinergic neurons from the different Ch1 to Ch8 subdivisions differ in size and shape and are interspersed among non-cholinergic neurons. The ratio of cholinergic versus non-cholinergic neurons differs among sectors and the perikarya of the cholinergic neurons, as well as non-cholinergic radiations to these neurons, contain AChE.

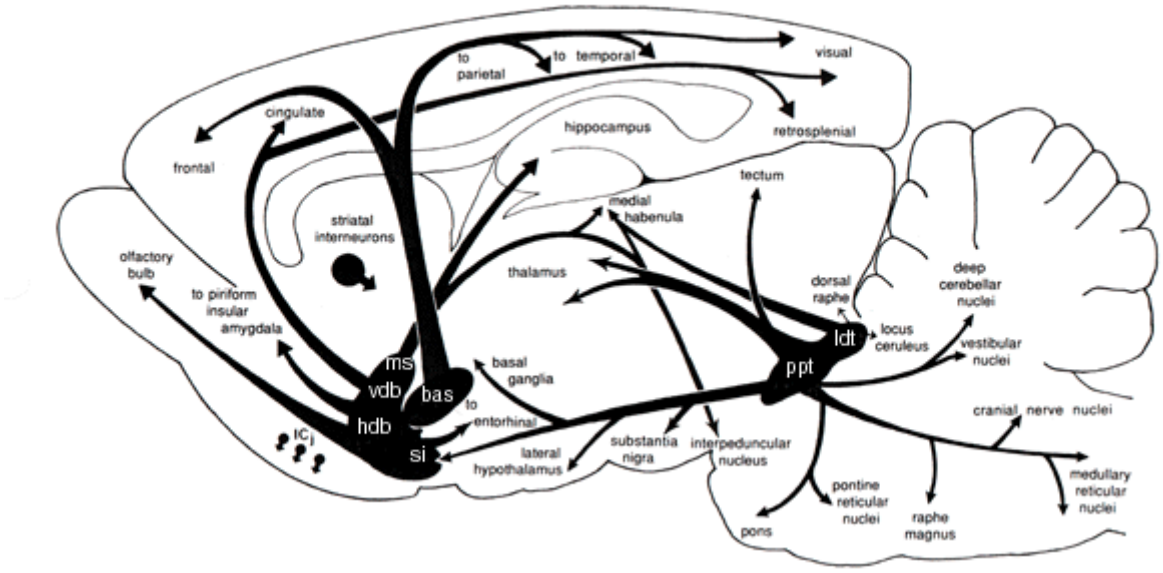

Figure 2. Schematic summary of the distribution of cholinergic neurons and their projections in the rat brain. Abbreviations: MS, medial septum (cell group Ch1); VDB, vertical limb nucleus of the diagonal band of Broca (Ch2); HDB, horizontal limb nucleus of the diagonal band of Broca (Ch3); Bas, nucleus basalis magnocellularis (Ch4); ppt, pedunculopontine tegmental nucleus (Ch5); dlt, laterodorsal tegmental nucleus (Ch6); PFC, prefrontal cortex; ICj, islands of Calleja (Modified from Woolf et al., 1997).

1.3.1. Basal forebrain cholinergic system

The basal forebrain cholinergic system is composed by clusters of cholinergic cells, going from Ch1 to Ch4, to provide the main source of cortical and hippocampal cholinergic innervation. Ch1 neurons are contained in the medial septal nucleus or medial septum (MS), lengthwise to midline and the external part of septum and mostly compound by non-cholinergic neurons (Mesulam et al., 1983a). Ch1 forms a continuum with the Ch2 sector, the vertical limb of the diagonal band of Broca (VDB); the major neurons of Ch2 are the BFCN. The main projections of

the Ch1-Ch2 BFCN are to the hippocampus, hypothalamus and occipital cortex. The Ch3 sector is comprised of neurons of the horizontal limb of the diagonal band of Broca (HDB), with approximately 25% of neurons displaying a cholinergic phenotype innervating the olfactory bulb. The Ch4 sector of both human and monkey brain is the major source of cholinergic projections to the cortical mantle (Mesulam et al., 1983b). The Ch4 sector corresponds to the denominated nbM.

Pedunculopontine tegmental nucleus and laterodorsal pontine tegmentum

The pedunculopontine nucleus (Ch5) is a heterogeneous nucleus and is comprised of neurons within a sector located in the pontomesencephalic reticular formation. The Ch5 sector connects with several thalamic nuclei and sends a minor projection to the neocortex. In the laterodorsal tegmental nucleus is found the Ch6 cluster, which innervates to various thalamic nuclei (Mesulam et al., 1983b). The Ch7 sector is located in the medial habenula and projects to the interpeduncular nucleus (Kasa, 1986). Finally, the Ch8 sector corresponds to the parabigeminal nucleus of the pontomesencephalic region, and its neurons project to the superior colliculus and the lateral geniculate (Mufson et al., 1986).

The nucleus basalis of Meynert

Theodor Meynert first described a group of magnocellular hyperchromic neurons located in the human basal forebrain, naming it the nucleus of the ansa lenticularis. This structure was later renamed as the **nucleus basalis of Meynert** (nbM) and was considered to be homologous with the nucleus basalis magnocellularis (B) of the rat (Adams et al., 1997). The nbM is located at the plane of the intermediate Ch4 region. Mesulam and colleagues found that over 90 % of the magnocellular neurons in the nbM are cholinergic and that the Ch4 group is the largest out of the four basal forebrain cholinergic groups. Furthermore, the Ch4 can be subdivided into five groups in monkeys (Mesulam et al., 1983a): the anterior part (Ch4a) including the anteromedial (Ch4am) and anterolateral (Ch4al); the intermediate part (Ch4i) including the intermediodorsal (Ch4id) and intermedioventral (Ch4iv); and a posterior group (Ch4p) (Mesulam and Geula, 1988). In the human brain, Ch4 neurons express ChAT, the vesicular ACh transporter, AChE, calbindin-d28k, the high affinity nerve growth factor receptor (NGFr) trkA, and the low affinity p75 NGFr ($p75^{NTR}$). A minority of Ch4 neurons are NGFr-negative and, at least in the rat, project preferentially to the amygdala. The nucleus basalis also contains a complex mosaic of non-cholinergic neurons that are nicotinamide adenine dinucleotide phosphate diaphorase (NADPHd)-positive, γ-aminobutyric acid (GABA)ergic, peptidergic, or tyrosine hydroxylase-positive (Mesulam and Geula, 1988; Gritti et al., 1994; Mufson et al., 2003).

Afferent projections to the nbM

The afferent projections to the nbM were demonstrated at the subcellular level by the ultrastructural localization of different markers. Immunohistochemical studies in rodents reveal a substantial number of catecholaminergic projections from the ventral tegmental area and substantia nigra pars compacta, serotonergic projections from the dorsal raphe and ventral tegmental area, and cholinergic innervations from the pedunculopontine nucleus and laterodorsal tegmental area (Jones and Cuello, 1989). Dendrites of Ch4 BFCN receive innervations from cholinergic (ChAT-positive), GABAergic and dopaminergic neurons (Smiley and Mesulam, 1999). The cholinergic contacts usually form asymmetric synapses and could represent local collaterals or projections from Ch5–Ch6. The GABAergic input occurs through symmetric synapses and could represent input from inhibitory neurons within the basal forebrain. The human nbM contains numerous dopaminergic, serotonergic, and noradrenergic axons from the neurons of the ventral tegmental area/substantia nigra, the midbrain raphe and the nucleus locus coeruleus, respectively. In the rat, all of these nuclei, together with the cholinergic Ch5–Ch6 cell groups, have been shown to project to Ch4 (Jones and Cuello, 1989). Galanin, glutamate and estrogen receptors have also been found in the human Ch4 sector as postsynaptic components of extrinsic afferents to Ch4 (Mufson et al., 2003).

Efferent projections from the nbM

The human and primate nbM and the B in rodents, provides the main source of cortical cholinergic innervation (Mesulam et al. 1983). The specific depletion of BFCN in the Ch4 of rodents and primates significantly reduces the cortical densities of ACh and AChE (McGeer and McGeer, 1986; Wenk et al., 1994). Ch4a mainly innervates the most rostral part of the brain. The neurons from Ch4am provide the major cholinergic innervation to frontal, parietal and cingulate cortices. A more modest number of projections are directed to the inferior parietal lobule including hypothalamus, hippocampus, somatosensory cortex, amygdala and parahippocampal regions among others. The Ch4al subsector mainly projects to the frontoparietal cortex and the amygdala and, to a lesser degree, to the olfactory bulb, motor cortex, ventrolateral orbital cortex, insular and parahippocampal areas. The BFCN of the Ch4i subsector are located in the middle of the nucleus and send projections to orbital, insular, periarcuate, peristriate, inferotemporal and parahippocampal areas, and to the inferior parietal lobule, but project more modestly to the medial frontal pole, dorsomedial motor cortex, amygdala, anterior auditory cortex and the temporal pole. Lastly, the BFCN from the Ch4p subsector mainly innervate the superior temporal pole and few projections are directed to inferotemporal and posterior insular regions (Mesulam et al., 1983b; Mesulam and Geula, 1988). The same regions can be innervated by different Ch4 subsectors, which show that there is a considerable overlap of BFCN from individual subsectors. The lack of

anatomical separation of BFCN in discrete subpopulations would represent a challenge for the identification of the degeneration of a specific Ch4 subsector. Immunohistochemical studies in *postmortem* brain samples from human subjects show that cholinergic innervations from the nbM are mostly unmyelinated and leave the nucleus in two highly discrete organized fiber bundles which form the medial and lateral cholinergic pathways (Selden et al., 1998).

Therefore, it is reasonable to compare human connectivity with that found in primates and rodents and, indeed, human pathological data give indirect support to this assumption (Mesulam, M. M. and Geula, 1988). The cholinergic innervation form a dense plexus of fibers in all regions of the human neocortex displaying synaptic specializations, as they are often in close contact with cortical cholinoceptive neurons (Mesulam, M. M. and Geula, 1988). Overall, the heterogeneous neural input to the nucleus from predominantly limbic structures, combined with the massive cholinergic output to the almost entire neocortical mantle, makes the nbM the principal candidate for the modulation or influence of several aspects of complex and organized behavior such as learning, executive functions and working memory (Gratwicke et al., 2013).

2. Basal forebrain cholinergic system and cognition

Memory is the ability to recall past experiences and define our identity making us who we are (Dudai, 2004). The brain receives the information by three basic forms. First, we process stimuli instantaneously with our sensory memory, this information held in the human brain for less than one second (Vandenbroucke et al., 2014). Next, the information is transferred to our short-term memory (also known as working memory), which allows us to mull things over in the present (D'Esposito and Postle, 2015). Finally, we store past events and patterns learned over time in our long-term memory, also known as episodic or semantic memory (Pastotter et al., 2017). When a progressive deterioration of memory is detected and other cognitive functions become altered, appears the disabling syndrome of the brain called dementia (Qiu and Fratiglioni, 2015). The prevalence of older people diagnosed with dementia is reported to be around 6% worldwide (Prince et al., 2013). The total global cost of dementia was estimated at US$818 billion in 2015 and will rise above US$1 trillion in 2018 (Vos et al., 2015). Therefore, dementia is considered the greatest global challenge for health and social care in the current century (Livingston et al., 2017). Cognition-approach treatments aim to redress cognitive deficits, the most prevalent and important element of suffering from dementia (Office, 2017). The cholinergic system has been found to be crucially involved in cognitive functions, with cholinergic dysfunction playing a pivotal role in the pathophysiology of dementia (Roy et al., 2016). Concretely, the functionality of basal forebrain cholinergic pathways has an important role in correct process of memory (Solari and Hangya, 2018; Aitta-Aho et al., 2018). In this connection, AD is the most common irreversible cause of dementia. The memory dysfunction was attributed to the profound degeneration of Ch4 neurons and the further loss of cortical cholinergic innervations (Mesulam, 2004). Experiments performed in both animals and humans have shown learning and memory impairments after treatment with anticholinergic drugs. Altogether, it has led to "the cholinergic hypothesis of geriatric memory dysfunction," by Bartus et al. (1982). However, in the last decades, the role of ACh in memory has been debated (Blokland, 1995a; Gold, 2003), mainly due to conflicting results obtained with cholinergic lesions (Easton et al., 2012).

Dysfunctions in BFCS may underlie some of the behavioral symptoms in patients with AD (Grothe et al., 2012). The decrease in the levels of presynaptic cholinergic markers in the neocortex was correlated with the degree of dementia (Perry et al., 1978). Because the BFCS is a major site of pathology associated with AD, animal models of this disease have placed special emphasis on the behavioral effects of destruction of the homologous area, the nucleus basalis magnocellularis (B) and medial septal area (MS), in rodents and non-human primates. The loss

of basal forebrain cholinergic cells in these models can induce an impairment of memory similar to the symptoms observed in patients with AD (Toledano and Alvarez, 2004).

A direct consequence of the cholinergic hypothesis of AD was the development of animal models of cholinergic system dysfunction based on the spontaneous or induced involution or experimental manipulation of the basalocortical cholinergic systems of the basal forebrain. Different lines of research have been developed in humans, animals, tissues, cells, and even at the subcellular and molecular levels, but the results obtained to date are far from solving the problem. As in other diseases, animal models could provide the key for discovering the changes that occur during the course of the pathological processes, and could help in developing a suitable treatment for each degenerative step. However, no animal suffers AD, nor any agent has been isolated that induces this disorder in animals. Nonetheless, experimental AD models have been developed for the study of selected aspects of the process, and for the examination of the possibilities of preventing, stopping or even reversing neurodegeneration and the cognitive deficits it causes. The results obtained in these models are not restricted to AD. The research in degeneration of BFCS is also involved in other disorders such as Parkinson's disease (Liu, A. K. et al., 2015). They also have a role into physiological senile cognitive deficits (Price et al., 1991), and other borderline situations such as mild cognitive impairment and age-associated memory impairment (Mufson et al., 2002).

2.1. Cholinergic dysfunction models

Different types of normal and experimental cholinergic dysfunction models have been described or developed:

Normal aged animals

The first one and more simple corresponds to senile animals models. This model, based on ChAT and $p75^{NTR}$ changes together with cell loss, has been reported in basal forebrain of senile animals (Biegon et al., 1986; Fischer et al., 1992). Some studies relate this to a deficit in cortical markers (Michalek et al., 1989), and only in some monkeys is accompanied by some degree of amyloid deposition (Sani et al., 2003). Although it is well established the differences between brain senility and sporadic AD, similar cholinergic mechanisms are seen in both processes. Moreover, there is strong evidence of pathological change from senility to AD (Mann et al., 1984), which involves passing through stages of mild cognitive and age-associated memory impairment (Pagani et al., 2016; Davis, M. et al., 2018). This has very important practical implications, however, factors related to ageing hinder the interpretation of results.

Pharmacological models

The importance of cholinergic activity in the brain to learning and memory function was first recognized more than 30 years ago, when relatively low doses of certain muscarinic acetylcholine-receptor antagonists (e.g., the belladonna alkaloids atropine and scopolamine) were found to induce transient cognitive deficits in young human volunteers that resembled those observed in elderly subjects (Drachman and Leavitt, 1974). Several studies indicate thast antimuscarinics disrupt attention. The scopolamine and cholinergic blockade models have confirmed the close relationships among cognitive function, cortical neuronal transmission and baso-cortical cholinergic innervation, suggesting that cholinergic therapies might be useful for the treatment of AD (Delvalle and Greengard, 1976; Nieto-Escamez et al., 2002). Scopolamine could alter certain features of the human electroencephalogram (e.g., delta, theta, alpha, and beta activity) in a fashion that mimics some of the changes observed in patients with AD (Ebert and Kirch, 1998). Interestingly, muscarinic antagonists appear to negatively affect cognitive performance to a greater extent in elderly subjects than in younger subjects (Zemishlany and Thorne, 1991), and they impair subjects with AD more dramatically than in non-demented elderly subjects (Sunderland et al., 1987). In human studies, the use of cholinergic drugs with young or aged healthy individuals were of some use several years ago but ethical concerns have restricted their use (Sunderland et al., 1986).

Basal forebrain cholinergic lesion models

As previously mentioned, different lesion or dysfunction of BFCN have been developed to produce a broad range of models.

a) Electrolytic lesions

These lesions were abandoned several years ago because they cause alterations to fibers passing in affected area, and the combination of this technique with other types of models was necessary to differentiate cholinergic and non-cholinergic effects (Sabbatini et al., 1999; Shimizu et al., 2003).

b) Excitotoxic non-selective cholinergic lesions/dysfunctions of the distinct forebrain cholinergic subareas performed by stereotactic injections

These lesions provoke the death of cholinergic cells around the injection area but the excitotoxins are not specific for cholinergic degeneration. They produce cortical cholinergic dysfunction without other deficits. Lesion in septum, diagonal band, gyrus cingularis and other limbic areas provoke higher cholinergic hypofunctioning in the hippocampus and amygdala. On the contrary the lesions in the B lead to cortical cholinergic changes. The widely used toxins are those acting in glutamatergic receptors: (N-methyl-D-aspartate (NMDA) and non-NMDA agonists such as ibotenic (IBO) (Hepler et al., 1985; Singewald et al., 2011), quisqualic (QUIS) (Marston et al., 1994; Winkler et al., 1998), quionilic (QUIN) (Boegman et al., 1992) and α-amino-3 hydroxy-5 methyl- 4 isoxazole- propionic (AMPA) acids (Waite et al., 1994). Controversial data have been obtained from the different toxins regarding projection cholinergic markers and the induced cognitive impairment (Muir et al., 1993; Gutierrez et al., 1999). Although this type of lesions produces a huge cognitive impairment the cholinergic projections did not seem to be very affected (Waite and Thal, 1996).

c) Cholinotoxic lesions; selective cholinergic lesions of the forebrain cholinergic nuclei

These tools have been considered closest to AD since they theoretically preserve non-cholinergic neurons, axons that pass thorough this area and selectively impaired cholinergic centers.

AF64

The cholinotoxin ethylcholine aziridinium ion (AF64A), which binds to the high affinity choline uptake system (HACU), provokes significant acquisition and retention deficits in different memory tasks by inducing extensive brain dysfunction which affect to different neuronal systems that are involved not only in cholinergic system (Nakamura et al., 1992).

Immunotoxins

Classical methods that rely on mechanical lesions, or the injection of cholinotoxins or excitotoxins have failed to induce complete and selective cholinergic cell death in the basal forebrain of rats (Smith, G., 1988). In the previous explained lesions, the GABAergic interneurons are directly affected since intermingle with cholinergic cells. A more efficient and selective tool to induce permanent cortical cholinergic hypoactivity makes use of a cholinergic 192IgG-saporin inmutoxin. During the early nineties, 192IgG-saporin, a powerful tool for selective BFCN lesioning, was developed by Wiley et al. (1991), and revolutionized research on the cognitive functions of the basal forebrain cholinergic system. The 192IgG-saporin immunotoxin consists of a monoclonal antibody 192IgG raised against the low affinity neurotrophin receptor $p75^{NTR}$ and the ribosome-inactivating protein saporin, which is coupled to the antibody via a disulfide bond. $P75^{NTR}$ is abundant and specific in cholinergic cells of the BFCS (Springer et al., 1987). The toxin follows receptor binding and internalization like the endogenous ligand of $p75^{NTR}$, and enzymatically inactivates the large ribosomal subunit, thereby blocking protein synthesis and ultimately resulting in cell death by apoptosis; the neurodegenerative process can be considered complete in about 2 weeks. Lesions of this selectivity and extent had proven impossible to produce using any other technique (Wrenn and Wiley, 1998).

After an intracerebroventricular (i.c.v.) injection of 192IgG-saporin, the immunotoxin is taken up by cholinergic terminals and retrogradely transported to cell soma in the basal forebrain (Heckers et al., 1994). Thus, the i.c.v. administration of 192IgG-saporin results in massive BFCN loss, including those from the medial septum, vertical and horizontal limb of the diagonal band of Broca and nucleus basalis magnocellularis, whereas cholinergic cells in the adjacent ventral pallidum and cholinergic interneurons within the caudate putamen are not affected (Rossner, Schliebs et al., 1995). The immunolesions keep loci of cholinergic degeneration free from mechanical damage and do not affect parvalbumin, calbindin or calretinin containing GABAergic neurons of the basal forebrain. The only additional non-cholinergic neurons known to be affected by the i.c.v. administration of 192IgG-saporin application are cerebellar Purkinje cells which also express $p75^{NTR}$ (Heckers et al., 1994; Waite et al., 1995).

Intraparenchymal injections of 192IgG-saporin directly into specific nuclei of the basal forebrain allow us to understand the specific role of the different BFCN populations in behavioral and neurochemical aspects. The infusion of 192IgG-saporin in the distinct nuclei induces profound specific BFCN losses and cholinergic hypoactivity in the innervated areas and permits us to assess the contributions of single projection systems in a variety of learning and memory tests, thereby demonstrating the effectiveness of 192IgG-saporin (Wenk et al., 1994).

Neurochemical effects of 192 IgG-saporin administration in B

Effects on cholinergic neurotransmission

The effects on cholinergic and non-cholinergic neurotransmission of 192IgG-saporin-induced BFCN depletion in the B have been extensively analyzed. Multiple neurotransmitter systems are affected in this lesion model, but cortical cholinergic neurotransmission becomes especially impaired. Profound alterations have been reported, such as reductions in several cortical cholinergic presynaptic markers including ChAT activity (up to 80%) and density (up to 50%), or AChE density (up to 90%) and SDHACU density ([^{3}H]HC-3 binding by up to 45%) (Gil-Bea et al., 2005; Ljubojevic et al., 2014). In addition, the cortical ACh supply and specific adaptations related to neurotransmitter receptors are also observed. Autoradiographic studies demonstrate that M_1 mAChR density is increased by up to 35% in the parietal cortex one week after the 192IgG-saporin infusion, whereas M_2 mAChR density is less affected (an increase of approximately 20%), which is in parallel with great reductions in AChE levels and choline uptake sites (Pellborn and Rossner, 1995; Rossner, 1997). The fact that M_2 mAChR is increased after immunolesions (having lost up to 80% of BFCN terminals), supports the hypothesis that a significant population of M_2 mAChR could exist postsynaptically to cholinergic terminals in the cerebral cortex (Rossner, 1997; Mesulam, 1998). *Ex vivo* autoradiographic studies have confirmed significant and widespread decreases in cortical presynaptic terminals by using [^{123}I]BVM, a radioligand which targets the VAChT (Quinlivan et al., 2007). Besides, *in vivo* PET neuroimaging studies, carried out in rats with a 192IgG-saporin-induced lesion of the B, have demonstrated a significant decrease in fronto-cortical cholinergic terminals (Parent et al., 2012; 2013), glucose metabolism (Mehlhorn et al., 1998) and neuronal metabolic activity by using [^{18}F]fluoroethoxybenzovesamicol to label the vesicular ACh transporter and [^{18}F]-2-fluoro-2-deoxyglucose and cytochrome oxidase activity assays (Gelfo et al., 2013).

Effects on other different neurotransmitter systems

As previously mentioned, specific basal forebrain cholinergic immunolesions also affect other neurotransmitter systems, including the glutamatergic, GABAergic, serotonergic and adrenergic and more recently also the cannabinoid system. While NMDA receptors are reduced by approximately 20%, AMPA and kainate binding sites are increased by up to 30% in several cortical regions seven days after the 192IgG-saporin-induced lesion of the B. Regarding GABAergic neurotransmission, the binding of [^{3}H]muscimol, but not [^{3}H]flunitrazepam, is increased by up to 20% after 192IgG-saporin administration in cortical regions, revealing a modulation of cortical inhibition (Gelfo et al., 2013). The selective BFCN damage in the B may

be associated with a functional decline in cortical GABAergic neurotransmission and cognitive deficits (Jeong et al., 2011). In this sense, our research group showed a decrease of GABAergic immunoreactivity in cortical areas together with increase in the activity of CB_1 receptors (Llorente-Ovejero et al., 2017). Moreover, deep brain stimulation of the remaining BFCN after B lesion improves spatial memory performance and partially restores the two isoforms of glutamic acid decarboxylase, GAD65kDa and GAD67kDa and glutamate to control levels (Lee et al., 2016). These findings clearly demonstrate that basal forebrain cholinergic innervation has a pivotal role in cognitive processes by fine-tuning the cortical excitatory-inhibitory balance.

Basal forebrain cholinergic immunolesions do not alter α_1-adrenoceptor and 5-HT_{1A} receptor binding in the neocortex, but α_2 and β-adrenoceptors and 5-HT_{2A} display significant reductions in neocortical brain regions in parallel with the loss of BFCN terminals (Heider et al., 1997). More recent studies show that B cholinergic deafferentation triggers a significant down-regulation of 5-HT_{2A} receptor levels in the frontal cortex, together with changes in serotonin and 5-hydroxytryptophan levels, suggesting a down-regulation of the rate-limiting enzyme for the synthesis of serotonin in combination with the cholinergic deficit (Severino et al., 2007). However, 5-HT_{1A} and 5-HT_{1B} receptors do not seem to mediate this process (Heider et al., 1997; Garcia-Alloza et al., 2006).

Effects on neurotrophin homeostasis

NGF plays a pivotal role in the development and maintenance of BFCN and neuronal plasticity (Conner and Varon, 1992). BFCN depletion in the B does not modify NGF protein levels in the basal forebrain but, considering that much of this protein is located in BFCN cell bodies, the remaining BFCN probably compensate for the loss of cholinergic innervation (Rossner, 1997). Interestingly, when NGF is administered i.c.v. to 192IgG-saporin-lesion rats, it displays a limited capacity to enhance the functioning of residual BFCN and increases fear-related behavior and adverse neuroproliferation (Winkler et al., 2000). The brain-derived neurotrophic factor (BDNF) has also been studied because of its role in survival, differentiation and the functioning of neurons (Mattson, 2008). Two weeks after a 192IgG-saporin-induced lesion of B, cortical BDNF protein levels are significantly reduced (Angelucci et al., 2011; Turnbull et al., 2018). The fact that NGF levels are increased, whereas BDNF is reduced after 192IgG-saporin lesioning of BFCN, suggests that there is a different regulation. Growth factors are very promising molecules, but neurotrophin-based therapeutic strategies should be handled cautiously until there is a complete understanding of their regulation in neurodegeneration, since some clinical trials have had to be halted because of safety-issues (Eriksdotter et al., 2018).

Effects on neurogenesis and neuronal plasticity

The i.c.v. administration of 192IgG-saporin in adult rats impairs adult neurogenic processes, increasing cell death in both the dentate gyrus and the olfactory bulb (Cooper-Kuhn et al., 2004). Impairment in spatial memory performance has also been observed in this lesion model, which is reverted by the systemic administration of physostigmine, presumably through M_1 and M_4 mAChR expressed in newly born cells (Mohapel et al., 2005). Moreover, a 192IgG-saporin-induced lesion of BFCN in the B disrupts cortical map reorganization and impairs motor learning, supporting the hypothesis that cortical plasticity is a key substrate for enabling an animal to effectively learn a skilled motor behavior (Conner et al., 2003). Further studies have demonstrated that following focal cortical injury, the basal forebrain cholinergic system is required for the necessary plasticity that behavioral recovery requires (Conner et al., 2005). These findings support the hypothesis that the basal forebrain cholinergic system is selectively required for modulating complex forms of cortical plasticity driven by behavioral experiences (Ramanathan et al., 2009).

Effects on gene regulation

Acquisition of new information is associated with changes in the cortical expression of several genes, some of which have been identified as playing a major role in learning and memory processes (Gusev and Gubin, 2010). The intraparenchymal administration of 192IgG-saporin directly in the B triggers profound regressive changes in dendritic morphology of frontal cortical neurons (Harmon and Wellman, 2003), and impairment of neuronal plasticity (Wellman and Sengelaub, 1991). When cDNA microarrays and qRT-PCR have been used to screen for the cortical gene expression profile in 192IgG-saporin-lesioned rats, specific changes in mRNA expression were reported in those behaviorally impaired animals, associated with the loss of BFCN in the B (Paban et al., 2011). Finally recent study shows that i.c.v. toxin administration is able to increase the expression of ribosome-forming proteins and microglia-specific genes in hippocampus (Dobryakova et al., 2018).

Effects on other molecules

Recent studies of our research group found changes in the lipid profile following the cholinergic cell loss induced by 192IgG-saporin. Decrease of some sulfatide species and increase of phosphatidylcholine species was shown in B (Martinez-Gardeazabal et al., 2017). One of the most consistent lipid changes that has been described in brains of AD patients is the decrease of

sulfatides during the early stages of disease (Han et al., 2002; Cheng et al., 2013; Gonzalez de San Roman, et al., 2017).

Behavioral effects of BFCN immunolesions in the B

It has been previously shown that a single intraparenchymal injection of 192IgG-saporin in the B results in an extensive and selective loss of BFCN, long-lasting cortical cholinergic hypoactivity and deficits in recognition memory capacity (nonmatching-to-position task, object recognition task and object location task), in delayed matching to position (T-maze task), configural association learning (operant conditioning task), spatial learning (Morris water maze) and aversive learning and memory (passive avoidance test) (Torres et al., 1994; Berger-Sweeney et al., 1994; Baxter et al., 1995; McGaughy and Sarter, 1998; Pizzo et al., 2002; Butt and Bowman, 2002; Han et al., 2002; Bailey et al., 2003; Paban et al., 2005; Gibbs and Johnson, 2007; Dashniani et al., 2009; Cheng et al., 2013; Rastogi et al., 2014; Lee et al., 2016; Martinez-Gardeazabal et al., 2017).

Further studies involving the lesioning of the B with 192IgG-saporin support the role of BFCN in an array of attentional functions including vigilance, reorienting of spatial attention and attentional resources directed at environmental stimuli (Bucci et al., 1998). All these previous results allow us to conclude that the B plays a major role in attention and that could have an influence on effects on learning and memory (Ljubojevic et al., 2014).

Conversely, the results of other studies based on 192IgG-saporin-induced lesion of the B indicate that the role of the basal forebrain cholinergic system in cognitive functions is considerably more limited than was previously believed. Thus, impairments in spatial learning and memory, which are commonly observed after basal forebrain lesions produced with less selective methods (excitotoxins), are not observed following selective immunotoxic lesions of specific BFCN. Some authors report impairment in spatial learning and memory by lesions of the basal forebrain, which are frequently attributed to BFCN loss, despite the lack of selectivity of the lesion method employed (Berger-Sweeney et al., 2001; Baxter and Bucci, 2013). Several studies using the intraparenchymal infusion of 192IgG-saporin in the B have failed to show impairment in spatial learning tasks, or have produced only mild performance deficits (Wenk et al., 1994c; Baxter and Gallagher, 1996). In contrast, when 192IgG-saporin is administered i.c.v., more consistent impairments in spatial learning and memory are reported (Berger-Sweeney et al., 1994). Some authors have reported a higher depletion of cortical ChAT activity following i.c.v. 192IgG-saporin administration than with intraparenchymal injections, leading them to propose that a severe loss of cortical cholinergic input is required to induce deficits in learning and memory (Baxter, 2001).

In conclusion, the controversial behavioral findings suggest that the surgical procedures as well as the dose of immunotoxin used are critical variables when 192IgG-saporin is administered intraparenchymally. This model of basal forebrain cholinergic dysfunction, induced by the administration of 192IgG-saporin in the B, produces neurochemical perturbations related to ACh-related enzymatic machinery, neurotransmitter receptors, neurotrophin homeostasis and neuronal plasticity, leading to learning, memory and attentional deficits similar to the cognitive impairment observed in AD patients. Therefore, this model is useful to assay a wide range of pharmacological interventions aimed at modulating or partially restoring basal forebrain cholinergic neurotransmission.

3. Cholinergic system in AD

The loss of BFCN in the nbM is one of the main hallmark features of AD brains and was originally described by Davies and Maloney (Davies and Maloney, 1976) and corroborated in subsequent studies (Whitehouse et al., 1981; Whitehouse et al., 1982). The loss of cortical cholinergic innervation in AD can be attributed to the loss of BFCN present in the nbM (Geula et al., 1998; Mesulam, 2004; Ikonomovic et al., 2007). The profound reductions in ChAT and AChE activities in cholinergic projecting areas of AD patients could result from impaired synthesis of these enzymes, from an abnormality in their axonal transport from BFCN bodies to terminals in the cortex, or from degeneration or atrophy of BFCN. The primary source of cholinergic innervation to cortex and hippocampal formation is derived from large BFCN in the nbM and the complex MS-diagonal band of Broca respectively, and these cholinergic nuclei have been extensively examined in patients with AD.

However, some immunohistochemical studies reported only changes in size, but not in the number of BFCN, and no significant loss of cortical ChAT was found in *postmortem* studies of mild AD patients (DeKosky, 2031).

Additional studies demonstrated that BFCN display hypertrophy in the early stages of AD, and gradually become atrophic in the advanced stages (Hayes and Lewis, 1992). Interestingly, a correlation between the number of neuritic plaques in several neocortical areas and the loss of BFCN was found (Arendt et al., 1984). Besides, by using AChE-staining histochemical assay, a marked decrease in the density of stained BFCN, together with abundant neurofibrillary tangles were found in the nbM of AD patients (McGeer, P. L. et al., 1986).

Due to the large number of neurochemical, neuropathological and functional observations which have been made in *postmortem* samples from AD patients, it is reasonable to think that the nbM is deeply involved in the manifestation and progression of AD. ChAT activity and AChE-positive fibers are markedly reduced in the frontal, parietal, temporal and visual cortices in AD. The depletion of cholinergic structures in the temporal lobe, including its limbic, paralimbic and associated components is similar to the distribution of the senile plaques (Mesulam and Geula, 1994).

The cholinergic innervation of the hippocampal formation is thought to play an important role in memory processes and there is a large body of evidence supporting that the basal forebrain cholinergic innervation of the hippocampus becomes reduced in the elderly as well as in AD

patients. The distribution of AChE in AD hippocampal samples revealed reduced levels of both AChE activity and stained fiber densities (Green and Mesulam, 1988).

In *postmortem* samples from AD patients, ChAT activity was significantly reduced in the amygdala (Rossor et al., 1982). The density of senile plaques and the extent of neurofibrillary tangles in the amygdala do not apparently correlate with the loss of either the cholinergic innervation or the BFCN density (Emre et al., 1993).

3.1. Cholinergic receptors in AD

When the supply of cortical ACh is interrupted as a consequence of BFCN degeneration and/or ChAT down-regulation, the cholinergic receptors located in projecting areas are devoid of the endogenous ligand and one should expect to observe a regulation to compensate for that loss of cholinergic input. The two classes of cholinergic receptors, the G protein-coupled mAChR and the ligand-gated ion channel nAChR, are not equally affected in AD, the mAChR are more affected in AD.

Muscarinic acetylcholine receptors in AD

The studies performed in tissue homogenates using radioligands selective for mAChR have shown discrepancies in brain tissue samples from AD patients. [^{3}H]pirenzepine, a relatively selective M_1 mAChR radioligand, shows that binding parameters are generally unaltered in brain tissue samples from AD patients (Araujo et al., 1988). Since M_1 mAChR are mainly located in postsynaptic cholinoceptive neurons, they are probably conserved after the loss of BFCN. A significant loss of M_2 mAChR has been observed in specific brain areas of *postmortem* AD patients, including cortical areas and the hippocampal formation, and this is consistent with the idea that M_2 mAChR could be located on degenerating BFCN nerve terminals (Mash et al., 1985; Quirion et al., 1989).

Autoradiography represents a powerful pharmacological tool to analyze the radioligand binding in discrete and small brain areas or subfields in brain slices. Moreover, the density and distribution of receptors can readily be correlated with the density of neurons, neuritic plaques and neurofibrillary tangles, or with the degree of cholinergic dysfunction in the brain area of interest on slices consecutive to those processed for autoradiography. The first autoradiographic studies for mAChR in AD patients showed that the densities and the proportions of the M_1 and M_2 mAChR subtypes in autopsied AD brain samples were not significantly different in slices of hippocampal tissue compared to those observed in non-demented controls (Griffiths et al., 1994). Conversely, further autoradiographic studies showed significant reductions of both [^{3}H]pirenzepine binding in the presence of cold oxotremorine (M_1 mAChR subtype) and

[^{3}H]oxotremorine binding in the presence of an excess of cold pirenzepine (M_2 mAChR subtype) in entorhinal cortex and in most hippocampal strata in AD brain slices (Rodriguez-Puertas et al., 1997).

Immunohistochemical approaches have been used to anatomically describe the mAChR cellular distribution in *postmortem* brain samples from AD patients and have found a decrease in the M_1 protein in the cortex and hippocampus (Myers et al., 1996). In neocortical and hippocampal regions, M_1 mAChR is mainly expressed in all pyramidal neurons where it displays a somatodendritic distribution (Levey et al., 1995). Behavioral studies have demonstrated deficits in learning and memory in mice lacking M_2 mAChR, which suggests that the M_2 mAChR subtype plays a crucial role in cognitive processes (Tzavara et al., 2003). In this sense, hippocampal muscarinic activation, through the high affinity M_2 mAChR subtype, promotes a rise in AMPA receptor sensitivity to glutamate, which finally leads to the so-called 'muscarinic long term potentiation', essential to explain hippocampal neuronal plasticity (Segal and Auerbach, 1997). Regarding the distribution of the M_2 mAChR subtype, and consistent with radioligand binding assays, a decrease in protein levels was also found in AD patients that could probably be explained by the loss of BFCN during the disease. Cortical M_4 mAChR, which are expressed in the neuropil and in scattered perikarya, have been found to be significantly up-regulated in AD patients (Flynn et al., 1995). The M_4 loss in rodents leads to dysfunction in hippocampal synaptic transmission, suggesting that this subtype could be involved in neuronal plasticity-associated with memory formation (Mulugeta et al., 2006).

The expression of the genes for M_1 and M_2 mAChR were found to be unchanged in AD patients (Ohara et al., 1994). However, other authors reported increased mRNA levels of the M_1 mAChR subtype in the temporal and occipital cortices (Harrison et al., 1991).

In reference to the functionality of mAChR, a significant loss of high-affinity agonist binding to M_1 mAChR was described in the frontal cortex of patients with AD (Flynn et al., 1991). The first evidence of the relationship between cholinergic muscarinic activation and amyloid precursor protein processing was demonstrated in carbachol-treated cell cultures which overexpressed M_1 and M_3 mAChR (Nitsch et al., 1992). More recent studies found that the attenuation of G-protein coupling to M_1 mAChR in the neocortex was associated with dementia severity, and indeed, correlated with reductions in PKC activity and NMDA receptor density, suggesting a postsynaptic cholinergic dysfunction in AD (Tsang et al., 2007). [^{35}S]GTPγS binding to G proteins combined with immunoblot analysis of G protein subunits, also revealed that the receptor-mediated activation of G proteins was reduced in brain cortex of AD patients (Hernandez-Hernandez et al., 1995). Oxotremorine-M-mediated activation of the M_2 mAChR subtype did not trigger any change in the functional coupling of M_2 mAChR to G protein in the

neocortex of patients with AD. Further studies have provided evidence of the loss of muscarinic receptor-G protein coupling in AD and support the hypothesis that muscarinic receptor-mediated cortical activation may be compromised in this disease (Ferrari-DiLeo et al., 1995).

4. AD treatments

Current treatments available include cholinesterase inhibitors for patients with any stage of AD dementia, and memantine for people with moderate-to-severe AD dementia. These medications have been shown to enhance the quality of life for both patient and caregivers when prescribed at the appropriate time during the course of illness. However, they do not change the course of illness or the rate of decline (Mossello and Ballini, 2012). At present, only two classes of pharmacological therapies are available for patients with AD. The cholinesterase inhibitors donepezil, rivastigmine, and galantamine are the recommended therapy for patients with mild, moderate, or severe AD dementia as well as Parkinson's disease dementia. On the other hand, memantine, a non-competitive N-methyl-D-aspartate receptor antagonist approved for use in patients with moderate to severe AD. Other alternative therapies, for example huperzine A, that seems to significantly improve cognitive performance in patients with AD or vascular dementia (VD), is not regulated by the US Food and Drug Administration and may be subject to fluctuations in potency and purity (Xing et al., 2014). The treatments also go in other directions, due to the inflammation that is produced in the development of AD, the use of non-steroidal anti-inflammatory drugs could reduce the risk to develop AD. However, recent investigations failed to note any significant difference in cognitive performance in patients with those treatments (Gupta et al., 2015).

In the past decade, omega-3 fatty acid supplements including fish oil have received much attention owing to their cardiovascular benefits. A recent randomized, controlled, double-blinded studies showed cognitive improvement function in people with MCI who took fish oil supplements, though these studies were limited, since different fish oil dosages, longer intervention periods, and larger sample sizes should be investigated (Bo et al., 2017).

Finally, control of cardiovascular risk factors contributes to overall brain health in both cerebrovascular disease and neurodegenerative diseases (Gorelick et al., 2017). A systematic review of many studies showed an association between the Mediterranean diet and cognitive impairment (Singh et al., 2014).

Aerobic exercise was also associated with a reduction in the neuropsychiatric symptoms and contributed to attenuate the caregivers' burden (Stella et al., 2011). Although larger controlled studies are still needed to examine the long-term effects of physical activity in patients with biomarker-proven AD pathology, the inherent systemic benefits and lack of health risks should

lead all healthcare providers to recommend regular exercise for their patients, regardless of cognitive function (Smith, J. C. et al., 2014).

Future treatments

Research into future treatments for AD could involve targeting of the etiologic pathologies: neurofibrillary tangles (composed of p-tau) and senile plaques (Aβ). However, a debate remains regarding to which abnormality is the best target to slow down or halt the neurological decline, including the question about the origin of this histopathological features (Mann and Hardy, 2013). Another approach could be the preservation of transcortical networks and enhancing inter-neuronal connections in order to improve cognitive functions (Kosik, 2013). AD therapies represented in phase I, phase II, and phase III obtained in Clinicaltrials.gov as of January 30, 2018, showed that there are 112 agents in the current AD treatment pipeline. There are 23 agents in 25 trials in phase I, 63 agents in 75 trials in phase II and 26 agents in 35 trials in phase III. 63% of them are disease-modifying therapies, 22% are symptomatic cognitive enhancers, and 12% are symptomatic agents addressing neuropsychiatric and behavioral changes (Figure 3) (Cummings et al., 2018).

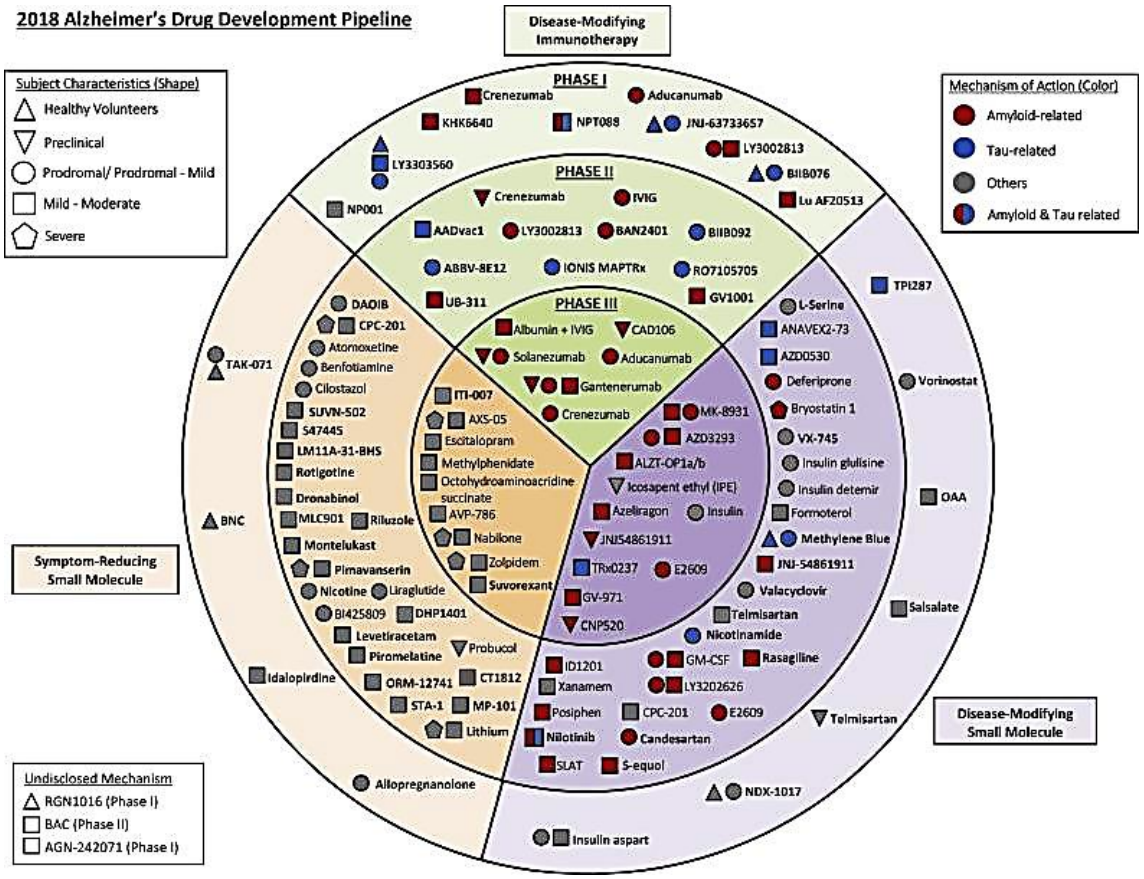

Figure 3. Agents in clinical trials for treatment of Alzheimer's disease in 2018 (from clinicaltrials.gov accessed January 30, 2018). Obtained from Cummings et al., 2018.

Very few new drugs ever make it past Phase II research. In fact, only 1/3 of those drugs ever make it to Phase III clinical trials. The drugs that progress to Phase III are definitively tested for effectiveness in the treatment or cure of a specific condition. These clinical research studies are intrinsically more complicated than other phases, as these trials are the longest and largest out of all the studies conducted. Phase III of the 2018 AD pipeline has 26 agents, 17 disease-modifying therapies, one cognitive-enhancing, and eight drugs for behavioral symptoms. Among the disease modifying therapies, 14 addressed amyloid targets, and only one involved a tau-related target or involved neuroprotection or metabolic mechanism of action (Cummings et al., 2018).

The early detection of biomarkers of the disease will continue still being the best option to an early possible treatment of the disease (Aisen et al., 2017). Other multiple alterations converge in the pathogenesis of AD, including synaptic degeneration, mitochondrial defects, and increased production of reactive oxygen species. Therefore, two of the major goals of current research in AD are to develop new tools for early diagnosis and to search for treatments that are more effective (or simply with some effectiveness), aimed at curbing or retarding disease progression toward dementia by acting on multiple targets during the prodromal period of the

disease. In this respect, the cannabinoid compounds have attracted increasing interest during the last decade based on that the stimulation of the endocannabinoid (eCB) system may help to modulate in parallel several of the pathological processes occurring during the early stages of AD.

5. The endocannabinoid system

The therapeutic value of cannabis was scientifically assessed for the first time in the early 19th century, demonstrating the clinical utility of cannabis in several disorders including cholera, rheumatic diseases, delirium tremens and infantile convulsions (Anonymous, 1843). Δ9-tetrahydrocannabinol (Δ9-THC) would prove to be the most pharmacologically interesting compound of cannabis since it is responsible for its psychotropic activity. Δ9-THC was isolated from hashish and its chemical structure was established by the pioneering studies (Tasker et al., 2015).

The endocannabinoid system include: 1) two 7-transmembrane-domain receptors named as cannabinoid receptor type-1 (CB_1) and cannabinoid receptor type-2 (CB2); 2) their 2 most studied endogenous ligands, the "endocannabinoids" N-arachidonoylethanolamine (anandamide) and 2-arachidonoylglycerol (2-AG); and 3) the 5 enzymes believed, at that time, to be uniquely responsible for endocannabinoid biosynthesis [i.e., N-acyl-phosphatidyl-ethanolamine-selective phospholipase D (NAPE-PLD) and diacylglycerol lipases (DAGL) α and β, for anandamide and 2-AG, respectively] and hydrolytic inactivation [i.e., fatty acid amide hydrolase (FAAH) and monoacylglycerol lipase (MAGL), for anandamide and 2-AG, respectively] (Watkins and Kim, 2015).

5.1. CB_1 receptor

The subtype 1 of cannabinoid receptors (CB_1 receptor) is a member of the rhodopsin-like family of seven TM domain receptors that are coupled to G proteins at their intracellular surface. This receptor was initially cloned in the rat brain (473 amino acids) and subsequently in human (472 amino acids) and in mouse (473 amino acids), sharing a 97-99% amino acid sequence homology (Matsuda et al., 1992).

The development of the [^{3}H]CP55,940 radioligand allowed the anatomical localization of cerebral cannabinoid receptors by using autoradiographic techniques (Herkenham et al., 1990). The mapping of [^{3}H]CP55,940 binding sites showed a preferential localization of CB_1 receptors in specific areas of gray matter, thereby predicting the action of cannabinoids reported in behavioral experiments, and this led to intense research into eCB signaling (Freund et al., 2003). The highest levels of [^{3}H]CP55,940 binding were observed in the olfactory bulb, the nigrostriatal pathway including the globus pallidus, the cerebellar molecular layer and specific layers of the

hippocampus. Ligand binding experiments pointed to CB_1 receptors as one of the most abundant GPCR in CNS. The first electron microscopy studies carried out in rodents, as well as in human CNS, suggested that CB_1 receptors are located in specific types of axon terminals (Katona et al., 1999a; Hajos et al., 2000). Boutons engaged in asymmetrical (excitatory) synapses seem to be devoid of CB_1 receptors, whereas symmetrical (inhibitory) synapses display a profuse distribution of CB_1 receptors, indicating that GABAergic, but not glutamatergic, axon terminals contain CB_1 receptors. However, further studies demonstrated that CB_1 receptors are also present in glutamatergic synapses, but at much lower levels (Hajos et al., 2001; Katona et al., 2006).

Regarding the physiological actions mediated by CB_1 receptors, the tetrad test has been used for screening drugs that induce cannabimimetic effects, consisting of four behavioral components: spontaneous activity, catalepsy, hypothermia and analgesia (Little et al., 1988). Two brain regions that are intimately involved in the control of movement, the basal ganglia and the cerebellum, display very high densities of cannabinoid binding sites which are compatible with the effects of cannabinoids on both motor and cognitive functions, according to the first behavioral paradigm of the tetrad test. The moderate levels of CB_1 receptors reported in basal forebrain-emerging pathways, including the frontal, parietal, and cingulated cortices, septum and amygdala may be an indication of the effects of the cannabinoids on cognitive functions, such as learning, memory and emotional behavior.

On the other hand, the moderate levels of binding in the hypothalamus, lateral subnucleus of interpeduncular nucleus, parabrachial nucleus, nucleus of solitary tract and spinal dorsal horn are probably related to the potent analgesic and antihyperalgesic properties of cannabinoid agonists and their orexigenic effects (Freund and Hajos, 2003). In contrast, the reported low levels of cannabinoid ligand binding in the brainstem areas that control cardiovascular and respiratory functions may explain the tolerability to high doses of cannabinoids (Mailleux et al., 1992; Kano et al., 2009). These overall binding properties are preserved in mammals (Herkenham et al., 1990). During the last decade, there has been increasing evidence of the presence of CB_1 receptors at other locations such as postsynaptic terminals, intracellular organelles, such as the mitochondria, which regulate cell metabolism and memory (Hebert-Chatelain et al., 2016), and in astrocytes, which regulate gliotransmission (Navarrete and Araque, 2008; Bilkei-Gorzo et al., 2018).

In CNS, pharmacological, electrophysiological and neurochemical studies have all shown that CB_1 receptors are located presynaptically and regulate the release of certain types of neurotransmitters. CB_1 receptor activation decreases cellular cyclic adenosine monophosphate (cAMP) levels and elicits cannabimimetic responses. CB_1 receptors also interact with voltage-gated ion channels and inhibit potassium, sodium, and N- and P/Q-type- calcium channels by

reducing membrane potentials (Pertwee, 2010). CB_1 receptor-mediated suppression of neurotransmitter release leads to several forms of synaptic plasticity, such as transiently short-term depression (STD) or persistently long-term depression (LTD) and long-term potentiation (LTP). Both, STD and LTD are mediated by 2-AG. CB_1 receptors have shown a measurable constitutive activity, indicative of G protein activation in the absence of agonists, which could be related to their high abundance and localization (Kendall and Yudowski, 2017). Therefore, inverse agonists specific for CB_1 receptors, such as SR141716A, have also been described (Arnold et al., 2001). The activation of CB_1 receptors is critically involved in many cellular functions such as cell growth, transformation and apoptosis (Galve-Roperh et al., 2002). The CB_1 receptor also activates other intracellular kinases including the phosphatidylinositol 3-kinase (Bouaboula et al., 1997), the focal adhesion kinase (Kendall and Yudowski, 2017), and some enzymes involved in energy metabolism (Derkinderen et al., 1996). The particular distribution of CB_1 receptors and the biosynthesis of eCB in the CNS is induced after the activation of multiple signaling systems, e.g., dopaminergic, serotonergic, (Giuffrida et al., 1999; Mateo et al., 2017; Fantegrossi et al., 2018; Mendiguren et al., 2018), noradrenergic (Mendiguren et al., 2018), cholinergic (Kim et al., 2002a; Ohno-Shosaku et al., 2003), glutamatergic (Ohno-Shosaku et al., 2002) or GABAergic (Musella et al., 2017; Cruz-Martinez et al., 2018). All this observations further support the involvement of the eCB system in the modulation of CNS neurotransmission and control of neuronal network activity.

The inhibitory effects of cannabinoids are directly related to GABA release. Evidence of these effects is further supported by the fact that cannabinoid agonists modulate presynaptic GABA release, decrease amplitude and frequency of $GABA_A$ receptor-mediated inhibitory postsynaptic currents and fail to block the postsynaptic response induced by GABA or muscimol. This process is specifically mediated by CB_1 receptor-dependent activation because it is blocked by two independent antagonists of CB_1 receptors, rimonabant (SR141716A) and AM251, and is completely absent in CB_1 receptor knockout mice (Freund et al., 2003b; Tanimura et al., 2009; Kano, 2014). Other evidences are the activation of CB_1 receptors specifically in GABAergic neurons that inhibit LTD in the amygdala (Marsicano et al., 2002). CB_1 receptor stimulation during adolescence is sufficient to elicit an enduring state of prefrontal network disinhibition resulting from a developmental impairment of local prefrontal GABAergic transmission (Cass et al., 2014).

The development of cell-type specific CB_1 receptor-knockout models has helped us to study how eCB signaling in specific neuronal circuits (i.e. CB_1 receptor-mediated regulation of GABAergic or glutamatergic transmission) contributes to neuronal network activity, synaptic plasticity and behavior. The inactivation of CB_1 receptors exclusively in forebrain GABAergic

neurons (GABA-CB1-KO) leads to diminished hippocampal LTP formation (Monory et al., 2015).

Presynaptic release of glutamate activates AMPA receptors and mGluR on the postsynaptic membrane and induces 2-AG release, which activates CB_1 receptors in the same presynaptic terminals that release glutamate (homosynaptic) or in neighboring presynaptic terminals (heterosynaptic). This phenomenon has not only been observed in excitatory synapses in the dorsal striatum, nucleus accumbens, cerebral cortex, dorsal cochlear nucleus, cerebellum, and hippocampus, and in inhibitory synapses in the hippocampus, amygdala and ventral tegmental area, but also in cholinergic synapses (Heifets and Castillo, 2009). Some studies have revealed that the lack of CB_1 receptors in glutamatergic neurons (Glu-CB1-KO) facilitates hippocampal LTP formation (Monory et al., 2015). CB_1 activation could also increase extracellular levels of glutamate in the nucleus accumbens shell, ventral tegmental area, and medial prefrontal cortex (Grzeda et al., 2017). Surprisingly, cannabinoid agonists are able to reduce glutamatergic-mediated responses in CB_1 receptor knockout mice to the same levels as they do in wild-type mice (Hajos and Freund, 2002). Glutamatergic axon terminals must contain a novel cannabinoid-sensitive site, which is indeed blocked by SR141716A, but it would be molecularly distinct from the cloned CB_1 receptor (Freund et al., 2003).

CB_1 receptors and the cholinergic system

BFCN mediated control of learning and memory processes suggests the existence of finely-tuned modulations of synaptic transmission involving eCB signaling. There are only a few immunohistochemical studies studying the anatomical distribution of the different elements of the eCB system in the mammalian central cholinergic system. These studies indicate that rodent BFCN of the B are devoid of CB_1 receptors, but contain the AEA degrading enzyme FAAH, and display a fine CB_1 receptor fiber meshwork surrounding the perikarya which further suggests that BFCN may utilize eCB for the retrograde control of neurotransmission (Harkany et al., 2003). Similar results were obtained in the gray mouse lemur, revealing evolutionarily conserved networks (Harkany et al., 2005). However, there are controversial anatomical data regarding the CB_1 receptor expression in BFCN (Harkany et al., 2003). Previous light and electron microscopy studies reported a dense labeling of CB_1 receptors in ChAT positive neurons in monkey, and the existence of differentiated BFCN in the medial septum of the rat where cholinergic innervation of the hippocampus originates, some of which express CB_1 receptors (Lu et al., 1999; Nyiri et al., 2005).

A significant decrease of electrically evoked ACh release in rodent brain can be induced by various cannabinoid receptor agonists (Steffens et al., 2003). This effect is completely blocked by the CB_1 receptor antagonists SR141716A and AM281, and absent in CB_1 receptor knockout mice (Gifford et al., 2000). Moreover, the eCB-mediated ACh release is increased in "knockdown" experiments with antisense oligonucleotides complementary to CB_1 receptor mRNA and in the hippocampus and the neocortex of CB_1 receptor knockout mice (Kathmann et al., 2001). Comparable effects had been described in hippocampal slices in a CB_1 receptor activation-dependent manner (Gifford and Ashby, 1996). However, in vivo administration of cannabinoid compounds reveals contradictory results. The administration of Δ9-THC or the synthocannabinoid WIN55,212-2 reduces hippocampal ACh release (Gessa et al., 1997; Mishima et al., 2002a; Pisanu et al., 2006). Other authors report increased rates of ACh release by cannabinoid agonists (Acquas et al., 2001). Interestingly, cannabinoid agonists, in a dose-dependent manner, trigger biphasic effects on functional responses (Margulies and Hammer, 1991), cortical evoked potentials (Turkanis and Karler, 1981), locomotion (Davis, W. M., Moreton, King and Pace, 1972) and on the CB_1 receptor-mediated release of ACh (Tzavara et al., 2003). This study shows that a low dose of WIN55,212-2 (0,5 mg/kg) induces a transient stimulation, whereas a higher dose (5 mg/kg) triggers persistent inhibition of hippocampal ACh release, probably involving dopamine D_1 and D_2 receptors.

On the other hand, the cholinergic agonist carbachol transiently suppresses inhibitory synaptic transmission in CA1 pyramidal cells in a CB_1 receptor activation-dependent manner (Kim et al., 2002). The mAChR-driven eCB-mediated STD is also found in hippocampal excitatory synapses and in striatal inhibitory synapses, leading to the phenomena of DSE and DSI, respectively (Narushima et al., 2007; Straiker and Mackie, 2007).

CB_1 receptor-mediated LTD dependent on mAChR stimulation has been described in both inhibitory synapses (Younts and Castillo, 2014), and excitatory synapses (Zhao and Tzounopoulos, 2011). A recent study provides evidence of a 2-AG mediated LTD of glutamatergic synaptic transmission in the prefrontal cortex induced by specific stimulation of M_1 mAChR, since it is abolished by selective M_1 mAChR antagonism (Martin et al., 2015). The above-mentioned findings represent different examples of the crosstalk between eCB and cholinergic systems, which reveal the CB_1 receptor-mediated short- and long-term cholinergic synaptic plasticity.

5.2. CB_2 receptor

In 1993 the second subtype of cannabinoid receptors, named the CB_2 receptor was identified (Munro et al., 1993). A human cDNA cloning revealed that it is a GPCR consisting of 360 amino acids, located in chromosome 1p35-p36 and that it shares a 44% homology with the human CB_1 receptor. It was subsequently cloned in several mammalian species, including mouse (347 amino acids) (Shire et al., 1996) and rat (410 amino acids) (Brown et al., 2002).

CB_2 receptors are widely distributed in peripheral tissues, and particularly in immune system cells. CB_2 mRNA has been identified in many immune tissues displaying the highest levels in macrophages, CD4+ T cells, CD8+ T cells, B cells, natural killer cells, monocytes and polymorphonuclear neutrophils. Interestingly, CB_2 mRNA has been found in CNS microglia, regulating its migration (Walter et al., 2003), with variations in CB_2 receptor level expression depending on the state of activation of the cell in response to specific damage such as neurodegenerative processes (Ashton and Glass, 2007). However, CB_2 receptors can be detected in neuritic plaque-associated microglia in AD brain tissue (Benito et al., 2003). In addition, there is molecular and pharmacological evidence of the distribution of CB_2 receptors in several tissues including pulmonary endothelial cells, bone tissue, the gastrointestinal system, mouse spermatogonias, mature and precursor adipocytes, cirrhotic liver, cardiomyocytes, pancreas and spleen (Atwood and Mackie, 2010).

In summary, the distribution of CB_2 in the CNS remains controversial. In addition to its expression in the microglia under particular circumstances, exists pharmacological and physiological evidence of its presence in astrocytes (Sanchez et al., 2001), brainstem neurons (Van Sickle et al., 2005) and in culture neurons of Purkinje and granular cells of mice cerebellum (Skaper et al., 1996), as well as in neural progenitor cells (Palazuelos et al., 2006). The presence of CB_2 receptors in the CNS at detectable and functionally relevant levels has been detected in rodent and human whole brain, brainstem, cerebellum, cortex, hippocampus, thalamus, olfactory bulb, thalamic nuclei and in several additional brain regions (Atwood and Mackie, 2010). Interestingly, recent work also indicates that CB_2 receptors expressed in neurons modulate the rewarding sensations obtained from cocaine (Xi et al., 2011; Bystrowska et al., 2018), and mediate hippocampal synaptic function (Stempel et al., 2016). Although, no clear evidences for CB_2 expression in the healthy CNS have been found, an up-regulation of this receptor in the context of amyloid-triggered neuroinflammation has been reported (Lopez, A. et al., 2018).

5.3. Endocannabinoids

Lipid signaling molecules (neurolipids) are emerging as key modulatory elements in CNS neurotransmission in which GPCR for multiple neurolipid systems are being identified. Lipids represent the main structural components of the cell membranes, but some phospholipid species present in the membranes of neurons, glia and other cells may serve as precursors for the synthesis of neurolipids, such as the eCB. The eCB are defined as endogenous compounds, generated by different tissues and organs, capable of binding to and activate cannabinoid receptors. They are synthesized through cleavage of phospholipid precursors and may be released on demand when evoked by postsynaptic depolarization or GPCR activation (Di Marzo et al., 1994; Maejima et al., 2001).

AEA and 2-AG

AEA belongs to the family of the N-acylethanolamines, which are biosynthesized via a membrane phospholipid-dependent pathway, i.e. the enzymatic hydrolysis of the corresponding N-acyl-phosphatidylethanolamines (NAPE) by a phospholipase D selective for NAPE (NAPE-PLD) (Hansen et al., 1998). Although most of the neurotransmitters are water-soluble and require specific TM proteins to transport them across the cell membrane, the eCB are non-charged lipids that readily cross lipid membranes and it is reasonable to hypothesize that there is no need for an eCB carrier. However, several structural analogs of AEA have been reported to inhibit the AEA uptake (Beltramo et al., 1997). Nevertheless, AEA transport meets four key criteria of a carrier-mediated process: saturability, fast rate, temperature dependence and substrate selectivity (Freund et al., 2003). The uptake of AEA does not require cellular energy or external Na^+, suggesting that it is mediated through facilitated diffusion and its immediate intracellular hydrolyzation probably contributes to the rate of AEA transport. To date, four models have been proposed: 1) AEA uptake occurs by facilitated diffusion through a membrane carrier; 2) AEA crosses the membrane by enzyme-mediated cleavage of AEA; 3) AEA undergoes endocytosis through a caveolae-related uptake process; 4) Simple diffusion driven by intracellular sequestration of AEA (Di Marzo, 2008).

The enzymatic degradation of AEA was first reported in neuroblastoma and glioma cells as anandamide amidase (Deutsch and Chin, 1993). Later it was identified as anandamide amidohydrolase in the brain, and finally renamed as fatty acid amide hydrolase (FAAH) when purified and cloned from rat liver (Cravatt et al., 1996). Rat, mouse, and human FAAH proteins are all 579 amino acids in length. The FAAH gene was mapped to human chromosome 1p34-p35. FAAH is detected in many organs including brain and recognizes a variety of fatty acid amides, but its preferred substrate is AEA. FAAH also catalyzes the hydrolysis of the ester bond of 2-AG

in vitro. FAAH-knockout mice exhibit an increased responsiveness to exogenous administration of AEA, further demonstrating the direct involvement of FAAH in AEA degradation (Cravatt et al., 2001).

The levels of 2-AG in tissues, cells or cerebrospinal fluid (CSF) are usually much higher than those of AEA, and may be sufficient to permanently activate cannabinoid receptors (Sugiura et al., 1995). Similarly to AEA, the enhancement of intracellular Ca^{2+} induces the synthesis of 2-AG. The most important biosynthetic precursors of 2-AG are the sn-1-acyl-2-arachidonoylglycerols (DAG) from membrane phospholipids.

The main enzyme responsible for the degradation of 2-AG is the monoacylglycerol lipase (MAGL) identified by Tornqvist and Belfrage (1976) (Dinh et al., 2002). The MAGL was cloned from a mouse adipocyte cDNA library (Karlsson et al., 1997). Several studies suggest the existence of additional 2-AG hydrolyzing enzymes in brain microglial cells (Muccioli and Stella, 2008).

The mechanism for 2-AG uptake is also unclear. Some studies propose that that 2-AG and AEA are transported by the same system (Piomelli et al., 1999; Bisogno et al., 2001). Evidence for this assumption is that cold 2-AG prevents [^{3}H]-AEA uptake, suggesting that both eCB may compete for the same transport system. AEA and 2-AG also share similar kinetic properties, and their transport is inhibited by AM404, (Freund et al., 2003).

5.4. Synthocannabinoid agonists

Synthetic cannabinoids (SC) are a heterogeneous group of compounds developed to probe the endogenous cannabinoid system or as potential therapeutics (Wiley et al., 2014). The majority of SC detected in herbal products display a greater binding affinity for the cannabinoid CB_1 receptor than the Δ9-THC. Δ9-THC is the primary psychoactive compound in the cannabis plant, with greater affinity for the CB_1 than for the CB_2 receptor. *In vitro* and animal *in vivo* studies show that the pharmacological effects of the SC are 2-100 times more potent than Δ9-THC, including analgesic, anti-seizure, weight-loss, anti-inflammatory, and anti-cancer growth effects. SC produce physiological and psychoactive effects similar to Δ9-THC, but with greater intensity, resulting their abuse in medical and psychiatric emergencies (Castaneto et al., 2014).

Synthetic cannabinoid agonists or synthocannabinoids can be divided into four groups according to their chemical structures. The first group (classical cannabinoids) involves dibenzopyran derivatives that are both natural constituents of cannabis (e.g., Δ9-THC and Δ8-THC) and their synthetic analogues (HU 210). The first generation of classical cannabinoids

lacked CB_1/CB_2 receptor selectivity, as they were synthesized by inducing minor modifications of the Δ9-THC molecule. CB_2 receptor-selective agonists such as JWH-133 and HU-308 were also modified from Δ9-THC (Huffman et al., 1996; Hanus et al., 1999). The second group (non-classical cannabinoids) was developed as bicylic and tricyclic analogues of Δ9-THC, lacking the pyran ring (Melvin et al., 1993). This group includes CP55,940, which binds to both CB_1 and CB_2 receptors with a similar affinity. CP55,940 is a full agonist for both receptor types and significantly contributed to both the *in vitro* and *in vivo* pharmacological characterization of CB_1 receptors. The third group of cannabimimetic compounds consists of the aminoalkylindoles. This series is represented by WIN55,212-2 which also displays a high affinity for both cannabinoid receptors. Some of these aminoalkylindoles, such as JWH-015, display significant selectivity for the CB_2 receptors (Showalter et al., 1996). The prototype of the fourth eicosanoid group, which involves arachidonic acid derivatives, is AEA, the first eCB isolated from mammalian brain (Devane et al., 1992). Some examples of eicosanoid-based cannabinoid agonists are AM356, arachidonyl-2´-chloroethylamide (ACEA) and arachidonylcyclopropyl-amida (ACPA).

Some synthetic agonists display more selectivity for the CB_1 receptor subtype including (+)-methanandamide, ACEA and ACPA. Examples of the CB_2 receptor-selective agonists most frequently used are JWH-133, HU-308, JWH-015 and AM-1241 (Pertwee, 2008).

5.5. Synthocannabinoid antagonists

The first specific cannabinoid antagonist developed and pharmacologically characterized was SR141716A (Rinaldi-Carmona et al., 1994). It blocks the actions of various cannabinoid agonists both *in vitro* and *in vivo* (Kano et al., 2009). This compound is a pure antagonist at nanomolar concentrations but it is not CB_1 receptor-specific and it blocks both CB_1 and CB_2 receptors (Pertwee, 1999). It displays inverse agonism under certain experimental conditions. Two analogues of SR141716A have also been developed, AM251 and AM281 (Howlett, 2002). Some selective antagonists for CB_2 receptors are SR144528, AM630 and surinabant, which display considerably more affinity for CB_2 receptors than for CB_1 receptors (Rinaldi-Carmona et al., 1998). However, most of the pharmacodynamic features were studied in cell cultures overexpressing CB_2 receptors, but not by using *in vivo* experiments. One *in vivo* experiment on cannabinoid-induced antinociception demonstrated that low doses of both SR141716A and SR144528 contributed to prolonging and enhancing pain induced by tissue damage, which indicates that peripheral CB_1 and CB_2 receptors are participating in the intrinsic control of pain (Calignano et al., 1998).

6. Endocannabionid system in AD

The eCB system has provided a strong rationale for research in therapeutic targets for autoimmune diseases, stroke and some other severe neurodegenerative diseases, including Alzheimer's disease (AD). An increasing number of studies in the recent years suggest the involvement of the endocannabinoid system in the regulation of Aβ clearance, oxidative stress, ACh homeostasis and inflammation processes occurring during AD progression (Lopez, J. A. et al., 1990). In this context, the eCB system becomes profoundly altered, with modifications ranging from changes in anandamide (AEA) and 2-arachidonoylglycerol (2-AG) levels to modulations in the expression pattern of their regulatory enzymes and of cannabinoid receptors (Fernandez-Ruiz et al., 2015). Data obtained from human *postmortem* samples from AD patients suggest that the eCB system is modulated during the course of disease.

Westlake and colleagues analyzed both the mRNA expression for CB_1 receptors and [^{3}H]CP55,940 binding in *postmortem* brain samples from AD patients (Westlake et al., 1994). [^{3}H]CP55,940 binding was reduced in cortex, but no alterations in levels of CB_1 mRNA expression were observed in comparison with aged-matched controls. Although [^{3}H]CP55,940 binding was reduced, it was not selectively associated with AD-pathology and failed to dissociate changes in CB_1 receptor expression from normal aging. Other research groups found that both cortical and hippocampal CB_1 receptor levels remain unaltered in AD (Benito et al., 2003). In contrast, other authors reported decreased levels of highly nitrosylated CB_1 receptor expression in cortical areas containing activated microglia (Ramirez et al., 2005). Furthermore, autoradiographic studies using the selective CB_1 receptor radioligand, [^{125}I]SD7015, revealed increased levels of CB_1 receptor expression in the frontal cortex in the early stages of AD (Braak I-II), and a decline during the later stages (Braak V-VI), which indicates that CB_1 receptor density inversely correlate with Braak tau pathology (Farkas et al., 2012). A recent detailed autoradiographic study showed increased levels of [^{3}H]CP55,940 binding in the frontal cortex during the middle stages of AD (Braak III-IV), but no changes in the early stages (Manuel et al., 2014). Increased CB_1 receptor activity during the initial stages of AD might be an indication of neuroprotective mechanisms mediated by eCB signaling in response to initial neuronal damage. Finally, no changes in CB_1 receptor levels were found by immunoblotting and receptor binding in human brain samples (Lee, J. H. et al., 2010). An *in vivo* study conducted in 11 patients with AD and 7 healthy volunteers by using the specific radiotracer, [^{18}F]MK-9470, for positron emission tomography (PET) of CB_1 receptors, found no significant differences in CB_1 receptor availability in any of the brain regions studied (Ahmad et al., 2014).

The analysis of CB_2 receptors in human samples from AD patients by immunohistochemistry revealed the absence of signal for CB_2 receptors in brains of the control group (with a limited presence in a subset of microglial cells such as the perivascular microglia), but an intense level of staining in AD samples (Benito et al., 2003). In addition, increase of CB_2 receptors have been found in brain tissue samples from AD patients, which seem to be associated with the activation of the microglia surrounding senile plaques (Ramirez et al., 2005). These results suggest a positive correlation with the density of the glial fibrilar acidic protein (GFAP) marker for astrocytes and senile plaques, but not with the cognitive status (Solas et al., 2013).

Moreover, FAAH density and activity is significantly increased and is associated with the overexpression of glial CB_2 receptors, which probably contributes to inflammatory processes by increasing arachidonic acid as a consequence of the increased AEA metabolism in senile plaque enriched brain areas (Benito et al., 2003). Similarly to what has been observed in CB_1 receptor studies, the literature fails to report consistent results related to the regulation of eCB metabolism in AD. The increased levels of FAAH in AD brains support the idea that eCB and/or their precursors could be regulated in some way. Some studies reported decreased brain, but not plasmatic, levels of AEA and its precursor NArPE in cortical regions from AD patients, which positively correlated with cognitive deficiencies and, inversely, with senile plaque pathology, suggesting a possible involvement of AEA deregulated metabolism in cognitive dysfunction (Koppel et al., 2009; Jung et al., 2012). In these studies no alterations were observed in the levels of 2-AG in brain samples from AD patients. However, Mulder et al. (2011) reported that 2-AG-mediated signaling in the late stages of AD was deregulated in *postmortem* brain samples. The increased expression of DAGL-α, together with the decreased activity of MAGL and ABHD6, could contribute to 2-AG signaling-mediated synapse silencing. The absence of altered eCB plasmatic levels means that we cannot consider them as plasmatic biomarkers for AD.

6.1. Preclinical evidence for the therapeutic potential of cannabinoids in AD

Clinical data modestly support the beneficial effects of nabilone or dronabinol (cannabinoid agonist analog of Δ9-THC). These treatments during several weeks showed a significant reduction in agitation and aggression refractory to antipsychotics and anxiolytics, together with weight gain in individuals previously rejecting food, although no reduction in other neuropsychiatric symptoms was observed. One clinical trial including 15 AD patients resulted in a decrease in the severity of altered behavior after 6 weeks of dronabinol treatment, with its side effects limited to euphoria and somnolence (Volicer et al., 1997). Further clinical trials including eight patients with dementia reported a reduction in nighttime agitation and behavioral disturbances, without adverse effects during the trial periods with dronabinol (Walther et al., 2006; Walther et al., 2011). Moreover, the administration of nabilone to an advanced AD patient who was refractory to antipsychotic and anxiolytic medications, promptly and significantly improved the agitation and aggressiveness (Passmore, 2008). However, no evidence of cannabinoid-based improvement of dementia has yet been observed (Krishnan et al., 2009). Recently, a clinical trial with Δ9-THC in 24 patients with dementia and relevant neuropsychiatric symptoms, revealed the absence of side and/or beneficial effects after its daily oral administration for 3 weeks, suggesting that higher doses could be efficacious and equally well tolerated (van den Elsen, G A et al., 2015). Equally important is the almost total absence of side effects observed during treatment with Δ9-THC in these patients, and beyond a certain euphoria, drowsiness or fatigue (Volicer et al., 1997; van den Elsen et al., 2015; van den Elsen et al., 2017).

Cannabinoids are compounds with a broad spectrum of effects, which makes them suitable to target the multiple pathological features that characterize neurodegenerative diseases. Preclinical studies provide evidence to support the potential of cannabinoid pharmacology for the treatment of these diseases.

Objectives

The basal forebrain cholinergic system is severely affected in Alzheimer's disease and is responsible for most of the clinical alterations in learning and memory processes. The loss of cholinergic neurons and muscarinic receptors in the nucleus basalis of Meynert has been reported in Alzheimer's disease. The treatments with inhibitors of AChE approved for Alzheimer's disease enhance the cholinergic tone as symptomatic therapy. On the other hand, endocannabinoid signaling is also altered during the progression of Alzheimer's disease. The endocannabioid system modifies learning and memory processes and is a neuromodulator of the basal forebrain cholinergic system. Cannabinoid receptor activation modulates the release of ACh but there are controversial reports regarding the cannabinoid effects in learning and memory processes.

The research on new experimental animal models of Alzheimer's disease and in new drugs in preclinical and clinical stages is contributing to the development of new treatments to slow down the progression of the Alzheimer's disease, but with little success. Therefore, the aim of this Thesis was to investigate in a new treatment based on activation of the cannabinoid system to improve the clinical symptoms of Alzheimer's disease. The objectives of the present study are:

1. To evaluate the effects on the spatial and aversive memory of rats after specific lesion of the nucleus basalis magnocellularis by intraparenchymal administration of 192IgG-saporin (model of basal forebrain cholinergic lesion), using the Barnes Maze and Passive Avoidance tests respectively, and to analyze the cannabinoid and cholinergic systems by histochemical and autoradiographic studies.

2. To examine the effect of a low dose of WIN55,212-2 (0.5 mg/kg) administration in learning and memory processes in a pharmacological model of cholinergic antagonism by Barnes Maze and Passive Avoidance tests, and to analyze the cannabinoid and cholinergic system by histochemical and autoradiographic studies. Furthermore, to study the possible bias of the cognitive behavior by the analgesic effects of the treatment by both hot plate and electrical shock-evoked pain threshold test.

3. To analyze the effect of sub-chronic intraperitoneal administration of WIN55,212-2 at a dose of 0.5 mg/kg in learning and memory using the rat model of basal forebrain cholinergic lesion, and study the cannabinoid and cholinergic system in their brains.

4. To evaluate the CB_1 cannabinoid receptor-mediated specificity of the effect in spatial and aversive memory by co-administration of WIN55,212-2 together with SR141716A, a cannabinoid antagonist, at the same dose (0.5 mg/kg) in the rat model of basal forebrain cholinergic lesion, and study the cannabinoid and cholinergic system in their brains.

5. To explore the dose-dependency of the effect at high doses of WIN55,212-2 (3 mg/kg) in spatial and aversive memory in the rat model of cholinergic lesion, and to study the cannabinoid and cholinergic system in their brains.

6. To evaluate the effect in spatial and aversive memory of SR141716A at a dose of 0.5 mg/kg in learning and memory in a model of basal forebrain cholinergic lesion in Barnes Maze and Passive Avoidance test respectively and to analyze the activity and density of muscarinic and cannabinoid receptors by autoradiography.

Animals, material and methods

1. Animals

1.1. Sprague-Dawley rats

A total of 225 adult male Sprague-Dawley rats weighing 200-250 g were used in the present study. Rats were housed four or five per cage (50 cm length x 25 cm width x 15 cm height) at a temperature of 22°C and in a humidity-controlled (65%) room with a 12:12 hours light/dark cycle, with access to food and water *ad libitum.* These type of animals were used for all treatments including the *in vivo* administration of 192IgG-saporin followed by behavioral tests, histochemical, immunohistochemical and autoradiography assays. The number of animals used in each procedure and treatment is detailed later in the treatments section (Table 2). Every effort was made to minimize animal suffering and to use the minimum number of animals. All procedures were performed in accordance with European animal research laws (Directive 2010/63/EU) and the Spanish National protocols were approved by the Local Ethical Committee for Animal Research of the University of the Basque Country (CEEA 388/2014).

2. Materials

2.1.Reagents

192IgG-saporin (Batch 2441969) was acquired from Millipore (Temecula, CA, USA). [^{3}H]CP55,940 (131.8 Ci/mmol), [^{3}H]-N-methyl scopolamine (81 Ci/mmol) and [^{35}S]GTPγS (1250 Ci/mmol) from PerkinElmer (Boston MA, USA). The [^{3}H]-microscales and [^{14}C]-microscales used as standards in the autoradiographic experiments were purchased from ARC (American Radiolabeled Chemicals, Saint Louis, MO, USA). The β-radiation sensitive films, Kodak Biomax MR, bovine serum albumin (BSA), DL-dithithreitol (DTT), adenosine deaminase (ADA), guanosine 5'-diphosphate (GDP), guanosine5'-O-3-thiotriphosphate (GTPγS), ketamine, xylazine, acetylthiocholine iodide were all acquired from Sigma-Aldrich (St Louis, MO, USA). The compounds necessary for the preparation of the different buffers, the fixation and the treatment of slides were of the highest commercially available quality for the purpose of our studies.

2.2. Drugs

(-)-*cis*-3-[2-Hydroxy-4-(1,1-dimethylheptyl)phenyl]-*trans*-4-(3-hydroxypropyl)cyclohexanol (**CP55,940**), (α,*S*)-α-(Hydroxymethyl)benzeneacetic acid (1α,2β,4β,5α,7β)-9-methyl-3-oxa-9-azatricyclo[3.3.1.02,4]non-7-yl ester hydrobromide (**Scopolamine**), (2-Hydroxyethyl)trimethylammonium chloride carbamate (**Carbachol**) were acquired from Sigma-Aldrich; (R)-(+)-[2,3-Dihydro-5-methyl-3[(4-morpholinyl)methyl]pyrrolo[1,2,3-de]-1,4-benzoxazinyl]-(1-naphthalenyl)methanone mesylate (**WIN55,212-2**), 5-(4-Chlorophenyl)-1-(2,4-dichlorophenyl)-4-methyl-N-1-piperidinyl-1H-pyrazole-3-carboxamide hydrochloride (**SR141716A**) from Tocris (Bristol, UK).

TABLE 1. Functions of the drugs used in all procedures

Drug	Function
CP55,940	CB_1 and CB_2 agonist
WIN55,212-2	CB_1 and CB_2 agonist
SR141716A	CB_1 antagonist
Carbachol	M_1-M_5 agonist
Scopolamine	M_1-M_5 agonist

3. Methods

3.1. Behavioral studies

BARNES MAZE (BM)

Equipment

The BM is a behavioral test that was originally developed by Carol Barnes to study spatial memory in rats (Barnes, 1979). The maze is a white circular platform (130 cm of diameter) elevated one meter above the floor containing 20 equally spaced holes (10 cm diameter, 2.5 between holes). Only one hole lead to dark chamber located under the target hole named "scape box". Two bright lights (400 W) were around de platform. To stimulate de spacial memory of the rat, visual cues (circle, rectangle, triangle and square with different colors and textures) enclosing the room were used. To analyze all the parameters of the animal Smart 3.0 software (Panlab Harvard apparatus, Barcelona, Spain) was used.

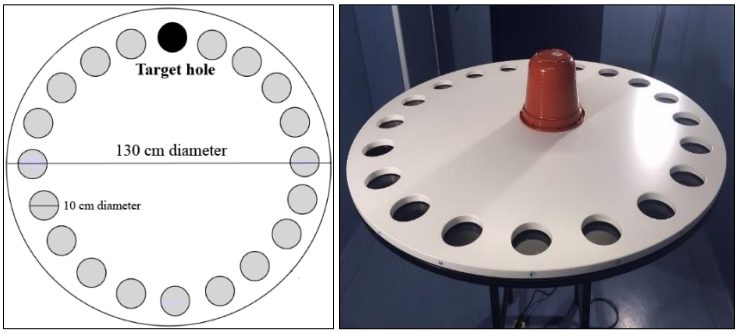

Figure 1. A scheme and real photo of the Barnes maze used is shown. The initial box, where the animal is introduced, is shown in the middle of the maze.

Procedure

Adaptation period. During the adaptation period, the rat was placed in a cylindrical start chamber, initial box, in the middle of the maze. The initial box was removed after a minute to start with the adaptation period. The animal was gently guided to the target hole (each rat had its own preselected hole). The rat must stay in darkness in the scape box for a minute.

Spatial acquisition. Before the acquisition phase beginning, the maze was cleaned using a 10 % ethanol solution. (This action was done after each animal was removed from the maze). Then, the rat was placed in the initial box in the middle of the maze. After a minute, the initial box was removed and the rat was allowed to explore the maze for 3 minutes. During this time, the following parameters were measured: total latency (time spent by each animal to found the target hole), total path length (distance covered by each animal to found the target hole) and speed (mean speed of

each animal till the target hole was found). The trial finished when the animal entered into the target hole or after 3 min had elapsed. If the animal did not reach the goal within 3 minutes, it was gently guided to the escape box where remained for 1 min. Finally, the rat was placed in its home cage until the next trial. Animals conducted 4 trials per day with an inter-trial interval of 15 minutes during 4 days. The interval of 15 minutes was used to test another 4 to 5 animals.

Probe trail. On day 5, 24 h after the last training day, the probe trial was performed with the target hole closed. Firstly, the animal was placed for a minute in the initial box in the middle of the maze. After a minute the initial box was lifted to release the animal that was allowed to explore the maze for 3 minutes. During this probe trial the time spent in each quadrant was also measured (the maze was divided in four quadrant: target, positive, negative and opposite). Finally, the rat was placed in its home cage.

All the procedures were analyzed by SMART 3.0 video tracking software.

PASSIVE AVOIDANCE (PA)

Equipment

The passive avoidance apparatus for rats consists of two methacrylate compartments separated by a guillotine door. The first compartment is large, white, illuminated an open-topped: 31 cm (W) x 31 cm (D) x 24 cm (H), and the other is small, dark and closed: 19.5 cm (W) x 10.8 cm (D) x 12 cm (H).

Figure 2. PanLab passive avoidance box LE870 used shown.

Procedure

Acquisition phase. Each animal was gently placed in the illuminated compartment with is head facing the closed door and allowed to explore it for 30 sec. Then, the guillotine door automatically opened and the animal was allowed to enter in the dark compartment for 60 sec. When the animal entered in the dark compartment the guillotine door was closed, then a foot shock (0.4 mA/2 sec) was delivered. 10 sec after the foot shock, the animal was given back to its home cage. The acquisition latency was measured (time spent for each animal to enter into the dark

compartment). The animals that did not enter in the dark compartment were removed from the study.

Retention phase. 24 h after the acquisition session, the retention session was performed. The animals were placed again in the white compartment and allowed to explore for 30 sec. Then, the guillotine-door was opened allowing the animal to enter in the dark compartment. The step-through latency was measured (time necessary to enter into the dark compartment during the retention phase) up to a maximum cut-off time of 300 sec. No foot shock was delivered in the retention session.

HOT PLATE

Equipment

Hot plate apparatus (Leica Scientific Instruments, Figure 3), consist in a cylindrical see-through plexiglass wall (19 cm x 30 cm) located above a plate. It heats up through an electric resistance and is equipped with a timer and a thermostat. On the top of the cylinder a metal grating to hold the animal when it jumps is put.

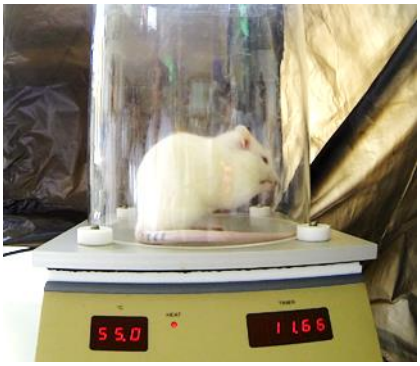

Figure 3. The hot plate apparatus LE 7406 used is shown.

Procedure

Animals were placed in the metal plate that was warmed previously (55 ± 0.5 °C). Then, the time spent by the animal till jumping was recorded (jump latency). The parameter of latency to start licking paws was also measured.

ELECTRICAL SHOCK EVOKED PAIN THRESHOLD

Equipment

The white compartment (31 cm (W) x 31 cm (D) x 24 cm (H)) of PA was used. This compartment has a grid floor and electrical footshocks of different potency can be delivered.

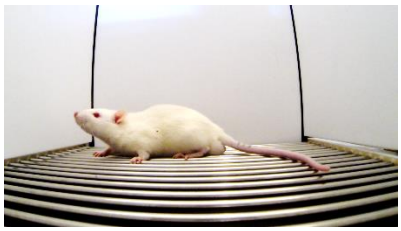

Figure 4. The white compartment of PanLab passive avoidance box used is shown.

Procedure

Rats were placed in the white compartment and received a gradual intensity electrical footshock beginning at 0.0 mA, and ending as soon as the animal showed discomfort. The time spent to first vocalization was measured.

3.2. Animal models

Pharmacological model of muscarinic antagonism in rat

The scopolamine was dissolved in saline 0.9 % and was administered intraperitoneally (2 mg/kg) in a volume of 10 ml/kg, thirty minutes before the BM probe trial and PA acquisition session.

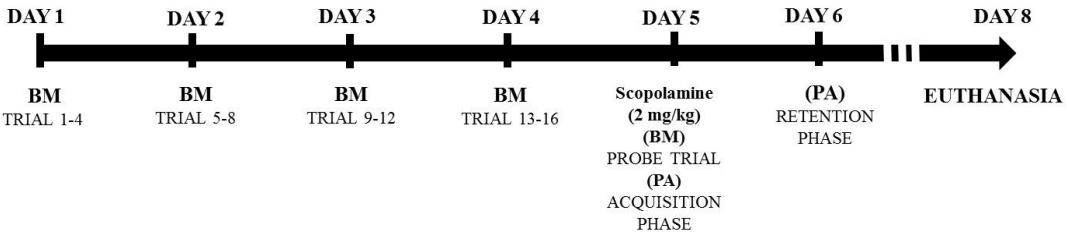

Figure 5. Synopsis of the experimental design showing the behavioral schedule in a pharmacological model of muscarinic antagonist.

Model of basal forebrain cholinergic lesion in rat

192IgG-saporin is commonly used to selectively depletion BFCN in the B. The controls of the lesion were two groups, the sham-operated rats (SHAM) and the administration of artificial cerebrospinal fluid as vehicle following the same stereotaxic coordinates (CONTROL). 192IgG-saporin administered rats were named as LESION group. Rats were randomly assigned to one of three groups. The vehicle was prepared mixing 0.15 M NaCl, 2.7 mM KCl, 0.85 mM $MgCl_2$ (pH 7.4) and sterilized by filtration with 0.4 µm-Ø filters (EMD Millipore, CA, USA). Rats were anesthetized with ketamine/xylazine (90/10 mg/kg; s.c.) and then place in stereotaxic instrument (kopf, Tujunga, CA). After an incision was made in the skin along the midline of the skull, two holes were practiced. A 10-µl Hamilton syringe (Neuros^{TM} syringe, 1701RN; Bonaduz, Switzerland) with a 0.210 mm diameter needle was carefully used to minimize brain damage. The intraparenchymal infusions were made into the B: - 1.5 mm anteroposterior from Bregma, ± 3 mm mediolateral from midline, + 8 mm dorso-ventral from the cranial surface (Paxinos and Watson, 2005). 192IgG-saporin was dissolved in vehicle under aseptic conditions to a final concentration of 130 ng/µl. Vehicle or 192IgG-saporin was bilaterally administered (1 µl/hemisphere) at a constant rate of 0.2 µl/min. The needle was kept in for 5 min before carefully removal during another 5 min to avoid a possible backflow and to allow complete diffusion. During surgery, the body temperature was controlled and the eyes were kept hydrated with warm saline

solution (0.9 % NaCl). After the administration ends, the wounds were closed with braided silk sutures and a broad-spectrum intramuscular antibiotic (2.25 mg/kg oxytetracycline) injection was given. The rats were allowed to recover from surgery for seven days. On day eight started with BM and consecutively PA test to evaluate the learning and memory of these animals before the dissection of the brain for use in the neurochemical studies.

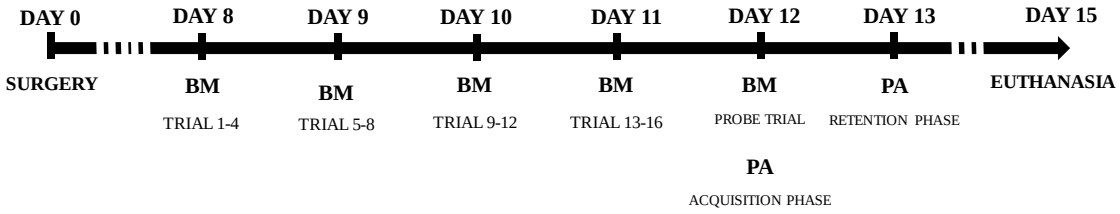

Figure 6. Synopsis of the experimental design showing surgery and behavioral schedule in a model of basal forebrain cholinergic lesion.

3.3. Treatments

WIN55,212-2 administration in a pharmacological model of muscarinic antagonism

WIN55,212-2 was intraperitoneally administered once daily (0.5 mg/kg), one hour before every BM trial started, for four consecutive days, the fifth day before the probe trial the animals received one dose of WIN55,212-2 and one dose of scopolamine (Figure 7, Table 2). WIN55,212-2 was dissolved in pure DMSO and diluted with kolliphor EL (Sigma-Aldrich) and 0.9 % saline to a proportion of (1:1:18), as vehicle. The effects of vehicle and WIN55,212-2 without scopolamine were tested in both test.

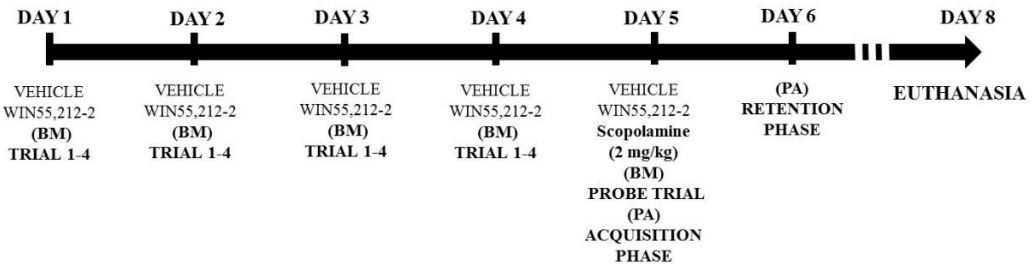

Figure 7. Synopsis of the experimental design showing the treatment schedule with scopolamine and WIN55,212-2, behavioral tests and euthanasia in a pharmacological model of muscarinic antagonism.

WIN55,212-2 and/or SR141716A administration in a model of basal forebrain cholinergic lesion

WIN55,212-2 and/or SR141716A were intraperitoneally administered once daily, one hour and half an hour, respectively, before BM trials started, for five consecutive days (Figure 8, Table 2). Both drugs were dissolved in pure DMSO and diluted with kolliphor EL (Sigma-Aldrich) and 0.9 % saline to a proportion of (1:1:18) as vehicle. The group of animals with vehicle administration was also analyzed in both tests.

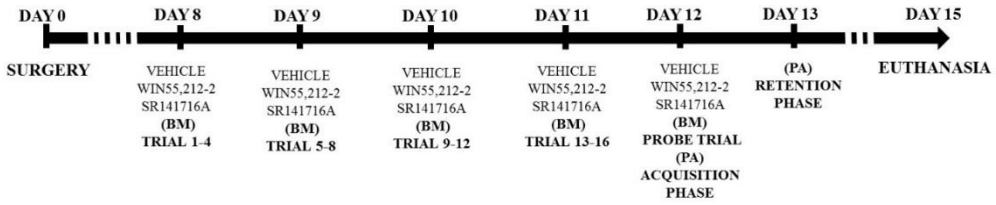

Figure 8. Synopsis of the experimental design showing the treatment schedule with WIN55,212-2 and/or SR141716A, behavioral tests and euthanasia in the model of basal forebrain cholinergic lesion.

Table 2. Summary of all treatments and/or lesion procedures. The number of animals used in each experimental group is indicated.

Experimental Group	Treatment	N
SHAM	Sham-operated	7
CONTROL	Artificial cerebrospinal fluid administration (CSF)	33
LESION	Toxine administration disolved in CSF (T)	55
CONTROL+W0.5	CSF + WIN55212-2 (0.5 mg/kg)	12
LESION+W0.5	T + WIN55212-2 (0.5 mg/kg)	12
LESION+W+SR	T + WIN55212-2 + SR141716A (0.5 mg/kg)	9
CONTROL+SR	CSF + SR141716A (0.5 mg/kg)	10
LESION+SR	T + SR141716A (0.5 mg/kg)	9
CONTROL+W3	CSF + WIN55212-2 (3 mg/kg)	8
LESION+W3	T + WIN55212-2 (3 mg/kg)	8
VEHICLE	VEHICLE	21
WIN55,212-2	WIN55212-2 (0.5 mg/kg)	21
SCOPOLAMINE	VEHICLE + SCOPOLAMINE (2 mg/kg)	10
WIN+SCOP	WIN55,212-2 (0.5 mg/kg) + SCOPOLAMINE (2 mg/kg)	10
TOTAL		**225**

WIN55,212-2 and SR141716A were administered daily for five consecutive days.

3.4. Tissue preparation

All animals used in the present study were anesthetized with ketamine/xylazine (90/10 mg/kg; i.p.) and then sacrificed before the dissection of their brains.

Fresh tissue

Animals were sacrificed by decapitation after anesthesia. The brain samples were quickly removed by dissection (4° C), fresh frozen and kept at -80°C. Later they were cut into 20 µm slices and mounted onto gelatin-coated slices and stored at -25°C until used. These slices were used for the autoradiographic studies.

Fixed tissue

Animals were transcardially perfused via the ascending aorta with 50 ml warm (37°C), calcium-free Tyrode's solution (0.15 M NaCl, 5 mM KCl, 1.5 mM $MgCl_2$, 1 mM $MgSO_4$, 1.5 mM NaH_2PO_4, 5.5 mM Glucose, 25 mM $NaHCO_3$; pH 7.4) and 0.5% heparinized, followed by 4% paraformaldehyde and 3% picric acid in 0.1 M phosphatase buffer (4°C) (100 ml/100 g b.w.). Their brains were subsequently removed and post-fixed in the same fixative solution for 90 min at 4°C, and then were immersed in a cryoprotective solution of 20% sucrose in PB overnight at 4°C, and then tissue was frozen by immersion in isopentane and kept at -80°C. The brains were cut into 12 µm coronal slices using a Microm HM550 cryostat (Thermo Scientific) at -25°C and mounted onto gelatin-coated slides an finally stored at -25°C until used. These slices were used for immunohistochemical studies ($p75^{NTR}$ positive cells, AChE activity).

Different brain areas related with learning and memory processes were analyzed using both types of tissue, fixed or fresh frozen (Figure 9).

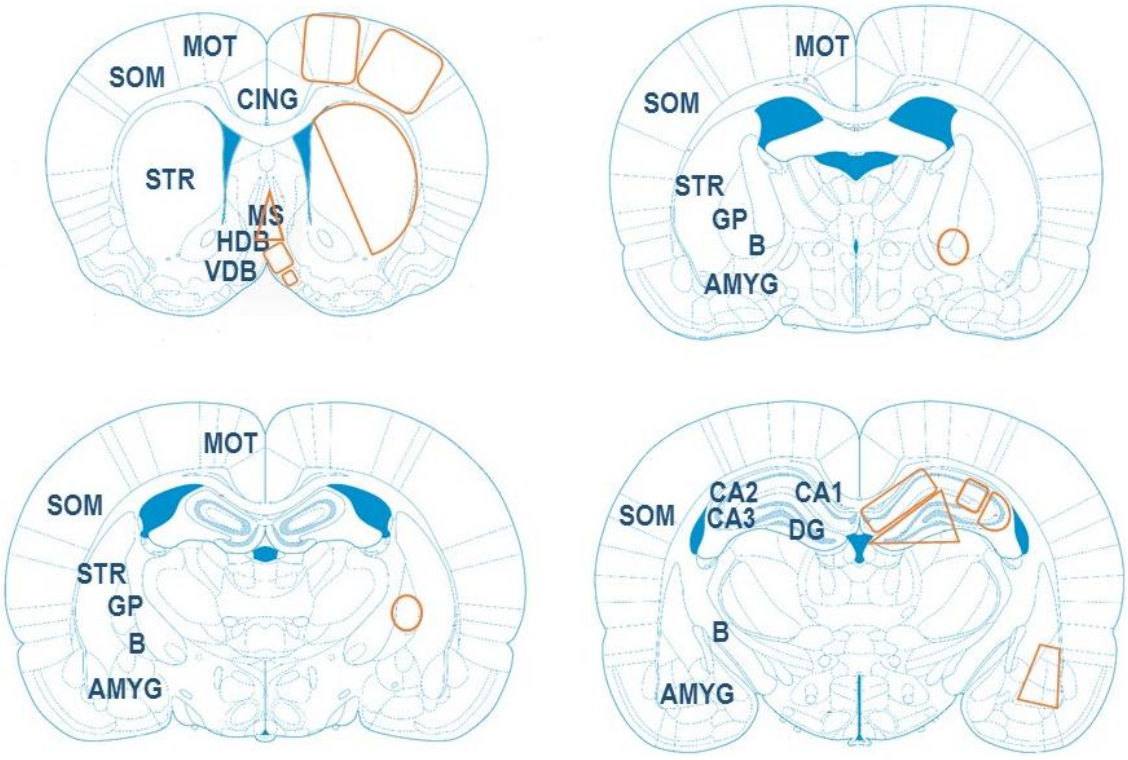

Figure 9. Coronal rat brain sections of Paxinos atlas. In the right part of every brain section is shown the name of the areas analyzed related with learning and memory processes, and in the left part it is shown the areas where the measurements were done (different nucleus of layers were analyzed inside of some of the areas). This general outline was followed in all the neurochemical studies. CING: cingulate, MOT: motor cortex (layers I-VI), SOM: Somatosensorial cortex (layers I-VI), STR: striatum, GP: Globus pallidus, SM: medial septum, B: nucleus basalis magnocellularis, HDB: horizontal diagonal band, VDB: vertical diagonal band, Hippocampus CA1: Oriens, pyramidal, radiatum; CA2: Oriens, pyramidal, radiatum; CA3: Oriens, pyramidal, radiatum; DG: dentate gyrus: Granular, molecular, polymorphic, AMYG: amygdala).

3.5. Autoradiographic studies

Labeling of activated $G\alpha_{i/o}$ proteins by the [^{35}S]GTPγS binding assay

Fresh 20 µm slices from all the animals groups were dried, followed by two consecutive incubations in HEPES-based buffer (50 mM HEPES, 100 mM NaCl, 3 mM $MgCl_2$, 0.2 mM EGTA and 0.5% BSA, pH 7.4) for 30 min at 30°C to remove the endogenous ligands. Briefly, slices were incubated for 2 h at 30°C in the same buffer but supplemented with 2 mM GDP, 1 mM DTT, adenosine deaminase (3-Units/l) and 0.04 nM [^{35}S]GTPγS. Basal binding was determined in two consecutive slices in the absence of the agonist. The agonist-stimulated

binding was determined in another consecutive slice with the same reaction buffer, but in the presence of the corresponding receptor agonists, WIN55,212-2 for CB_1/CB_2 receptors and carbachol for M_2/M_4 receptors. Non-specific binding was defined by competition with [^{35}S]GTPγS (10 µM) in another section. Then, slices were washed twice in cold (4°C) 50 mM HEPES buffer (pH 7.4), dried and exposed to β-radiation sensitive film with a set of [^{14}C] standards calibrated for ^{35}S.

Cannabinoid receptor autoradiography

Fresh 20 µm slices from all the animals groups were air-dried and submerged in 50 mM Tris-HCl buffer containing 1% of BSA (pH 7.4) for 30 min at room temperature to remove the endogenous ligands. They were then incubated in the same buffer but in the presence of the CB_1/CB_2 receptor radioligand, [^{3}H]CP55,940 (3 nM) for 2 h at 37°C. Non-specific binding was measured by competition with non-labeled CP55,940 (10 µM) in another consecutive slice. Then, slices were washed in ice-cold buffer to remove unbound radioligand (4°C). Autoradiograms were generated by exposure (4º C) of the tissues for 21 days to β-radiation sensitive films together with [^{3}H]-microscales used to calibrate the optical densities to fmol/mg tissue equivalent (fmol/mg t.e.).

Muscarinic receptor autoradiography

Fresh 20 µm slices from all the animals groups were air-dried and submerged in 50 mM phosphate buffer (pH 7.4) for 20 min to remove the endogenous ligands. They were then incubated in the same buffer but in presence of the M_1-M_5 receptor radioligand, [^{3}H]N-Methyl-scopolamine (1.5 nM) for 1 hour at room temperature. Non-specific binding was measured by competition with non-labeled scopolamine (1µM) in another consecutive slice. Then, slices were washed in ice-cold buffer (4°C). Autoradiograms were generated by exposure of the tissues for 40 days at 4°C to β-radiation sensitive films together with [^{3}H]-microscales used to calibrate the optical densities to fmol/mg tissue equivalent (fmol/mg t.e.).

3.6. Histochemical methods

Histochemistry for AChE detection in fixed and fresh tissue

Fresh slices from all experimental groups were air dried for 20 min at room temperature, post-fixed in 4% paraformaldehyde in PBS for 30 min at 4°C and washed in 0.1 M PBS, pH 7.4 (PBS) for 20 min. BFCN in the B and cholinergic innervations were stained using the "direct coloring" thiocoline method for AChE (karnovsky and Roots, 1964). The slices were rinsed twice in 0.1 M Tris-maleate buffer (pH 6.0) for 10 min and incubated in complete darkness, with constant and gentle agitation in the AChE reaction buffer: 0.1 M Tris-maleate; 5 mM sodium citrate; 3 mM $CuSO_4$; 0.1 mM iso-OMPA; 0.5 mM $K_3Fe(CN)_6$ and 2 mM acetylthiocholine iodide as reaction substrate. The incubation times were calculated from 30 min for optimal staining cholinergic somas in B to100 min for staining cholinergic fibers. Finally, the enzymatic reaction was stopped by two consecutive washes (2x10 min) in 0.1 M Tris-maleate (pH 6.0). Slices were then dehydrated in increasing concentrations of ethanol and covered with di-n-butyl phthalate in xylene (DPX) as the mounting medium. Finally, the stained slices were scanned at 600 ppi of resolution, the images were converted to 8-bit gray-scale mode and AChE positive fiber density was quantified by Image J software (NIH, Bethesda, MD, USA). The software measured the optical density of the tissues (O.D.) of each anatomical area (Figure 9).

Immunohistochemistry for $p75^{NTR}$ receptor detection

12 µm slices were simultaneously blocked and permeabilized with 4% NGS in 0.3% Triton X-100 in PBS (0.1 M, pH 7.4) for 2 h at room temperature (22 ± 2°C). The slices were incubated at 4°C overnight with anti-$p75^{NTR}$ antibody (1:750; Cell signaling, MA, USA), diluted in 0.3% Triton X-100 in PBS with 5% BSA. The primary antibody was then revealed by incubation for 30 min at 37°C in the darkness with Alexa fluor-488 (1:250; Donkey anti-rabbit; Cell signaling, MA, USA) diluted in Triton X-100 (0.3%) in PBS.

Quantitative analyses of BFCN (AChE and $p75^{NTR}$ positive cells/mm^3)

200-fold magnification photomicrographs of the B were acquired by means of an Axioskop 2 Plus microscope (Carl Zeiss) equipped with a CCD imaging camera SPOT Flex Shifting Pixel. Both AChE stained and $p75^{NTR}$ immunoreactive BFCN were counted at three different stereotaxic levels (-1.08 mm, -1.56 mm and -2.04 mm from Bregma), and the total

number of BFCN in the whole image was obtained. The density of BFCN was expressed as AChE or $p75^{NTR}$ positive cells/mm^3.

3.7. Statistical analyses

The statistical analysis used is specified below. Different statistical studies were made depending on the groups of animals.

Table 3. Summary of all the statistical analysis used with the different groups of animals.

Procedure	Comparison groups	Statistical analysis
BM	SHAM / CONTROL / LESION	One-way analysis of variance (ANOVA) Bonferroni's or Dunn's
PA adquisition	VEHICLE / SCOPOLAMINE / WIN55,212-2 / SCOP+WIN	
	CONTROL / LESION / CONTROL+W0.5 / LESION+W0.5	Two-way analysis of variance (ANOVA)
	LESION / LESION+W0.5 / LESION+W+SR	
	CONTROL / LESION / CONTROL+W3 / LESION+W3	
	CONTROL / LESION / CONTROL+SR / LESION+SR	
PA retention	All the comparations	Log-Rank/Mantel-Cox test
Autoradiographic & histochemical studies	CONTROL/LESION	Two-tailed unpaired Student T test in each area analyzed
	VEHICLE/WIN55,212-2	
	CONTROL/CONTROL+W0.5	
	LESION/LESION+W0.5	
	LESION+W0.5/LESION+W+SR	
	CONTROL/CONTROL+W3	
	LESION/LESION+W3	
	CONTROL/CONTROL+SR	
	LESION/LESION+SR	
Number of BFCN	CONTROL/LESION	Two-tailed unpaired Student T test
	CONTROL / LESION / CONTROL+W0.5 / LESION+W0.5	Two-way analysis of variance (ANOVA)

Results

1. MODEL OF BASAL FOREBRAIN CHOLINERGIC LESION

The spatial and aversive learning and memory was evaluated in the model of basal forebrain cholinergic lesion in rat designing a specific schedule compatible also with subchronic treatments. Therefore, different schedule combinations were assayed for analyzing the Barnes maze and Passive avoidance tests in the same animals. The schedule design showed in figure 1 was also followed for the next treatments with minor modifications.

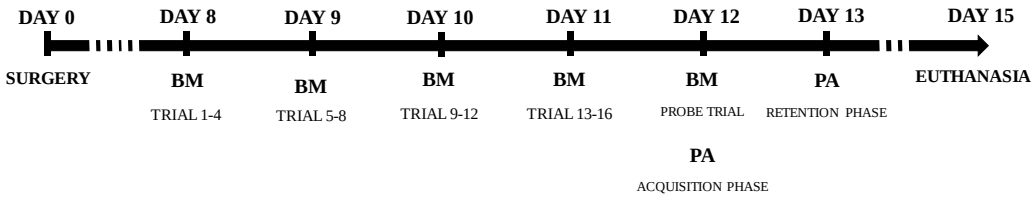

Figure 1. The basic schedule was designed to be compatible with lesion recovery, the necessary trials and probes for learning and memory tests, and for future drug treatments.

1.1. The specific lesion of BFCN leads to spatial and aversive memory impairment

To examine spatial learning and memory, rats were trained in a **Barnes Maze test** (**BM)** seven days after the intraparenchymal infusion of 192IgG-saporin into the B. Spatial acquisition parameters such as total latency (sec); total path length (cm) and speed (cm/sec) to reach the target hole were evaluated by the tracking software. Both parameters total latency and total path length, decreased during the acquisition phase for all animals (Figure 2A and 2B). However, during the trial 13 (day 11) both parameters showed significant differences for the LESION group. (Figure 2D; Total latency. SHAM: 7.4 ± 2 sec, CONTROL: 9.3 ± 1 sec, LESION: 17 ± 2 sec, **p≤0.01. Figure 2E; Total path length. SHAM: 130 ± 33 cm, CONTROL: 156 ± 19 cm, LESION: 292 ± 30 cm, **p≤0.01). On the contrary, the speed was increasing progressively in each new trial. The LESION rats were faster than the CONTROL and SHAM animals (Figure 2C; Mean of speed during all the trials: LESION: 17 ± 0.8 cm/sec; CONTROL: 14 ± 0.6 cm/sec and SHAM cm/sec,*p≤0.05 LESION *vs* CONTROL, #p≤0.05 LESION *vs* SHAM).

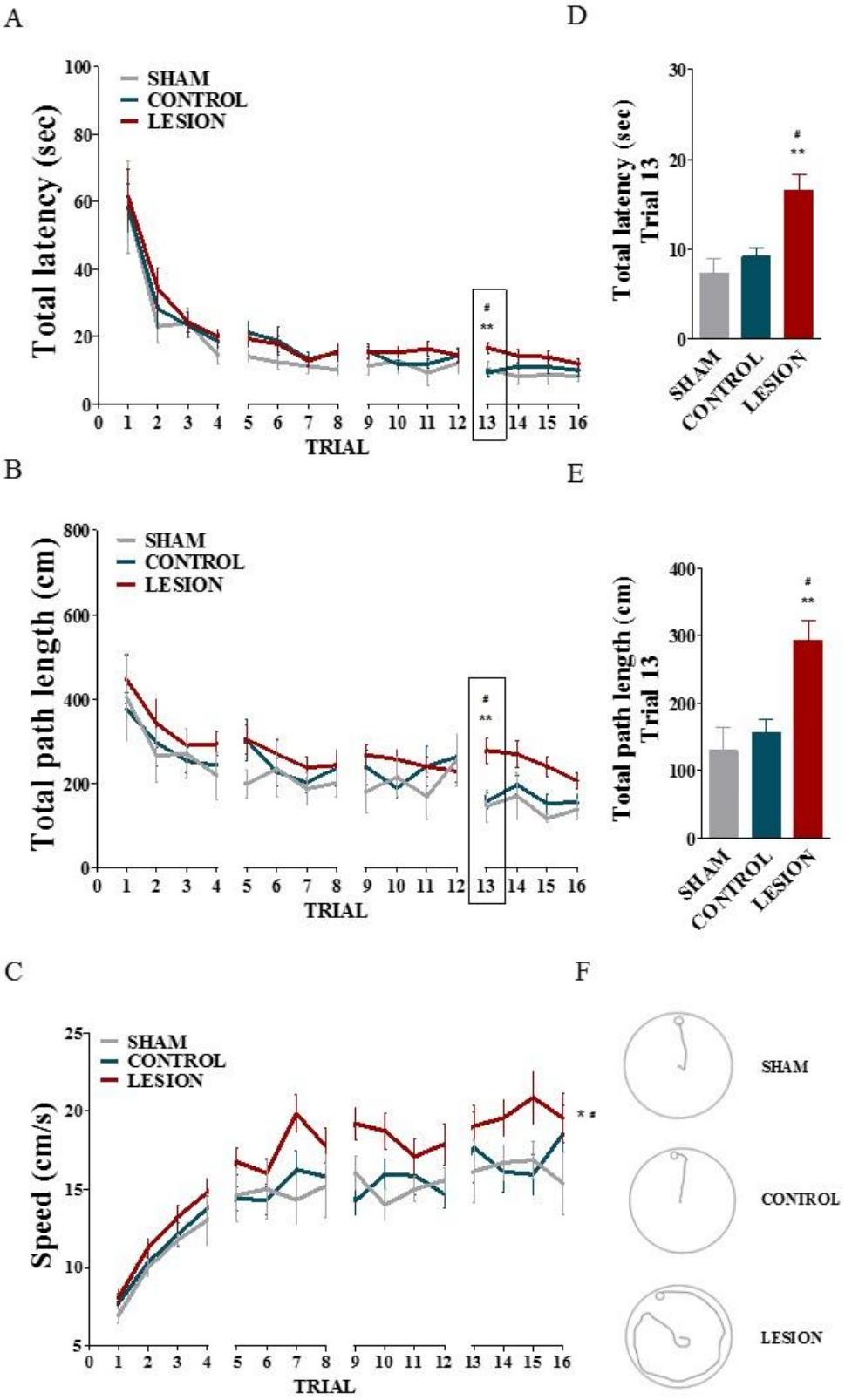

Figure 2. (A) Total latency, (B) total path length and (C) mean of speed during all sixteen trials in the acquisition phase of the three experimental groups, comparison between different curves, *p≤0.05 LESION *vs* CONTROL, #p≤0.05 LESION *vs* SHAM. (D) Total latency in trial 13. (E) Total path length in trial 13 (day 11). Data are (mean ± S.E.M.). *p≤0.05 SHAM *vs* LESION, **p≤0.01 SHAM *vs* LESION. #p≤0.05 CONTROL *vs* LESION. (F) Representative trajectory of trial 13 for the three experimental groups.

On probe trial (day 12), after the last training day, latency in the target quadrant was measured for every experimental group. LESION group spent less time in the target quadrant than SHAM and CONTROL rats. (Figure 3A; Latency in target quadrant. SHAM: 93.3 ± 6 sec, CONTROL: 88.7 ± 4 sec, LESION: 53.5 ± 3 sec, ***p≤0.001). There were no statistically significant differences for any of the recorded parameters in the BM test between SHAM and CONTROL animals, which revealed absence of significant damage due to the needle or the vehicle used that could have any effect on the analyzed behavior.

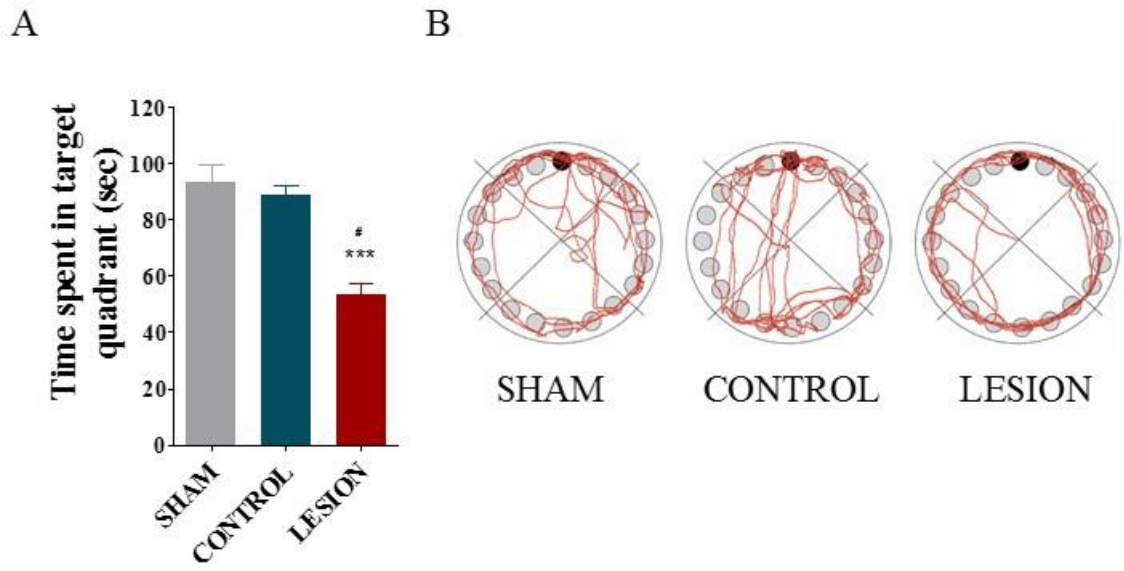

Figure 3. (A) Time spent in target quadrant on probe trial (mean ± S.E.M.). ***p≤0.001 SHAM *vs* LESION; #p≤0.01 CONTROL *vs* LESION. (B) Representative trajectory for each experimental group during the probe trial (180 sec). Note the accumulation of trajectories in the target quadrant for both sham and control groups.

To examine learning and memory associated to an aversive stimulus the **passive avoidance (PA)** was followed after the probe trial of BM (day 12). We also evaluated in the PA test the acquisition latency parameter as the time that rats remained in the open compartment before entering the dark one. LESION group exhibited lower acquisition latency than the other groups. (Figure 4A; SHAM: 12 ± 2 sec, CONTROL: 12 ± 1 sec, LESION: 6 ± 1 sec). 24 hours later, all trained animals were tested again to evaluate aversive memory. The step-through latency time was measured and represented as Kaplan-Meier survival curves to determine the estimated probability of a positive response; i.e., to reach the cut-off time. In general, all the SHAM rats and most of the CONTROL animals were able to remember the aversive stimulus (100 % and 77 %, respectively). However, only a 27 % of the LESION animals were able to remember the aversive stimulus (Figure 4B).

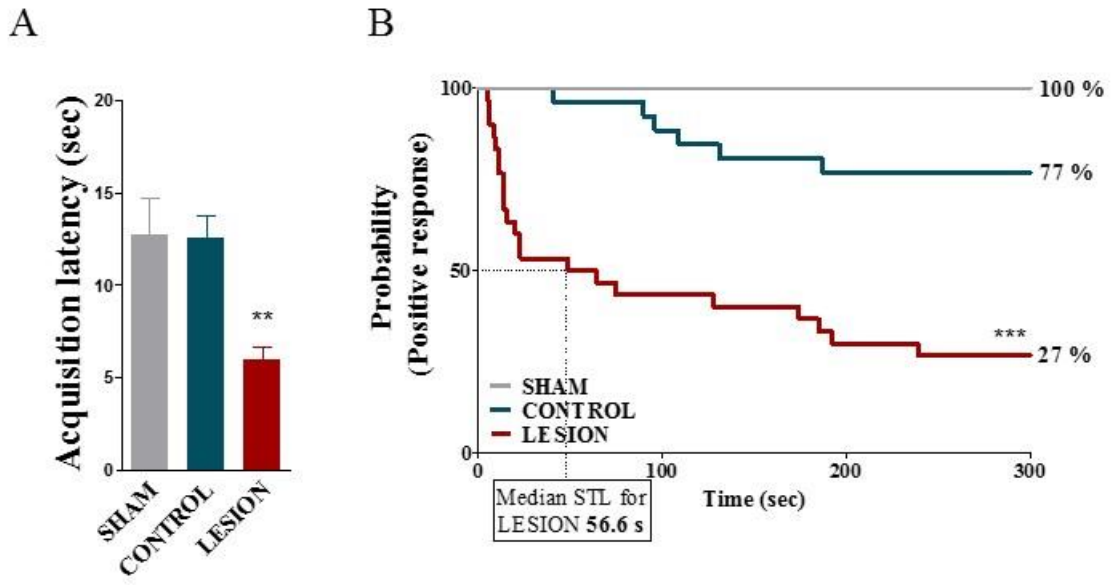

Figure 4. (A) Acquisition latency times during the learning trial of the passive avoidance test (mean ± S.E.M.). **p≤0.01 CONTROL *vs* LESION. (B) Step-Through latency times of passive avoidance test represented as Kaplan-Meier survival curves (***p ≤0.001 *vs* CONTROL, Log-Rank/Mantel-Cox test).

Considering, than rats in the SHAM group had the same behavior than the CONTROL animals in all of analyzed parameters during BM and PA tests, these later animals will be considered as the "control" group and will be named as CONTROL from now on.

1.2. Effect of specific lesion in BFCN on long-term memory

To examine the effect of the lesion on long-term memory the BM and PA test were also used measuring the different parameters, latency per quadrant and step-through latency every two months on all animals (Figure 5A). The term "0 month" was used to designate the first trials and probes for these groups of animals. The first results observed in these new animals showed that the time necessary to forget the BM spatial acquisition was up to 6 months in CONTROL rats (0 month: 90.27 ± 8 sec *vs* 6 months: 51.32 ± 5 sec. Figure 5B, ***p≤0.001), and up to 7 months to forget the aversive stimulus in PA (0 months: 80 % positive responses *vs* 7 month: 27 % positive responses (Figure 5C).

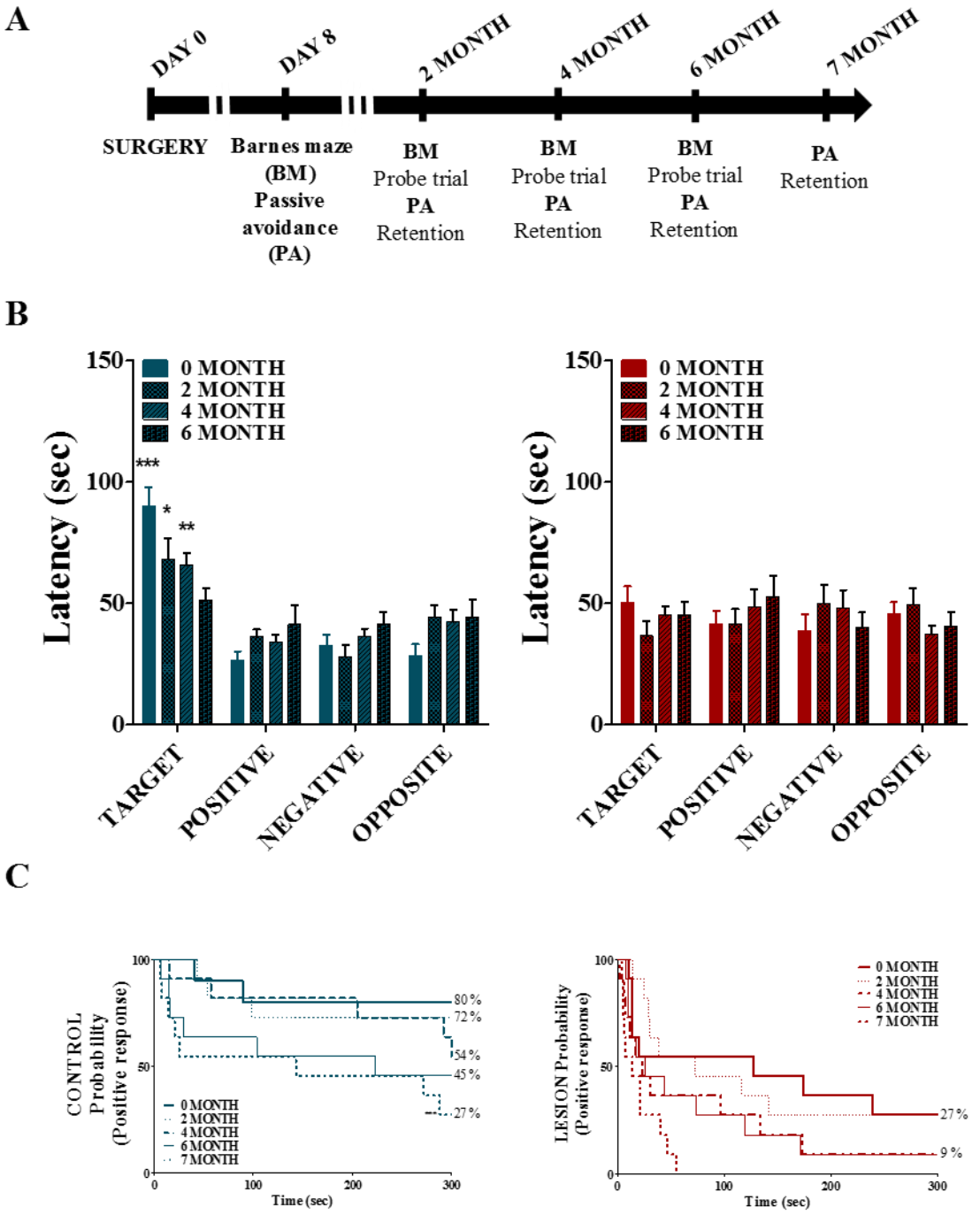

Figure 5. CONTROL in blue and LESION in red. (A) Training schedule to evaluate the long-term memory until month 7 after surgery. (B) Latency of BM over the time. Note CONTROL animals forget the BM training at 6 months. *p≤0.05; **p≤0.01; ***p≤0.001. (C) Step-Through latency times of passive avoidance test represented as Kaplan-Meier survival curves (***p≤0.001, Log-Rank/Mantel-Cox test). The CONTROL animals forget the aversive stimulus learned in the PA at 7 month after surgery.

1.3. Specific lesion in BFCN leads to decrease muscarinic signaling

15 days after the deletion of cholinergic neurons at the nucleus basalis magnocellularis, the density and activity of muscarinic receptors was analyzed by means of autoradiography.

The [^{35}S]GTPγS binding stimulated by carbachol was measured in brain areas related to learning and memory to localize and quantify the activity of the M_2/M_4 receptors. Basal binding was similar in both groups LESION and CONTROL, in all the analyzed brain areas. The M_2/M_4 receptor activity induced by carbachol was decreased in different layers of the motor cortex (**Layer I**: CONTROL: 281 ± 14 % *vs* LESION: 86 ± 19 %; **layer II-V**: CONTROL: 294 ± 40 % *vs* LESION**:** 167 ± 32 %, *p≤0.05), in septal nuclei (medial septum or **MS**: CONTROL: 387 ± 46 % *vs* LESION: 229 ± 34 %) and vertical diagonal band or **VDB** (CONTROL: 334 ± 15 % *vs* LESION: 216 ± 32 %, *p≤0.05, Figure 6, Table 1).

The [^{3}H]-N-methyl-scopolamine binding was also measured in consecutive sections to analyze density and distribution of the total population of muscarinic receptors. The lesion in the B did not modify the density of total muscarinic receptors in areas related to learning and memory such as the hippocampus (Table 2).

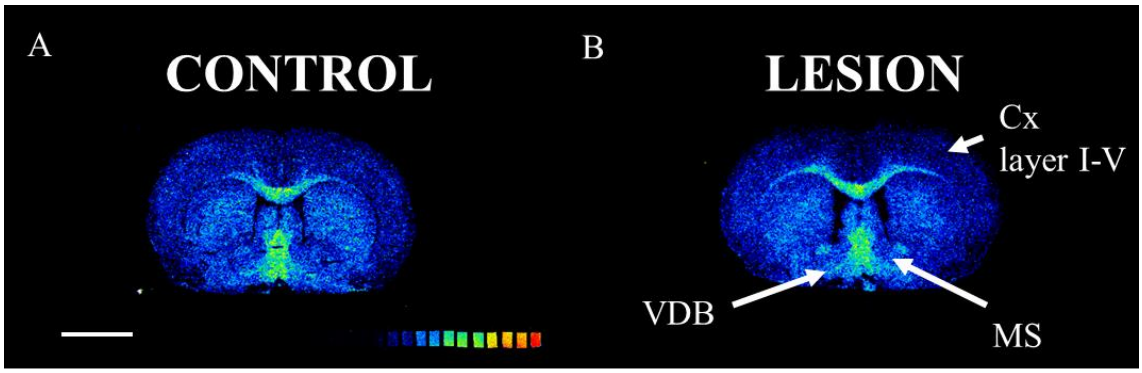

Figure 6. Representative autoradiograms corresponding to coronal sections from (A) CONTROL and (B) LESION rats that show the [^{35}S]GTPγS binding stimulated by carbachol (100 µM) in vertical diagonal band (VDB), motor cortex layer I-V (Mot Cx I-V) and medial septum (MS) . Scale bar: 4 mm.

Table 1. [^{35}S]GTPγS basal and 100 µM carbachol-induced binding expressed as percentage of stimulation over the basal binding in the different areas related to learning and memory

	Basal binding (nCi/g t.e.)		**Carbachol stimulation (% over basal)**	
Brain region	CONTROL	LESION	**CONTROL**	**LESION**
Cerebral cortex				
Cingulate	162 ± 32	192 ± 39	223 ± 39	193 ± 51
Motor				
Layer I	118 ± 23	200 ± 58	281 ± 14	86 ± 19**
Layer II-V	136 ± 30	192 ± 38	294 ± 40	167 ± 32*
Layer VI	160 ± 30	157 ± 33	160 ± 30	157 ± 33
Somatosensory				
Layer I-V	201 ± 28	253 ± 73	125 ± 27	121 ± 30
Layer VI	209 ± 42	259 ± 52	153 ± 36	122 ± 30
Basal ganglia				
Globus pallidus	364 ± 48	381 ± 55	97 ± 15	108 ± 28
Striatum	241 ± 34	295 ± 53	150 ± 22	118 ± 24
Diencephalon				
B	478 ± 32	550 ± 56	74 ± 14	69 ± 36
HDB	292 ± 20	337 ± 31	168 ± 43	153 ± 28
VDB	304 ± 30	409 ± 62	334 ± 15	216 ± 32*
Medial septum	242 ± 33	332 ± 53	387 ± 46	229 ± 34*
Hippocampus				
CA1	161 ± 43	186 ± 40	150 ± 33	180 ± 29
Oriens	362 ± 57	337 ± 50	141 ± 47	115 ± 31
Pyramidal	386 ± 53	330 ± 30	141 ± 54	138 ± 49
Radiatum	300 ± 54	283 ± 36	126 ± 42	123 ± 24
CA2	189 ± 41	181 ± 39	163 ± 39	230 ± 50
CA3	208 ± 42	214 ± 45	144 ± 28	196 ± 82
Oriens	231 ± 47	263 ± 49	91 ± 11	126 ± 28
Pyramidal	194 ± 37	195 ± 48	173 ± 25	147 ± 59
Radiatum	280 ± 58	322 ± 50	88 ± 28	78 ± 18
Dentate gyrus	197 ± 39	188 ± 44	178 ± 57	137 ± 45
Granular	248 ± 29	168 ± 36	96 ± 28	163 ± 32
Molecular	253 ± 42	245 ± 49	115 ± 33	136 ± 46
Polimorphic	198 ± 54	222 ± 31	103 ± 24	99 ± 20
Amygdala	342 ± 83	399 ± 56	95 ± 21	77 ± 17

HDB: horizontal diagonal band, VDB: vertical diagonal band and B: nucleus basalis magnocellularis. Data are mean ± S.E.M. values from CONTROL and LESION rats. *p≤0.05 , ** p≤0.01 when compared to CONTROL group.

Table 2. Autoradiographic densities of muscarinic receptors expressed in fmol/mg t.e., obtained as specific binding of [^{3}H]-N-methyl-scopolamine.

Specific binding of [^{3}H]N-METHIL-SCOPOLAMINE (Fmol/g t.e.)		
Brain region	CONTROL	LESION
Cerebral cortex		
Cingulate	309 ± 34	303 ± 39
Motor		
Layer I	512 ± 72	536 ± 74
Layer II-V	291 ± 37	296 ± 32
Layer VI	202 ± 15	236 ± 22
Somatosensory		
Layer I-V	349 ± 36	392 ± 27
Layer VI	209 ± 24	240 ± 18
Basal ganglia		
Globus pallidus	24 ± 3	29 ± 2
Striatum	268 ± 32	321 ± 39
Diencephalon		
NBM	51 ± 9	57 ± 5
HDB	129 ± 26	144 ± 13
VDB	106 ± 9	128 ± 14
Medial septum	103 ± 8	125 ± 14
Hippocampus		
CA1	307 ± 37	330 ± 42
Oriens	348 ± 45	393 ± 46
Pyramidal	317 ± 34	352 ± 52
Radiatum	254 ± 43	298 ± 39
CA2	302 ± 36	347 ± 57
CA3	216 ± 25	254 ± 28
Oriens	232 ± 28	257 ± 27
Pyramidal	189 ± 19	209 ± 22
Radiatum	182 ± 19	217 ± 26
Dentate gyrus	258 ± 26	305 ± 33
Granular	280 ± 31	341 ± 30
Molecular	165 ± 16	194 ± 28
Polimorphic	303 ± 41	315 ± 32
Amygdala	304 ± 39	296 ± 27

HDB: horizontal diagonal band, VDB: vertical diagonal band and B: nucleus basalis magnocellularis. Data are mean ± S.E.M. values from CONTROL and LESION rats groups.

1.4. Specific lesion of BFCN leads to decrease of cholinergic innervations

The loss of BFCN 15 days after the lesion provoked a reduction in AChE positive fibers in brain areas innervated by the BFCN (Figure 7). The motor and somatosensory cortices were the more denervated brain areas as a consequence of the lesion (**motor cortex**: CONTROL 16 ± 2 *vs* LESION 8 ± 1 a.u..; expressed as arbitrary units or a.u., and **somatosensory cortex**: CONTROL: 19 ± 1 *vs* LESION 11 ± 1 a.u., ***p≤0.001) in different layers (Table 3).

Table 3. $AChE^+$ optical densities (arbitrary units or a.u.) obtained as enzymatic AChE staining.

	$AChE^+$ Optical Density (a.u.)	
Brain region	CONTROL	LESION
Cerebral cortex		
Cingulate	19 ± 1	19 ± 1
Motor		
Layer I	16 ± 2	8 ± 1***
Layer II-V	17 ± 2	8 ± 1***
Layer VI	17 ± 2	8 ± 1***
Somatosensory		
Layer I-V	18 ± 1	9 ± 1***
Layer VI	19 ± 1	11 ± 1***
Basal ganglia		
Globus pallidus	13 ± 1	12 ± 2
Striatum	67 ± 2	57 ± 5
Diencephalon		
B	36 ± 3	24 ± 3*
HDB	60 ± 4	59 ± 3
VDB	47 ± 5	44 ± 2
Medial septum	50 ± 2	49 ± 3
Hippocampus		
CA1	19 ± 1	20 ± 1
Oriens	20 ± 1	22 ± 3
Pyramidal	27 ± 1	26 ± 2
Radiatum	14 ± 1	17 ± 2
CA2	18 ± 1	21 ± 2
CA3	25 ± 1	24 ± 1
Oriens	22 ± 4	28 ± 3
Pyramidal	40 ± 1	36 ± 2
Radiatum	24 ± 1	21 ± 1
Dentate gyrus	22 ± 1	22 ± 0.5
Granular	27 ± 2	26 ± 1
Molecular	22 ± 2	23 ± 1
Polimorphic	22 ± 1	25 ± 2
Amygdala	51 ± 3	47 ± 4

HDB: horizontal diagonal band, VDB: vertical diagonal band and B: nucleus basalis magnocellularis. Data are mean ± S.E.M. values from CONTROL and LESIONED rats groups. ***p≤0.001 when compared to CONTROL group.

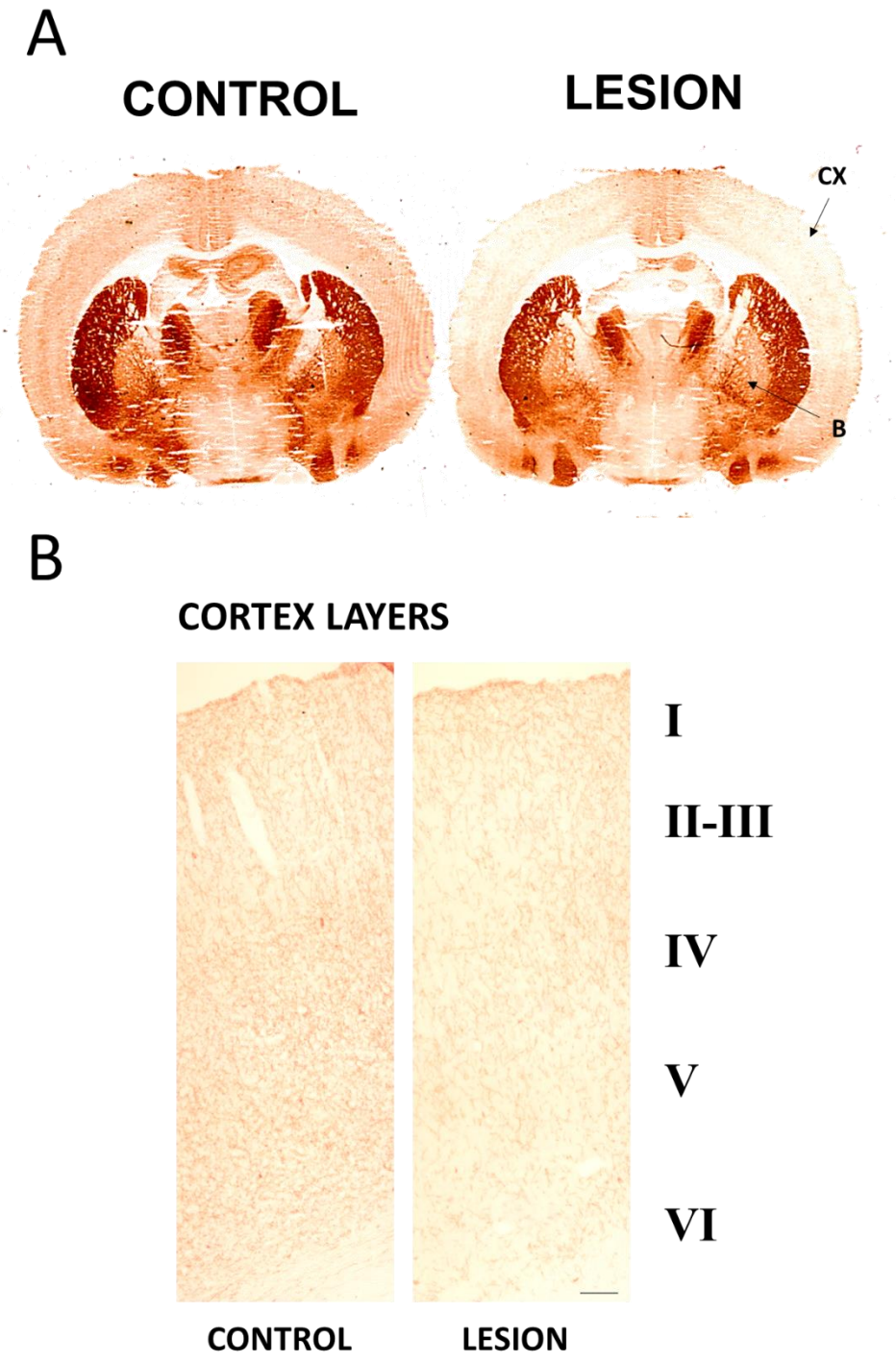

Figure 7. (A) AChE staining in representative brain coronal slices of CONTROL and LESION rats. Scale bar = 4 mm. (B) Microphotographs showing the different cortical layers of motor cortex. Scale bar = 500 µm.

1.5. Specific lesion of BFCN leads to altered CB_1 functionality

The effect of the depletion of B cholinergic cells on cannabinoid receptors was also analyzed 15 days after the lesion. Both density and activity of CB_1 receptors were analyzed by autoradiography in tissue sections.

The [^{35}S]GTPγS binding stimulated by WIN55,212-2 was measured in brain areas related to learning and memory to localize and quantify the activity of CB_1 receptors. The CB_1 receptor activity induced by WIN55,212-2 was exclusively decreased in septal nuclei (**MS**: CONTROL: 426 ± 95 % *vs* LESION: 160 ± 25 %; **HDB**: CONTROL: 314 ± 55 % *vs* LESION: 132 ± 23 % and **VDB**: CONTROL: 352 ± 76 % *vs* LESION: 162 ± 23 %, *p≤0.05; Table 4 and Figure 8).

The CB_1 receptor density was studied in the same brain areas by analyzing the [^{3}H]CP55,940 binding. The loss of BFCN increased CB_1 receptor densities in areas receiving cholinergic innervation from the basal forebrain, such as hippocampus and amygdala (**CA1**: CONTROL: 175 ± 23 *vs* LESION: 325 ± 52 fmol/g t.e; **CA2**: CONTROL: 221 ± 22 *vs* LESION: 310 ± 34 fmol/g t.e and **DG granular**: CONTROL: 158 ± 28 *vs* LESION: 277 ± 43 fmol/g t.e, *p≤0.05) (Table 5 and Figure 9).

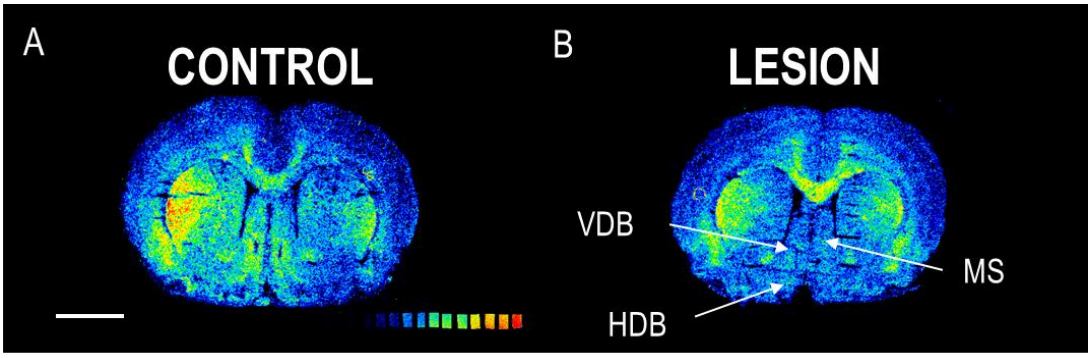

Figure 8. Representative autoradiograms corresponding to coronal sections of representative (A) CONTROL and (B) LESION rats, that show [^{35}S]GTPγS binding stimulated by WIN55,212-2 (10 µM) in HDB: horizontal diagonal band, VDB: vertical diagonal band and MS: medial septum. Scale bar: 4 mm.

TABLE 4. [^{35}S]GTPγS basal and WIN55,212-2-induced (10 μM) binding expressed as percentage of stimulation over the basal binding in different areas related with learning and memory control.

	Basal binding (nCi/g t.e.)		**WIN55,212-2 stimulation (% over basal)**	
Brain region	CONTROL	LESION	**CONTROL**	**LESION**
Cerebral cortex				
Cingulate	303 ± 48	328 ± 48	380 ± 91	257 ± 67
Motor				
Layer I	271 ± 34	286 ± 53	258 ± 54	191 ± 52
Layer II-V	299 ± 52	320 ± 43	213 ± 50	144 ± 22
Layer VI	305 ± 64	320 ± 46	430 ± 92	376 ± 91
Somatosensory				
Layer I-V	290 ± 54	292 ± 45	193 ± 49	170 ± 73
Layer VI	298 ± 60	323 ± 53	281 ± 64	202 ± 53
Basal ganglia				
Globus pallidus	467 ± 90	461 ± 34	1833 ± 370	1119 ± 131
Striatum	392 ± 55	402 ± 52	334 ± 78	217 ± 35
Diencephalon				
B	363 ± 68	409 ± 63	205 ± 61	236 ± 60
HDB	370 ± 42	390 ± 34	314 ± 55	132 ± 23*
VDB	383 ± 57	413 ± 37	352 ± 76	162 ± 23*
Medial septum	427 ± 75	408 ± 55	426 ± 95	160 ± 25*
Hippocampus				
CA1	213 ± 47	227 ± 44	294 ± 56	388 ± 53
Oriens	313 ± 49	298 ± 35	453 ± 59	407 ± 62
Pyramidal	293 ± 48	267 ± 28	461 ± 65	432 ± 62
Radiatum	320 ± 51	306 ± 28	234 ± 41	316 ± 39
CA2	260 ± 41	232 ± 40	359 ± 71	381 ± 74
CA3	323 ± 46	296 ± 39	434 ± 65	405 ± 61
Oriens	294 ± 48	298 ± 29	460 ± 70	489 ± 78
Pyramidal	300 ± 48	299 ± 29	373 ± 54	346 ± 47
Radiatum	360 ± 50	368 ± 32	331 ± 54	319 ± 42
Dentate gyrus	312 ± 45	292 ± 39	411 ± 69	369 ± 71
Granular	330 ± 53	341 ± 48	276 ± 68	249 ± 48
Molecular	330 ± 41	337 ± 32	316 ± 76	236 ± 24
Polimorphic	323 ± 50	340 ± 46	414 ± 75	452 ± 79
Amygdala	332 ± 58	332 ± 53	190 ± 62	252 ± 70

HDB: horizontal diagonal band, VDB: vertical diagonal band and B: nucleus basalis magnocellularis. Data are mean ± S.E.M. values from CONTROL and LESION rats. *$p \leq 0.05$ when compared to CONTROL group.

TABLE 5. Autoradiographic densities of CB_1 receptors expressed in fmol/mg t.e., obtained as specific binding of [^{3}H]CP55,940

Specific binding of [^{3}H]CP55,940 (fmol/g t.e.)		
Brain region	CONTROL	LESION
Cerebral cortex		
Cingulate	149 ± 15	130 ± 19
Motor		
Layer I	173 ± 19	140 ± 16
Layer II-V	120 ± 16	103 ± 11
Layer VI	170 ± 23	146 ± 19
Somatosensory		
Layer I-V	75 ± 10	73 ± 11
Layer VI	123 ± 10	150 ± 32
Basal ganglia		
Globus pallidus	980 ± 180	883 ± 98
Striatum	313 ± 36	292 ± 27
Diencephalon		
B	122 ± 37	56 ± 14
HDB	102 ± 16	99 ± 10
VDB	159 ± 33	169 ± 17
Medial septum	144 ± 28	136 ± 12
Hippocampus		
CA1	175 ± 23	325 ± 52*
Oriens	250 ± 39	288 ± 41
Pyramidal	225 ± 15	386 ± 59*
Radiatum	192 ± 39	226 ± 27*
CA2	221 ± 22	310 ± 34*
CA3	282 ± 28	306 ± 28
Oriens	302 ± 14	324 ± 31
Pyramidal	323 ± 30	317 ± 27
Radiatum	211 ± 24	282 ± 30
Dentate gyrus	199 ± 31	256 ± 23
Granular	158 ± 28	277 ± 43*
Molecular	154 ± 22	169 ± 26
Polimorphic	258 ± 47	299 ± 58
Amygdala	103 ± 19	185 ± 24*

HDB: horizontal diagonal band, VDB: vertical diagonal band and B: nucleus basalis magnocellularis. Data are mean ± S.E.M. values from CONTROL and LESION rats. *$p \leq 0.05$ when compared to CONTROL group.

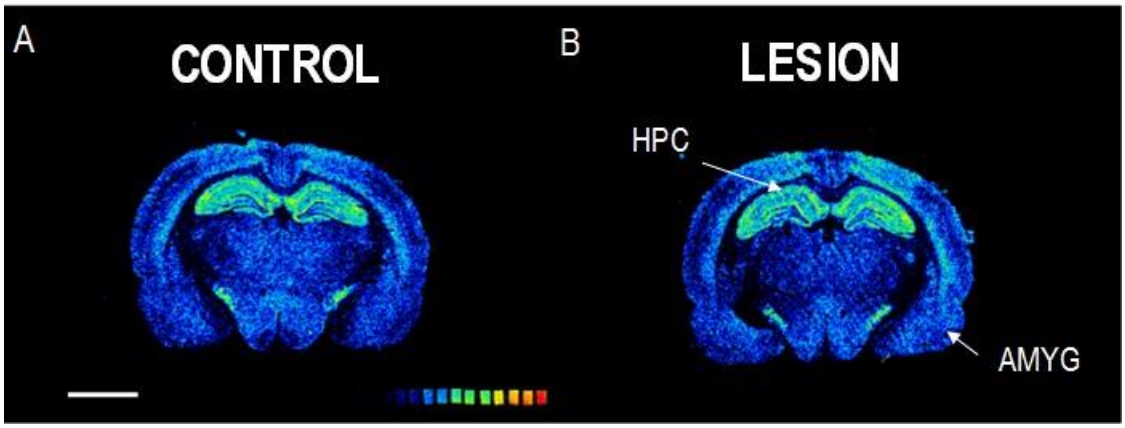

Figure 9. Representative autoradiograms of (A) CONTROL and (B) LESION rat coronal sections that show [^{3}H]CP55,940 binding (3 nM) in HPC: hippocampus and AMYG: amygdala. Scale bar: 4 mm.

1.6. The specific loss of BFCN in the B positively correlates with a dysfunction of M_2/M_4 receptor activity in areas related to learning and memory processing

The $p75^{NTR}$ immunofluorescence assay was used to stain the surviving target BFCN after the administration of 192IgG-saporin. The toxin administration in the B reduced the number of BFCN (Figure 10A, 863 ± 64 cells/mm^3 in CONTROL group and 257 ± 32 in LESION group) and in a number of $AChE^+$ cells (Figure 10A, 789 ± 41 cells/mm^3 in CONTROL group and 165 ± 38 cells/mm^3 in LESION group). The decrease of $p75^{NTR}$ and $AChE^+$ cells in B correlated positively with the time in the target quadrant of BM ($r^2 = 0.72$ and $r^2 = 0.71$, respectively for $p75^{NTR}$ and $AChE^+$ cells, $p \leq 0.05$, Figure 10C). In addition, the linear regression analysis verified that the relationship between the depletion of BFCN and muscarinic M_2/M_4 dysfunction both in the cortex and in the septal nuclei (Figure 11, Table 6).

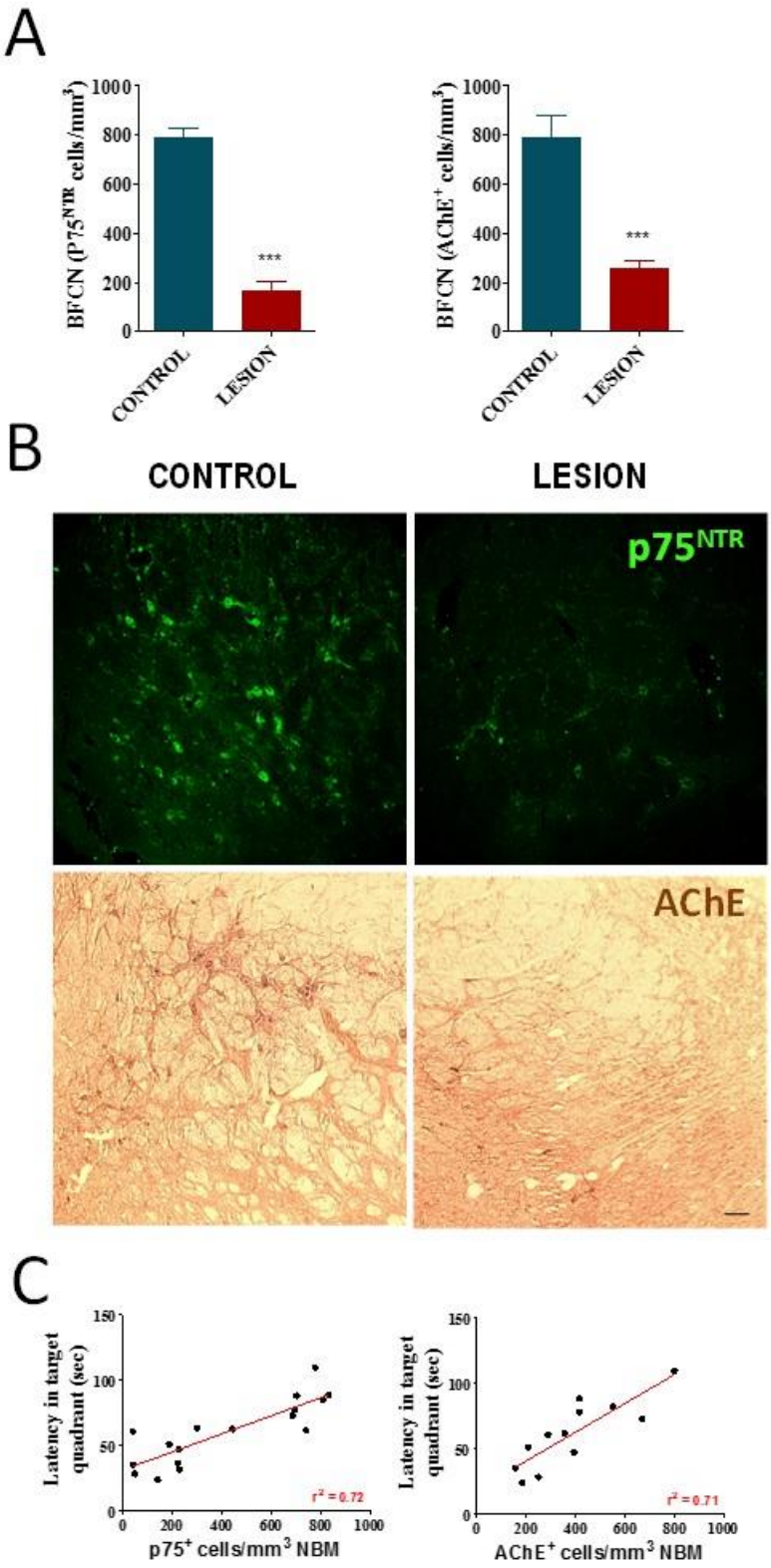

Figure 10. (A) Number of $p75^{NTR}$ and $AChE^{+}$ cells in the B of CONTROL and LESION groups. (B) AChE enzymatic staining and $p75^{NTR}$ immunofluorescence in the B. (C) Correlation analysis between latency in target quadrant in BM and $p75^{NTR}$ positive cells in the B for the LESION experimental group. Scale bar 100µM.

TABLE 6. Linear regression analysis between CB_1 and M_2/M_4 stimulation and number of BFCN expressing $P75^{NTR}$.

Linear regresion analysis						
	$p75^{NTR}$					
	CB_1 stimulation % over basal			M_2/M_4 stimulation % over basal		
Brain region	**p**	**Pearson r**	**r squared**	**p**	**Pearson r**	**r squared**
Cerebral cortex						
Motor						
Layer I	0.67	-0.12	0.01	**0.004**	0.79	0.62
Layer II-V	0.7	-0.1	0.01	**0.03**	0.63	0.4
Layer VI	0.74	-0.09	0.009	0.49	0.22	0.05
Basal ganglia						
Diencephalon						
B	0.25	-0.33	0.11	0.94	-0.02	0.0003
HDB	0.53	0.17	0.03	0.1	0.55	0.3
VDB	0.59	0.15	0.02	0.98	-0.006	0.00003
Medial septum	0.74	0.08	0.0007	**0.003**	0.79	0.63

HDB: horizontal diagonal band, VDB: vertical diagonal band and B: nucleus basalis magnocellularis. In bold the positive correlated. Data expresses as Pearson's r and r^2 coefficients. **$p \leq 0.01$, *$p \leq 0.05$.

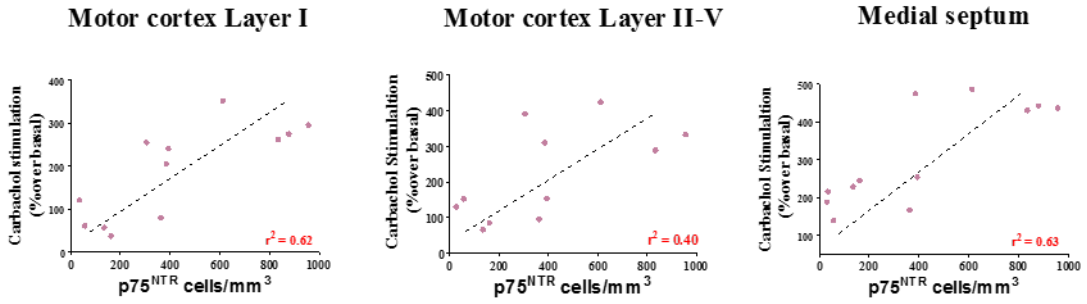

Figure 11. Positive correlation analysis between carbachol stimulation (% over basal) of motor cortex layers I-V and medial septum and $p75^{NTR}$ positive cells in the B for the LESION experimental group.

2. SUBCHRONIC WIN55,212-2 ADMINISTRATION EFFECTS ON THE PHARMACOLOGICAL MODEL OF MUSCARINIC RECEPTOR ANTAGONIMS

Previous results of our group showed WIN55,212-2 had potential neuroprotective effects by using the *in vitro* model of cholinergic lesion in brain organotypic cultures (unpublished results). Therefore, WIN55,212-2 was the best compound candidate to be used *in vivo*, firstly in one of the most commonly used models of cholinergic cognitive deficit in rodents, induced by a single acute administration of 2 mg/kg of the muscarinic antagonist, scopolamine. The following four treatment schedules (VEHICLE, WIN55,212-2, SCOP and WIN+SCOP groups) were designed after different previous trials to evaluate the effects of the CB_1 cannabinoid agonist, WIN55,212-2 (0,5 mg/kg, i.p., 5 days), in this *in vivo* model of amnesia induced by cholinergic blockade (Figure 12).

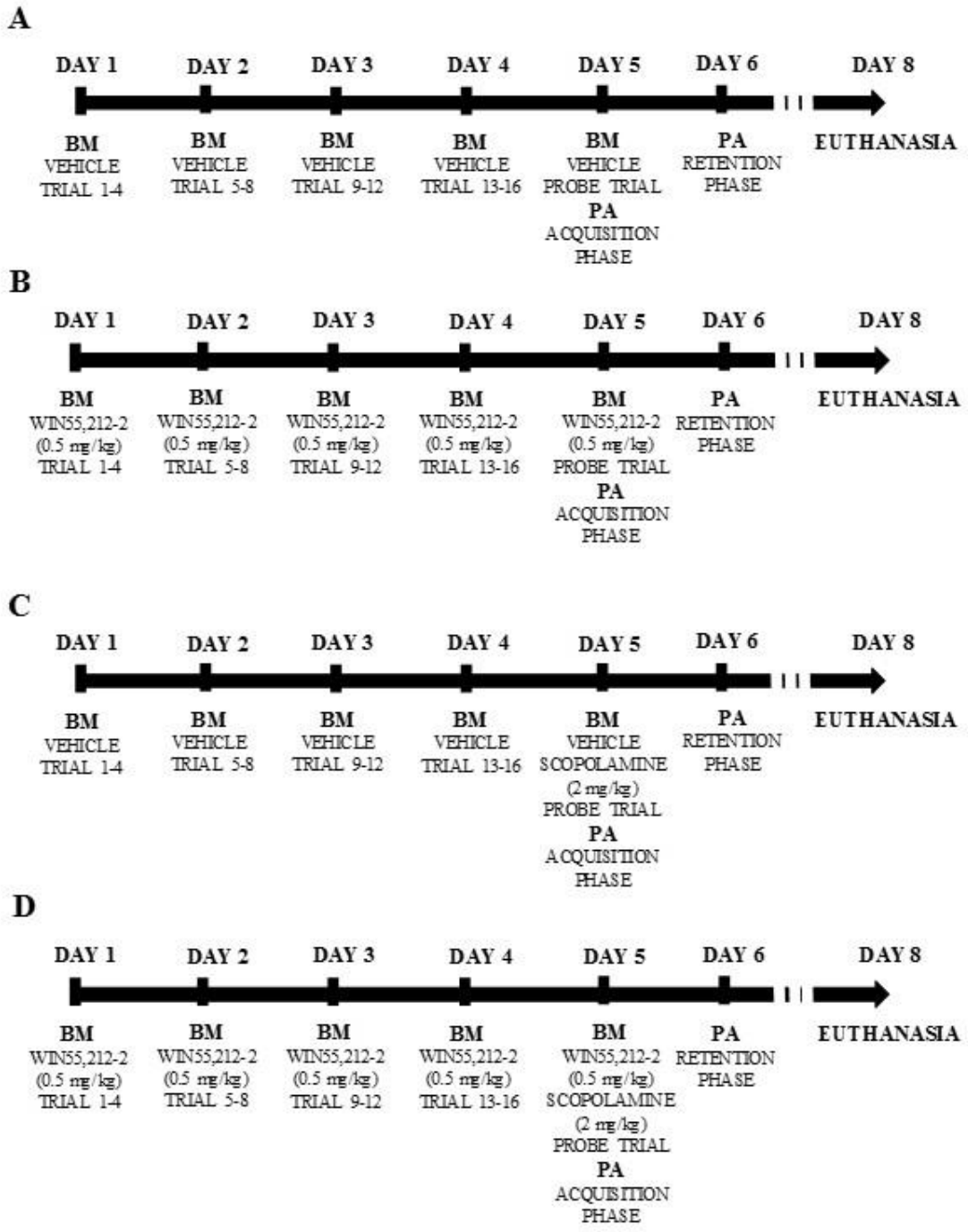

Figure 12. Training schedules followed for each of the four groups of treatment designed to evaluate the effects of WIN55,212-2 in both spatial and aversive memory.

2.1. Subchronic WIN55,212-2 treatment prevents from amnesic effects induced by scopolamine

To examine spatial learning and memory behavior all rats were firstly trained in a Barnes maze test. The two groups of rats that were subchronically treated with WIN55,212-2 (were also trained for the BM test from the first day of treatment). During the treatments and trainings, different behavioral parameters were evaluated by using the tracking software, including total latency (sec), total path length (cm) and mean speed (cm/sec) to reach the target hole. The first observations showed that the total latency and total path length were decreasing during the acquisition phase for all groups of treatment, but in a different way (Figure 13A, 13C). Total latency showed significant differences between VEHICLE and WIN55,212-2 groups during the first trial. (Figure 13A, Trial 1 VEH: 40 ± 5 sec *vs* Trial 1 WIN0.5: 101 ± 25 sec,). The average speed increased for each trial, but WIN-treated rats were walking more slowly than vehicle-treated rats (Figure 13C, *p≤0.05).

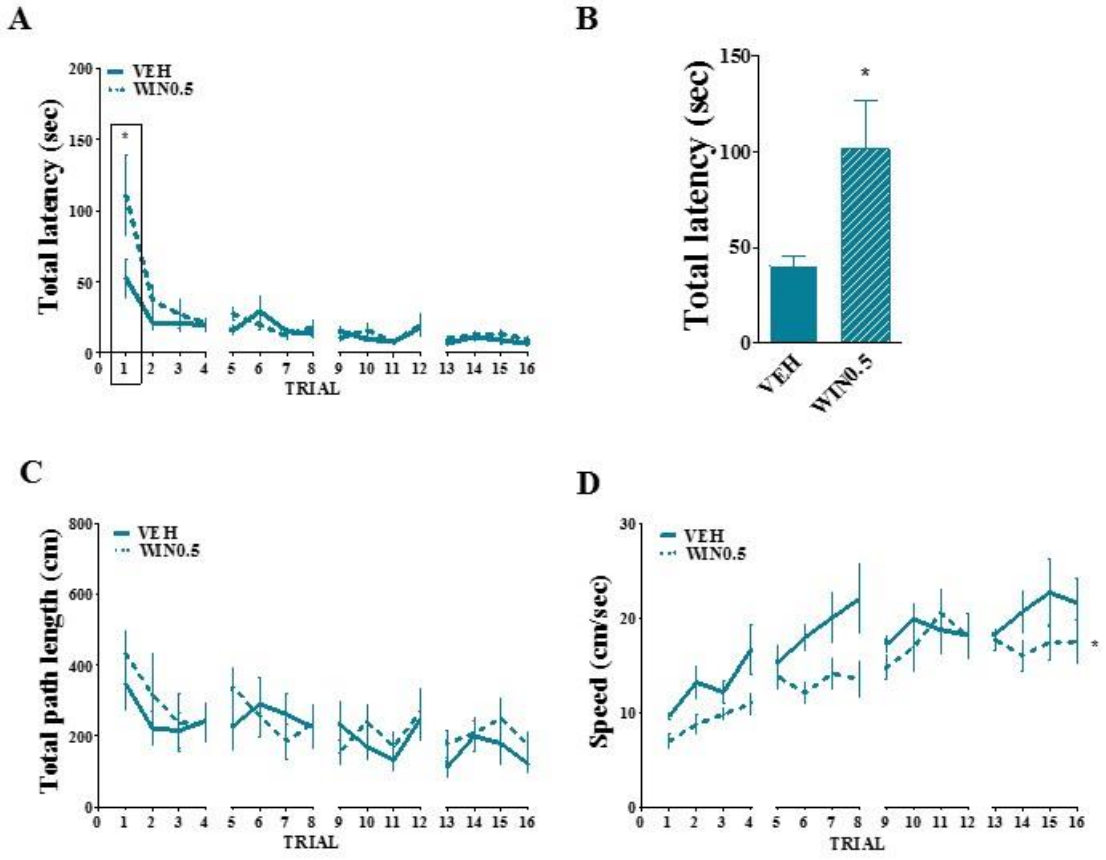

Figure 13. (A) Total latency, (B) Total latency in trial 1, and (C) Total path length. (D) Average speed during each of the sixteen trials of the acquisition phase, comparison between different curves, *p≤0.05. Data are (mean ± S.E.M.) *p≤0.05. VEH *vs* WIN0.5.

On probe trial, after the last training day, latency in target quadrant was measured in four groups. VEHICLE, WIN0.5 and WIN+SCOP groups spent more time in the target quadrant than SCOP group. (Figure 14A, Time spent in target quadrant. VEH: 94 ± 7 sec, SCOP: 38 ± 4 sec, WIN0.5: 88 ± 5 sec, WIN+SCOP: 80 ± 11 sec)

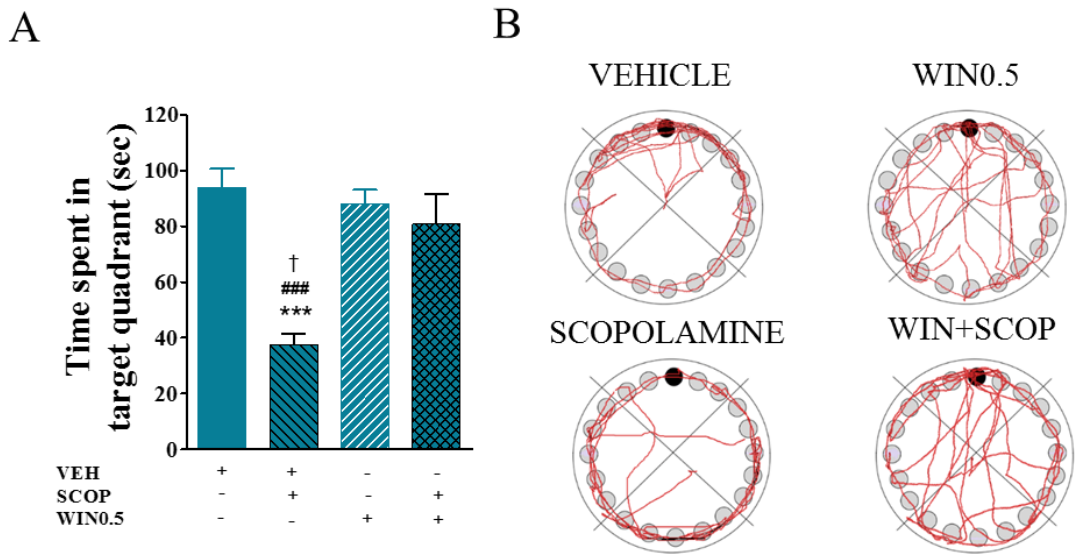

Figure 14. (A) Time spent in target quadrant on probe trial (mean ± S.E.M.). VEH *vs* SCOP ***p≤0.001. SCOP *vs* WIN55,212-2 ###p≤0.001, SCOP *vs* WIN+SCOP †p≤0.05. (B) Representative trajectory during 180 sec in the probe trial. Note the accumulation of trajectories in the target quadrant for VEHICLE, WIN0.5 and WIN+SCOP.

The learning and memory associated to the learning of an aversive stimulus was evaluated by using the PA test. The day of the probe trial of BM test (fifth and last day of treatment) we also evaluated the acquisition latency in the PA test. The animals of the SCOP group exhibited a higher acquisition latency in PA test than the other groups (Figure 15A, VEH: 9 ± 2 sec, SCOP: 30 ± 9 sec, WIN0.5: 13 ± 2 sec and WIN+SCOP: 10 ± 3 sec, **p≤0.01 VEH *vs* SCOP). 24 hours later, the step-through latency time was measured in the PA test. The results indicated that only VEHICLE group rats were able to remember the aversive stimulus (100 %). The other groups, WIN0.5, WIN+SCOP and SCOP showed that only 14 %, 10 % and 0 % of the animals were able to remember it, respectively (Figure 15B).

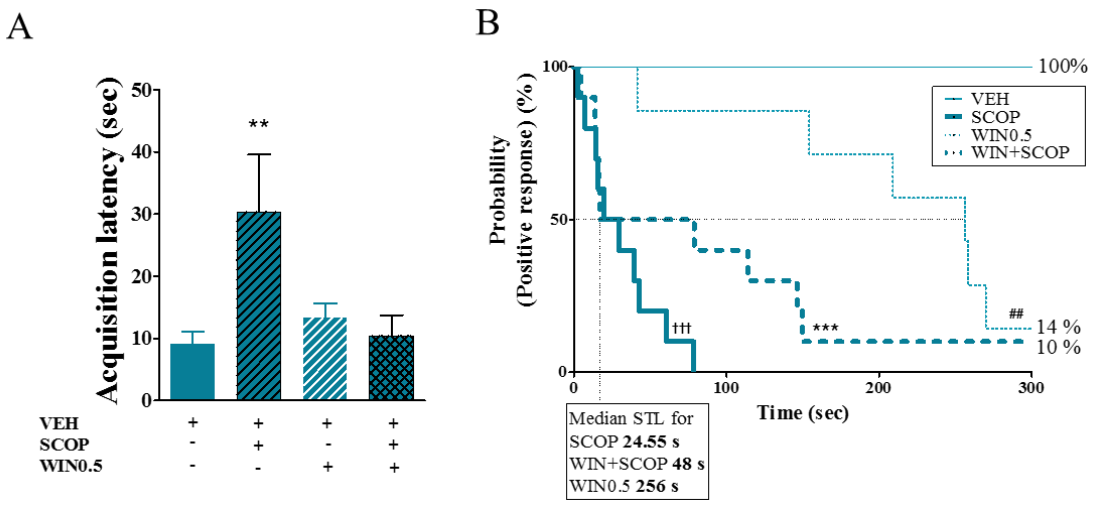

Figure 15. (A) Acquisition latency times in the learning trial of the PA test (mean ± S.E.M.)**p≤0.01, VEH *vs* SCOP. (B) Step-through latency times of PA test represented as Kaplan-Meier survival curves. ##p≤0.01 WIN0.5*vs* VEH, ***p≤0.001 WIN+SCOP *vs* VEH, †††p≤0.001 SCOP *vs* VEH, Log-Rank/Mantel-Cox test).

2.2. Subchronic WIN55,212-2 administration leads to altered response to pain stimulus

It is well established that cannabinoids are able to induce analgesic effects. Learning and memory (step-through latency times) of an aversive electrical stimulus during the PA test could be biased or misunderstood by the possible analgesic effects of the cannabinoid treatment, therefore we evaluated the effect of WIN55,212-2 treatment on pain sensitivity. The pain response in treated rats was measured by hot plate test, measuring two parameters, time-latency to start licking their paws and to jump. In addition, we designed a more specific test for the PA test, evaluating the pain threshold to an increasing intensity of electrical shock in their paws.

The results obtained in hot plate test showed an analgesic effect in the WIN0.5 group of rats (Figure 16A, latency licked paw, VEH: 7 ± 0.5 sec *vs* WIN0.5: 9.2 ± 0.6 sec, Figure 16B, jump latency, VEH: 16 ± 4 sec *vs* WIN0.5: 32 ± 5 sec, *p≤0.05). In the electrical shock-evoked pain threshold test, the latency time to start vocalization (indicative of pain) of WIN0.5 group of rats was also higher than for VEHICLE group (Figure 16C, VEH: 0.03 ± 0.008 sec *vs* WIN0.5: 0.071 ± 0.01 sec, p≤0.05). The results obtained in both pain tests indicated a possible bias of the step-through latency times measured in PA for WIN0.5 group of rats.

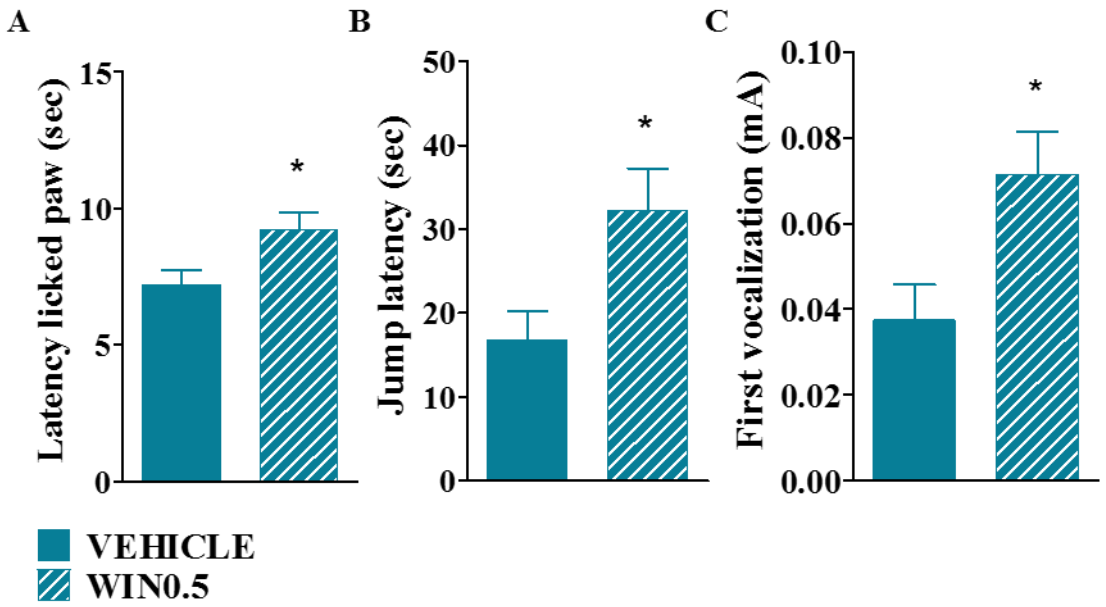

Figure 16. (A) Latency licked paw in hot plate test, (B) Jump latency in hot plate test and (C) First vocalization in the electrical shock-evoked pain threshold test (mean ± S.E.M, *p≤0.05) compared to VEHICLE group.

2.3. Subchronic WIN55,212-2 administration leads to increased muscarinic signaling

The effect of WIN55,212-2 administration on cholinergic receptors modulation was studied. The activity of muscarinic receptors was analyzed by means of autoradiography.

The [^{35}S]GTPγS binding stimulated by carbachol was measured in brain areas related to learning and memory to localize and quantify the activity of M_2/M_4 receptors. Basal binding was similar for VEH and WIN0.5 groups in all the brain areas that were analyzed. The $G_{i/o}$ coupled M_2/M_4 receptor activity induced by carbachol was increased in cortex layer (**Motor cortex layer I-V**: VEH: 88 ± 16 % *vs* WIN0.5: 154 ± 17 % *p≤0.05), in septal nuclei (**MS**: VEH: 268 ± 27 *vs* WIN0.5: 374 ± 43 %; **HDB:** VEH: 139 ± 23 % *vs* WIN0.5: 244 ± 37 %, *p≤0.05) and hippocampus (**CA3 pyramidal**: VEH: 25 ± 19 % *vs* WIN0.5: 95 ± 29) (Figure 17, table 7).

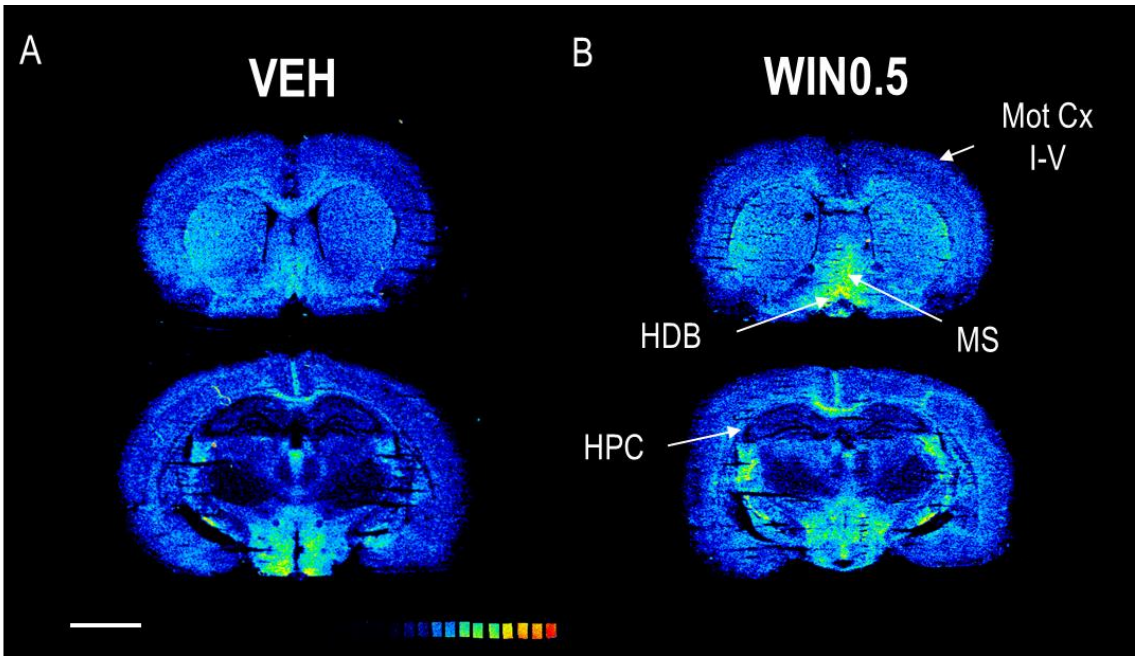

Figure 17. Representative autoradiograms corresponding to coronal sections from of (A) VEH and (B) WIN0.5 rats showing [^{35}S]GTPγS binding stimulated by carbachol (100 µM) in HDB: Horizontal diagonal band, Mot Cx I-V: Motor cortex layer I-V and MS: Medial septum. Scale bar: 4 mm.

TABLE 7. [^{35}S]GTPγS basal and carbachol-induced (100 µM) binding expressed as percentage of stimulation over the basal binding, in different brain areas related to learning and memory control.

	Basal binding (nCi/g t.e.)		Carbachol stimulation (% over basal)	
Brain region	VEH	WIN0.5	**VEH**	**WIN0.5**
Cerebral cortex				
Cingulate	286 ± 24	296 ± 28	102 ± 21	115 ± 19
Motor				
Layer I-V	236 ± 35	235 ± 30	88 ± 16	154 ± 17*
Layer VI	282	268 ± 32	169 ± 21	154 ± 34
Somatosensory				
Layer I-V	198 ± 24	199 ± 26	156 ± 28	164 ± 53
Layer VI	262 ± 75	252 ± 34	178 ± 21	194 ± 38
Basal ganglia				
Globus pallidus	369 ± 32	433 ± 52	76 ± 33	116 ± 75
Striatum	286 ± 30	286 ± 32	221 ± 22	188 ± 26
Diencephalon				
B	334 ± 22	392 ± 77	129 ± 26	195 ± 35
HDB	332 ± 16	302 ± 30	139 ± 23	244 ± 37*
VDB	320 ± 31	326 ± 45	247 ± 22	250 ± 36
Medial septum	329 ± 33	325 ± 46	268 ± 27	374 ± 43*
Hippocampus				
CA1	401 ± 43	433 ± 12	56 ± 17	62 ± 17
Oriens	392 ± 38	361 ± 63	51 ± 16	64 ± 23
Pyramidal	323 ± 28	354 ± 41	65 ± 15	88 ± 46
Radiatum	424 ± 26	432 ± 23	39 ± 7	49 ± 8
CA2	336 ± 24	385 ± 19	50 ± 9	47 ± 11
CA3	329 ± 19	368 ± 17	48 ± 5	36 ± 6
Oriens	298 ± 37	295 ± 56	64 ± 23	67 ± 18
Pyramidal	384 ± 26	393 ± 29	25 ± 19	95 ± 29*
Radiatum	319 ± 17	354 ± 31	34 ± 9	30 ± 8
Dentate gyrus	319 ± 22	362 ± 43	37 ± 7	48 ± 13
Granular	444 ± 43	468 ± 27	38 ± 10	42 ± 17
Molecular	230 ± 28	221 ± 21	40 ± 8	34 ± 11
Polimorphic	392 ± 28	361 ± 63	27 ± 10	27 ± 6
Amygdala	495 ± 29	433 ± 29	98 ± 18	75 ± 31

HDB: horizontal diagonal band, VDB: vertical diagonal band and B: nucleus basalis magnocellularis. Data are mean ± S.E.M. values from VEH and WIN0.5 groups of rats. *p≤0.05 when compared to VEH group.

2.4. Subchronic treatment with WIN55,212-2 modifies AChE activity

The effect of WIN55,212-2 administration on AChE activity was studied in brain areas related to learning and memory by AChE histochemistry. The WIN55,212-2 administration decreased the AChE positive ($AChE^+$) fiber density in motor cortex (**Motor cortex layer I-V**: VEH: 11 ± 0.5 *vs* WIN0.5: 9 ± 0,5 O.D. (a.u.) **Motor cortex layer VI**: VEH: 12 ± 0.3 *vs* WIN0.5: 10 ± 0.4 O.D. (a.u.)) and in hippocampus (**CA1**: VEH: 14 ± 0.6 % *vs* WIN0.5: 12 ± 0.6 O.D. (a.u.)) (Figure 18, Table 8).

TABLE 8. $AChE^+$ fiber densities expressed in optical density (a.u.), obtained as AChE enzymatic staining.

$AChE^+$ Optical Density (a.u.)		
Brain region	VEH	WIN0.5
Cerebral cortex		
Cingulate	13 ± 0.5	12 ± 1
Motor		
Layer I-V	11 ± 0.5	9 ± 0.4*
Layer VI	12 ± 0.3	10 ± 0.4*
Somatosensory		
Layer I-V	12 ± 0.8	11 ± 0.5
Layer VI	14 ± 0.7	13 ± 0.6
Basal ganglia		
Globus pallidus	15 ± 2	13 ± 1
Striatum	54 ± 3	49 ± 2
Diencephalon		
B	30 ± 1	31 ± 3
HDB	49 ± 4	49 ± 3
VDB	41 ± 2	43 ± 2
Medial septum	42 ± 2	42 ± 1
Hippocampus		
CA1	14 ± 0.6	12 ± 0.6*
Oriens	13 ± 0.6	13 ± 1
Pyramidal	20 ± 0.6	18 ± 1
Radiatum	9 ± 0.5	8 ± 0.4
CA2	13 ± 0.5	12 ± 0.4
CA3	18 ± 0.8	17 ± 0.4
Oriens	16 ± 1	16 ± 1
Pyramidal	30 ± 1	28 ± 2
Radiatum	15 ± 0.8	13 ± 0.7
Dentate gyrus	15 ± 0.6	15 ± 0.6
Granular	19 ± 1	18 ± 1
Molecular	14 ± 0.4	15 ± 0.8
Polimorphic	15 ± 1	16 ± 1
Amygdala	39 ± 5	39 ± 3

HDB: horizontal diagonal band, VDB: vertical diagonal band and B: nucleus basalis magnocellularis. Data are mean ± S.E.M. values from VEH and WIN0.5 rats groups. *p≤0.05 when compared to VEHICLE group.

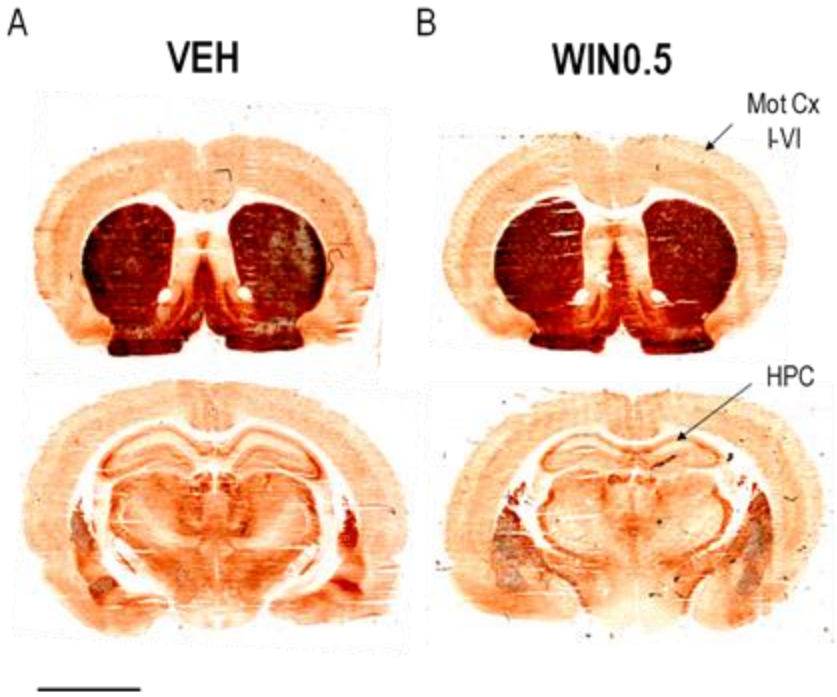

Figure 18. AChE staining in brain coronal slices at two different levels of (A) VEH and (B) WIN0.5 treated groups. Mot Cx I-VI: Motor cortex layer I-VI. HPC: Hippocampus. Scale bar: 4 mm.

2.5. Subchronic WIN55,212-2 administration leads to altered CB_1-mediated activity

The effect of WIN55,212-2 (0.5 mg/kg) administration on cannabinoid receptors modulation was studied. The activity and density of CB_1 receptors was analyzed by means of autoradiography.

The [^{35}S]GTPγS binding was stimulated *in vitro* also by WIN55,212-2 (10 μM) and the percentage over the basal was measured in brain areas related to learning and memory to localize and quantify the activity of CB_1 receptors. . The activity mediated by $G_{i/o}$-coupled CB_1 receptors was increased following the WIN55,212-2 treatment in several areas related to learning and memory processes. (**Motor cortex layer I-V**: VEH: 216 ± 41 % *vs* WIN0.5: 405 ± 72 %. **Striatum**: VEH: 452 ± 57 % *vs* WIN0.5: 758 ± 143 %. **VDB**: VEH: 224 ± 58 % *vs* WIN0.5: 613 ± 179 %. **CA1 oriens**: VEH: 17 ± 5 *vs* WIN0.5: 62 ± 12 %. **CA1 radiatum**: 230 ± 41 % *vs* WIN0.5: 350 ± 87 %. **CA3**: VEH: 276 ± 42 % *vs* WIN0.5: 425 ± 58 %. **CA3 radiatum**: VEH: 74 ± 21 % *vs* WIN0.5: 184 ± 44 %. **Dentate gyrus**: VEH: 277 ± 51 % *vs* WIN0.5: 484 ± 66 %, Figure 19, Table 9).

TABLE 9. [^{35}S]GTPγS basal and WIN55,212-2 (10 µM)-induced binding expressed as percentage of stimulation over the basal binding in different areas related to cholinergic control of learning and memory.

	Basal binding (nCi/g t.e.)		WIN55,212-2 stimulation (% over basal)	
Brain region	VEH	WIN0.5	**VEH**	**WIN0.5**
Cerebral cortex				
Cingulate	113 ± 14	124 ± 19	248 ± 36	298 ± 55
Motor				
Layer I-V	91 ± 13	110 ± 15	216 ± 41	405 ± 72*
Layer VI	110 ± 15	121 ± 17	353 ± 51	354 ± 39
Somatosensory				
Layer I-V	90 ± 18	90 ± 23	156 ± 47	259 ± 41
Layer VI	117 ± 13	113 ± 26	353 ± 66	378 ± 96
Basal ganglia				
Globus pallidus	566 ± 50	512 ± 35	874 ± 115	890 ± 103
Striatum	176 ± 21	170 ± 31	452 ± 57	738 ± 143*
Diencephalon				
B	475 ± 59	482 ± 69	231 ± 51	277 ± 46
HDB	177 ± 21	174 ± 34	230 ± 40	257 ± 48
VDB	283 ± 62	292 ± 53	224 ± 58	613 ± 179*
Medial septum	240 ± 52	292 ± 53	206 ± 37	356 ± 61
Hippocampus				
CA1	407 ± 58	454 ± 53	104 ± 27	175 ± 22
Oriens	532 ± 14	579 ± 22	17 ± 5	62 ± 12*
Pyramidal	222 ± 39	289 ± 71	230 ± 41	312 ± 93
Radiatum	335 ± 61	355 ± 95	137 ± 23	350 ± 87*
CA2	252 ± 39	272 ± 34	199 ± 45	234 ± 49
CA3	158 ± 23	188 ± 36	276 ± 42	425 ± 58*
Oriens	575 ± 30	499 ± 72	58 ± 19	57 ± 12
Pyramidal	205 ± 50	229 ± 55	305 ± 110	323 ± 130
Radiatum	389 ± 50	359 ± 50	74 ± 21	184 ± 44*
Dentate gyrus	160 ± 28	190 ± 34	277 ± 51	484 ± 66*
Granular	117 ± 28	105 ± 29	318 ± 101	398 ± 104
Molecular	245 ± 50	297 ± 28	174 ± 38	308 ± 90
Polimorphic	168 ± 18	187 ± 36	324 ± 45	338 ± 76
Amygdala	468 ± 65	498 ± 70	213 ± 59	407 ± 87

HDB: horizontal diagonal band, VDB: vertical diagonal band and B: nucleus basalis magnocellularis. Data are mean ± S.E.M. values from VEH and WIN0.5 groups. *p≤0.05 when compared to VEH group.

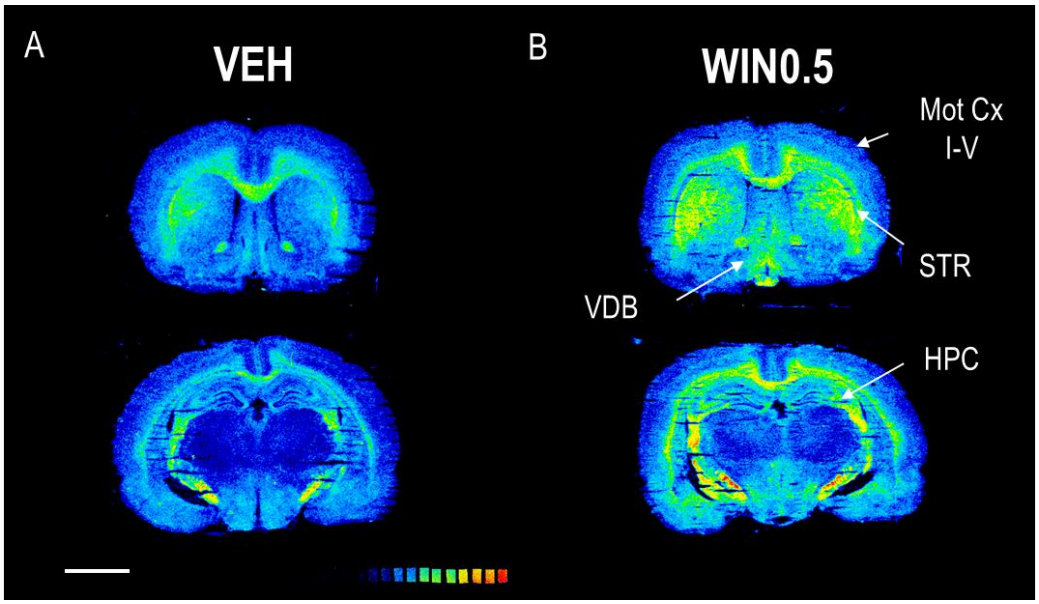

Figure 19. Representative autoradiograms corresponding to coronal sections from (A) VEHICLE and (B) WIN55,212-2 (0.5 mg/kg)-treated rats, that showed [^{35}S]GTPγS stimulated by WIN55,212-2 (10 μM) in Mot Cx I-V: Motor cortex layer I-V, VDB: vertical diagonal band, STR: striatum and HPC: hippocampus. Scale bar: 4 mm.

The CB_1 receptor densities were studied in the same brain areas by [^{3}H]CP55,940 binding. The treatment with the cannabinoid agonist WIN55,212-2 increased CB_1 receptors in the cerebral cortex (**Motor cortex layer I-V**: VEH: 247 ± 13 fmol/g t.e. *vs* WIN0.5: 296 ± 13 fmol/g t.e.; **Motor cortex layer VI**: VEH: 262 ± 34 fmol/g t.e. *vs* WIN0.5: 346 ± 13 t.e. fmol/g and **Somatosensorial cortex layer VI**: VEH: 194 ± 31 fmol/g t.e. *vs* WIN0.5: 273 ± 26 fmol/g t.e., *$p \leq 0.05$, Figure 20, Table 10).

TABLE 10. Autorradiographic densities of CB_1 receptors expressed in fmol/mg t.e., obtained as specific binding of [^{3}H]CP55,940.

Specific binding of [^{3}H]CP55,940 (fmol/g t.e.)		
Brain region	VEH	WIN0.5
Cerebral cortex		
Cingulate	272 ± 16	299 ± 29
Motor		
Layer I-V	247 ± 13	296 ± 13*
Layer VI	262 ± 34	346 ± 13*
Somatosensory		
Layer I-V	211 ± 20	212 ± 20
Layer VI	194 ± 31	273 ± 26*
Basal ganglia		
Globus pallidus	1274 ± 93	1314 ± 121
Striatum	586 ± 35	589 ± 62
Diencephalon		
B	307 ± 41	325 ± 41
HDB	189 ± 22	172 ± 32
VDB	229 ± 21	250 ± 23
Medial septum	237 ± 25	259 ± 21
Hippocampus		
CA1	413 ± 16	394 ± 20
Oriens	435 ± 29	413 ± 22
Pyramidal	428 ± 35	384 ± 24
Radiatum	475 ± 33	447 ± 41
CA2	428 ± 26	407 ± 24
CA3	485 ± 18	448 ± 23
Oriens	414 ± 18	402 ± 32
Pyramidal	349 ± 22	301 ± 30
Radiatum	483 ± 33	454 ± 31
Dentate gyrus	355 ± 14	308 ± 20
Granular	116 ± 20	117 ± 22
Molecular	352 ± 13	318 ± 21
Polimorphic	450 ± 26	438 ± 31
Amygdala	202 ± 23	206 ± 21

HDB: horizontal diagonal band, VDB: vertical diagonal band and B: nucleus basalis magnocellularis. Data are mean ± S.E.M. values from VEH and WIN0.5 groups of rats. *$p \leq 0.05$ when compared to VEH group.

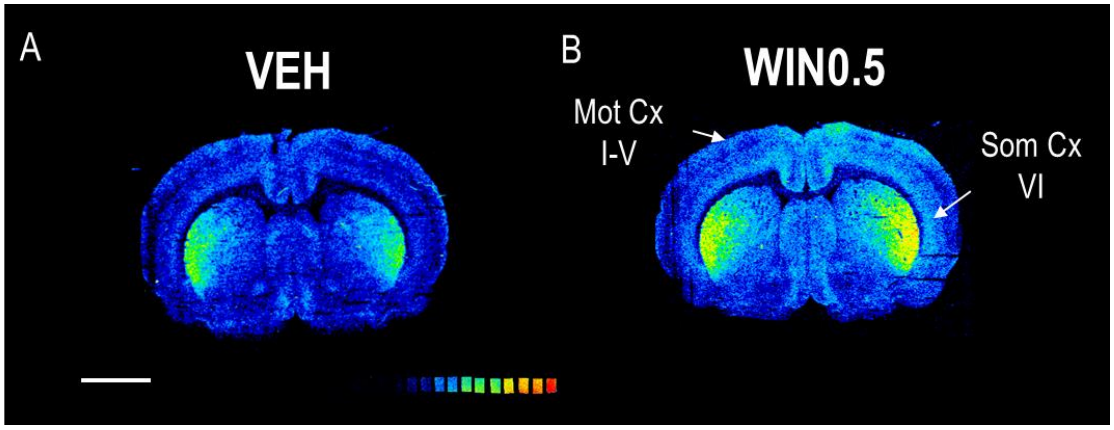

Figure 20. Representative autoradiograms corresponding to coronal sections from (A) VEHICLE and (B) WIN55,212-2 (0.5 mg/kg)-treated rats showing up-regulation of the [^{3}H]CP55,940 binding (3 nM) in Mot Cx I-V: Motor cortex layer I-V and Som Cx VI: Somatosensorial cortex layer VI. Scale bar: 4 mm.

3. EFFECTS OF THE SUBCHRONIC WIN55,212-2 ADMINISTRATION ON A RAT MODEL OF BASAL FOREBRAIN CHOLINERGIC LESION

As previously described in the present study, WIN55,212-2 (0.5 mg/kg) was able to prevent scopolamine-elicited amnesic effects. The next step we raised was to follow a similar treatment in a more specific animal model of cerebral cholinergic dysfunction of learning and memory abilities such us the model of basal forebrain cholinergic lesion induced by intraparenquimal 192IgG-saporin. We mixed the schedules described in the previous sections to obtain the best possible instructions that would allow us to combine lesion, administration of the drug and performing the BM and PA learning and memory tests. The figure 21 illustrates the followed treatment schedules and groups of treatment.

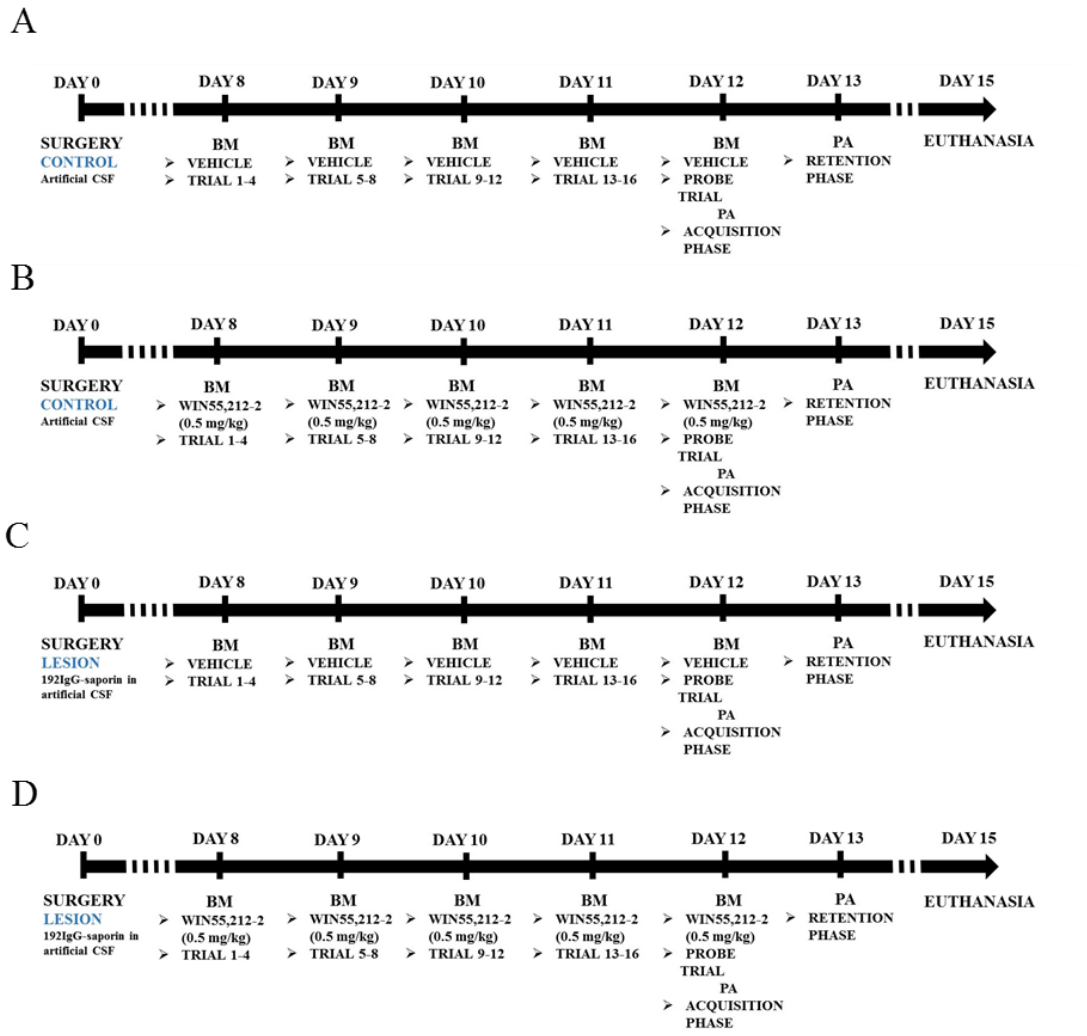

Figure 21. Training schedules followed for each of the four groups of treatment designed to evaluate the effects of WIN55,212-2 (0.5 mg/kg i.p. during 5 days) in both spatial and aversive memory in lesion and corresponding control animals.

3.1. Subchronic WIN55,121-2 administration reverted the cognitive impairment induced by 192IgG-saporin in basal forebrain

To evaluate the spatial learning and memory behavior the rats were trained in the BM test. During the treatment, we evaluated 3 spatial acquisition parameters such as total latency (sec), total path length (cm) and speed (cm/sec). Total latency and total path length were decreased during the acquisition phase (Figure 22 A and B), however the total latency showed significant differences between all groups during the first trial of days 1 and 4 of the acquisition or learning, i.e. during trial 1 and trial 13 (Trial 1 CONTROL: 58 ± 7 sec, LESION: 62 ± 8 sec, C+W0.5: 116 ± 15 sec, L+W0.5: 108 ± 14 sec. Trial 13 CONTROL: 9 ± 1 sec, LESION: 17 ± 2 sec, C+W0.5: 11 ± 2 sec, L+W0.5: 9 ± 1 sec, Figure 22D). The speed was increasing with each trial, but WIN55,121-2 -treated rats moved more slowly than vehicle-treated rats during all 16 trials (Speed CONTROL: 14 ± 1 cm/sec, LESION: 17 ± 1 cm/sec, C+W0.5: 11 ± 0.6 cm/sec, L+W0.5: 11 ± 0.6 cm/sec Figure 22 C).

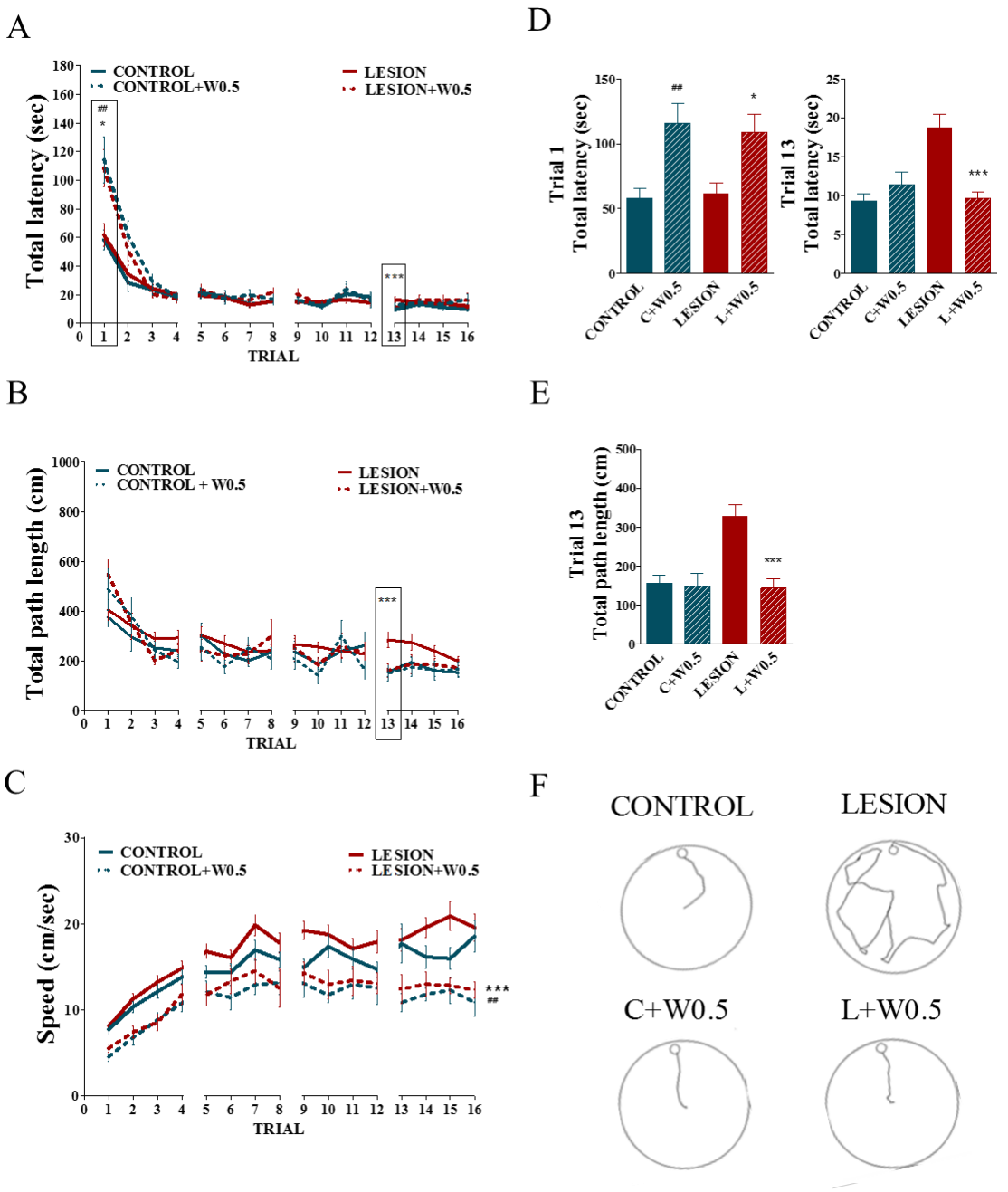

Figure 22. (A) Total latency, (B) Total path length and (C) Average speed during each of the sixteen trials of the acquisition phase (***p≤0.01 LESION *vs* L+W0.5; ##p≤0.01 CONTROL *vs* C+W0.5). (D) Total latency of trials 1 (*p≤0.05 LESION *vs* L+W0.5, ##p≤0.01 CONTROL+W0.5 *vs* CONTROL) and 13. (***p≤0.01 LESION *vs* L+W0.5). (E) Trial 13 total path length (***p≤0.01 LESION *vs* L+W0.5). (F) Representative trajectory of trial 13 in the experimental groups. Data are (mean ± S.E.M.)

On probe trial, after the last training day, the latency in target quadrant was measured for the four groups of rats. CONTROL, C+W0.5 and L+W0.5 groups took more time in the target quadrant than LESION group (Figure 23 A, time spent in target quadrant: CONTROL: 89 ± 4 sec, C+W0.5: 76 ± 7 sec, LESION: 50 ± 3 sec, L+W0.5: 82 ± 7 sec. CONTROL *vs* LESION †††p≤0.001, C+W0.5 *vs* LESION ##p≤0.01, L+W0.5 *vs* LESION ***p≤0.01).

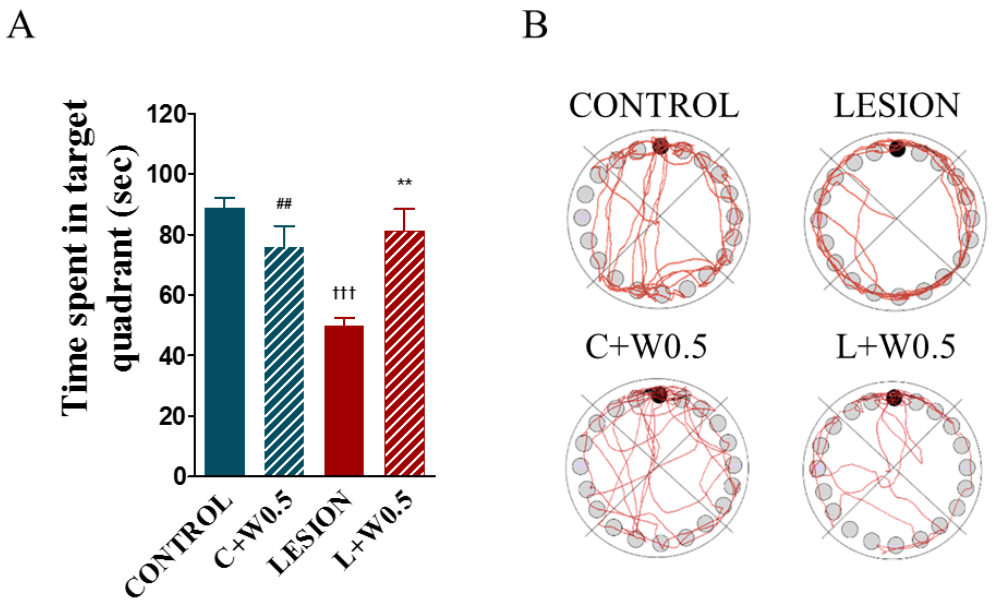

Figure 23. (A) Time spent in target quadrant on probe trial (B) Representative trajectory during 180 sec of the probe trial. Data are mean ± S.E.M. CONTROL *vs* LESION †††p≤0.001, C+W0.5 *vs* LESION ##p≤0.01, L+W0.5 *vs* LESION ***p≤0.01. Note the accumulation of trajectories in the target quadrant for CONTROL, C+W0.5 and L+W0.5.

The passive avoidance test was used to analyze the learning and memory of an aversive stimulus. The day of the probe trial of Barnes Maze (12th day) and after the final probe trial, the acquisition latency parameter was evaluated in the passive avoidance test. LESION group exhibited less latency than the other groups. (Figure 24 A, LESION: 6 ± 1 sec, L+W0.5: 13 ± 2 sec, CONTROL: 12 ± 2 sec and C+W0.5: 12 ± 2 sec, **p≤0.01 CONTROL *vs* LESION). 24 hours later, all trained animals were tested again to evaluate aversive memory. Then, the step-through latency time was measured. The four groups of rats were analyzed and only the CONTROL group was able to remember the aversive stimulus (100 %). The other groups, LESION, W0.5 and C+WIN0.5 showed that just a 14 %, 10 % and 0 % of the animals respectively, were able to remember the aversive stimulus. (Figure 24 B).

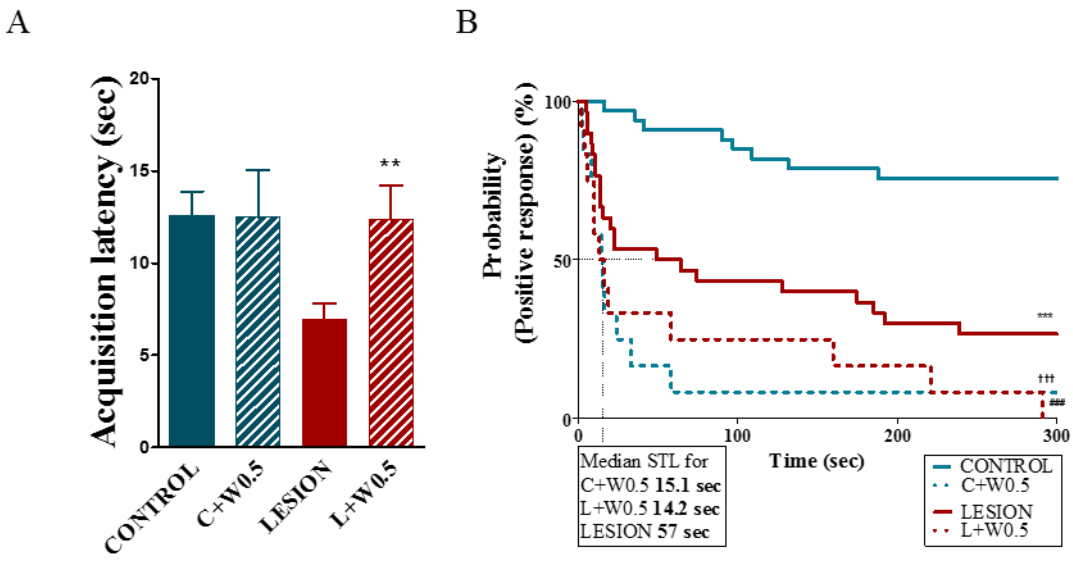

Figure 24. (A) Acquisition latency times in the learning trial of the passive avoidance test (mean ± S.E.M., **p≤0.01, CONTROL *vs* LESION). (B) Step-Through latency times of passive avoidance test represented as Kaplan-Meier survival curves CONTROL *vs* LESION: ***p≤0.001, CONTROL *vs* C+W0.5: ###p≤0.001 and CONTROL *vs* L+W0.5: †††p≤ 0.001, Log-Rank/Mantel-Cox test).

3.2. WIN55,212-2 subchronic treatment is able to restore cognitive impairment induced by both short-term and long-term cholinergic lesions with 192IgG-saporin in basal forebrain

The effect of subchronic treatment with WIN55,212-2 (0.5 mg/kg i.p.) on learning and memory was also analyzed at two different post-lesion times. To study the effects of WIN55,212-2 in short-term lesion, two different BM test were assayed in the same animals. Firstly, 7 days after the lesion, the rats were trained during the 16 spatial acquisition trials and the probe trial (BM1) without any treatment, then, 10 days later a second BM test was assayed (BM2) but together with the subchronic treatment with WIN55,212-2 (0.5 mg/kg i.p.; 5 days). The obtained results showed that WIN55,212-2 treatment was able to enhance the time in target quadrant during BM2 in those LESION animals that previously, were not able to remember the escape hole during the probe trial in BM1 (LESION: 52 ± 3 sec *vs* L+W0.5: 90 ± 31 sec, LESION vs L+W0.5 ***p≤0.001. Figure 25 F).

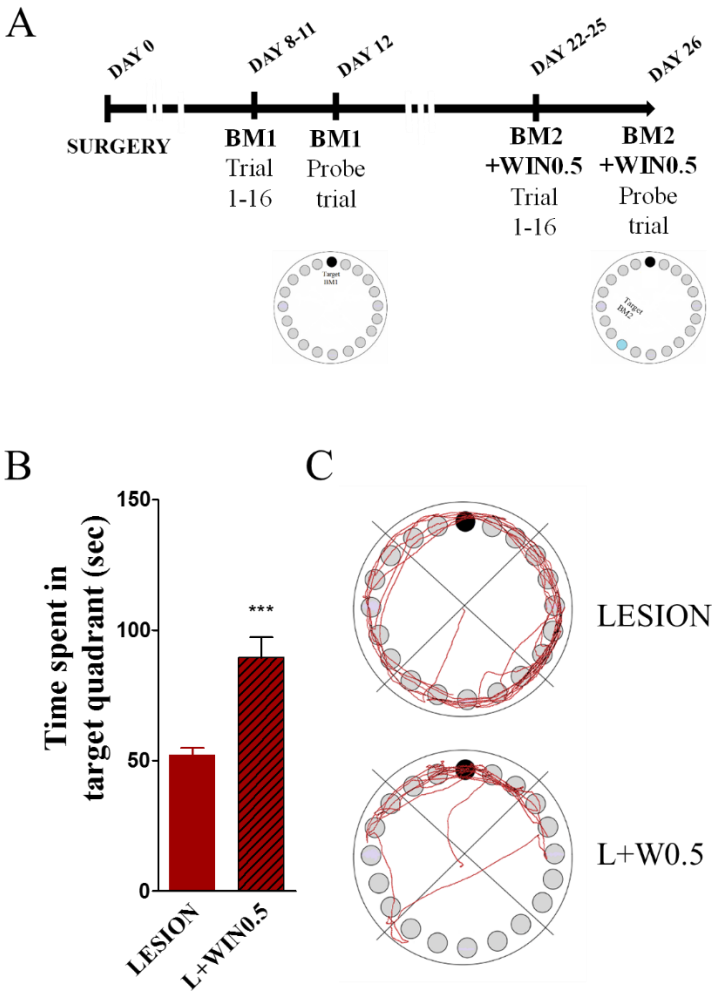

Figure 25. (A) A Schedule to follow the spatial learning and memory in the same rats before (12 days after lesion) and after the subchronic treatment with WIN55,212-2; 0.5 mg/kg (at day 22 after lesion) at a short time after the lesion. LESION *vs* L+W0.5 ***p≤0.001. (B) Time spent in target quadrant on probe trial. Data are mean ± S.E.M. (B) Representative trajectory on probe trial (BM1 *vs* BM2) for the same animal before and after the treatment.

To examine the effect of WIN55,212-2 subchronic treatment in a long-term lesion, firstly we evaluated if the effects of the lesion on learning and memory were able to remain during 8 months. The same animal executed a total of three BM tests, the first was initiated 7 days after the lesion (BM1), the second was evaluated 8 months after the lesion (BM2) and the third, together with the WIN55,212-2 subchronic treatment, 15 days after the BM2 (BM3). 8 months after the lesion the animals did not perform correctly the probe trial of BM, i.e., the animals remained cognitive impaired 8 months after the lesion. When WIN55,212-2 was subchronically administered to animals after 8 months of lesion a huge improvement in the time spent in the target quadrant was recorded. (0 MONTH: 50 ± 6 sec, 8 MONTH: 66 ± 5 sec and 8M+W0.5: 103 ± 6 sec. 0 MONTH *vs* 8M+W0.5 ***p≤0.001, 8 MONTH *vs* 8M+W0.5 ###p≤0.001. Figure 26 B).

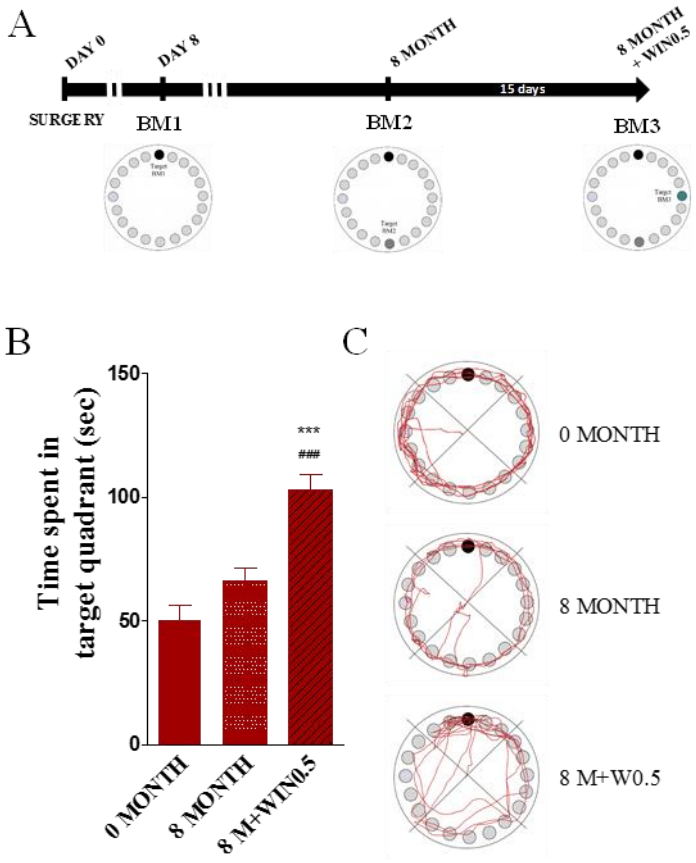

Figure 26. (A) Schedule followed for a LESION group of rats during eight months. The same animals were evaluated in a total of three BM tests: one 7 days after the lesion (BM1), the second 8 months after the lesion (BM2) and the third, together with the WIN55,212-2 subchronic treatment, 15 days after the BM2 (BM3). (B) Time spent in target quadrant on probe trial. Data are mean ± S.E.M. 0 MONTH *vs* 8M+W0.5 ***p≤0.001 and 8 MONTH *vs* 8M+W0.5 ###p≤0.001. (B) Tracking of 180 sec of representative trajectory during the probe trial of the same animal over the time at BM1 (0 month), BM2 (8 month) and BM3 (8 month + W0.5).

3.3. Subchronic WIN55,212-2 administration leads to increased muscarinic signaling after basal forebrain cholinergic lesion

The effect of WIN55,212-2 administration on cholinergic receptors was studied in animals with basal forebrain cholinergic lesion. The activity of muscarinic receptors was analyzed by means of autoradiography.

The [^{35}S]GTPγS binding stimulated by carbachol (100 µM) was measured in brain areas related to learning and memory to localize and quantify the activity of M_2/M_4 receptors. Basal binding was similar in the four groups analyzed in this section (CONTROL, C+W0.5, LESION and L+W0.5) in all the brain areas analyzed. The subchronic treatment of CONTROL rats with WIN55,212-2 (0.5 mg/kg i.p., 5 days) elicited an increase on M_2/M_4 receptor activity (when induced *in vitro* by carbachol 100 µM) in different areas that control learning and memory processes. (**Motor cortex layer I**: CONTROL: 281 ± 14 % *vs* C+W0.5: 395 ± 35 %, **Motor cortex layer II-V**: CONTROL: 266 ± 44 % *vs* C+W0.5: 546 ± 103 % , **Somatosensorial cortex layer VI**: CONTROL: 153 ± 36 % *vs* C+W0.5: 345 ± 66 %, **Striatum**: CONTROL: 160 ± 18 % *vs* C+W0.5: 313 ± 44 %, **HDB**: CONTROL: 129 ± 23 % *vs* C+W0.5: 294 ± 31 %, **Amygdala**: CONTROL: 95 ± 6 % *vs* C+W0.5: 231 ± 39 % , *p≤0.05. Figures 27 and 28).

On the other hand, the treatment of a lesion group of rats (L+W0.5) also was able to the M_2/M_4 receptor activity in cortex in a similar way, increasing the activity(**Motor cortex layer I**: LESION: 87 ± 19 % *vs* L+W0.5: 226 ± 41 %, **Motor cortex layer II-V**: LESION: 147 ± 30 % *vs* L+W0.5: 242 ± 35 %). But, the treatment induced a decrease in M_2/M_4 receptor activity in the hippocampus of L+W0.5 group of rats (**CA1**: LESION: 147 ± 30 % *vs* L+W0.5: 242 ± 35 %, **CA2**: LESION: 230 ± 41 % *vs* L+W0.5: 111 ± 22 %, **CA3**: LESION: 196 ± 36 % *vs* L+W0.5: 51 ± 14 % ##p≤0.01. Figures 27 and 28).

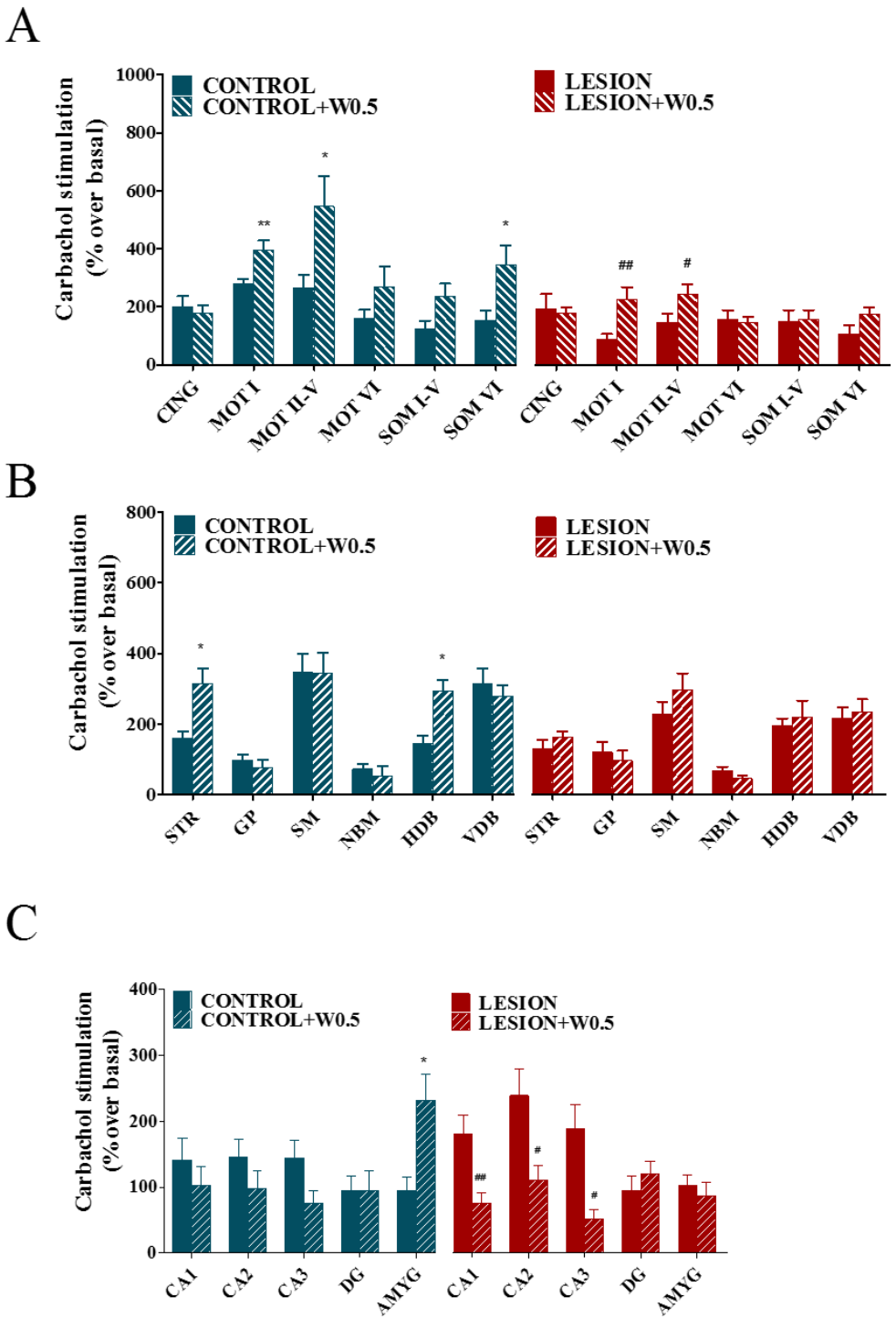

Figure 27.[^{35}S]GTPγS binding stimulated by carbachol (100 μM) in different brain areas represented as % stimulated over the basal levels. (A) Cerebral cortex (CING: cingulate, MOT I: motor cortex layer I, MOT II-V: motor cortex layer II-V, MOT VI: motor cortex layer VI, SOM I: Somatosensorial cortex layer I, SOM VI: Somatosensorial cortex layer VI). (B) Basal ganglia (STR: striatum, GP: Globus pallidus, MS: medial septum, B: nucleus basalis magnocellularis, HDB: horizontal diagonal band, VDB: vertical diagonal band). (C) hippocampus and amygdala (CA1: Oriens, pyramidal, radiatum; CA2: Oriens, pyramidal, radiatum; CA3: Oriens, pyramidal, radiatum; DG: dentate gyrus: Granular, molecular, polymorphic, AMYG: amygdala). (Data are mean ± S.E.M.). *p≤0.05, **p≤0.01 CONTROL *vs* C+W0.5; #p≤0.05, ##p≤0.01 LESION *vs* L+W0.5.

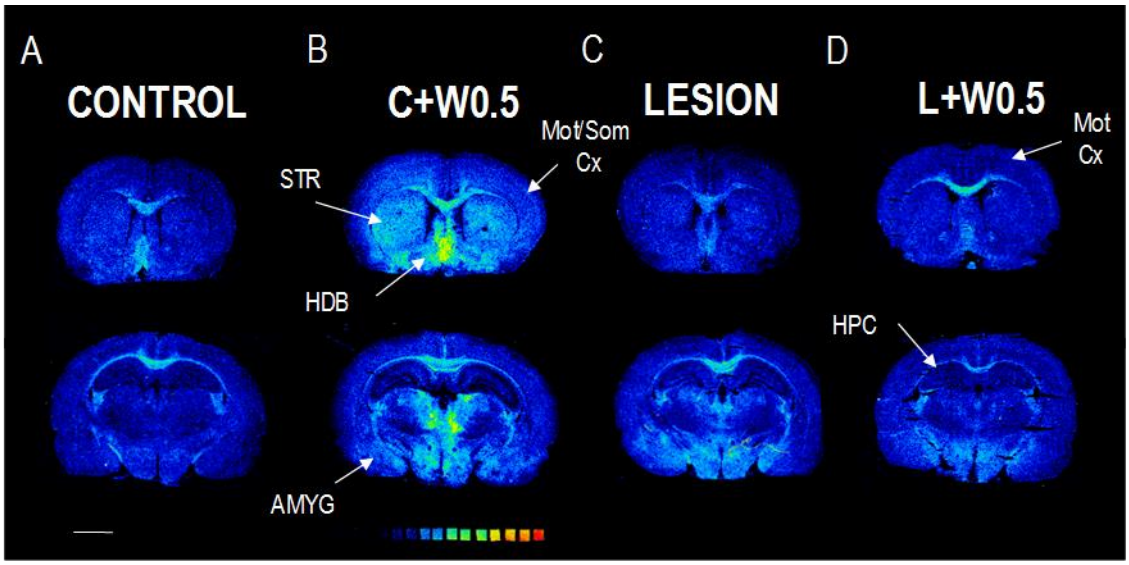

Figure 28. Representative autoradiograms of (A) CONTROL, (B) C+W0.5, (C) LESION and (D) L+W0.5 in rat coronal sections that show [^{35}S]GTPγS stimulated by carbachol (100 µM) in Mot Cx I-V: Motor cortex layer I-V, Som Cx: Somatosensorial cortex layer VI, HDB: Horizontal diagonal band, AMYG: Amygdala and HPC: hippocampus. Scale bar: 4 mm.

The muscarinic receptor density was studied in the same brain areas by measuring the [^{3}H]N-Methyl-Scopolamine specific binding. The WIN55,212-2 administration to the CONTROL group only modified (increase) the density of muscarinic receptors in the most superficial layer of the motor cortex (Figure 29 A). But, when the same treatment was applied to a lesion group of rats, a broad decrease in the densities of muscarinic receptors was recorded in cerebral cortex, basal ganglia and hippocampus. (**Motor cortex layer VI**: LESION: 236 ± 23 *vs* L+W0.5: 187± 27 fmol/g t.e; **Somatosensorial cortex layer I-V**: LESION: 392 ± 27 *vs* L+W0.5: 293 ± 36 fmol/g t.e, **Somatosensorial cortex layer VI**: LESION: 240 ± 18 *vs* L+W0.5: 164 ± 19 fmol/g t.e, **Striatum**: LESION: 338 ± 37 *vs* L+W0.5: 169 ± 20, fmol/g t.e., **B**: LESION: 57 ± 5 *vs* L+W0.5: 37 ± 3 fmol/g t.e., **Amygdala**: LESION: 296 ± 28 *vs* L+W0.5: 205 ± 28 fmol/g t.e. #p<≤0.05 LESION *vs* L+W0.5. Figures 29 and 30).

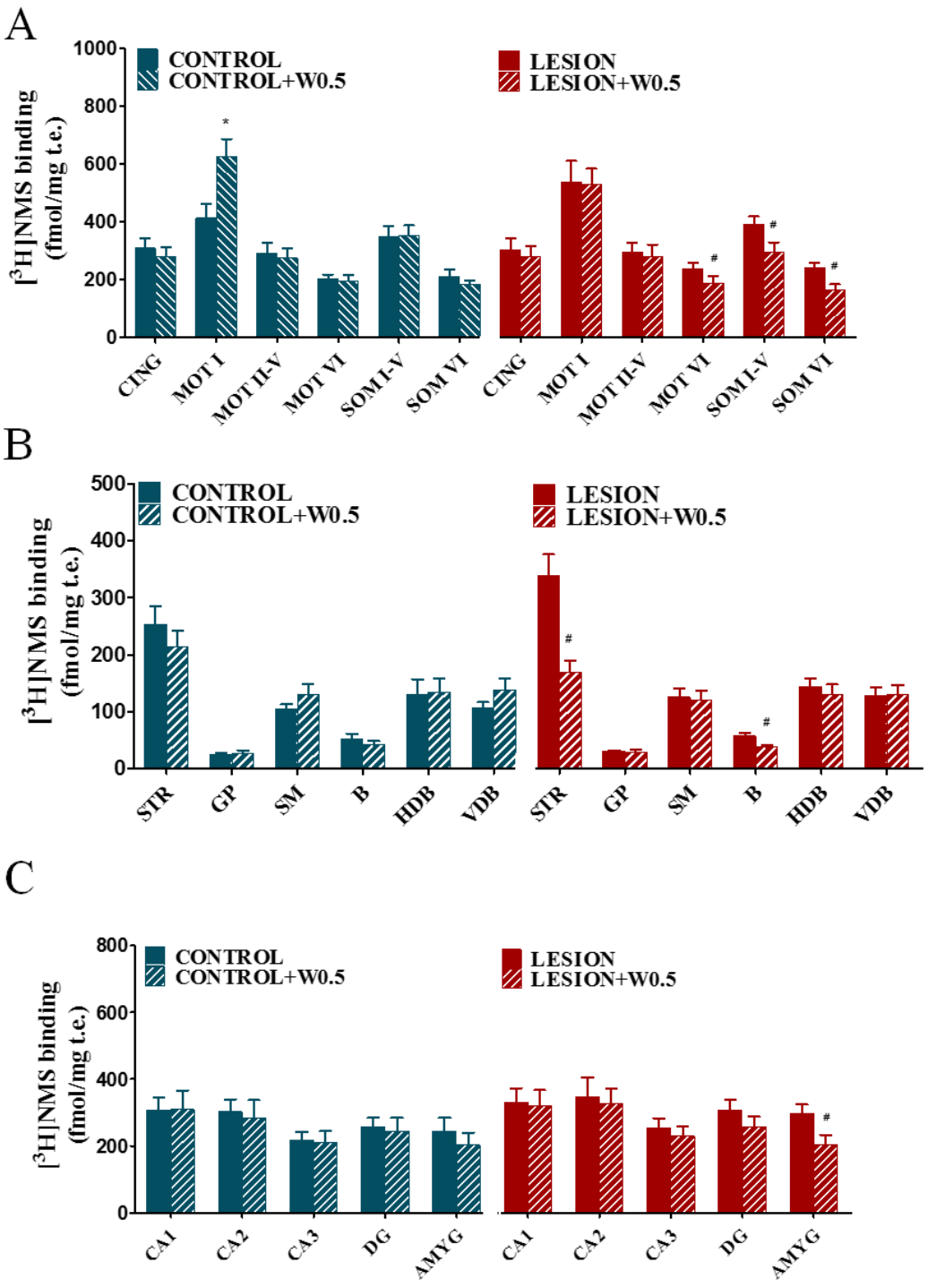

Figure 29. The [^{3}H]NMS binding in different brain areas expressed in fmol/mg t.e. (A) Cerebral cortex (CING: cingulate, MOT I: motor cortex layer I, MOT II-V: motor cortex layer II-V, MOT VI: motor cortex layer VI, SOM I: Somatosensorial cortex layer I, SOM VI: Somatosensorial cortex layer VI). (B) Basal ganglia (STR: striatum, GP: Globus pallidus, MS: medial septum, B: nucleus basalis magnocellularis, HDB: horizontal diagonal band, VDB: vertical diagonal band). (C) Hippocampus and amygdala (CA1: Oriens, pyramidal, radiatum; CA2: Oriens, pyramidal, radiatum; CA3: Oriens, pyramidal, radiatum; DG: dentate gyrus: Granular, molecular, polymorphic, AMYG: amygdala). (Mean ± S.E.M.) *p≤0.05 CONTROL *vs* C+W0.5, #p≤0.05 LESION *vs* L+W0.5.

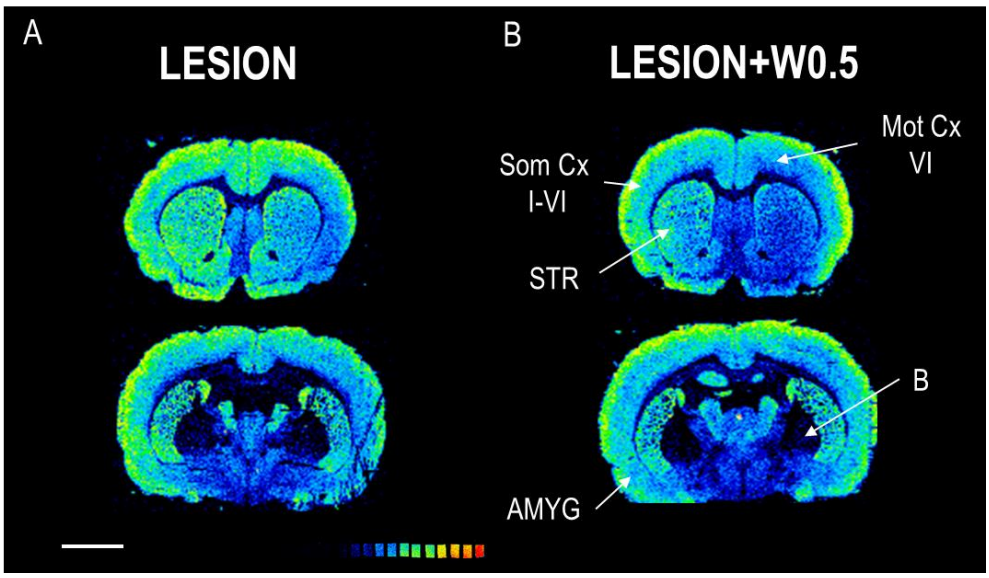

Figure 30. Representative autoradiograms of (A) LESION and (B) L+W0.5 rat coronal sections that show [^{35}S]GTPγS stimulated by carbachol (100 µM) in Mot Cx I-V: Motor cortex layer I-V, Som Cx: Somatosensorial cortex layer VI, HDB: Horizontal diagonal band, AMYG: Amygdala and HPC: hippocampus. Scale bar: 4 mm.

3.4. Subchronic WIN55,212-2 administration modifies cholinergic innervation after basal forebrain lesion

The effect of WIN55,212-2 administration on AChE activity was studied in brain areas related to learning and memory after basal forebrain lesion. The WIN55,212-2 administration to CONTROL rats was able to increase $AChE^{+}$ fiber density in septal nuclei (**MS**: CONTROL: 50 ± 2 *vs* C+W0.5: 59 ± 2 O.D. a.u.; **VDB**: CONTROL: 44 ± 2 *vs* C+W0.5: 65 ± 3O.D. a.u., *p≤0.05. Figure 31 B). Moreover, the WIN55,212-2 administration to a lesion group of rats reverted the decreased of the AChE activity that was induced by the lesion in cortex and B (see results in previous sections) (**Motor cortex layer I**: CONTROL: 17 ± 1, C+W0.5: 15 ± 1, LESION: 9 ± 1, L+W0.5: 14 ± 1 O.D. a.u., **Motor cortex layer II-V**: CONTROL: 18 ± 1, C+W0.5: 17 ± 1, LESION: 8 ± 1, L+W0.5: 16 ± 2 O.D. a.u., **Motor cortex layer VI**: CONTROL: 17 ± 1, C+W0.5: 17 ± 1, LESION: 8 ± 1, L+W0.5: 15 ± 1 O.D. a.u., **Somatosensorial cortex layer I-V**: CONTROL: 18 ± 1, C+W0.5: 17 ± 1, LESION: 9 ± 1, L+W0.5: 16 ± 1 O.D. a.u., **Somatosensorial cortex layer VI**: CONTROL: 20 ± 1, C+W0.5: 18 ± 1, LESION: 11 ± 1, L+W0.5: 18 ± 1 O.D. a.u. and **B:** CONTROL: 36 ± 3, C+W0.5: 33 ± 2, LESION: 23 ± 3, L+W0.5: 31 ± 4 O.D. a.u., ##p≤0.01. Figures 31 and 32).

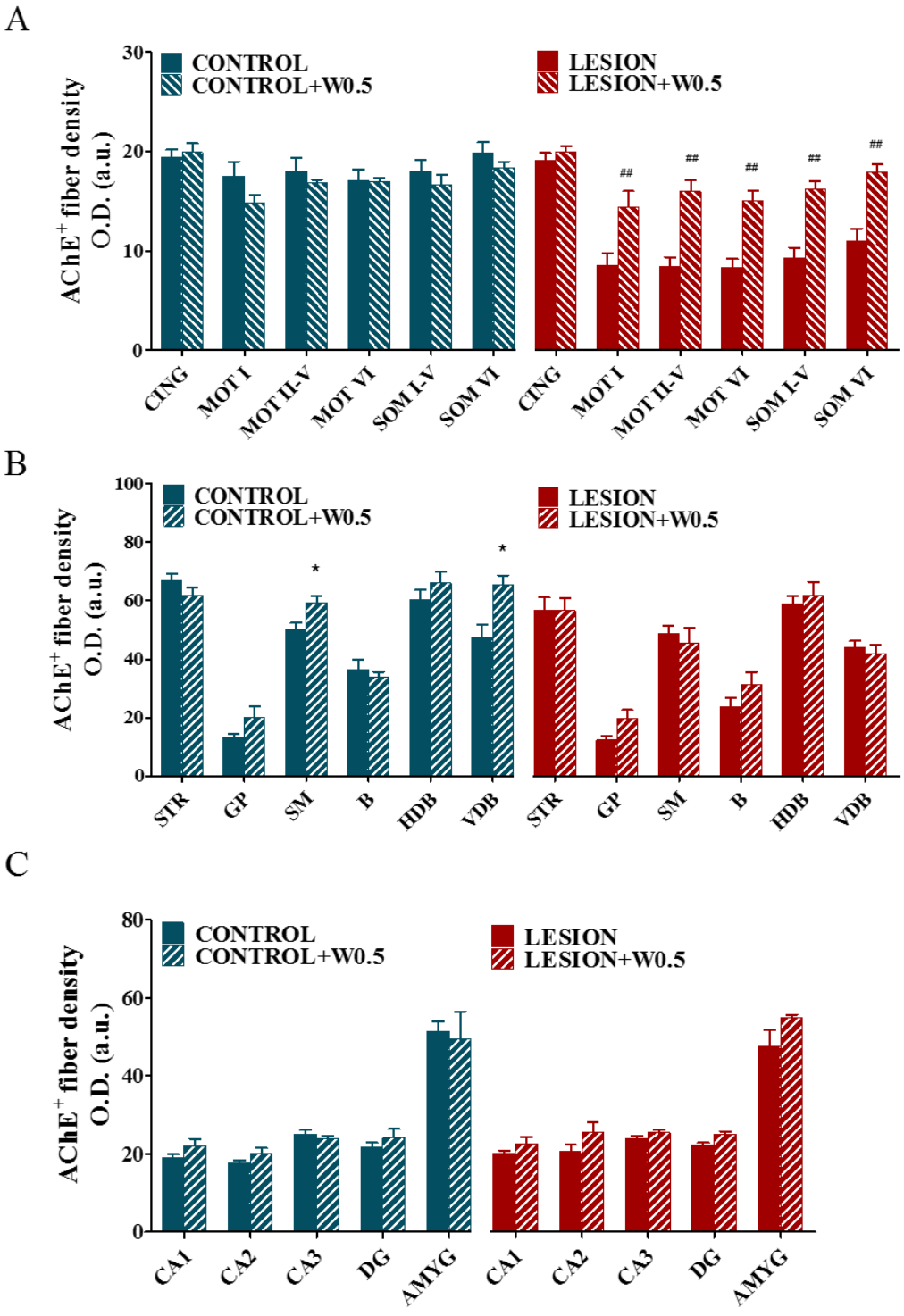

Figure 31. AChE staining in different brain areas represented as O.D. a.u. (A) Cerebral cortex (CING: cingulate, MOT I: motor cortex layer I, MOT II-V: motor cortex layer II-V, MOT VI: motor cortex layer VI, SOM I: Somatosensorial cortex layer I, SOM VI: Somatosensorial cortex layer VI). (B) Basal ganglia (STR: striatum, GP: Globus pallidus, MS: medial septum, B: nucleus basalis magnocellularis, HDB: horizontal diagonal band, VDB: vertical diagonal band). (C) Hippocampus and amygdala (CA1: Oriens, pyramidal, radiatum; CA2: Oriens, pyramidal, radiatum; CA3: Oriens, pyramidal, radiatum; DG: dentate gyrus: Granular, molecular, polymorphic, AMYG: amygdala). (Data are mean ± S.E.M.) *p≤0.05 CONTROL *vs* C+W0.5, ##p≤0.01 LESION *vs* L+W0.5.

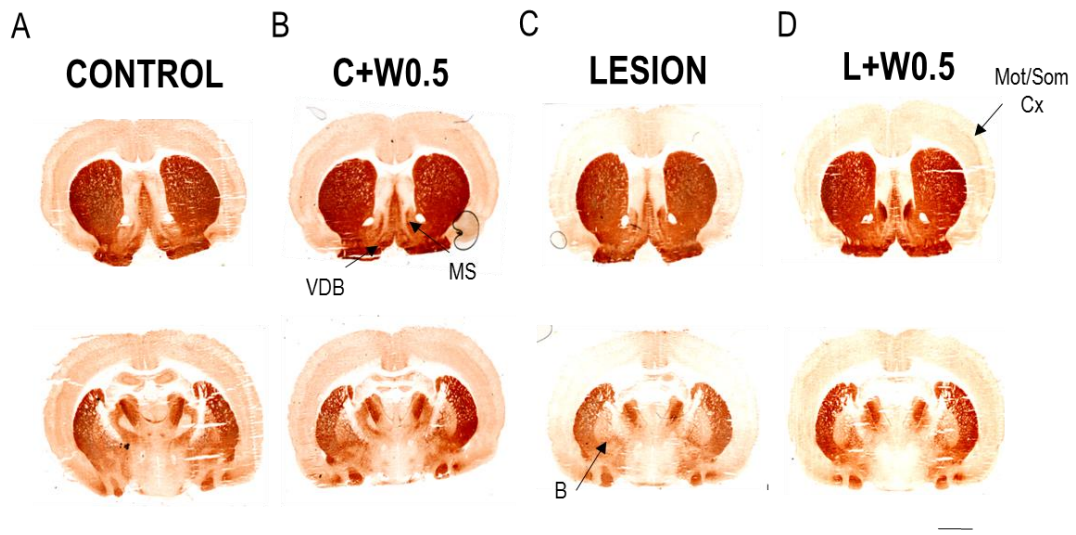

Figure 32. AChE staining in brain coronal slices at different levels of (A) CONTROL, (B) C+W0.5, (C) LESION and (D) L+W0.5 groups of rats. Mot:Motor cortex layer I-VI. Som: Somatosensorial cortex layer I-VI. VDB: vertical diagonal band. MS: medial septum. B: nucleus basalis magnocellularis. Scale bar: 4 mm.

3.5. Subchronic WIN55,212-2 administration modifies CB_1 activity after basal forebrain cholinergic lesion

The effect of subchronic WIN55,212-2 (0.5 mg/kg i.p.) administration to rats after basal forebrain cholinergic lesion on cannabinoid receptors brain densities and activity was also analyzed studied by receptor and [^{35}S]GTPγS autoradiography.

The [^{35}S]GTPγS binding stimulated by WIN55,212-2 (10μM) was measured in brain areas related to learning and memory to localize and quantify the activity of CB_1 receptors. The subchronic treatment with WIN55,212-2 (0.5 mg/kg i.p.) of control rats induced a dramatic increase of CB_1 receptor activity in different areas that control learning and memory processes. (**Motor cortex layer I**: CONTROL: 258 ± 54 % *vs* C+W0.5: 630 ± 121 %, **Motor cortex layer II-V**: CONTROL: 212 ± 50 % *vs* C+W0.5: 469 ± 63 % , **Somatosensorial cortex layer I-V**: CONTROL: 193 ± 49 % *vs* C+W0.5: 482 ± 109 %, **CA1**: CONTROL: 294 ± 56 % *vs* C+W0.5: 635 ± 117 %, **CA2**: CONTROL: 360 ± 71 % *vs* C+W0.5: 684 ± 76 %, **CA3**: CONTROL: 434 ± 64 % *vs* C+W0.5: 677 ± 86 % , **DG**: CONTROL: 412 ± 69 % *vs* C+W0.5: 747 ± 87 %, **AMYG**: CONTROL: 190 ± 62 % *vs* C+W0.5: 406 ± 74 %. *p≤0.05 Figure 33).

In addition, the same treatment applied to lesion rats also increased CB_1 receptor activity, in both cortical and basal ganglia brain areas recovering the control levels that were down-regulated by the lesion (**Motor cortex layer I**: LESION: 191 ± 51 % *vs* L+W0.5: 380 ± 90 %, **Motor cortex layer II-V**: LESION: 144 ± 22 % *vs* L+W0.5: 365 ± 77 %, **Striatum**: LESION: 217 ± 35 % *vs* L+W0.5: 393 ± 44 %, **MS**: LESION: 160 ± 25 % *vs* L+W0.5: 330 ± 52 %, **VDB**: LESION: 185 ± 30 % *vs* L+W0.5: 348 ± 62 %, Figures 33 and 34).

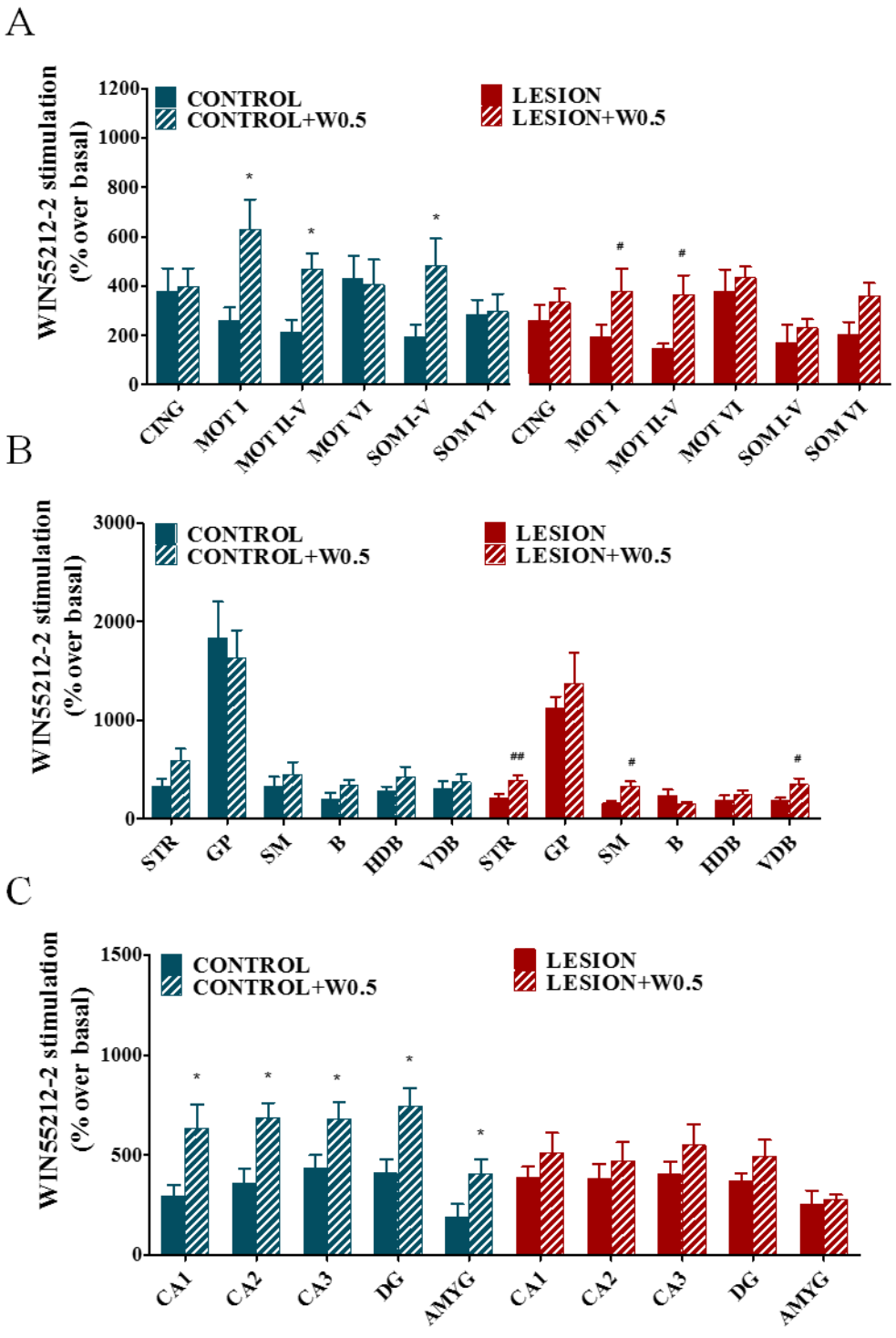

Figure 33. [^{35}S]GTPγS binding stimulated by WIN55,212-2 (10μM) in different brain areas represented as % stimulated over the basal values. (A) Cerebral cortex (CING: cingulate, MOT I: motor cortex layer I, MOT II-V: motor cortex layer II-V, MOT VI: motor cortex layer VI, SOM I: Somatosensorial cortex layer I, SOM VI: Somatosensorial cortex layer VI). (B) Basal ganglia (STR: striatum, GP: Globus pallidus, MS: medial septum, B: nucleus basalis magnocellularis, HDB: horizontal diagonal band, VDB: vertical diagonal band). (C) Hippocampus and amygdala (CA1: Oriens, pyramidal, radiatum; CA2: Oriens, pyramidal, radiatum; CA3: Oriens, pyramidal, radiatum; DG: dentate gyrus: Granular, molecular, polymorphic, AMYG: amygdala). (mean ± S.E.M.) *p≤0.05 CONTROL *vs* C+W0.5; #p≤0.05 ##p≤0.01 LESION *vs* L+W0.5.

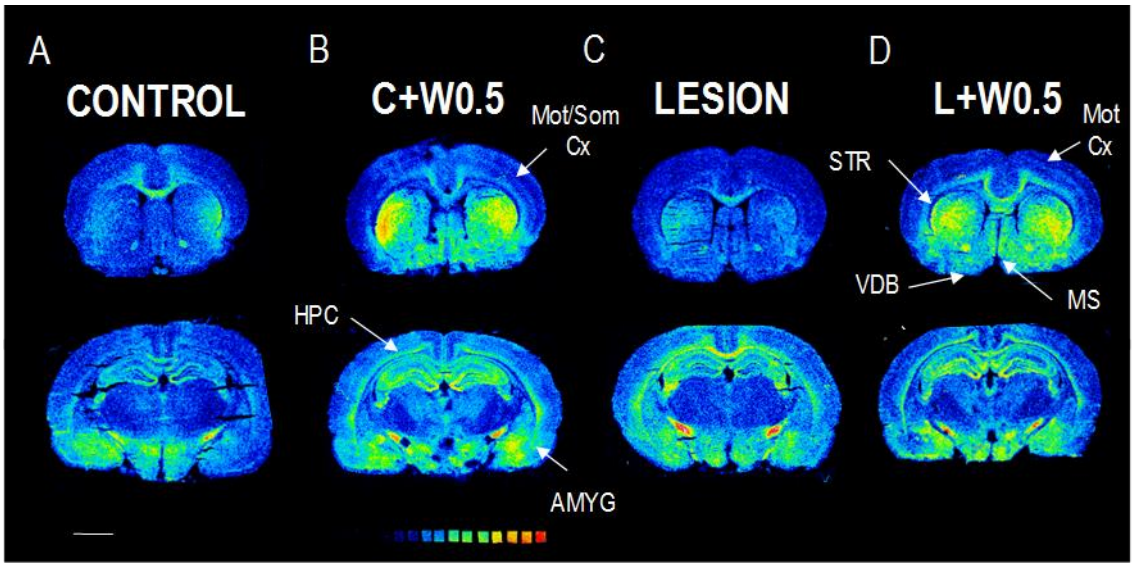

Figure 34. Representative autoradiograms of (A) CONTROL, (B) C+W0.5, (C) LESION and (D) L+W0.5 of rat coronal sections that show [^{35}S]GTPγS stimulated by WIN55,212-2 (10 µM) in Mot Cx: Motor cortex, Som: Somatosensorial cortex, MS: Medial septum, VDB: Vertical diagonal band, STR: Striatum, AMYG: Amygdala, HPC: hippocampus. Scale bar: 4 mm.

CB_1 receptor density was studied in the same brain areas by measuring the [^{3}H]CP55,940 specific binding. The WIN55,212-2 administration to a control group of rats was able to increase the CB_1 densities in cortex and hippocampus (**Cingulate**: CONTROL: 149 ± 15 *vs* C+W0.5: 199 ± 13 fmol/g t.e; **Motor cortex layer I** : CONTROL: 173 ± 19 *vs* C+W0.5: 239 ± 15 fmol/g t.e, **CA1:** CONTROL: 175 ± 23 *vs* C+W0.5: 360 ± 25 fmol/g t.e, **CA3:** CONTROL: 282 ± 28 *vs* C+W0.5: 406 ± 28 fmol/g t.e ; **Dentate gyrus**: CONTROL: 219 ± 32 *vs* C+W0.5: 359 ± 37 fmol/g t.e. Figure 34). Furthermore, when the same treatment was applied to a lesion group of rats there were also up-regulations of CB_1 receptor densities compared to lesion but untreated animals in cerebral cortex, basal ganglia and hippocampus. (**Cingulate**: LESION: 130 ± 19 *vs* L+W0.5: 245 ± 38 fmol/g t.e; **Motor cortex layer I**: LESION: 139 ± 16 *vs* L+W0.5: 335 ± 57 fmol/g t.e, **Motor cortex layer II-V**: LESION: 102 ± 11 *vs* L+W0.5: 179 ± 24 fmol/g t.e, **Striatum**: LESION: 292 ± 27 *vs* L+W0.5: 405 ± 43, fmol/g t.e., **B**: LESION: 65 ± 11 *vs* L+W0.5: 124 ± 28 fmol/g t.e., **HDB**: LESION: 98 ± 9 *vs* L+W0.5: 136 ± 28 fmol/g t.e, **CA2:** LESION: 284 ± 37 *vs* L+W0.5: 393 ± 27 fmol/g t.e, **CA3:** LESION: 305 ± 28 *vs* L+W0.5: 424 ± 34 fmol/g t.e and **Dentate gyrus**: LESION: 238 ± 25 *vs* L+W0.5: 352 ± 34 fmol/g t.e, ##p≤0.01, Figures 35 and 36).

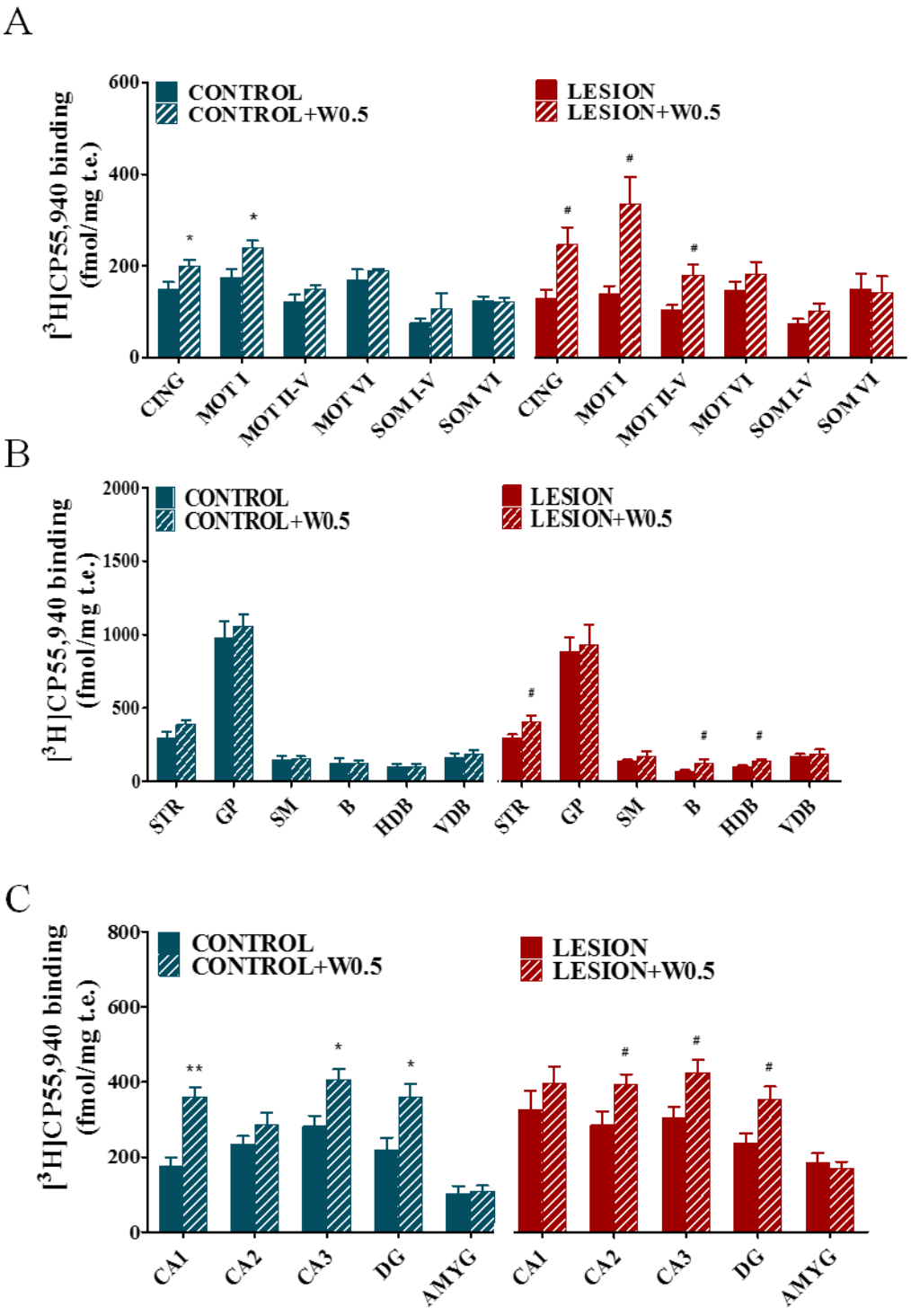

Figure 35. [^{3}H]CP55,940 binding in different brain areas expressed in fmol/mg t.e. (A) Cerebral cortex (CING: cingulate, MOT I: motor cortex layer I, MOT II-V: motor cortex layer II-V, MOT VI: motor cortex layer VI, SOM I: Somatosensorial cortex layer I, SOM VI: Somatosensorial cortex layer VI). (B) Basal ganglia (STR: striatum, GP: Globus pallidus, MS: medial septum, B: nucleus basalis magnocellularis, HDB: horizontal diagonal band, VDB: vertical diagonal band). (C) Hippocampus and amygdala (CA1: Oriens, pyramidal, radiatum; CA2: Oriens, pyramidal, radiatum; CA3: Oriens, pyramidal, radiatum; DG: dentate gyrus: Granular, molecular, polymorphic, AMYG: amygdala). (Mean ± S.E.M.) *p≤0.05 CONTROL *vs* C+W0.5, #p≤0.05 LESION *vs* L+W0.5.

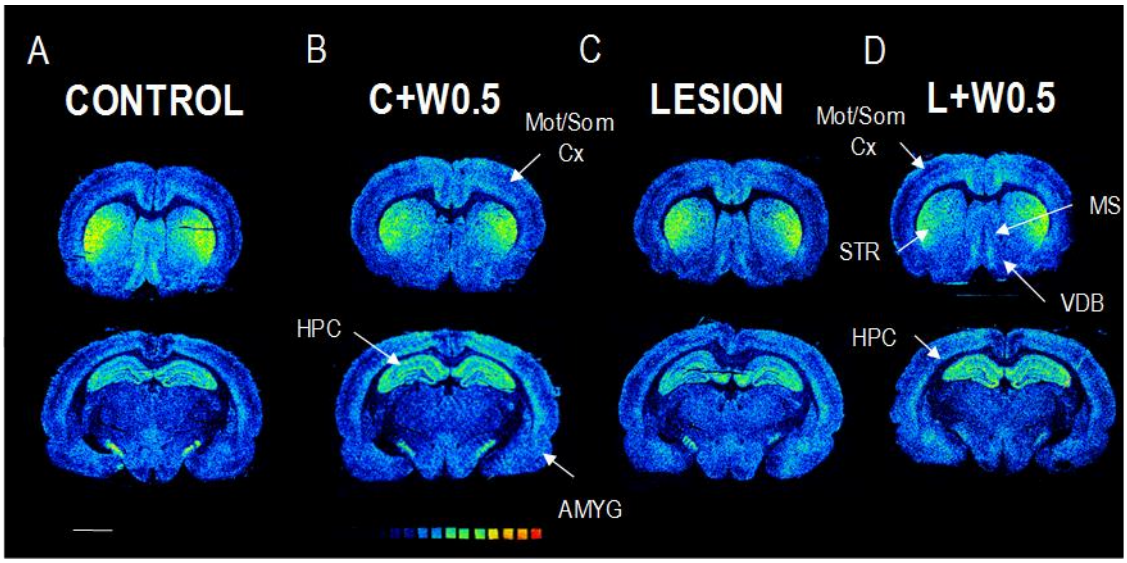

Figure 36. Representative autoradiograms of (A) CONTROL, (B) C+W0.5, (C) LESION and (D) L+W0.5 obtained from rat coronal sections that show [^{35}S]GTPγS stimulated by WIN55,212-2 (10 µM) in Mot: Motor cortex , Som Cx: Somatosensorial cortex, MS: Medial septum, VDB: Vertical diagonal band, AMYG: Amygdala and HPC: hippocampus. Scale bar: 4 mm.

3.6. Subchronic WIN55,212-2 administration did not modify the number of p75^{NTR}/AChE positive cells in B after basal forebrain cholinergic lesion

The number of p75^{NTR} and AChE^{+} cells in the B was not affected by the WIN55,212-2 subchronic treatment neither in control nor in lesion rats (**p75^{NTR}** CONTROL: 785 ± 64 cells/mm^3, LESION: 164 ± 32, CONTROL+W0.5: 701 ± 68 cells/mm^3 and LESION+W0.5: 201 ± 21; **AChE^{+}** CONTROL: 789 ± 41 cells/mm^3, LESION: 270 ± 38 cells/mm^3, CONTROL+W0.5: 701 ± 68 cells/mm^3 and LESION+W0.5: 368 ± 26 cells/mm^3 ***p≤0.001. Figure 37).

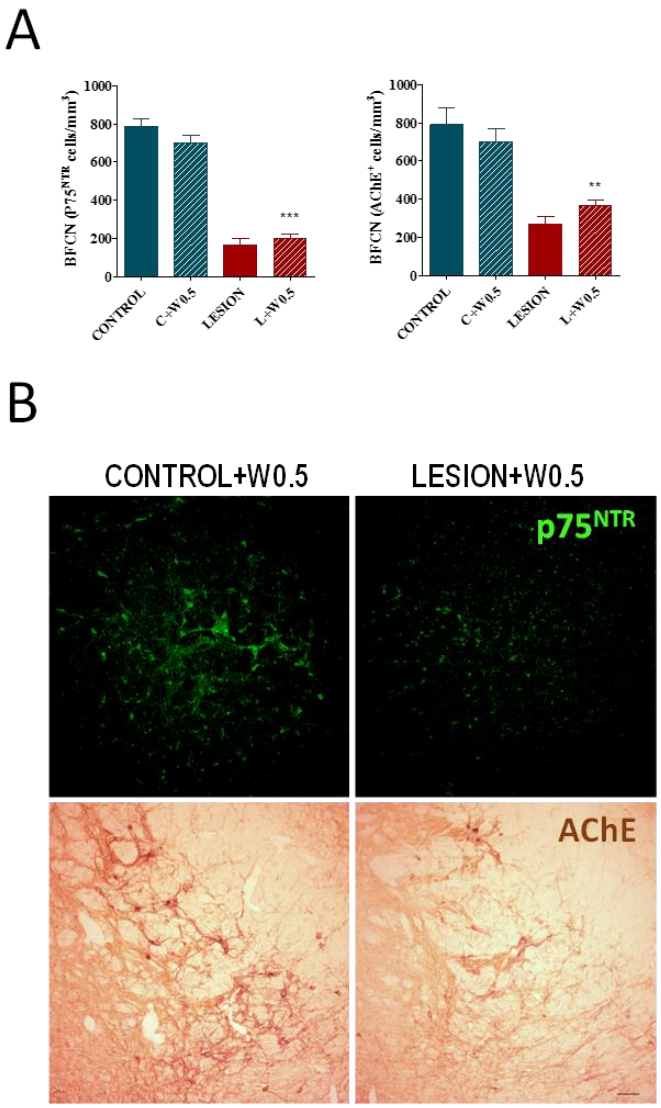

Figure 37. (A) Number of p75^{NTR} and AChE^{+} cells in the B of CONTROL, LESION, and WIN55,212-2 treated groups (C0.5 and W0.5). (B) AChE enzymatic staining and p75^{NTR} immunoflorescence in the B. Scale bar 100 µM.

4. SUBCHRONIC WIN55,212-2 AND SR141716A CO-ADMINISTRATION IN THE ANIMAL MODEL OF BASAL FOREBRAIN CHOLINERGIC LESION DEMONSTRATES THAT THE OBSERVED EFFECTS WERE MEDIATED BY CB_1 RECEPTORS

To examine if the positive effects observed in learning and memory were specifically mediated by CB_1 receptors, WIN55,212-2 and SR141716, an specific CB_1 antagonist in CNS, were co-administered to a group of rats with basal forebrain cholinergic lesion. A similar schedule than the already described for previous treatments was done for lesion, drugs treatments and behavior tests (Figure 38). Three groups of treatment were studied in this section: LESION, LESION+W0.5, L+W+SR. Both drugs, WIN55,212-2 and SR141716 share similar affinities for cerebral CB_1 receptors, therefore they were administered together at the same dose and periodicity during five days. In a next section are described the effects obtained after treatment only with the CB_1 specific antagonist, SR141716.

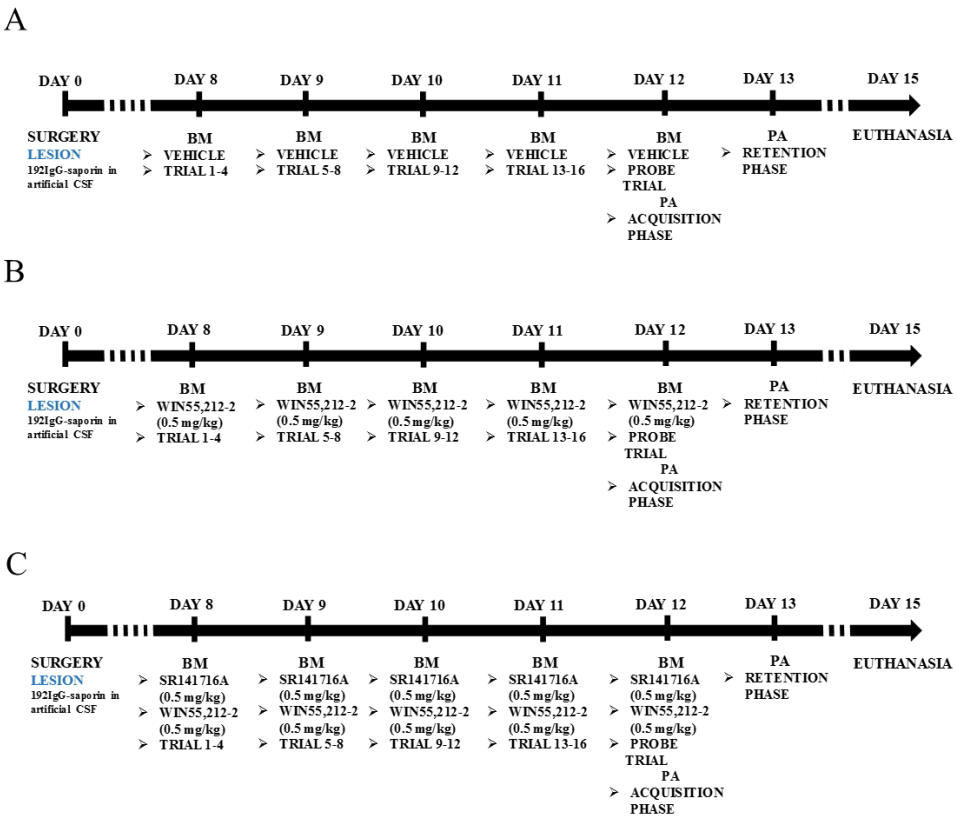

Figure 38. Training schedules followed for each of the three groups of treatment designed to evaluate the effects of WIN55,212-2 together with SR141716A in both spatial and aversive memory.

4.1. The cognitive improvement induced by the subchronic treatment with WIN55,212-2 in a rat model of basal forebrain cholinergic lesion is specifically mediated by CB_1 receptors

Spatial learning and memory behavior of treated rats was evaluated in the Barnes maze test. During the co-treatment with WIN55,212-2 together with SR141716A (L+W+SR group), we evaluated different spatial acquisition parameters such as total latency (sec), total path length (cm) and speed (cm/sec). The results indicated that total latency and total path length decreased during the acquisition phase for all groups of treatment (Figure 39 A and B). However, total latency showed significant differences during the first trial between L+W+SR group and the group of lesion rats only treated with the CB_1 agonist (L+W0.5). But, L+W+SR group took the same time to arrive to the target hole than LESION group (Trial 1 LESION: 61 ± 8 sec, LESION+W0.5: 108 ± 13 sec, L+W+SR: 61 ± 117 sec. Figure 39 A and D). Total path length also showed significant differences in trials 1 and 13 (Trial 1, LESION: 405 ± 42 cm, LESION+W0.5: 548 ± 56 cm, L+W+SR: 956 ± 151 cm, **p≤0.01 L+W0.5 *vs* L+W+SR and trial 13 LESION: 319 ± 29 cm, LESION+W0.5: 130 ± 22 cm, L+W+SR: 330 ± 56 cm, *p≤0.05 L+W0.5 *vs* L+W+SR). As usual, the speed was increasing with each trial for all groups of treatment. However, LESION+W0.5 moved more slowly than the other two groups, LESION and L+W+SR that showed a comparable speed. (LESION: 17 ± 1 cm/sec, LESION+W0.5: 11.8 ± 0.6 cm/sec, L+W+SR: 17 ± 0.7 cm/sec, Figure 39C).

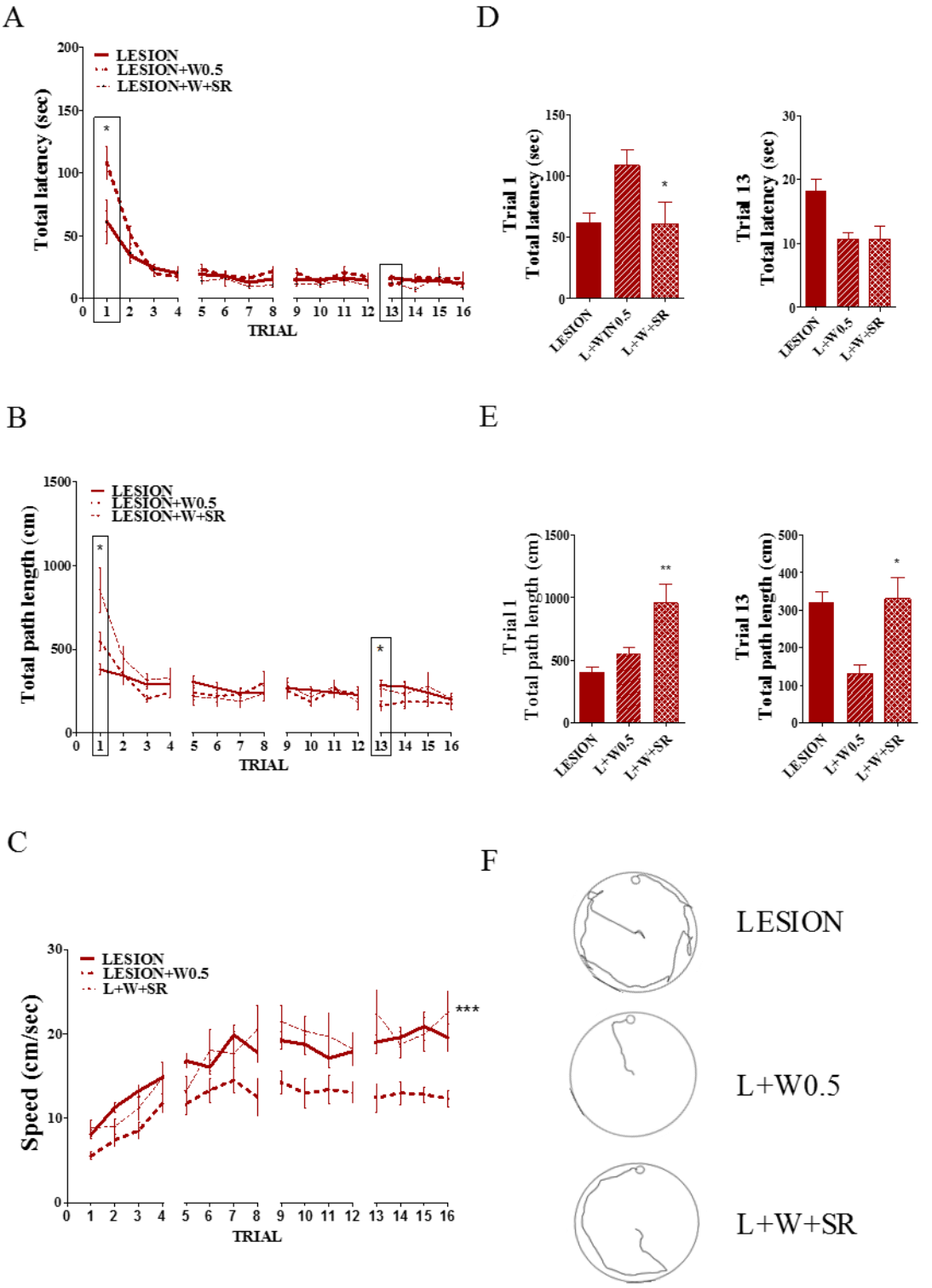

Figure 39. (A) Total latency, (B) Total path length and (C) average speed during each one of the sixteen trials in the acquisition phase for the three groups of treatments analyzed in the present section. ***p≤0.001 L+W0.5 *vs* L+W+SR. (D) Total latency of trial 1 and 13, *p≤0.05 L+W0.5 vs L+W+SR. (E) Total path length of trial 1 and trial 13, *p≤0.05, **p≤0.01 L+W0.5 vs L+W+SR. (F) Representative trajectory during trial 13 for each one of the experimental groups. Data are mean ± S.E.M.). Note that only comparison between L+W0.5 vs L+W+SR are shown, the comparison between LESION and L+W0.5 was described in a previous section.

On probe trial, after the last training day, the latency in target quadrant was measured for the three groups. Only L+W0.5 took more time in the target quadrant than the other two groups (Time spent in target quadrant. LESION: 49 ± 3 sec, L+W0.5: 81 ± 7 sec, L+W+SR: 48 ± 5 sec, Figure 40 A)

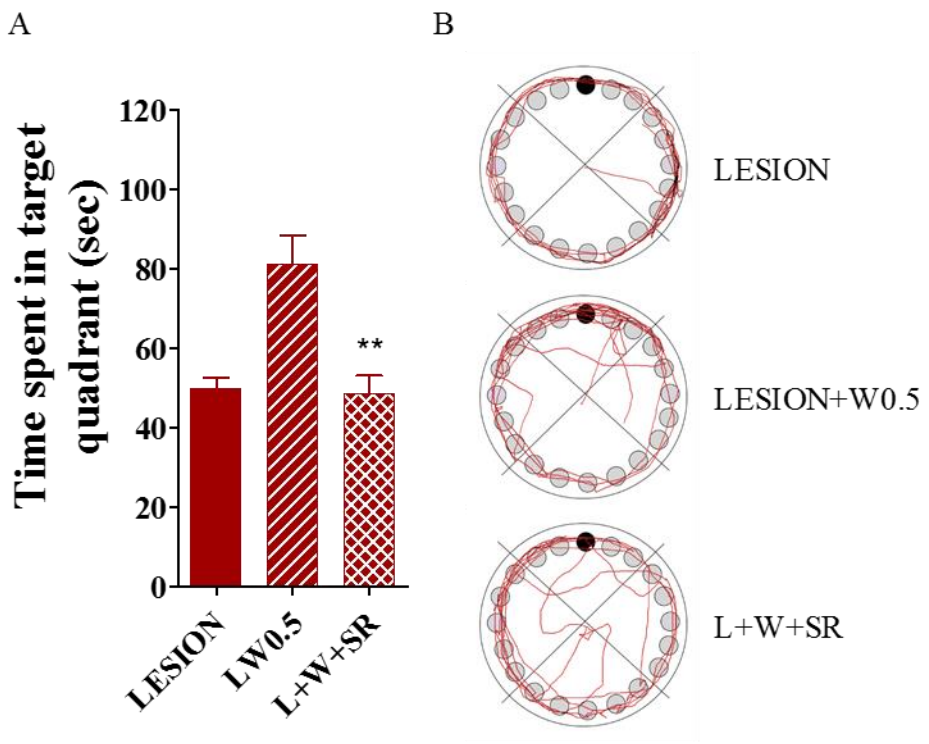

Figure 40. (A) Time spent in target quadrant on probe trial of the BM. (B) Representative trajectory during the 180 sec of the probe trial. Data are mean ± S.E.M. **p≤0.01, L+W+SR *vs* L+W0.5. Note that only comparison between L+W0.5 *vs* L+W+SR are shown, the comparison between LESION and L+W0.5 were described in a previous section.

The passive avoidance test was used to evaluate learning and memory associated to an aversive stimulus. The day of the probe trial of Barnes Maze (12th day) we also evaluated in the passive avoidance test the acquisition latency parameter. L+W0.5 group exhibited a higher latency than the other two groups. (LESION: 7 ± 1 sec, L+W0.5: 13 ± 2 sec, L+W+SR: 7 ± 2 sec, Figure 41 A). 24 hours later, all trained animals were tested again to evaluate aversive memory. Then, the step-through latency time was measured. None of the groups of treatment analyzed in this section remembered the aversive stimulus (LESION 25 %, LESION+W0.5 and LESION+W+SR 0 % of positive response).

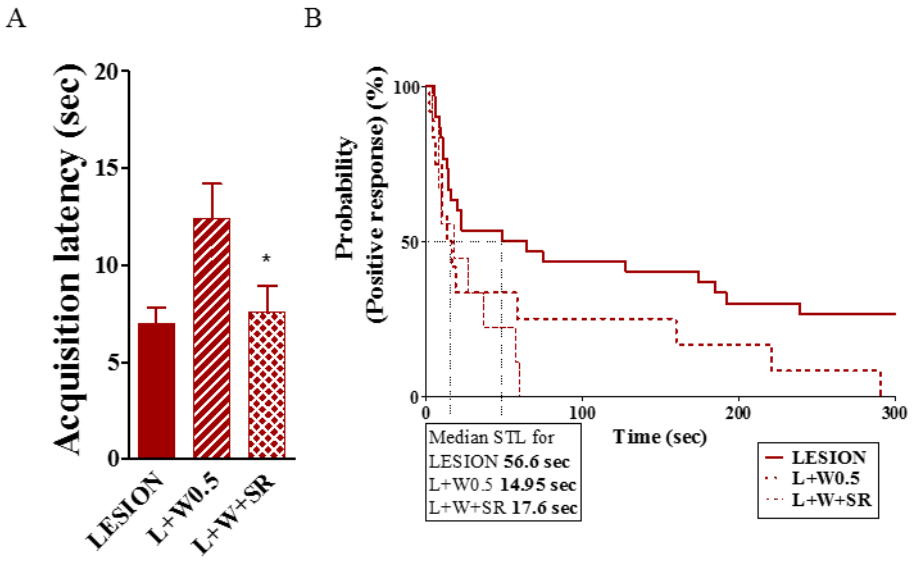

Figure 41. (A) Acquisition latency times during the learning trial of the passive avoidance test (mean ± S.E.M.) *p≤0.05, L+W0.5 *vs* L+W+SR. (B) Step-Through latency times of passive avoidance test represented as Kaplan-Meier survival curves, Log-Rank/Mantel-Cox test. Note that only comparison between L+W0.5 *vs* L+W+SR is shown, the comparison between LESION and L+W0.5 was described in a previous section.

4.2. Subchronic WIN55,212-2 and SR141716 co-administration leads to decrease muscarinic signaling on a model of basal forebrain cholinergic lesion

The effect of the subchronic co-administration of WIN55,212-2 and SR141716 on muscarinic cholinergic receptors was studied by autoradiography.

Firstly the [^{35}S]GTPγS binding stimulated by carbachol (100 µM) was measured in brain areas related to learning and memory control to localize and quantify the activity of M_2/M_4 receptors. Basal binding was similar in the three groups of treatment analyzed in this part of the study for all the analyzed brain areas (LESION, LESION+W0.5 and L+W+SR).

The subchronic co-administration of WIN55,212-2 and SR141716 to a group of lesion rats induced a decrease of M_2/M_4 receptor activity induced by carbachol in cerebral cortex and basal ganglia area compared with the activity of the group of rats treated only with WIN55,212-2 (**Motor cortex layer I**: LESION+W0.5: 256 ± 36 % *vs* L+W+SR: 119 ± 45 % , **Motor cortex layer II-V**: LESION+W0.5: 242 ± 35 % *vs* L+W+SR: 128 ± 56 % , **Somatosensorial cortex layer VI**: LESION+W0.5: 196 ± 10 % *vs* L+W+SR: 58 ± 17 %, **Striatum**: LESION+W0.5: 126 ± 17 % *vs* L+W+SR: 36 ± 16 %, **GP**: LESION+W0.5: 117 ± 25 % *vs* L+W+SR: 29 ± 12 %, **MS**: LESION+W0.5: 296 ± 47 % *vs* L+W+SR: 92 ± 23 % , **VDB**: LESION+W0.5: 234 ± 35 % *vs* L+W+SR: 102 ± 20 %. Figure 42). Note that the CONTROL group results are not included because they have been described in a previous section.

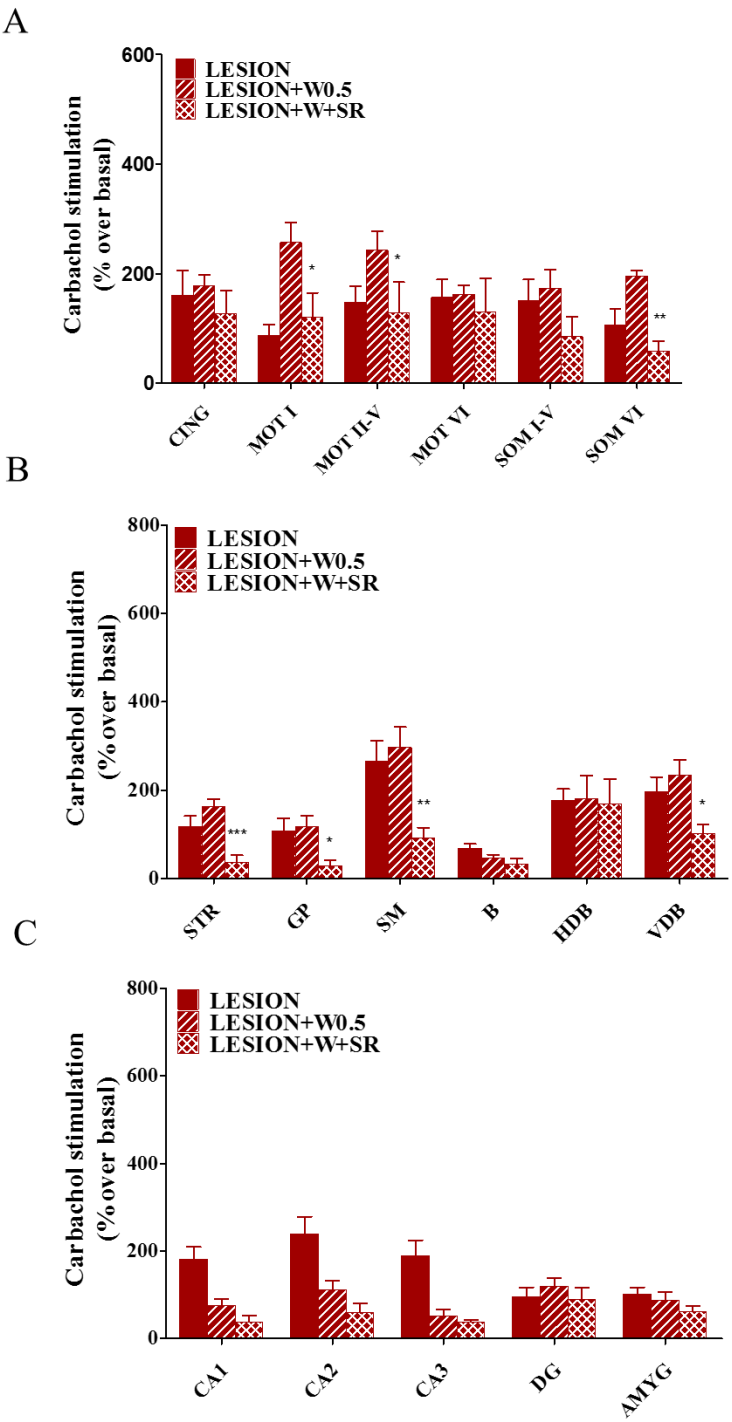

Figure 42. [^{35}S]GTPγS binding stimulated by carbachol in different brain areas represented as % stimulated by carbachol over the basal levels. (A) Cerebral cortex (CING: cingulate, MOT I: motor cortex layer I, MOT II-V: motor cortex layer II-V, MOT VI: motor cortex layer VI, SOM I: Somatosensorial cortex layer I, SOM VI: Somatosensorial cortex layer VI), (B) Basal ganglia (STR: striatum, GP: Globus pallidus, MS: medial septum, B: nucleus basalis magnocellularis, HDB: horizontal diagonal band, VDB: vertical diagonal band).(C) Hippocampus and amygdala (CA1: Oriens, pyramidal, radiatum; CA2: Oriens, pyramidal, radiatum; CA3: Oriens, pyramidal, radiatum; DG: dentate gyrus: Granular, molecular, polymorphic, AMYG: amygdala). (Data are mean ± S.E.M.) *p≤0.05, **p≤0.01 LESION+W0.5 *vs* LESION+W+SR. Only comparison between L+W0.5 *vs* L+W+SR are shown, the comparison between LESION and L+W0.5 were described in a previous section.

4.3. Subchronic WIN55,212-2 and SR141716 co-administration modifies cholinergic innervation following basal forebrain lesion

The effects of WIN55,212-2 and SR141716 co-administration on AChE activity were also analyzed in brain areas related to learning and memory control. The WIN55,212-2 and SR141716 co-administration to a group of lesion rats induced an increase of AChE staining (fiber density) in HDB (**HDB**: LESION+W0.5: 42 ± 3 O.D. a.u. *vs* L+W+SR: 57 ± 5 O.D. a.u.), and decrease in striatum and hippocampus when compared to the group of rats only treated with the CB_1 agonist (**Striatum**: LESION+W0.5: 61 ± 5 O.D. a.u. *vs* L+W+SR: 45 ± 4 O.D. a.u., **CA1**: LESION+W0.5: 25 ± 2 O.D. a.u. *vs* L+W+SR: 17 ± 1 O.D. a.u. and **CA2**: LESION+W0.5: 28 ± 3 O.D. a.u. *vs* L+W+SR: 15 ± 1 O.D. a.u.. Figure 43). Note that the CONTROL group results are not included in this section because they have been described in a previous section.

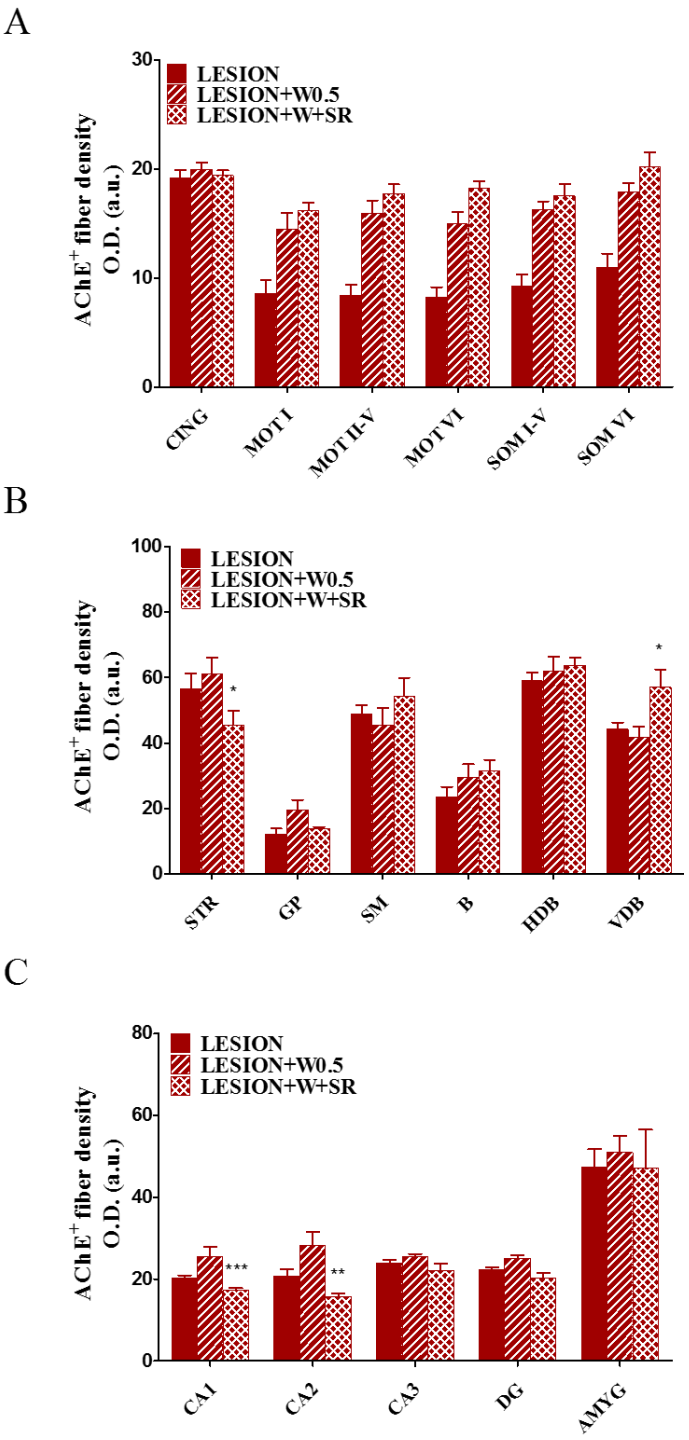

Figure 43. AChE staining in different brain areas represented as O.D. a-u. (A) Cerebral cortex (CING: cingulate, MOT I: motor cortex layer I, MOT II-V: motor cortex layer II-V, MOT VI: motor cortex layer VI, SOM I: Somatosensorial cortex layer I, SOM VI: Somatosensorial cortex layer VI), (B) Basal ganglia (STR: striatum, GP: Globus pallidus, MS: medial septum, B: nucleus basalis magnocellularis, HDB: horizontal diagonal band, VDB: vertical diagonal band).(C) Hippocampus and amygdala (CA1: Oriens, pyramidal, radiatum; CA2: Oriens, pyramidal, radiatum; CA3: Oriens, pyramidal, radiatum; DG: dentate gyrus: Granular, molecular, polymorphic, AMYG: amygdala). (Data are mean ± S.E.M.) *p≤0.05, **p≤0.01, ***p≤0.001 LESION+W0.5 *vs* L+W+SR. Only comparisons between L+W0.5 and L+W+SR are shown, the comparisons between LESION and L+W0.5 are described in a previous section.

4.4. Subchronic WIN55,212-2 and SR141716 co-administration leads to altered CB_1 activity following basal forebrain cholinergic lesion

In the present study we also analyzed the effect of WIN55,212-2 and SR141716 co-administration on cannabinoid receptor brain density by using the receptor autoradiography technique.

The [^{35}S]GTPγS binding stimulated by WIN55,212-2 (10 μM) was measured in brain areas related to learning and memory control to localize and quantify the activity of CB_1 receptors. The subchronic co-administration of the CB_1 agonist and antagonist to a group of lesion rats was able to down-regulate the CB_1 receptor activity induced by WIN55,212-2 in different brain areas involved in the control of learning and memory processes, when compared to the LESION+W0.5 group. (**Motor cortex layer I**: LESION+W0.5: 379 ± 90 % *vs* L+W+SR: 130 ± 44 %, **Motor cortex layer II-V**: LESION+W0.5: 365 ± 77 % *vs* L+W+SR: 92 ± 22 % , **Somatosensorial cortex layer I-V**: LESION+W0.5: 229 ± 35 % *vs* L+W+SR: 89 ± 42 %, **Somatosensorial cortex layer VI**: LESION+W0.5: 329 ± 54 % *vs* L+W+SR: 120 ± 37 %, **Striatum**: LESION+W0.5: 394 ± 44 % *vs* L+W+SR: 106 ± 13 %, **GP**: LESION+W0.5: 1132 ± 242 % *vs* L+W+SR: 531 ± 58 %, **MS**: LESION+W0.5: 330 ± 52 % *vs* L+W+SR: 93 ± 58 %, **B**: LESION+W0.5: 155 ± 13 % *vs* L+W+SR: 57 ± 12 %, **VDB**: LESION+W0.5: 311 ± 64 % *vs* L+W+SR: 91 ± 24 %, **CA1**: LESION+W0.5: 509 ± 102 % *vs* L+W+SR: 40 ± 13 %, **CA2**: LESION+W0.5: 468 ± 95 % *vs* L+W+SR: 37 ± 15 %, **CA3**: LESION+W0.5: 496 ± 79 % *vs* L+W+SR: 49 ± 13 %, **DG**: LESION+W0.5: 496 ± 79 % *vs* L+W+SR: 49 ± 13 % and **amygdala**: LESION+W0.5: 274 ± 27 % *vs* L+W+SR: 44 ± 7 %. Figure 44). Note that the CONTROL group results are not included because they have been described in a previous section.

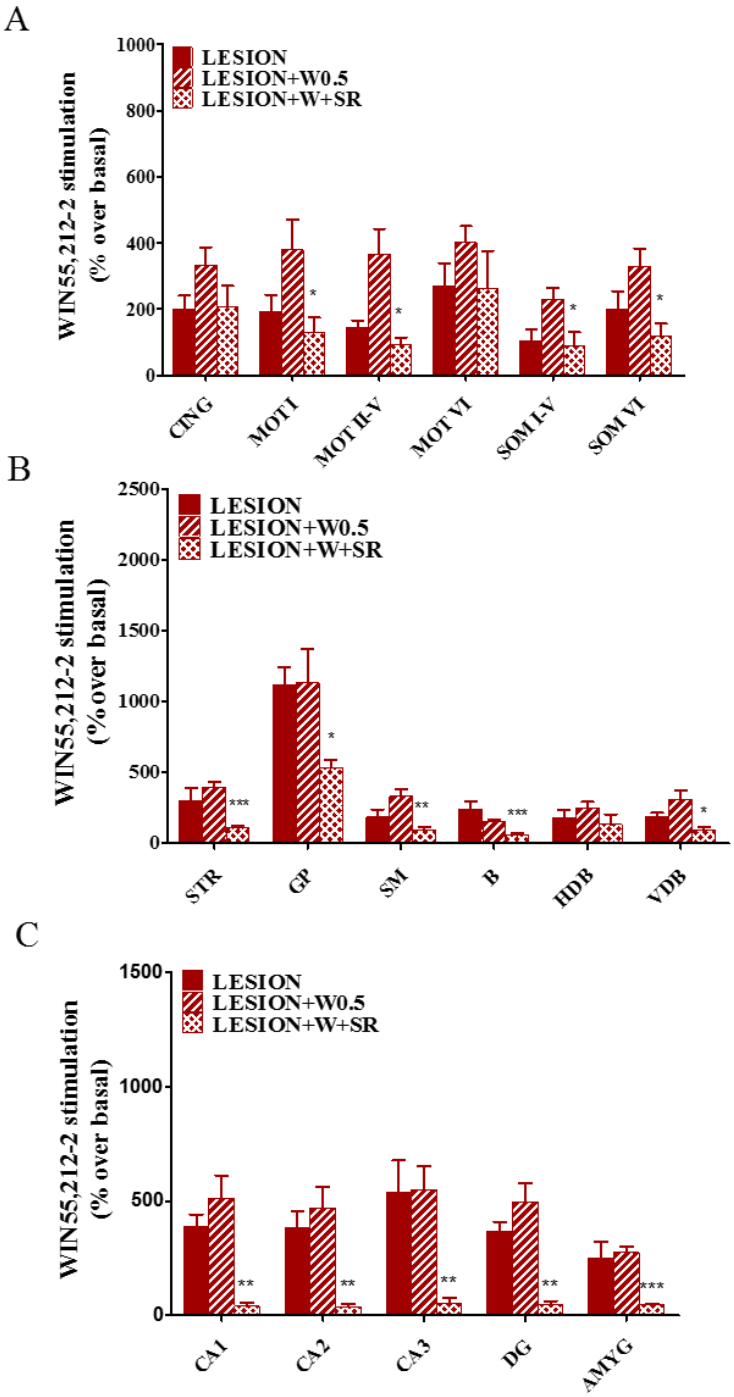

Figure 44. [^{35}S]GTPγS binding stimulated by WIN55,212-2 (10μM) in different brain areas represented as % stimulated over the basal values. (A) Cerebral cortex (CING: cingulate, MOT I: motor cortex layer I, MOT II-V: motor cortex layer II-V, MOT VI: motor cortex layer VI, SOM I: Somatosensorial cortex layer I, SOM VI: Somatosensorial cortex layer VI). (B) Basal ganglia (STR: striatum, GP: Globus pallidus, MS: medial septum, B: nucleus basalis magnocellularis, HDB: horizontal diagonal band, VDB: vertical diagonal band). (C) Hippocampus and amygdala (CA1: Oriens, pyramidal, radiatum; CA2: Oriens, pyramidal, radiatum; CA3: Oriens, pyramidal, radiatum; DG: dentate gyrus: Granular, molecular, polymorphic, AMYG: amygdala). (Data are mean ± S.E.M.). *p≤0.05, **p≤0.01, ***p≤0.001 LESION+W0.5 *vs* LESION+W+SR. Only comparison between L+W0.5 *vs* L+W+SR are shown, the comparison between LESION and L+W0.5 are described in a previous section.

The CB_1 receptor density was studied in the same brain areas by [^{3}H]CP55,940 binding. The co-administration of WIN55,212-2 and SR141716 to a group of lesion rats was able to increase the CB_1 density in almost all the analyzed brain areas . (**Cingulate**: LESION+W0.5: 245 ± 38 *vs* L+W+SR: 381 ± 40 fmol/mg t.e., **Motor cortex layer II-V**: LESION+W0.5: 179 ± 24 *vs* L+W+SR: 321 ± 44 fmol/mg t.e., **Motor cortex layer VI**: LESION+W0.5: 181 ± 29 *vs* L+W+SR: 388 ± 48 fmol/mg t.e., **Somatosensorial cortex layer I-V**: LESION+W0.5: 100 ± 15 *vs* L+W+SR: 246 ± 29 fmol/mg t.e., **Somatosensorial cortex layer VI**: LESION+W0.5: 142 ± 34 *vs* L+W+SR: 336 ± 43 fmol/mg t.e., **Striatum**: LESION+W0.5: 405 ± 43 % *vs* L+W+SR: 687 ± 91 fmol/mg t.e., **GP**: LESION+W0.5: 926 ± 139 *vs* L+W+SR: 1382 ± 140 fmol/mg t.e., **MS**: LESION+W0.5: 179 ± 34 *vs* L+W+SR: 337 ± 45 fmol/mg t.e., **B**: LESION+W0.5: 124 ± 28 *vs* L+W+SR: 212 ± 20 fmol/mg t.e., **HDB**: LESION+W0.5: 136 ± 13 *vs* L+W+SR: 252 ± 20 fmol/mg t.e., **VDB**: LESION+W0.5: 187 ± 28 *vs* L+W+SR: 301 ± 21 fmol/mg t.e., **CA1**: LESION+W0.5: 397 ± 44 *vs* L+W+SR: 722 ± 86 fmol/mg t.e., **CA2**: LESION+W0.5: 393 ± 27 *vs* L+W+SR: 682 ± 91 fmol/mg t.e., **CA3**: LESION+W0.5: 424 ± 34 *vs* L+W+SR: 744 ± 64 fmol/mg t.e. and **DG**: LESION+W0.5: 353 ± 34 *vs* L+W+SR: 657 ± 82 fmol/mg t.e.. Figure 45). Note that the CONTROL group results are not included because they have been described in a previous section.

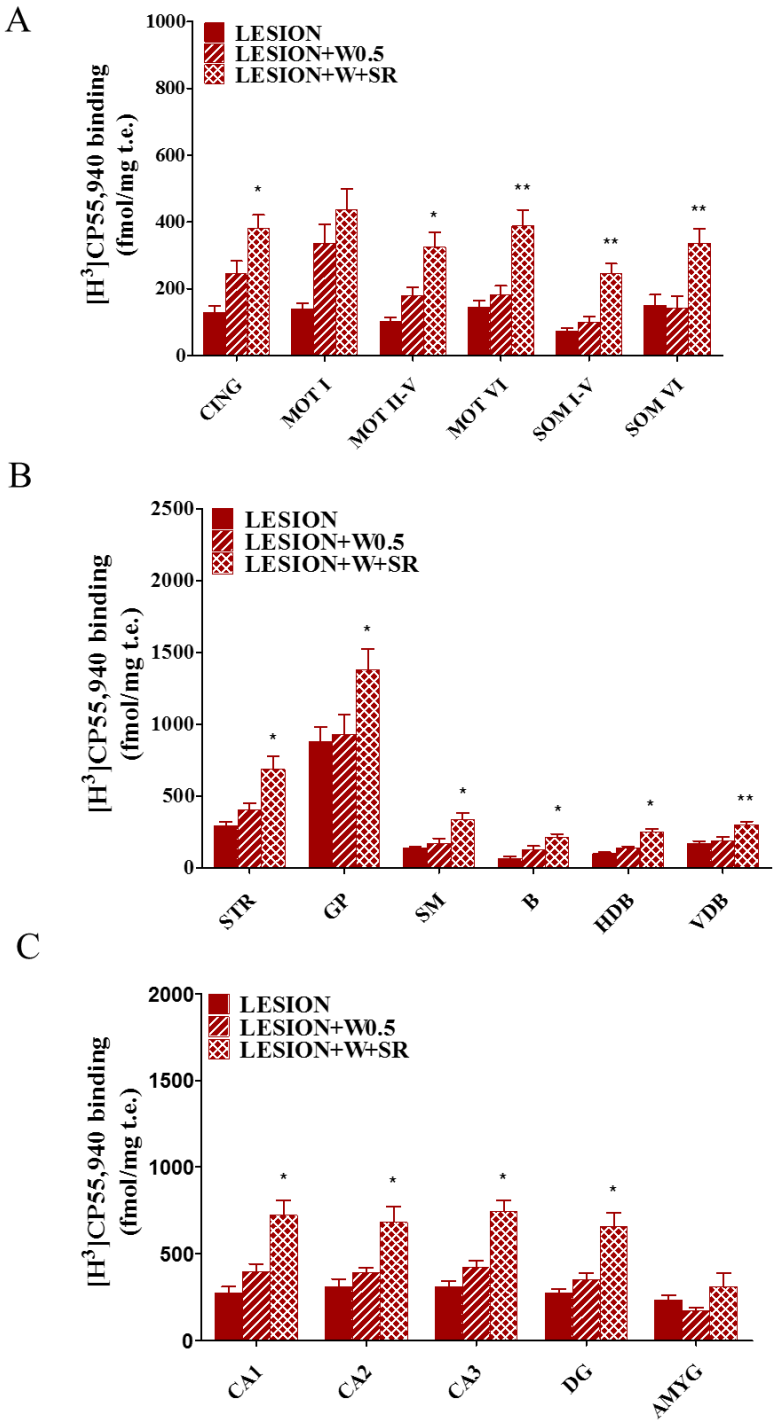

Figure 45. [^{3}H]CP55,940 binding in different brain areas represented as fmol/mg t.e. (A) Cerebral cortex (CING: cingulate, MOT I: motor cortex layer I, MOT II-V: motor cortex layer II-V, MOT VI: motor cortex layer VI, SOM I: Somatosensorial cortex layer I, SOM VI: Somatosensorial cortex layer VI), (B) Basal ganglia (STR: striatum, GP: Globus pallidus, MS: medial septum, B: nucleus basalis magnocellularis, HDB: horizontal diagonal band, VDB: vertical diagonal band).(C) Hippocampus and amygdala (CA1: Oriens, pyramidal, radiatum; CA2: Oriens, pyramidal, radiatum; CA3: Oriens, pyramidal, radiatum; DG: dentate gyrus: Granular, molecular, polymorphic, AMYG: amygdala). (Data are mean ± S.E.M.). *p≤0.05, **p≤0.01, LESION+W0.5 *vs* LESION+W+SR. Only comparison between L+W0.5 *vs* L+W+SR are showned, the comparison between LESION and L+W0.5 are described in a previous section.

5. EFFECTS OF A HIGH DOSE OF WIN55,212-2 (3 mg/kg) ON THE RAT MODEL OF BASAL FOREBRAIN CHOLINERGIC LESION

The effects elicited by a higher dose of WIN55,212-2 (3 mg/kg) on learning and memory behavior were evaluated in the model of basal forebrain cholinergic lesion an compared to vehicle treated animals following a schedule comparable to the described previous treatments.

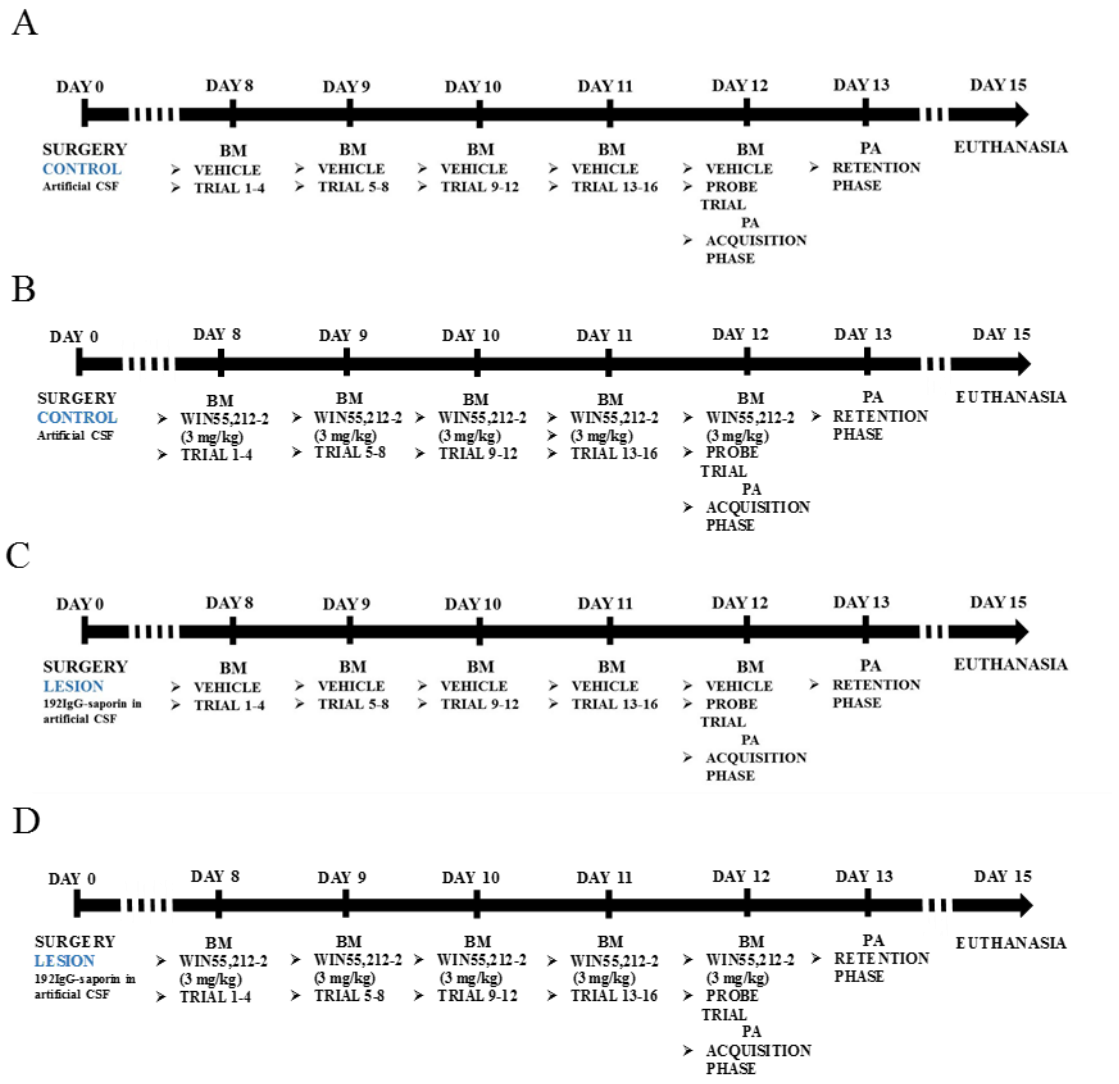

Figure 46. Lesion, treatment, training and behavior test different schedules followed for each of the four groups of treatment designed to evaluate the effects of high doses of WIN55,212-2 (3 mg/kg) in both spatial and aversive memory.

The rats included in every group of treatment were trained in a Barnes maze test to evaluate spatial learning and memory behavior. Total latency and total path length decreased during the spatial acquisition (Figure 47 A and B). Total latency showed significant differences between treated and non-treated groups during the first eight trials and L+W3 group reverted the increase induced in the LESION group during trial 13 (Total latency Trial 13; CONTROL: 9 ± 1 sec, LESION: 17 ± 2 sec, C+W3: 10 ± 3 sec, L+W3: 7 ± 3 sec). But, total path length showed significant changes specifically in trial 13 (CONTROL: 156 ± 19 sec, LESION: 309 ± 29 sec, C+W3: 253 ± 64 sec, L+W3: 155 ± 50 sec). The speed of the rats was increased with each trial as usual, for all the groups of treatment, but rats treated with WIN55,212-2 (3 mg/kg) were faster than vehicle treated rats during all the trials (CONTROL: 15 ± 0.6 cm/sec, LESION: 17 ± 0.8 cm/sec, C+W3: 24 ± 1 cm/sec, L+W3: 23 ± 2 cm/sec, Figure 47 C).

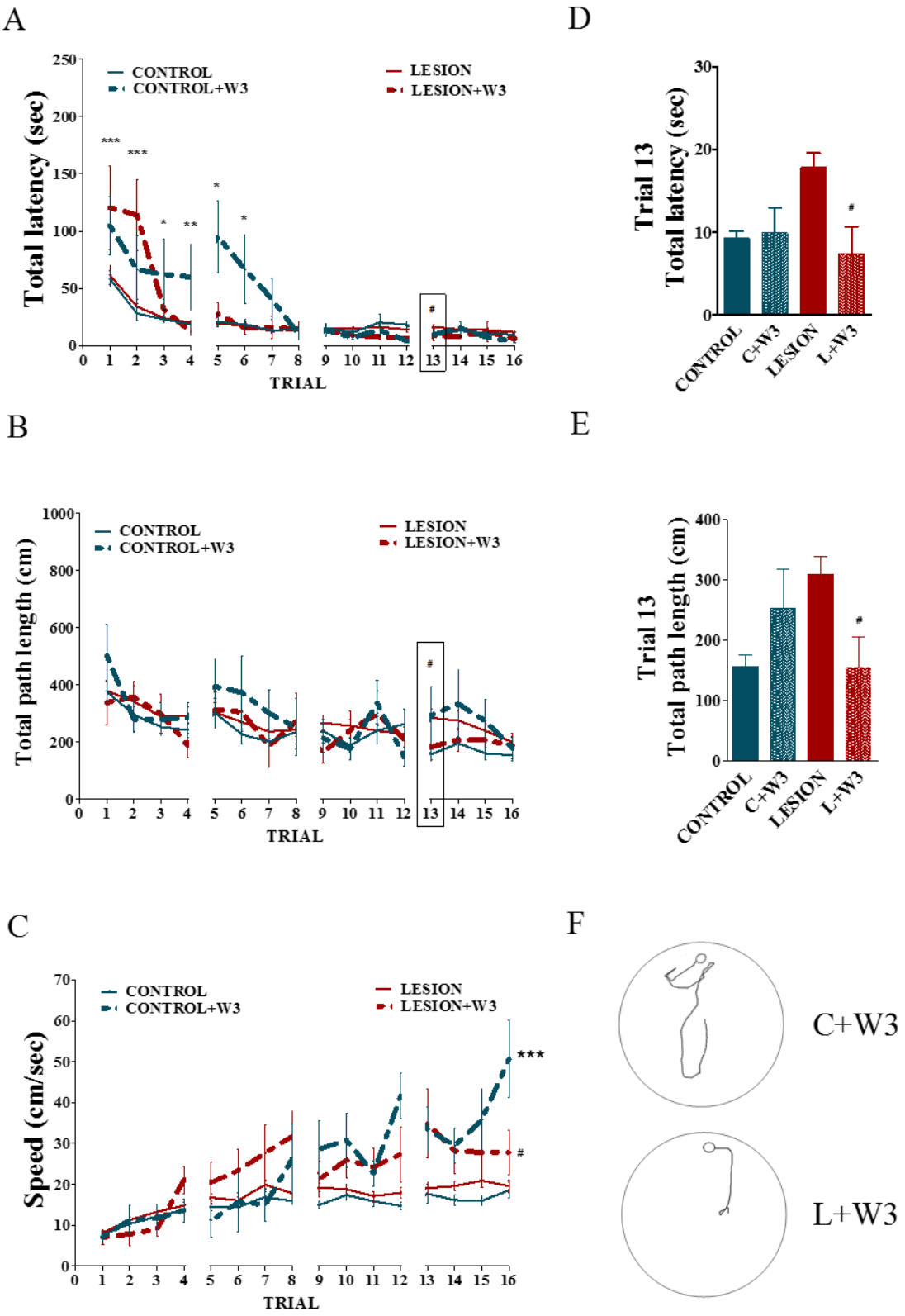

Figure 47. (A) Total latency, (B) Total path length and (C) average speed results are shown during each of the sixteen trials of the acquisition phase for the four groups of treatment (CONTROL, LESION, C+W3 and L+W3). (D) Total latency and (E) total path length during trial 13. (F) Representative trajectory of trial 13 for the groups of rats treated with WIN55,212-2 (3 mg/kg). Data are (mean ± S.E.M.). *p≤0.05, **p≤0.01, ***p≤0.001 CONTROL *vs* C+W3, #p≤0.05 LESION *vs* L+W3.

The latency in target quadrant was also measured during the probe trial, after the last training day, for each of the four experimental groups included in this section. Curiously, animals included in both LESION and C+W3 groups, took less time in the target quadrant than the other two groups, indicating that this higher dose of WIN55,212-2 of 3 mg/kg, was inducing an impairment in learning and memory spatial abilities in control animals comparable to those induced by the cholinergic lesion alone. (Figure 48, Time spent in target quadrant. CONTROL: 89 ± 3 sec, C+W3: 48 ± 3 sec, LESION: 49 ± 3, LESION+W3: 80 ± 12 sec).

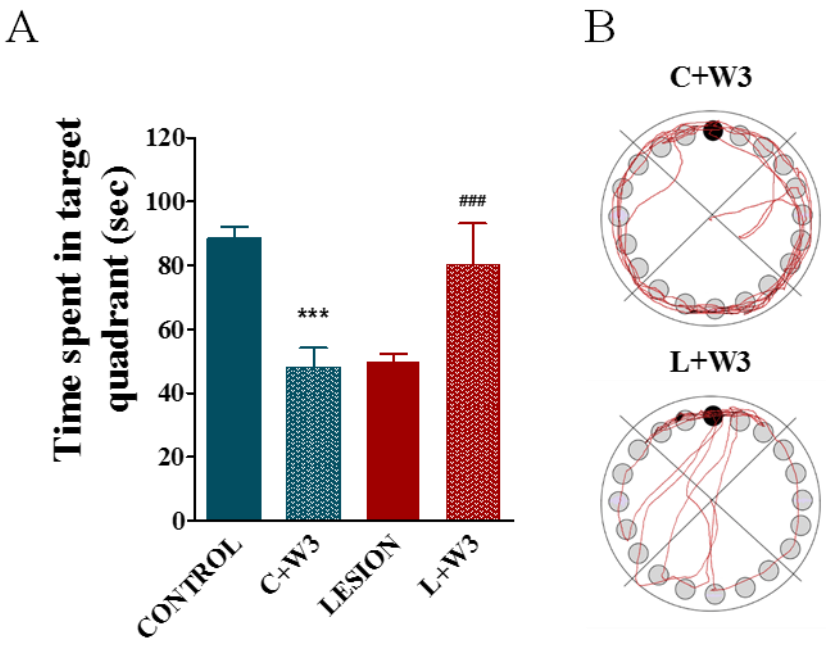

Figure 48. (A) Time spent in target quadrant on probe trial (B) Representative trajectories during 180 sec of the probe trial for both of the WIN55,212-2 (3 mg/kg) -treated groups. Data are mean ± S.E.M. ***p≤0.001 CONTROL *vs* C+W3. ### p≤0.001 LESION *vs* L+W3.

The aversive learning and memory behavior was evaluated using the passive avoidance (PA) test. After the probe trial of BM the acquisition latency parameter of the PA test was measured. The results indicated that the animals included in the LESION group exhibited lower acquisition latencies than those belonging to the other groups of treatment. (LESION: 6 ± 1 sec, L+W3: 15 ± 3 sec, CONTROL: 12 ± 1 sec and C+W3: 12 ± 2 sec. Figure 49 A). 24 hours later, all trained animals were tested again to evaluate aversive memory. Then, the step-through latency time was measured. When the four groups were compared only CONTROL group animals were able to remember the aversive stimulus (77 %). In the other groups, LESION, L+W3 and C+W3 only 26 %, 25 % and 25 % respectively of the animals were able to remember the aversive stimulus. (Figure 49 B). The PA results also indicated that the high dose of WIN55,212-2 of 3 mg/kg was impairing the aversive learning and memory in control animals in a similar way to that induced by the cholinergic lesion.

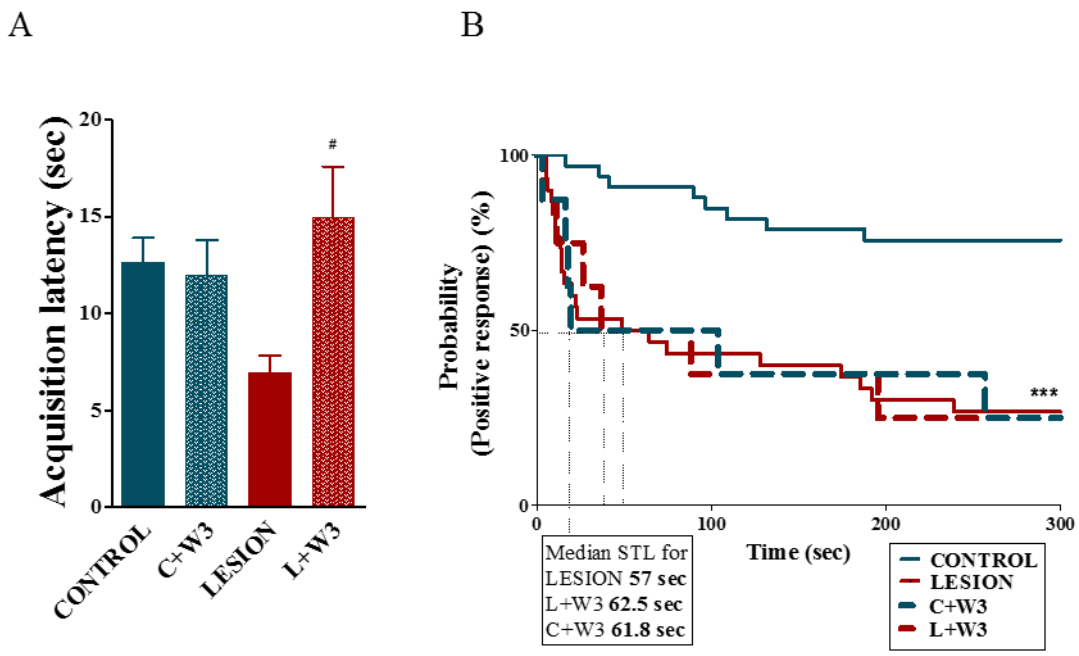

Figure 49. (A) Acquisition latency times during the learning trial of the passive avoidance test. Data are mean ± S.E.M. #p≤0.05 LESION *vs* L+W3. (B) Step-Through latency times of passive avoidance test represented as Kaplan-Meier survival, Log-Rank/Mantel-Cox test, ***p≤0.001 CONTROL *vs* C+W3.

5.1. Subchronic high doses of WIN55,212-2 administration leads to decreased muscarinic signaling in the rat model of basal forebrain cholinergic lesion

The effect of the subchronic administration of a high dose of WIN55,212-2 (3 mg/kg) on muscarinic cholinergic receptors was analyzed by autoradiography.

Firstly, the [^{35}S]GTPγS binding stimulated by carbachol (100 µM) was measured in brain areas related to learning and memory control, to localize and quantify the activity of M_2/M_4 receptors. Basal binding was similar in the four groups of treatment that were compared in this section and for all the analyzed brain areas. The WIN55,212-2 (3 mg/kg) treatment to CONTROL rats decreased M_2/M_4 receptor activity induced by carbachol in different brain areas that control learning and memory processes. (**Motor cortex layer I**: CONTROL: 281 ± 14 % *vs* C+W3: 78 ± 12 % **Motor cortex layer II-V**: CONTROL: 294 ± 44 % *vs* C+W3: 64 ± 25 %, **Somatosensorial cortex layer VI**: CONTROL: 153 ± 36 % *vs* C+W3: 30 ± 28 %, **Striatum**: CONTROL: 150 ± 20 % *vs* C+W3: 51 ± 28 %, **MS**: CONTROL: 387 ± 46 % *vs* C+W3: 137 ± 38 %, **CA1**: CONTROL: 105 ± 33 % *vs* C+W3: 36 ± 12 % , **CA2**: CONTROL: 163 ± 39 % *vs* C+W3: 42 ± 17 %. Figure 50).

On the other hand, the treatment with WIN55,212-2 (3 mg/kg) to a group of lesion rats also decreased the M_2/M_4 receptor activity (**striatum**: LESION: 118 ± 24 % *vs* L+W3: 51 ± 10 %, **CA1**: LESION: 210 ± 41 % *vs* L+W3: 76 ± 40 %, **CA2**: LESION: 230 ± 41 % *vs* L+W3: 73 ± 43 %. Figure 50).

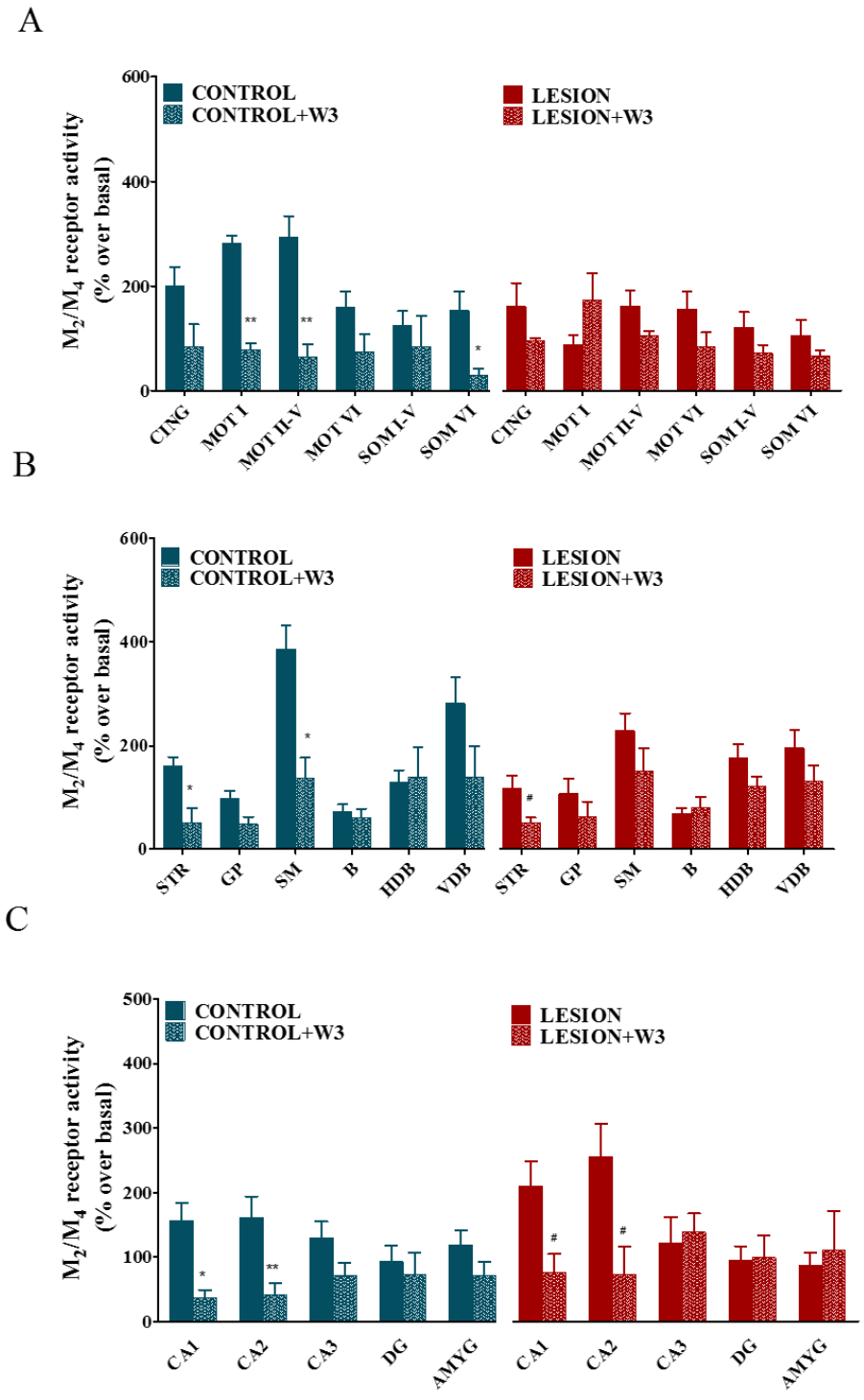

Figure 50. [^{35}S]GTPγS binding stimulated by carbachol (100µM) in different brain areas represented as % stimulated over the basal. (A) Cerebral cortex (CING: cingulate, MOT I: motor cortex layer I, MOT II-V: motor cortex layer II-V, MOT VI: motor cortex layer VI, SOM I: Somatosensorial cortex layer I, SOM VI: Somatosensorial cortex layer VI), (B) Basal ganglia (STR: striatum, GP: Globus pallidus, MS: medial septum, B: nucleus basalis magnocellularis, HDB: horizontal diagonal band, VDB: vertical diagonal band). (C) Hippocampus and amygdala (CA1: Oriens, pyramidal, radiatum; CA2: Oriens, pyramidal, radiatum; CA3: Oriens, pyramidal, radiatum; DG: dentate gyrus: Granular, molecular, polymorphic, AMYG: amygdala). (Data are mean ± S.E.M.) *p≤0.05, **p≤0.01 CONTROL *vs* C+W3, #p≤0.05 LESION *vs* L+W3.

5.2. Subchronic high doses of WIN55,212-2 administration leads to modify cholinergic innervation after basal forebrain lesion

The effects of WIN55,212-2 (3 mg/kg) administration on AChE activity were studied in brain areas related to learning and memory. The WIN55,212-2 administration to CONTROL rats increased the $AChE^+$ fiber density in striatum and B (Figure 51, **Striatum**: CONTROL: 70 ± 2 *vs* C+W3: 45 ± 4 O.D. (a.u.); **B**: CONTROL: 36 ± 3 *vs* LESION: 23 ± 3 O.D. (a.u.). Figure 51). Moreover, the WIN55,212-2 administration to LESION rats was able to increase the AChE activity in cortex to the control levels ((**Motor cortex layer I**: LESION: 9 ± 1, L+W3: 14 ± 1 O.D. (a.u.), **Motor cortex layer II-V**: LESION: 8 ± 1, L+W3: 17 ± 1 O.D. (a.u.), **Motor cortex layer VI**: LESION: 8 ± 1, L+W3: 18 ± 1 O.D. (a.u.), **Somatosensorial cortex layer I-V**: LESION: 9 ± 1, L+W3: 18 ± 1 O.D. (a.u.), **Somatosensorial cortex layer VI**: LESION: 11 ± 1, L+W3: 20 ± 1 O.D. (a.u.). Figure 51). The AChE activity was also increased in L+W3 group at some septal nuclei (**VDB:** LESION: 44 ± 2, L+W3: 60 ± 6 O.D. (a.u.). Figure 51).

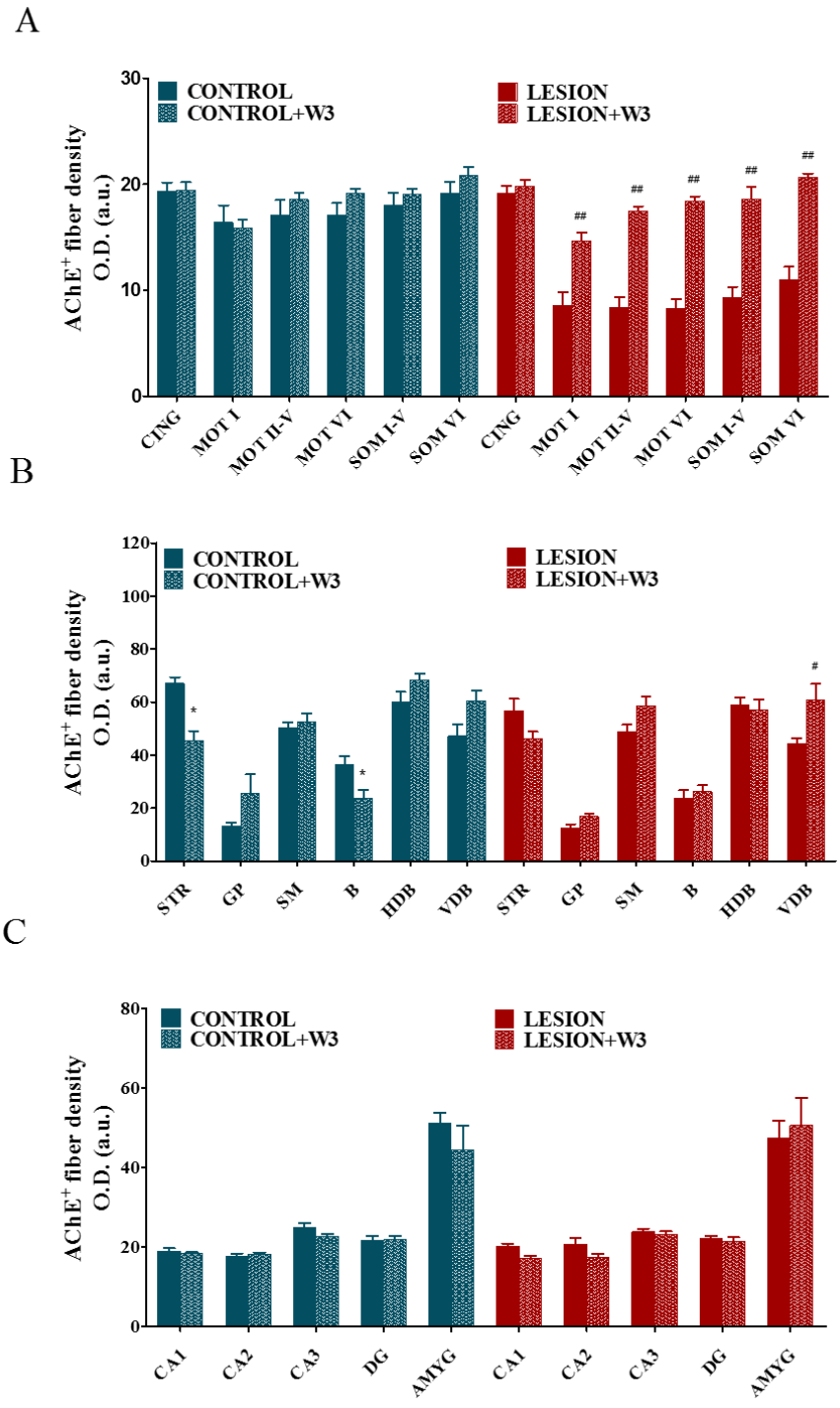

Figure 51. AChE staining in different brain areas represented as O.D. (a.u.). (A) Cerebral cortex (CING: cingulate, MOT I: motor cortex layer I, MOT II-V: motor cortex layer II-V, MOT VI: motor cortex layer VI, SOM I: Somatosensorial cortex layer I, SOM VI: Somatosensorial cortex layer VI), (B) Basal ganglia (STR: striatum, GP: Globus pallidus, MS: medial septum, B: nucleus basalis magnocellularis, HDB: horizontal diagonal band, VDB: vertical diagonal band) and (C) Hippocampus and amygdala (CA1: Oriens, pyramidal, radiatum; CA2: Oriens, pyramidal, radiatum; CA3: Oriens, pyramidal, radiatum; DG: dentate gyrus: Granular, molecular, polymorphic, AMYG: amygdala). (Data are mean ± S.E.M.) *p≤0.05 CONTROL *vs* C+W3, ##p≤0.01 LESION *vs* L+W3.

5.3. Subchronic treatment with a high dose of WIN55,212-2 (3 mg/kg) administration leads to altered CB_1 activity after basal forebrain cholinergic lesion

The effect of WIN55,212-2 administration on cholinergic receptors modulation was studied by autoradiography.

Firstly, he [^{35}S]GTPγS binding stimulated by WIN55,212-2 (10 µM) was measured in brain areas related to learning and memory to localize and quantify the activity of CB_1 receptors. The subchronic treatment with WIN55,212-2 (3 mg/kg) of CONTROL rats induced a down-regulation of CB_1 receptor activity induced by WIN55,212-2 in different brain areas involved in the control of learning and memory processes. (**Cingulate cortex:** 361 ± 74 % *vs* C+W3: 59 ± 5 % **Motor cortex layer I**: CONTROL: 258 ± 54 % *vs* C+W3: 78 ± 12 %, **Motor cortex layer VI**: CONTROL: 430 ± 29 % *vs* C+W3: 97 ± 23 %, **Somatosensorial cortex layer VI**: CONTROL: 281 ± 63 % *vs* C+W3: 42 ± 9 %, **Striatum**: CONTROL: 436 ± 88 % *vs* C+W3: 85 ± 36 %, **Globus pallidus**: CONTROL: 1833 ± 369 % *vs* C+W3: 547 ± 105 %, **MS**: CONTROL: 427 ± 95 % *vs* C+W3: 90 ± 18 %, **B**: CONTROL: 205 ± 61 % *vs* C+W3: 31 ± 8 %, **HDB**: CONTROL: 314 ± 55 % *vs* C+W3: 11 ± 45 %, **VDB**: CONTROL: 353 ± 77 % *vs* C+W3: 100 ± 34 %, **CA1**: CONTROL: 294 ± 56 % *vs* C+W3: 45 ± 7 %, **CA2**: CONTROL: 360 ± 71 % *vs* C+W3: 33 ± 7 %, **CA3**: CONTROL: 434 ± 64 % *vs* C+W3: 70 ± 34 %, %, **Dentate gyrus**: CONTROL: 412 ± 69 % *vs* C+W3: 81 ± 30 %. Figure 52). In addition, the treatment of LESION rats also was able to decrease CB_1 receptor activity, in cortex and basal glanglia (**Motor cortex layer VI**: LESION: 376 ± 91 % *vs* L+W3: 90 ± 12 %, **Somatosensorial cortex layer VI**: LESION: 202 ± 53 % *vs* L+W3: 72 ± 11 %, **B**: LESION: 236 ± 60 % *vs* L+W3: 64 ± 17 %, **CA1**: LESION: 389± 53 % *vs* L+W3: 78 ± 26 %, **CA2**: LESION: 381 ± 74 % *vs* L+W3: 75 ± 26 %, **CA3**: LESION: 359 ± 47 % *vs* L+W3: 104 ± 23 %, **Dentate gyrus**: LESION: 369 ± 39 % *vs* L+W3: 102 ± 26 %, **Amygdala:** LESION: 252 ± 69 % *vs* L+W3: 67 ± 20 %. Figure 52).

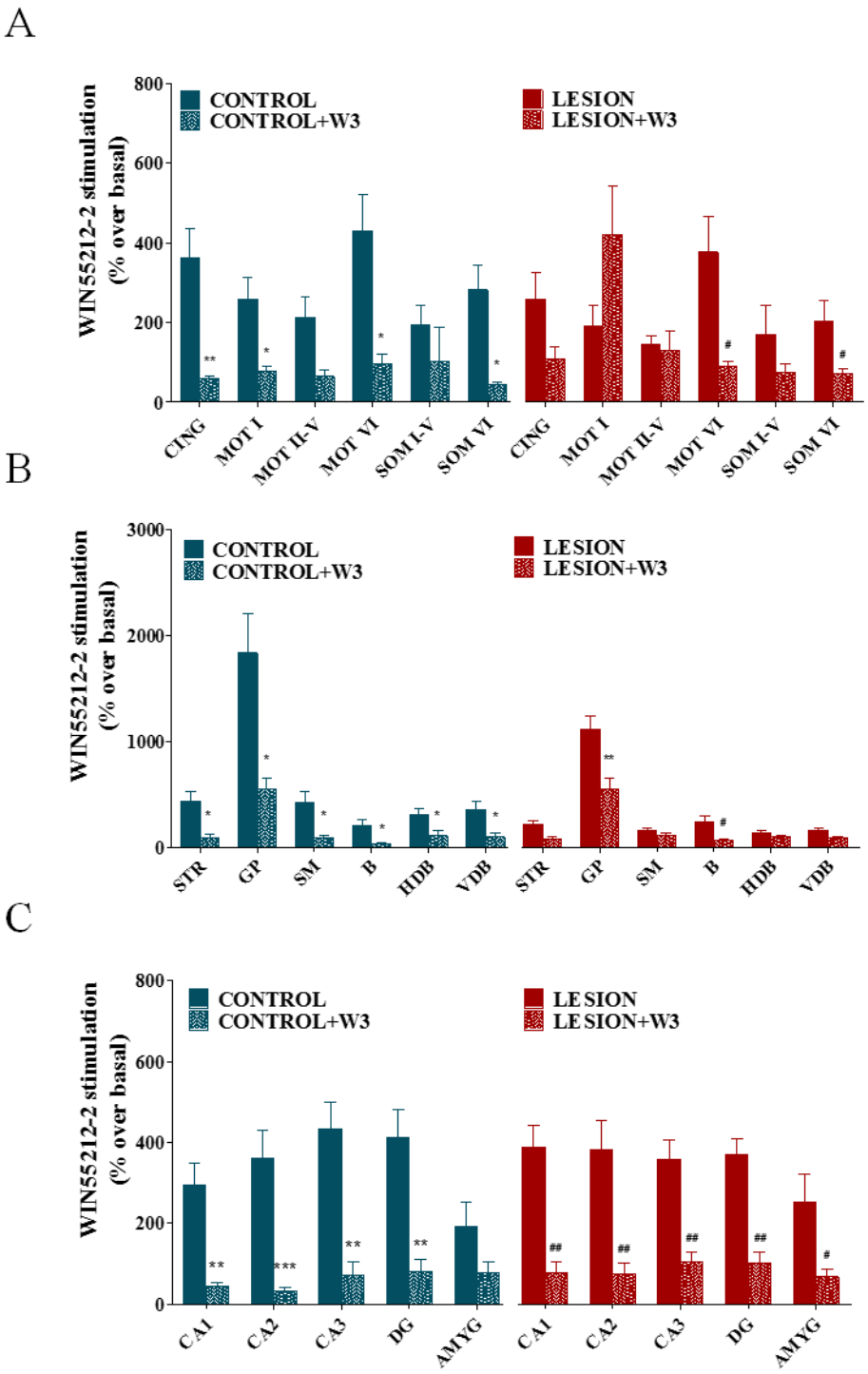

Figure 52. [^{35}S]GTPγS binding stimulated by WIN55,212-2 (10 µM) in different brain areas represented as % stimulated over the basal levels. (A) Cerebral cortex (CING: cingulate, MOT I: motor cortex layer I, MOT II-V: motor cortex layer II-V, MOT VI: motor cortex layer VI, SOM I: Somatosensorial cortex layer I, SOM VI: Somatosensorial cortex layer VI). (B) Basal ganglia (STR: striatum, GP: Globus pallidus, MS: medial septum, B: nucleus basalis magnocellularis, HDB: horizontal diagonal band, VDB: vertical diagonal band). (C) Hippocampus and amygdala (CA1: Oriens, pyramidal, radiatum; CA2: Oriens, pyramidal, radiatum; CA3: Oriens, pyramidal, radiatum; DG: dentate gyrus: Granular, molecular, polymorphic, AMYG: amygdala). (Data are mean ± S.E.M.) *p≤0.05 CONTROL *vs* C+W3, ##p≤0.01 LESION *vs* L+W3.

The CB_1 receptor density was also studied in the same brain areas by analyzing [^{3}H]CP55,940 binding. The administration of 3 mg/kg of WIN55,212-2 to control rats was able to induce an increase of the CB_1 densities in most of the analyzed brain areas (**Cingulate**: CONTROL: 149 ± 15 *vs* C+W3: 322 ± 54 fmol/g t.e.; **Motor cortex layer I**: CONTROL: 173 ± 19 *vs* C+W3: 310 ± 46 fmol/g t.e.; **Motor cortex layer II-V**: CONTROL: 136 ± 6 *vs* C+W3: 254 ± 33 fmol/g t.e.; **Motor cortex layer VI**: CONTROL: 170 ± 23 *vs* C+W3: 304 ± 48 fmol/g t.e.; **Somatosensorial cortex layer VI**: CONTROL: 75 ± 10 *vs* C+W3: 142 ± 32 fmol/g t.e.; **Striatum**: CONTROL: 313 ± 36 *vs* C+W3: 542 ± 103 fmol/g t.e.; **Medial septum**: CONTROL: 149 ± 28 *vs* C+W3: 266 ± 54 fmol/g t.e.; **HDB**: CONTROL: 102 ± 16 *vs* C+W3: 208 ± 32 fmol/g t.e.; **CA1:** CONTROL: 199 ± 30 *vs* C+W3: 516 ± 96 fmol/g t.e.; **CA2:** CONTROL: 234 ± 21 *vs* C+W3: 518 ± 92 fmol/g t.e..; **CA3:** CONTROL: 282 ± 28 *vs* C+W3: 596 ± 104 fmol/g t.e.; **Dentate gyrus**: CONTROL: 219 ± 32 *vs* C+W0.5: 520 ± 109 fmol/g t.e. Figure 53).

The subchronic treatment with 3 mg/kg of WIN55,212-2 to lesion rats also increased the CB_1 densities in the same brain areas. (**Cingulate**: LESION: 130 ± 19 *vs* L+W3: 312 ± 39 fmol/g t.e.; **Motor cortex layer I**: LESION: 140 ± 16 *vs* L+W3: 317 ± 62 fmol/g t.e.; **Motor cortex layer II-V**: LESION: 103 ± 11 *vs* L+W3: 275 ± 36 fmol/g t.e.; **Motor cortex layer VI**: LESION: 146 ± 19 *vs* L+W3: 327 ± 46 fmol/g t.e.; **Somatosensorial cortex layer I-V**: LESION: 73 ± 11 *vs* L+W3: 184 ± 29 fmol/g t.e.; **Striatum**: LESION: 292 ± 27 *vs* L+W3: 617 ± 56 fmol/g t.e.; **Globus pallidus**: LESION: 883 ± 98 *vs* L+W3: 1333 ± 144 fmol/g t.e.; **Medial septum**: LESION: 136 ± 11 *vs* L+W3: 267 ± 19 fmol/g t.e.; **B**: LESION: 66 ± 12 *vs* L+W3: 184 ± 41 fmol/g t.e.; **CA1:** LESION: 274 ± 38 *vs* L+W3: 519 ± 75 fmol/g t.e.;, **CA2:** LESION: 312 ± 43 *vs* L+W3: 494 ± 72 fmol/g t.e..; **CA3:** LESION: 312 ± 29 *vs* L+W3: 541 ± 56 fmol/g t.e.; **Dentate gyrus**: LESION: 276 ± 19 *vs* L+W3: 489 ± 55 fmol/g t.e. Figure 53).

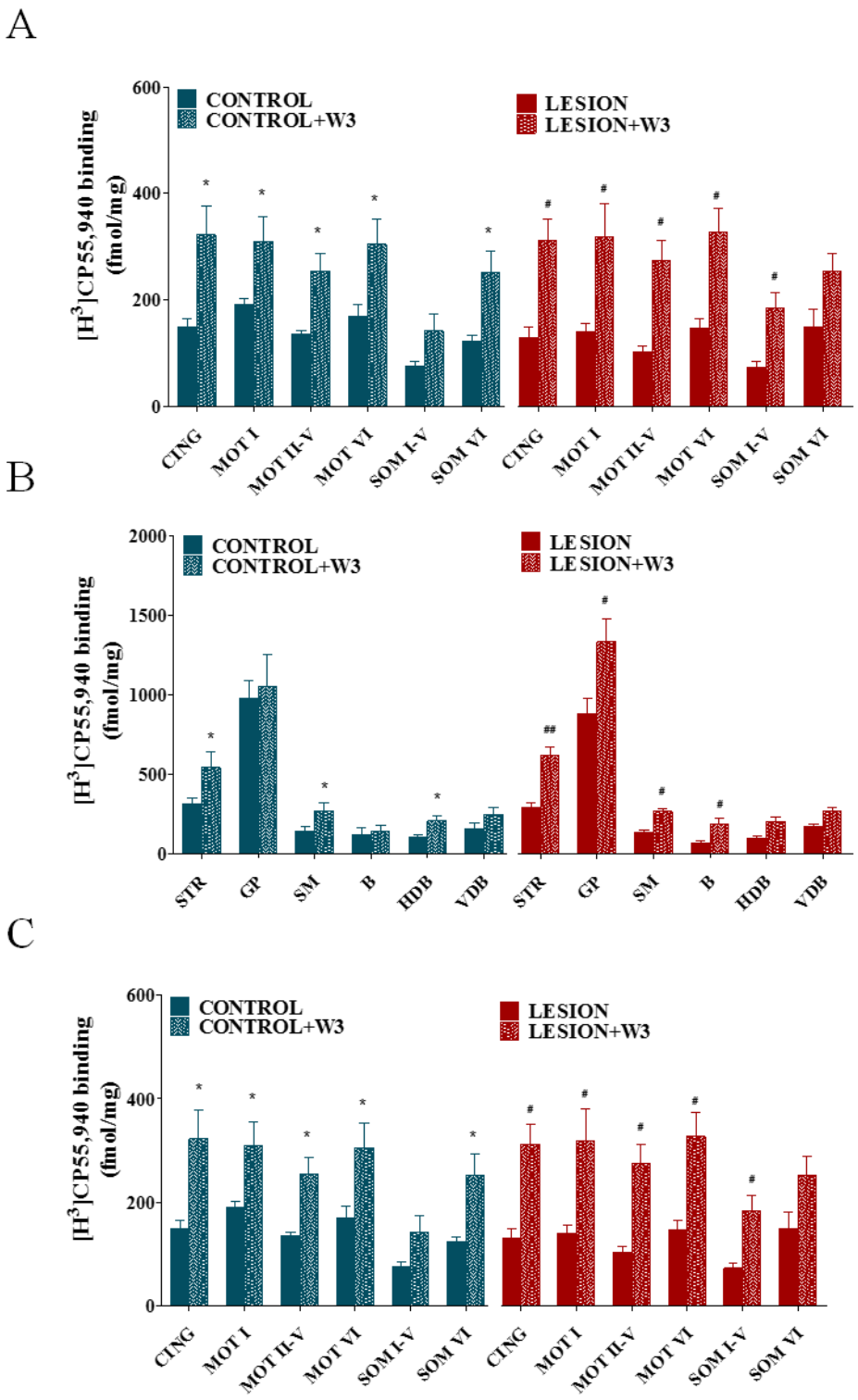

Figure 53. [^{3}H]CP55,940 binding in different brain areas represented as fmol/mg t.e. (A) Cerebral cortex (CING: cingulate, MOT I: motor cortex layer I, MOT II-V: motor cortex layer II-V, MOT VI: motor cortex layer VI, SOM I: Somatosensorial cortex layer I, SOM VI: Somatosensorial cortex layer VI). (B) Basal ganglia (STR: striatum, GP: Globus pallidus, MS: medial septum, B: nucleus basalis magnocellularis, HDB: horizontal diagonal band, VDB: vertical diagonal band). (C) Hippocampus and amygdala (CA1: Oriens, pyramidal, radiatum; CA2: Oriens, pyramidal, radiatum; CA3: Oriens, pyramidal, radiatum; DG: dentate gyrus: Granular, molecular, polymorphic, AMYG: amygdala). (Data are mean ± S.E.M.) *p≤0.05 CONTROL *vs* C+W3, #p≤0.05, ##p≤0.01 LESION *vs* L+W3.

6. ADMINISTRATION OF SR141716A ON A RAT MODEL OF BASAL FOREBRAIN CHOLINERGIC LESION

Finally, we analyzed the effects on learning and memory parameters induced by a subchronic treatment with the CB_1 antagonist SR1417161A (0.5 mg/kg) alone in the rat model of basal forebrain cholinergic lesion. The followed schedule for treatments and behavior test was similar to that described previously. .

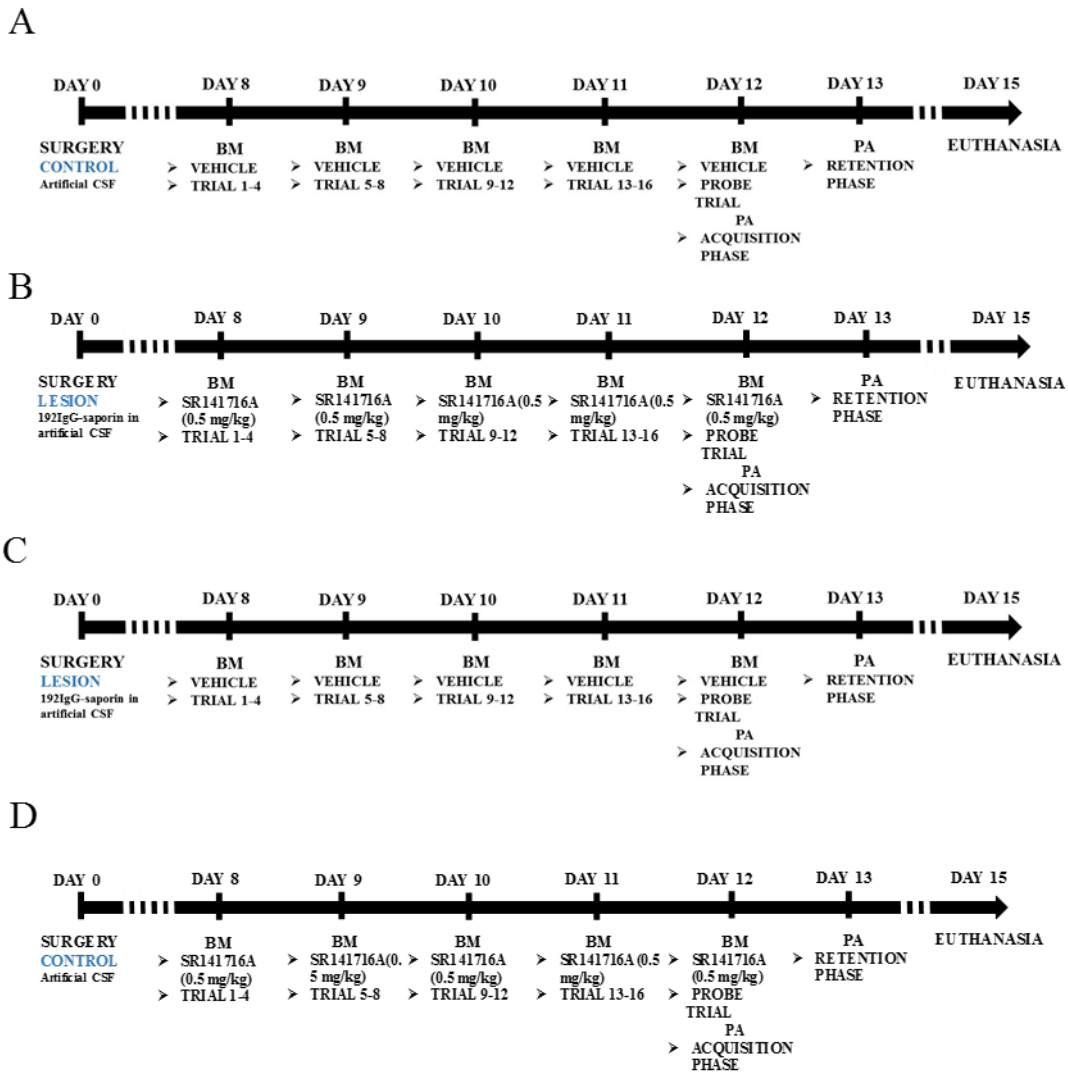

Figure 54. Treatment and behavior training and test schedules followed for each of the four groups of treatment designed to evaluate the effects of SR141716A (0.5 mg/kg) in both spatial and aversive memory.

To examine spatial learning and memory behavior the rats were trained for the Barnes maze test. Total latency and total path length were decreased as the 16 spatial acquisition trainings were completed (Figure 55 A and B). However, the speed was increasing with each trial for all groups of treatment. Usually rats treated with SR141716A (0.5 mg/kg) moved slightly more quick than vehicle-treated rats in all trials (Mean speed: CONTROL: 15 ± 0.6 cm/s, LESION: 17 ± 0.8 cm/s, C+SR0.5: 17 ± 1.4 cm/sec, L+SR0.5: 20 ± 0.7 cm/s, Figure 55 C).

Total latency showed significant differences in trial 13 for lesion rats, but those treated with the CB_1 antagonist showed similar latencies to control animals (Trial 13; CONTROL: 9 ± 1 sec, LESION: 18 ± 2 sec, C+SR0.5: 10 ± 3 sec, L+SR0.5: 9 ± 1 sec. #$p \leq 0.05$ LESION *vs* L+SR0.5. Figure 55 D). Total path length showed differences in trial 1 and trial 13 (Trial 1; CONTROL: 376 ± 39 cm, LESION: 446 ± 58 cm, C+SR0.5: 430 ± 77 sec, L+SR0.5: 767 ± 111 cm. #$p \leq 0.05$ LESION *vs* L+SR0.5 Trial 13; CONTROL: 156 ± 19 cm, LESION: 277 ± 30 cm, C+SR0.5: 210 ± 46 sec, L+SR0.5: 167 ± 24 cm. #$p \leq 0.05$ LESION *vs* L+SR0.5. Figure 55 E).

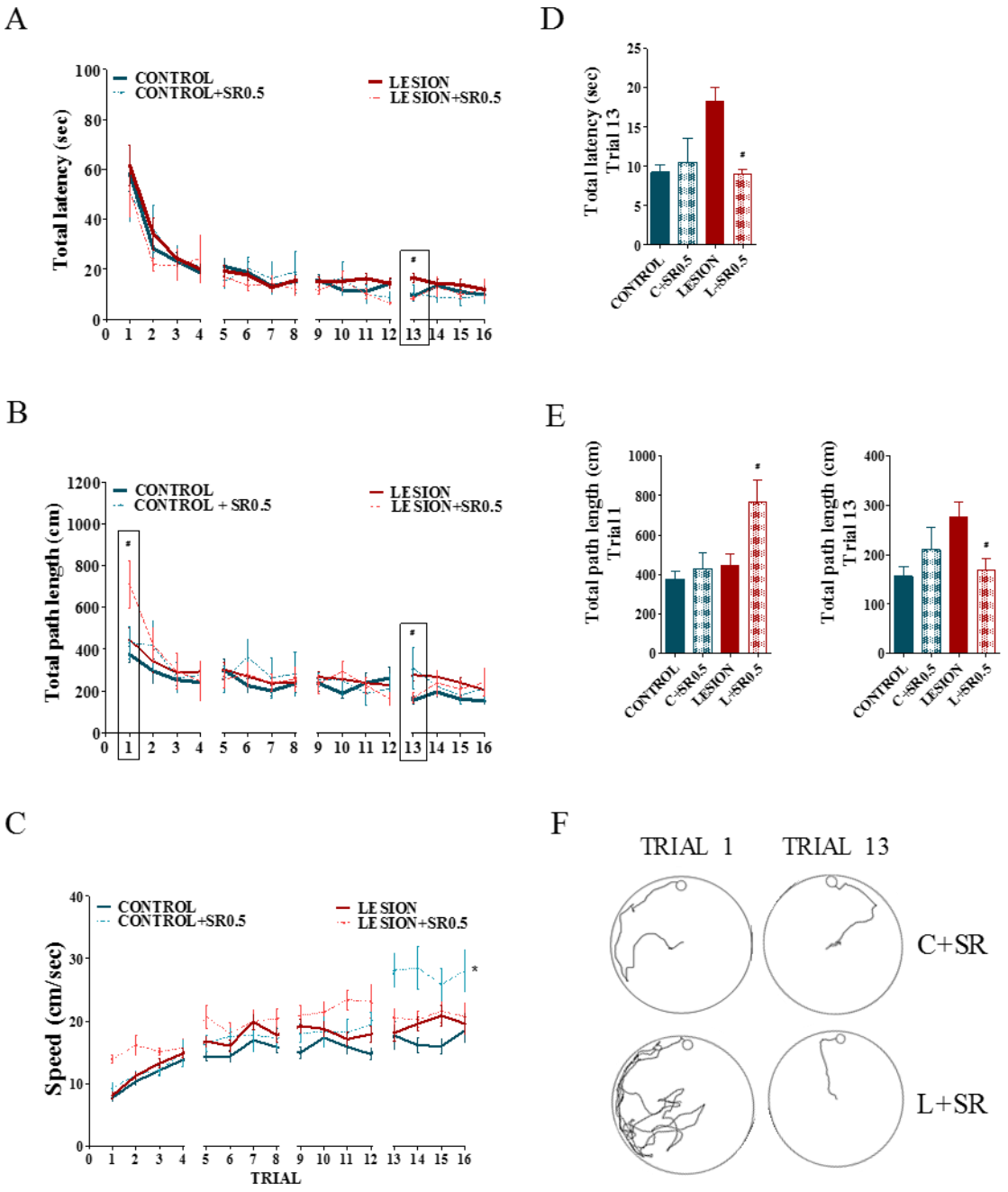

Figure 55. (A) Total latency. (B) Total path length. (C) Speed during each of the sixteen trials that constitute the acquisition phase for each of the four groups of animals. (D) Total latency. (E) Total path lengths covered during trials 1 and 13. (F) Representative trajectories during of trials 1 and 13 for the animals treated with SR141716A (0.5 mg/kg). (Data are mean ± S.E.M.). *p≤0.05 CONTROL *vs* C+SR0.5, #p≤0.05 LESION *vs* L+SR0.5.

On probe trial, after the last training day, the latency in target quadrant was measured for each of the experimental groups of treatment. Control rats treated with SR141716A (0.5 mg/kg) spent less time in the target quadrant than non-treated control rats. Conversely, treated lesion rats spent more time than non-treated lesion rats (Time spent in target quadrant. CONTROL: 89 ± 3 sec, C+SR0.5: 66 ± 3 sec, LESION: 48 ± 3, LESION+SR0.5: 68 ± 3 sec)

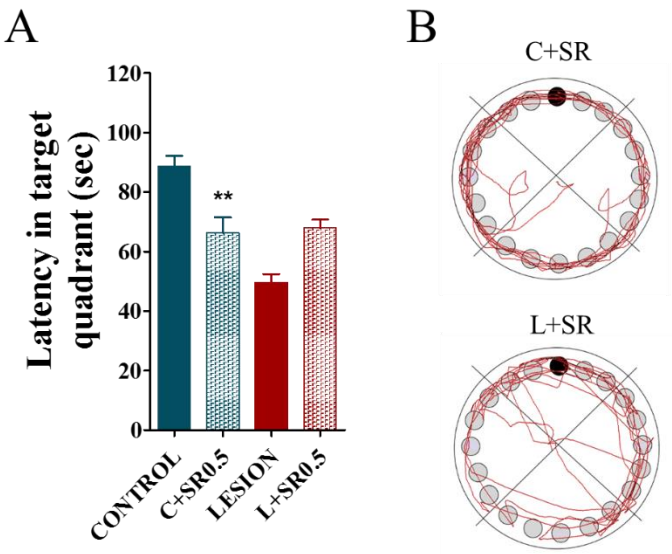

Figure 56. (A) Time spent in target quadrant on probe trial (B) Representative trajectory during 180 sec of the probe trial. Data are mean ± S.E.M. **p≤0.01 CONTROL *vs* C+SR0.5.

Learning and memory associated to aversive stimulus was evaluated in the passive avoidance test. The same day of the probe trial of Barnes Maze (12th day), we also evaluated the acquisition latency parameter in the passive avoidance test. LESION group exhibited lower latency times than the other groups of rats. (CONTROL: 12 ± 1 sec, C+SR0.5: 19 ± 4 sec, LESION: 6 ± 1 sec, L+SR0.5: 12 ± 2 sec. Figure 57 A). 24 hours later, all trained animals were tested again to evaluate aversive memory. Then, the step-through latency time was measured. When the four groups of treatment were compared only CONTROL and C+SR0.5 group were able to remember the aversive stimulus (CONTROL: 77 % and C+SR0.5: 80 % positive response). In the other two groups, LESION and L+SR0.5, only 26 % and 11 % of the animals were able to remember aversive stimulus, respectively. (Figure 57 B).

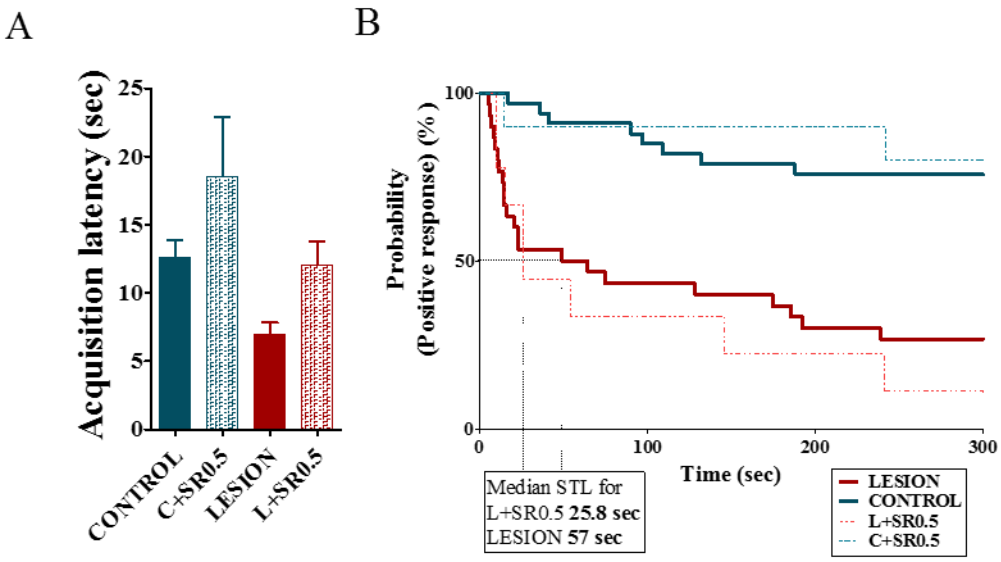

Figure 57. (A) Acquisition latency times during the learning trial of the passive avoidance test. Data are mean ± S.E.M. (B) Step-Through latency times of passive avoidance test represented as Kaplan-Meier survival, Log-Rank/Mantel-Cox test. No significant differences between control and C+SR0.5 and between lesion and L+SR0.5.

6.1. Subchronic administration of SR141716A (0.5 mg/kg) to rats with basal forebrain cholinergic lesion induce a decrease in muscarinic signaling

The effects on cholinergic muscarinic receptor activity induced by subchronic administration of SR141716A (0.5 mg/kg) to rats with basal forebrain cholinergic lesion was studied by autoradiography.

The [^{35}S]GTPγS binding stimulated by carbachol (100μM) was measured in brain areas related to learning and memory to localize and quantify the activity of M_2/M_4 receptors. The basal [^{35}S]GTPγS binding was similar in the four groups of treatment and in all the analyzed brain areas. The treatment with SR141716A (0.5 mg/kg) to CONTROL rats decreased M_2/M_4 receptor activity induced by carbachol in most of the analyzed brain areas. (**Cingulate**: CONTROL: 223 ± 36 % *vs* C+SR0.5: 38 ± 12 %, **Motor cortex layer I**: CONTROL: 281 ± 14 % *vs* C+SR0.5: 24 ± 11 %, **Motor cortex layer II-V**: CONTROL: 294 ± 44 % *vs* C+SR0.5: 31 ± 19 % , **Somatosensorial cortex layer I-V**: CONTROL: 125 ± 27 % *vs* C+SR0.5: 20 ± 10 %, **Somatosensorial cortex layer VI**: CONTROL: 153 ± 36 % *vs* C+SR0.5: 35 ± 14 %, **Striatum**: CONTROL: 150 ± 20 % *vs* C+SR0.5: 9 ± 5 %, **Globus pallidus**: CONTROL: 97 ± 15 % *vs* C+SR0.5: 14 ± 4 %, **MS**: CONTROL: 180 ± 32 % *vs* C+SR0.5: 31 ± 9 %, **B**: CONTROL: 73 ± 13 % *vs* C+SR0.5: 22 ± 3 %, **VDB**: CONTROL: 282 ± 49 % *vs* C+SR0.5: 30 ± 11 %, **CA1**: CONTROL: 105 ± 33 % *vs*

C+SR: 29 ± 10 % , **CA2**: CONTROL: 163 ± 39 % *vs* C+SR0.5: 38 ± 16 %, **CA3**: CONTROL: 143 ± 28 % *vs* C+SR0.5: 18 ± 11 %,. see Figure 58 for statistical data). In addition, the treatment with SR141716A to a group of lesion rats, was able to induce a down-regulation of M_2/M_4 receptor activity in cortex and in hippocampus (**Somatosensorial cortex layer I-V**: LESION: 150 ± 39 % *vs* L+SR: 26 ± 7 % and **CA2**: LESION: 238 ± 40 % *vs* L+SR0.5: 59 ± 31 %. see Figure 58 for statistical data).

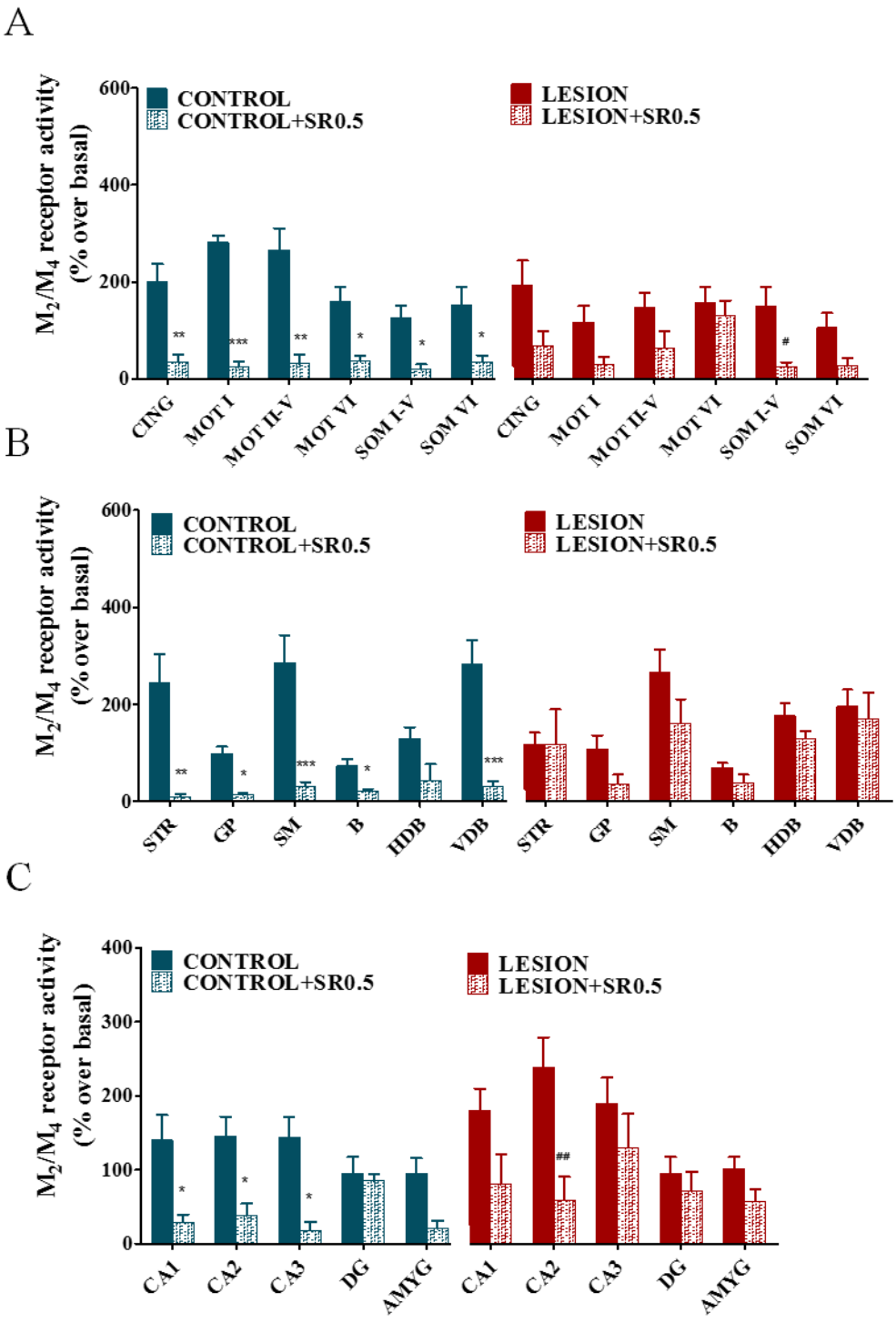

Figure 58. Percentage of stimulated [^{35}S]GTPγS binding by carbachol in different brain areas. (A) Cerebral cortex (CING: cingulate, MOT I: motor cortex layer I, MOT II-V: motor cortex layer II-V, MOT VI: motor cortex layer VI, SOM I: Somatosensorial cortex layer I, SOM VI: Somatosensorial cortex layer VI). (B) Basal ganglia (STR: striatum, GP: Globus pallidus, MS: medial septum, B: nucleus basalis magnocellularis, HDB: horizontal diagonal band, VDB: vertical diagonal band). (C) Hippocampus and amygdala (CA1: Oriens, pyramidal, radiatum; CA2: Oriens, pyramidal, radiatum; CA3: Oriens, pyramidal, radiatum; DG: dentate gyrus: Granular, molecular, polymorphic, AMYG: amygdala). (Data are mean ± S.E.M.). *p≤0.05, **p≤0.01, ***p≤0.001 CONTROL *vs* C+SR0.5; #p≤0.05, ##p≤0.01 LESION *vs* L+SR0.5.

6.2. Subchronic SR1417161A administration after basal forebrain lesion modifies the cholinergic innervation

The effect of subchronic SR141716A administration on AChE activity was studied in brain areas related to learning and memory. The CB_1 antagonist administration to CONTROL rats induced an increase of $AChE^+$ fiber densities in both basal ganglia and cortical areas (**Globus pallidus**: CONTROL: 13 ± 1 *vs* C+SR0.5: 41 ± 8 O.D. (a.u.), **Medial septum**: CONTROL: 50 ± 2 *vs* C+SR0.5: 77 ± 9 O.D. (a.u.), **HDB**: CONTROL: 60 ± 3 *vs* C+SR0.5: 78 ± 3 O.D. (a.u.), **VDB**: CONTROL: 47 ± 4 *vs* C+SR0.5: 78 ± 6 O.D. (a.u.).Figure 59). A similar effect was observed for the lesion rats treated with SR141716A (**Motor cortex layer I**: LESION: 9 ± 1, L+SR0.5: 15 ± 1 O.D. (a.u.), **Motor cortex layer II-V**: LESION: 8 ± 1, L+SR0.5: 17 ± 1 O.D. (a.u.), **Motor cortex layer VI**: LESION: 8 ± 1, L+SR0.5: 18 ± 1 O.D. (a.u.), **Somatosensorial cortex layer I-V**: LESION: 9 ± 1, L+SR0.5: 19 ± 1 O.D. (a.u.), **Somatosensorial cortex layer VI**: LESION: 11 ± 1, L+SR: 21 ± 1 O.D. (a.u.), **Globus pallidus:** LESION: 12 ± 1, L+SR0.5: 28 ± 1 O.D. (a.u.), **B:** LESION: 23 ± 3, L+SR0.5: 42 ± 3 O.D. (a.u.), **VDB:** LESION: 44 ± 2, L+SR0.5: 63 ± 4 O.D. (a.u.). Figure 59).

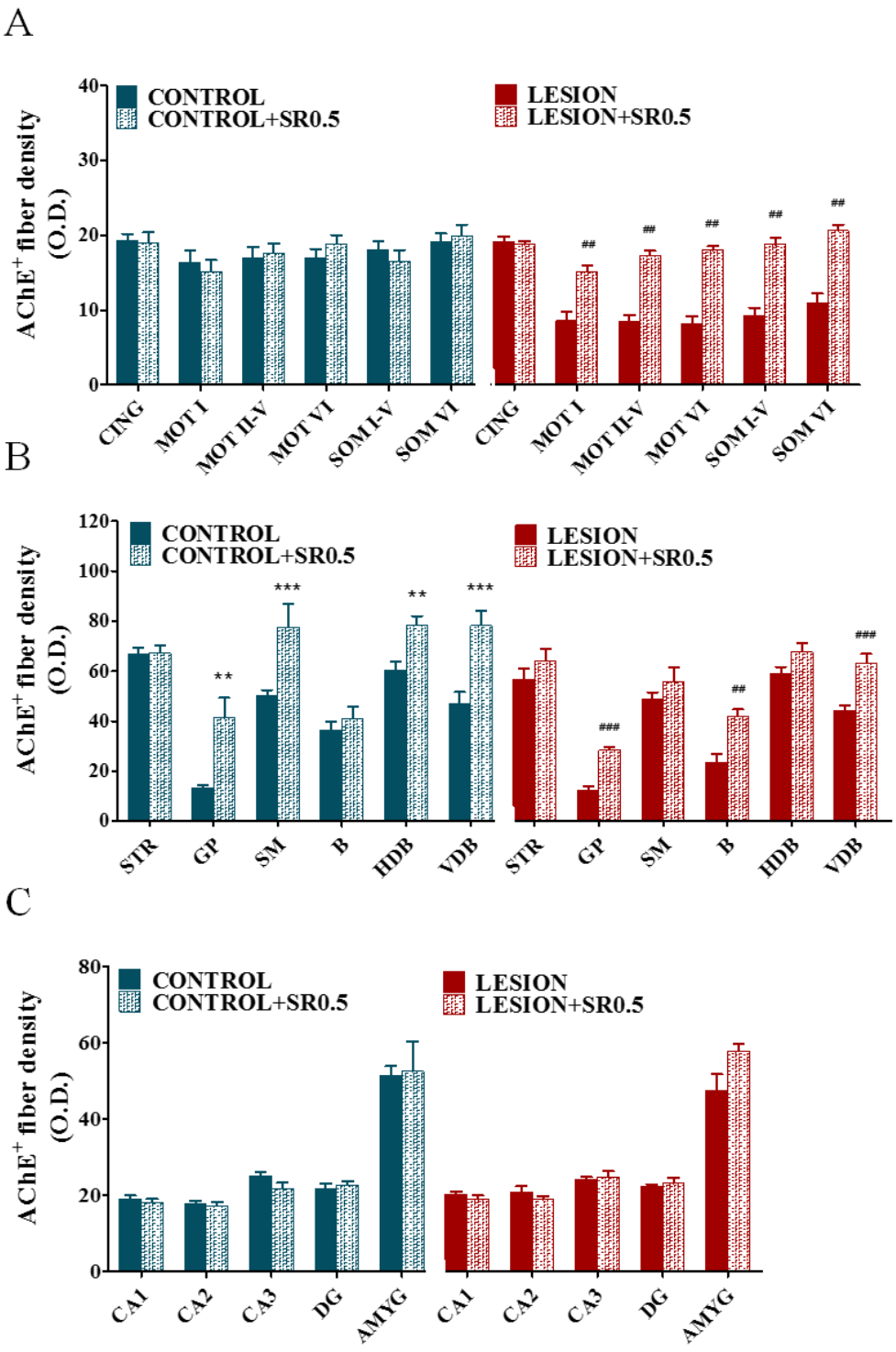

Figure 59. AChE staining in different brain areas represented as O.D. (a.u.). (A) Cerebral cortex (CING: cingulate, MOT I: motor cortex layer I, MOT II-V: motor cortex layer II-V, MOT VI: motor cortex layer VI, SOM I: Somatosensorial cortex layer I, SOM VI: Somatosensorial cortex layer VI), (B) Basal ganglia (STR: striatum, GP: Globus pallidus, MS: medial septum, B: nucleus basalis magnocellularis, HDB: horizontal diagonal band, VDB: vertical diagonal band). (C) Hippocampus and amygdala (CA1: Oriens, pyramidal, radiatum; CA2: Oriens, pyramidal, radiatum; CA3: Oriens, pyramidal, radiatum; DG: dentate gyrus: Granular, molecular, polymorphic, AMYG: amygdala). (Data are mean ± S.E.M.) *p≤0.05, **p≤0.01 CONTROL *vs* C+SR0.5; ##p≤0.01, ###p≤0.001 LESION *vs* L+SR0.5.

6.3. Subchronic SR141716A administration after basal forebrain cholinergic lesion leads to altered CB_1 activity and density

The effect of SR141716A administration on cannabinoid receptors was studied. The activity of cannabinoid receptors was analyzed by [^{35}S]GTPγS autoradiography. The [^{35}S]GTPγS binding stimulated by WIN55,212-2 (10 µM) was measured in brain areas related to learning and memory to localize and quantify the activity of CB_1 receptors. The SR141716A subchronic treatment of CONTROL rats induced a down-regulation in CB_1 receptor activity in different brain areas involved in the control of learning and memory processes. (**Cingulate:** 361 ± 74 % *vs* C+SR0.5: 75 ± 30 %, **Motor cortex layer I**: CONTROL: 258 ± 54 % *vs* C+SR0.5: 49 ± 12 %, **Motor cortex layer II-V**: CONTROL: 212 ± 50 % *vs* C+SR0.5: 40 ± 30 %, **Motor cortex layer VI**: CONTROL: 430 ± 29 % *vs* C+SR0.5: 137 ± 69 %, **Striaum**: CONTROL: 436 ± 88 % *vs* C+SR0.5: 79 ± 22 %, **Globus pallidus**: CONTROL: 1833 ± 369 % *vs* C+SR0.5: 369 ± 75 %, **MS**: CONTROL: 427 ± 95 % *vs* C+SR0.5: 75 ± 46 %, **B**: CONTROL: 205 ± 61 % *vs* C+SR0.5: 31 ± 15 %,**VDB**: CONTROL: 353 ± 77 % *vs* C+SR0.5: 58 ± 30 %, **CA1**: CONTROL: 294 ± 56 % *vs* C+SR0.5: 17 ± 5 %, **CA2**: CONTROL: 360 ± 71 % *vs* C+SR0.5: 47 ± 12 %, **CA3**: CONTROL: 434 ± 64 % *vs* C+SR0.5: 70 ± 40 %, **Dentate gyrus**: CONTROL: 412 ± 69 % *vs* C+SR0.5: 52 ± 14 % and **Amygdala**: CONTROL: 190 ± 62 % *vs* C+SR0.5: 40 ± 12 %. Figure 60). In addition, the same treatment applied to a group of lesion rats also decreased the CB_1 receptor activity, in different brain areas (**Cingulate**: LESION: 257 ± 67 % *vs* L+SR0.5: 53 ± 15 %, **Globus pallidus**: LESION: 1119± 122 % *vs* L+SR0.5: 402 ± 79 %, **B**: LESION: 236 ± 60 % *vs* L+SR0.5: 77 ± 24 %, **CA1**: LESION: 389± 53 % *vs* L+SR0.5: 38 ± 27 %, **CA2**: LESION: 381 ± 74 % *vs* L+SR0.5: 45 ± 29 %, **CA3**: LESION: 359 ± 47 % *vs* L+SR0.5: 114 ± 53 %, **Dentate gyrus**: LESION: 369 ± 39 % *vs* L+SR0.5: 76 ± 35 %, **Amygdala:** LESION: 252 ± 69 % *vs* L+SR0.5: 38 ± 12 %. Figure 60,).

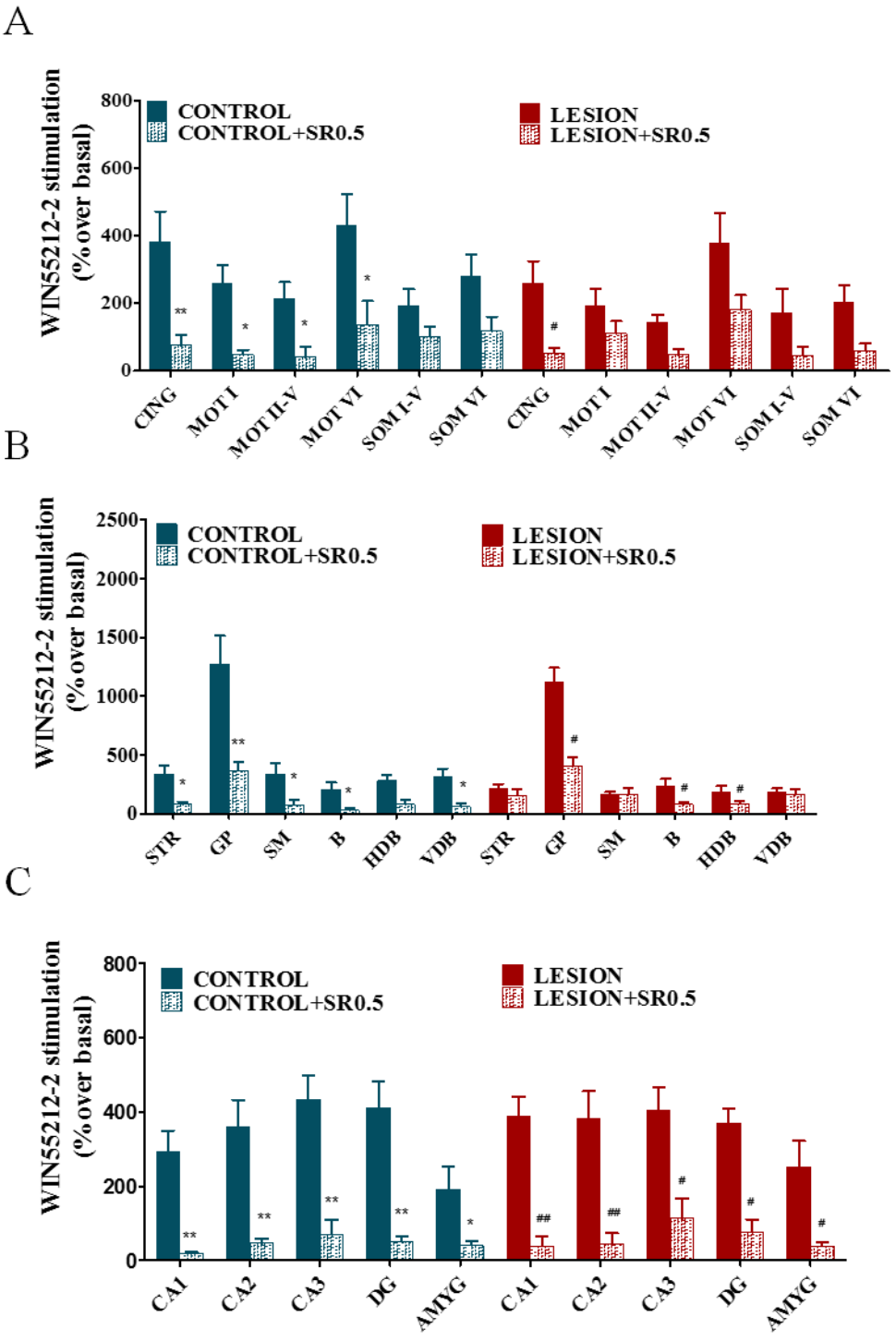

Figure 60. [^{35}S]GTPγS binding stimulated by WIN55,212-2 (10μM) in different brain areas represented as % stimulated over the basal. (A) Cerebral cortex (CING: cingulate, MOT I: motor cortex layer I, MOT II-V: motor cortex layer II-V, MOT VI: motor cortex layer VI, SOM I: Somatosensorial cortex layer I, SOM VI: Somatosensorial cortex layer VI). (B) Basal ganglia (STR: striatum, GP: Globus pallidus, MS: medial septum, B: nucleus basalis magnocellularis, HDB: horizontal diagonal band, VDB: vertical diagonal band). (C) Hippocampus and amygdala (CA1: Oriens, pyramidal, radiatum; CA2: Oriens, pyramidal, radiatum; CA3: Oriens, pyramidal, radiatum; DG: dentate gyrus: Granular, molecular, polymorphic, AMYG: amygdala). (Data are mean ± S.E.M.) *p≤0.05, *p≤0.01 CONTROL *vs* C+SR0.5; #p≤0.05##p≤0.01 LESION *vs* L+SR0.5.

Finally, the density of CB_1 receptors was also analyzed in the same brain areas by measuring the specific [^{3}H]CP55,940 binding. The administration of 0.5mg/kg of SR141716A to the CONTROL group induced an up-regulation of the CB_1 density in all the analyzed brain areas (**Cingulate**: CONTROL: 149 ± 15 *vs* C+SR0.5: 476 ± 67 fmol/g t.e.; **Motor cortex layer I**: CONTROL: 173 ± 19 *vs* C+SR0.5: 465 ± 67 fmol/g t.e.; **Motor cortex layer II-V**: CONTROL: 136 ± 6 *vs* C+SR0.5: 437 ± 51 fmol/g t.e.; **Motor cortex layer VI**: CONTROL: 170 ± 23 *vs* C+SR0.5: 536 ± 73 fmol/g t.e.; **Somatosensorial cortex layer I-V**: CONTROL: 75 ± 10 *vs* C+SR0.5: 142 ± 32 fmol/g t.e.; **Somatosensorial cortex layer VI**: CONTROL: 123 ± 10 *vs* C+SR0.5: 371 ± 69 fmol/g t.e.; **Striatum**: CONTROL: 313 ± 36 *vs* C+SR0.5: 781 ± 153 fmol/g t.e;, **Globus pallidus**: CONTROL: 980 ± 107 *vs* C+SR0.5: 1494 ± 179 fmol/g t.e.; **Medial septum**: CONTROL: 149 ± 28 *vs* C+SR0.5: 352 ± 49 fmol/g t.e.; **B**: CONTROL: 122 ± 37 *vs* C+SR0.5: 252 ± 18 fmol/g t.e.; **HDB**: CONTROL: 102 ± 16 *vs* C+SR0.5: 300 ± 39 fmol/g t.e.; **VDB**: CONTROL: 159 ± 32 *vs* C+SR0.5: 370 ± 58 fmol/g t.e.; **CA1:** CONTROL: 175 ± 30 *vs* C+SR0.5: 848 ± 135 fmol/g t.e.; **CA2:** CONTROL: 234 ± 21 *vs* C+SR0.5: 777 ± 119 fmol/g t.e.; **CA3:** CONTROL: 282 ± 28 *vs* C+SR0.5: 865 ± 100 fmol/g t.e.; **Dentate gyrus**: CONTROL: 219 ± 32 *vs* C+SR0.5: 750 ± 88 fmol/g t.e.; **Amygdala**: CONTROL: 103 ± 19 *vs* C+SR0.5: 252 ± 30 fmol/g t.e. Figure 61).

The same treatment applied to a group of lesion rats also increased the CB_1 density in the same brain areas. (**Cingulate**: LESION: 130 ± 19 *vs* L+SR0.5: 600 ± 78 fmol/g t.e.; **Motor cortex layer I**: LESION: 140 ± 16 *vs* L+SR0.5: 673 ± 138 fmol/g t.e.; **Motor cortex layer II-V**: LESION: 103 ± 11 *vs* L+SR0.5: 516 ± 83 fmol/g t.e.; **Motor cortex layer VI**: LESION: 146 ± 19 *vs* L+SR: 683 ± 128 fmol/g t.e.; **Somatosensorial cortex layer I-V**: LESION: 73 ± 11 *vs* L+SR0.5: 341 ± 69 fmol/g t.e.; **Somatosensorial cortex layer VI**: LESION: 150 ± 32 *vs* L+SR0.5: 511 ± 100 fmol/g t.e.; **Striatum**: LESION: 292 ± 27 *vs* L+SR0.5: 781 ± 153 fmol/g t.e.; **Globus pallidus**: LESION: 883 ± 98 *vs* L+SR: 1494 ± 179 fmol/g t.e., **Medial septum**: LESION: 136 ± 11 *vs* L+SR0.5: 352 ± 49 fmol/g t.e.; **B**: LESION: 66 ± 12 *vs* L+SR0.5: 252 ± 19 fmol/g t.e.; **HDB**: LESION: 66 ± 12 *vs* L+SR0.5: 300 ± 39 fmol/g t.e.; **VDB**: LESION: 168 ± 12 *vs* L+SR0.5: 370 ± 58 fmol/g t.e.; **CA1:** LESION: 274 ± 38 *vs* L+SR0.5: 848 ± 135 fmol/g t.e.; **CA2:** LESION: 312 ± 43 *vs* L+SR0.5: 777 ± 119 fmol/g t.e.; **CA3:** LESION: 312 ± 29 *vs* L+SR0.5: 865 ± 100 fmol/g t.e.; **Dentate gyrus**: LESION: 276 ± 19 *vs* L+SR0.5: 750 ± 88 fmol/g t.e.; **Amygdala**: LESION: 185 ± 24 *vs* L+SR0.5: 252 ± 30 fmol/g t.e. Figure 61).

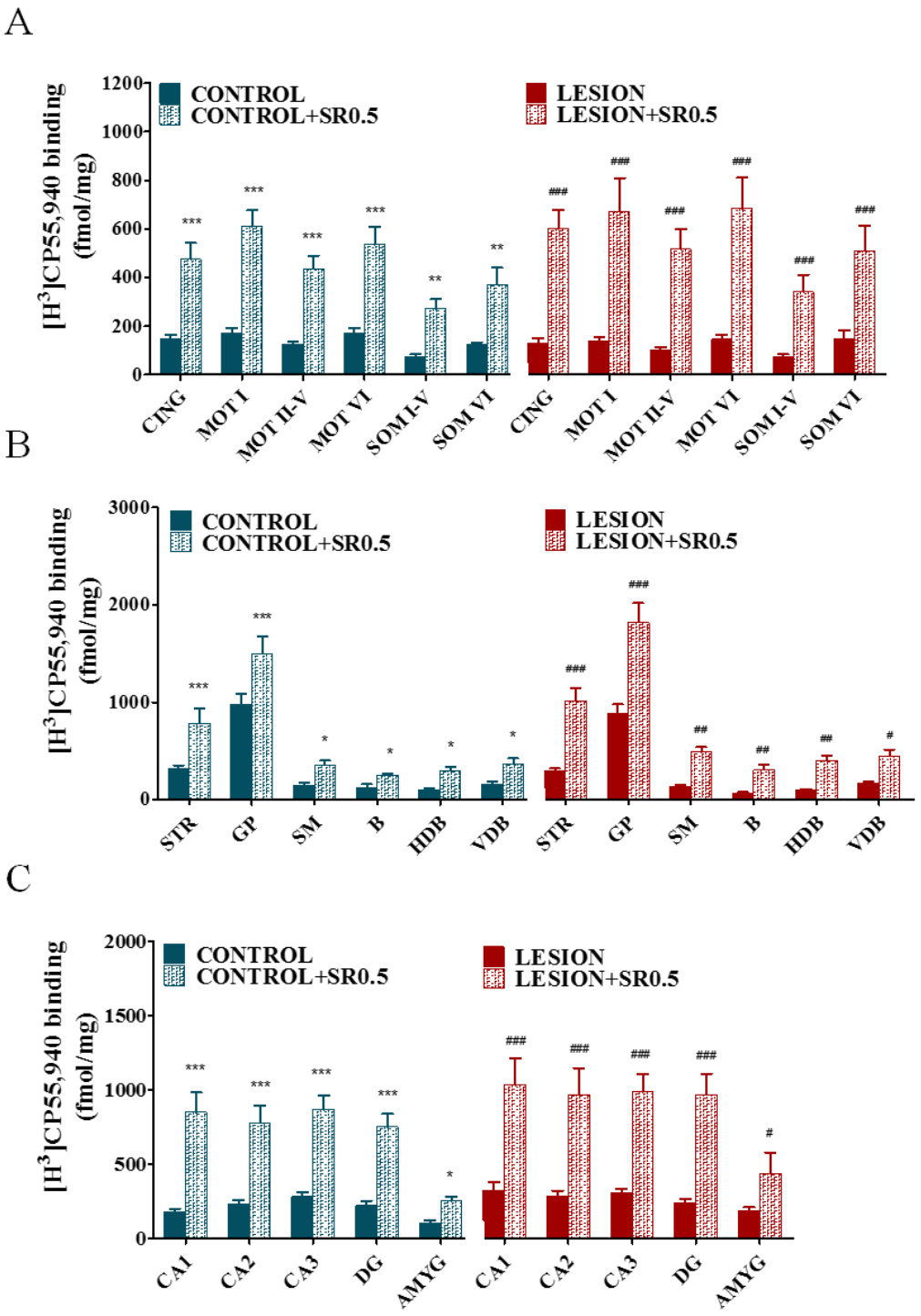

Figure 61. The [^{3}H]CP55,940 binding in different brain areas represented as fmol/mg t.e. (A) Cerebral cortex (CING: cingulate, MOT I: motor cortex layer I, MOT II-V: motor cortex layer II-V, MOT VI: motor cortex layer VI, SOM I: Somatosensorial cortex layer I, SOM VI: Somatosensorial cortex layer VI), (B) Basal ganglia (STR: striatum, GP: Globus pallidus, MS: medial septum, B: nucleus basalis magnocellularis, HDB: horizontal diagonal band, VDB: vertical diagonal band) and (C) Hippocampus and amygdala (CA1: Oriens, pyramidal, radiatum; CA2: Oriens, pyramidal, radiatum; CA3: Oriens, pyramidal, radiatum; DG: dentate gyrus: Granular, molecular, polymorphic, AMYG: amygdala). (Data are mean ± S.E.M.) *p≤0.05, **p≤0.01, ***p≤0.001 CONTROL *vs* C+SR0.5; #p≤0.05, ##p≤0.01, ###p≤0.001 LESION *vs* L+SR0.5.

DISCUSSION

The current treatments approved by the FDA for the Alzheimer disease include the acetylcholinesterase inhibitors that are based on the called cholinergic hypothesis. The origins of this hypothesis were studies initiated in the seventies that showed a cholinergic transmission disruption related to cognitive impairments in AD patients (Drachman, 1977). The goal of the treatments with acetylcholinesterase inhibitors is to enhance the cholinergic tone, but unfortunately the clinical outcome is only a moderate retardation in the advance of this devastating neurodegenerative disease (Bartus, 2000). Nowadays, only five medications are used in the clinical practice: donepezil, galantamine and rivastigmine from the "cholinesterase inhibitors", memantine as a NMDA glutamate receptor antagonist and the combination of donepezil and memantine. Moreover, these treatments were approved one hundred years after the first patient was diagnosed. These treatments cannot stop the progression of AD and are limited to temporary symptomatic relief and not exempt from side effects (Du et al., 2018).

The depletion of the cholinergic neurons in the basal forebrain, mainly in nucleus basalis of Meynert of AD patients was already identified during the eighties as one of the most plausible explanations to the damage in learning and memory processes, impairment that also was correlated to changes in neocortex(Whitehouse et al., 1982). Within this framework lie the animal models used in the present study based on muscarinic cholinergic antagonists and lesions in basal forebrain cholinergic system..

In this context, the neuromodulatory role of the endocannabinoid system (eCB) in the control of learning and memory has been emerging during the last few years, but the mechanism and interactions with the cholinergic are far of being understood. The eCB system is widely distributed in areas related to cognition such as the basal ganglia, hippocampus, amygdala and cortex. In addition the reported alterations under pathological conditions suggest that this system regulates essential processes altered during the development of different neurodegenerative diseases. The results described in the present Thesis supports recent preclinical evidences indicating that eCB-based therapies would be useful for dementia treatment in different neurological disorders, such as the Alzheimer's disease

In the present study to complementary models of cholinergic system dysfunction were used, pharmacological antagonism and lesion of the basal forebrain cholinergic pathway. Both models are used in many studies to understand pathological processes of cognitive impairments involving cholinergic dysfunction (Abdulla et al., 1997a; Berger-Sweeney et al., 2001; Fitz et al., 2008; Dashniani et al., 2009; Sadek et al., 2016a; Lee et al., 2016a).

The present study describes the positive effect of a relatively low dose (0.5 mg/kg) of the potent CB_1 receptor agonist, WIN55,212-2, restoring the cognitive impairment induced in both cholinergic dysfunction models. The pharmacological, histological and biochemical results

obtained in the brain of rats is discussed here below trying to elucidate the mechanism of action to explain those effects.

Impairment of spatial and aversive memory in rats following a cholinergic lesion of the basal forebrain

The cholinergic lesion of the basal forebrain (B) with 192IgG-saporin induced impairment in spatial and aversive memory when evaluated by Barnes Maze (BM) and passive avoidance (PA) tests PA, respectively. The group of rats with intraparenquimal administration of the vehicle (control) animals did not show any effect in both types of memories.

The BM is considered a hippocampal-dependent task where animals learn to associate visual stimuli in the surrounding environment with an escape hole location. Therefore, the associative neocortex is involved in the processing and integration of the spatial information. The Morris Water Maze (MWM) is the most widely employed behavioral test to study spatial acquisition in rodents, however, MWM use rodent's natural aversion to swimming in water as the motivation to learn the escape platform, but definitely the animals get very stressed during the test. Swimming is stressful, even to increase plasma corticosterone levels to a great extent (Brem et al., 2013; Vorhees and Williams, 2014). It should also be noted that pharmacological and/or genetic manipulations that increase anxiety could act as confounding factors on MWM performance. In the present study, the BM test offered several important advantages with regard to MWM. BM was used to evaluate spatial and working memory avoiding the stress to the maximum degree possible of the animal during the test (Barnes, 1979). Furthermore, BM was followed by PA test in the same animals to specifically evaluate learning and memory associated to aversive stimulus.

The basal forebrain cholinergic neurons (BFCN) constitute the predominant source of acetylcholine in these brain regions and have an important role in mediating fear and extinction memory. More specifically, the nucleus basalis magnocellularis cholinergic neurons innervating the basolateral amygdala (BLA) are critical for fear-associated memory and contextual fear extinction memory (Knox, 2016). Pharmacological treatments with both muscarinic and nicotinic compounds support the involvement of amygdala, hippocampus, and prefrontal cortex in the modulation of learning and extinction of contexts or cues associated with threat (Wilson and Fadel, 2017). PA was used in the present study to evaluate the degree of basal forebrain cholinergic dysfunction induced in the rats after the lesion of the BFCN. The different effects on memory elicited by toxin administration in basal forebrain will be discussed below.

The lesion rats that we used as a model of basal forebrain cholinergic dysfunction showed a clear disruption in memory and learning capabilities 15 days after the toxin administration. However, previous reports during the nineties shown controversial data regarding the memory effects in rodent models of 192 IgG-saporin administration in the basal forebrain. No cognitive disruption was described in the MWM following a complete cholinergic depletion after icv administration of 192IgG-saporin (Torres et al., 1994). Other authors also described that a selective loss of cholinergic cells in basal forebrain did not affect learning and memory parameters in the PA test, suggesting that this cholinergic dysfunction was not sufficient to produce functional impairments (Wenk et al., 1994). In contrast, it was reported that toxin administration induced dose-dependent memory impairment in both MWM and PA tests (Waite et al., 1995). In addition, previous result obtained by our own research group showed, that depletions of up to an 80 % of neurons in B by 192IgG-saporin intraparenquimal administration lead to aversive memory impairment in PA one week after the lesion. The main discrepancies in previous studies come from the schedule, dosing and pathways of administration of the toxin. Our model has been progressively refined to improve the number of lesion BFCN (around 80%) to optimize the results in selective dysfunction of the basal cholinergic pathway along with cognitive impairment, but preserving some cells for pharmacological interventions(Llorente-Ovejero et al., 2017).

In addition to the effects observed in learning and memory in lesion animals, we could measure also a regulation in locomotion parameters, showing more activity. The average speed of lesion rats during each of the sixteen BM trainings was evaluated. The alteration in locomotor activity by 192 IgG-saporin administration was already described by other authors (Walsh et al., 1995). The motor cortex modulates the animal locomotion and a correlation between numbers of neurons in this area with motor activity was recently described in Piavchenko et al., 2015. Moreover the basal cholinergic system modulates the dopamine release in cortex (Cohen et al., 2012). The hyperactivity of the lesion rats could be explained as a consequence of the dramatic reduction of cortical cholinergic input that would induce an increase in cortical dopamine in similar way to the known striatal equilibrium between both neurotransmitters. Nevertheless, lesion animals, even moving faster than controls spent more time to reach the escape hole in the last training day and during the final probe test, showing also longer trajectories. In other words, the hyperlocomotion was not the cause of the cognitive impairment observed in lesion animals.

Intraparenquimal administration of 192IgG-saporin in basal forebrain decrease cholinergic input

The lesion model of basal forebrain cholinergic denervation showed loss of different cholinergic makers.

The activity mediated by Gi/o coupled muscarinic receptors (M_2/M_4) was dramatically reduced in cortex and medial septum, together with a depletion of AChE activity in both cortical and basal forebrain areas. However, the total number of mAChR was not modified in B. The reduction in the number of cholinergic neurons (p75NTR positive cells) showed a correlation with the decrease in muscarinic activity in cortex and septal nuclei and also with the spatial learning and memory impairment parameters measured in the BM test. As previously indicated, depending on toxin administration area, dosing and especially post-injury time, different modification of cholinergic markers have been reported. Several studies have shown that 192IgG-saporin administration directly into the basal forebrain decreased different cholinergic markers in projection areas, such as cortex but also in hippocampus, but not always this decrease was enough to produce significant cognitive deficits (Baxter et al., 2013; Baxter and Bucci, 2013). Waite et al., 1995, reported that one week after icv administration of the toxin, there was a substantial loss of AChE staining in cortex and hippocampus, and that it was necessary around a 90% reduction in ChAT activity to induce behavioral deficits. Our results are supported by other authors that showed in models of mechanical or ibotenic acid-induced lesion of the basal-cortical pathway a moderate reduction in M_2 subtype of mAChR and M_2 and M_4 mRNA transcripts in frontal cortex, but no change in M_1 receptor (Schliebs et al., 1994).

Autoradiographic studies in *postmortem* tissue of AD patients showed comparable densities to matched controls of the total population of the five muscarinic receptors subtypes also analyzing the binding sites of tritiated scopolamine, and decrease of M_2 subtype in entorhinal cortex (Rodriguez-Puewrtas et al., 1997). The loss of cortical cholinergic innervation usually is accompanied by a depletion of M_2 but not subtypes such as the M_1, that would remain preserved in AD patients (Mufson et al., 2008).

The cortical reduction of AChE activity in lesion animals may be related to the observed cognitive impairment, but the decrease in the activity of M_2/M_4 receptors seems to have more weight in the cognitive disruption of this animals. Both muscarinic receptor subtypes, M_2 and M_4 are necessary in memory acquisition processes (Seeger, et al., 2004; Bainbridge et al., 2008; Bubser et al., 2014). M_2 and M_4 receptors mediate inhibitory responses but with quite different distribution and expression, e.g. M_4 subtype is less prevalent than M_2 in cortical areas (Ferrari-DiLeo et al., 1995). In our autoradiography assay we could not discriminate between M_2 an M_4 activities. The stimulation of the basal forebrain changes mRNA expression of M_4 (Groleau et

al., 2018). But the M_2 studies are more abundant, it is accepted that is a presynaptic auto-receptor located in neurites, fibers, or presumptive terminals. M_2 was detected in 10-30% of the total cholinergic cells in B of rat and monkey brains (Smiley et al., 1999; Medalla and Barbas, 2012). Although M_2 is predominantly presynaptic, also are on GABAergic interneurons in layers II/III and IV (Vilaro et al., 1992; Volpicelli and Levey, 2004). On GABAergic terminals, M_2 activation inhibits the release of GABA (Salgado et al., 2007).

A slight increase of M_2 receptor density was found after icv administration of 192 IgG-saporin (Rossner, 1997). All this data suggest that most of the activity of M_2/M_4 observed in our functional autoradiographyc study could come from the remaining BFCN projections. Previous result of our research group using a similar lesion procedure but dissecting the rat brains only one week after lesion, did not show significant differences in the activity of M_2/M_4 but a decrease of GABAergic cortical markers (Llorente-Ovejero et al., 2017). The GABA reduction after basal forebrain lesion has also been shown by other authors (Jeong et al., 2016). After one week of post-lesion time, the decrease of M_2/M_4 activity found in cortex 2 weeks post-lesion input was not detectable. The decrease of GABAergic cortical markers could progressively lead to the cortical M_2 reduction observed in our model. Most of the BFCN and their cortical projections that may have presynaptic M_2 could have been eliminated, with the consequent reduction in muscarinic receptor activity in cortex, but together with down-regulation of cortical GABAergic interneurons that express this receptor probably postsinaptically.

As previously indicated, the decrease in M_2/M_4 activity at the motor cortex, area that is obviously involved in motor function control, could also be responsible for the observed hyperlocomotion of the lesion rats. Cortical cholinergic denervation together with ACh decrease can cause locomotion activity alteration (Mattsson et al., 2004). M_4 muscarinic receptor control of cholinergic function produces dopaminergic hyperexcitability (Tzavara et al., 2004). These considerations suggest that BFCN depletion lead to decreased ACh cortical levels and finally to cholinergic tone disruption. Cortex processing malfunctions could produce the effects observed in learning, memory and motor functions.

Finally, we also found a modulation of M_2/M_4 receptors activity in septal nuclei, although this area should not be directly affected by the 192 IgG-saporin administration in B. Previous studies published that M_4 immunoreactivity in septal nuclei is negligible compared to M_2 (Levey et al., 1991). Accordingly, the muscarinic activity showed in the autoradiography study could be mediated mainly by the M2 subtype. Moreover, previous studies have demonstrated that the toxin administration in septal areas does not modify the M_2 immunoreactivity because only 8% of cholinergic cells in septal nuclei express the M2 receptor subtype. M_2 is principally expressed in GABAergic interneurons (Levey et al., 1991c; Levey, Edmunds, Hersch et al., 1995). It could be

plausible that 192 IgG-saporin would have diffused more than we expected, but then we should have observed changes in septal nuclei and hippocampus by the AChE staining, however we only found changes in cortical and in lesion areas. These results suggest a secondary response or regulation induced by the BFCN elimination interacting with GABAergic transmission directly related to septal nuclei cholinergic signaling. This possibility is further discussed within the context of the eCB in the next

Additionally, studies in M_2 mAChR knockout mice have reported significant deficits in learning and memory at the BM behavioral test (Seegeret al., 2004b). The cognitive deficits in these mice were associated with changes in neuronal plasticity studied at the Schaffer-CA_1 synapse in hippocampal slices by increase of the GABAergic signal. Although M_2/M_4 activity in hippocampus did not change with the lesion, we observed septal decrease of M_2 mAChR activity, and there are evidences showing that long term potentiation (LTP) in the rat hippocampus was attenuated after lesion in B, indicating that cholinergic plasticity could be indirectly affecting the hippocampus although B does not send direct cholinergic projections to it (Hosseini et al., 2017). Other important data is that these lesion rats had impaired spatial memory, a type of memory that is mainly processed by the septo-hippocampal pathway.

Other neurotransmitter systems could also be implicated in the cognitive impairment observed in our animal model. In this context, it is very well known that cannabinoids impair hippocampal-dependent learning and memory processes such as spatial learning and context-related memory task (Sullivan, 2000; Riedel and Davies, 2005). Therefore, we also studied the eCB signaling in the BFCN rat lesion model.

Modulation of the cannabinoid receptors in the brain of rats with basal forebrain cholinergic lesion

The receptors for eCB were analyzed in the brain of rats following the cholinergic lesion of the basal forebrain. The activity (CB_1 agonist-stimulated binding of [^{35}S]GTPγS mediated by CB_1 receptors in septal nuclei was significantly lower than that measured in control (sham-operated) animals. The regulation of the density of CB_1 receptors ([^{3}H]CP55,940 binding) was different, showing up-regulation in hippocampus and amygdala. The elimination of BFCN led to altered response of the eCB system, demonstrating the interaction between eCB and cholinergic systems. The endocannabinoids modulate synaptic plasticity of both excitatory and inhibitory synapses via CB_1 receptors (Riedel and Davies, 2005). CB_1 receptors, which constitute the predominant receptor subtype in CNS and neurons, are localized in presynaptic terminals and pre-terminal axon segments and are primarily localized to GABAergic basket cells (Katona et al.,

1999; Hajos et al., 2001). CB_1-mediated signaling is able to decrease GABA release in rat neocortex, hippocampus, amygdala and basal forebrain (Harkany et al., 2003; Hrabovszky et al., 2012). Morevover, the eCB system may directly regulate the release of ACh itself, at least in the hippocampus (Gifford and Ashby, 1996; Gifford et al., 2000; Kathmann et al., 2001). CB_1 like immunoreactive neurons and fibers were found in septum (Tsou et al., 1998). In septal nuclei, both CB_1 and muscarinic M_2 receptor subtypes could be expressed in GABAergic interneurons. In addition, both CB_1 and M_2 are preferentially presynaptic receptors with inhibitory effects, sharing also the coupling to the same type of Gi/o proteins. Similar interactions between presynaptic inhibitory receptors have been shown in noradrenergic neurons (Schlicker and Gothert, 1998). Also CB_1 receptors showed an inhibitory interaction with M_2 receptors on cholinergic neurons in mice hippocampus (Schulte et al., 2012). In our study, the reduction of the M_2 activity in lesion animals showed a correlation with the depletion of BFCN, but not the modulation of CB_1 activity or receptors. This data suggest that CB_1 and M_2 receptors could be expressed in different types of neurons. As previously mentioned, a decrease of CB_1 receptors in septal nuclei could lead to enhance inhibitory signaling in hippocampus. The activity mediated by M_2/M_4 receptors in hippocampus was not modified by the lesion, where the CB_1 receptor density was up-regulated. The different modulation of both systems could have a connection since cholinergic inputs from the septum modulate excitatory transmission at the hippocampus involving hippocampal presynaptic CB_1 cannabinoid receptors (Colgin et al., 2003). Two distinct mechanisms mediate the muscarinic suppression of hippocampal inhibitory synapses. In a subset of synapses, activation of M_2 receptors at presynaptic terminals suppresses GABA release directly. In contrast, in a different subset of synapses, activation of M_1/M_3 postsynaptic receptors initiate endocannabinoid production and subsequent suppression of GABA release by activating presynaptic CB_1 receptors (Fukudome et al., 2004). Nyiri and colleagues described that exist one type of septal cholinergic cell expressing $GABA_B$ and CB_1 receptor subtypes, and that this cells project to hippocampus (Nyiri et al., 2005). Specifically, activation of hippocampal CB_1 receptor decreases GABA release (Katona et al., 1999).

In summary, it is possible that in our model, a lesion-induced suppression of cholinergic input in the hippocampus would lead to increase the CB_1 density to compensate this cholinergic reduction. The CB_1 receptor activation found in the hippocampus of AD patients at initial Braak stages could be following similar mechanisms trying to maintain the physiological equilibrium between excitatory and inhibitory inputs in the hippocampus (Manuel et al., 2014). Although this CB_1 mediated compensatory mechanism would also exist in our cholinergic lesion model, it did not seem to be enough to restore the cognitive impairment found in these animals.

Another interesting finding was the up-regulation of CB_1 receptor density that we measured at basal forebrain (B) projecting areas such as the amygdala in lesion rats. In this area,

GABAergic interneurons may also modulate cholinergic signaling by CB_1 receptor activation (Marsicano and Lutz, 1999). Detailed electron microscopic investigation revealed that CB_1 receptors are located presynaptically on cholecystokinin-positive axon terminals, which establish symmetrical GABAergic synapses with their postsynaptic targets (Katona et al., 2001). The same, above-described mechanism for the hippocampus could be occurring in amygdala. Although there were no changes in AChE or M_2/M_4 receptor activities, CB_1 receptor density was found up-regulated in amygdala. . Since basal forebrain projections had been eliminated, the cannabinoid system could try to compensate the cholinergic transmission by GABAergic release inhibition.

This data suggested to us that if the cannabinoid system was trying to compensate the cholinergic transmission by GABA release diminution, external cannabinoid agonist supply could contribute to obtain the restoration of the impaired cholinergic transmission necessary for cognitive improvement in learning and memory functionality.

Subchronic WIN55,212-2 (0.5 mg/kg) administration prevent scopolamine amnesic effects

As we have previously stated, results of our group showed WIN55,212-2-mediated protective effects in the *ex vivo* model of basal forebrain cholinergic dysfunction. The cannabinoid agonist was able to induce a reduction of propidium iodide (PI) labeling, used as a marker or cell death after 192IgG-saporin treatment of organotypic cultures of rat hemibrain sections including the BFCN. Therefore, our next step was to imitate a similar treatment *in vivo* and firstly in a well characterized acute pharmacological model of cholinergic muscarinic blockade using the antagonist scopolamine (Marisco et al., 2013; El-Khadragy et al., 2014; Akinyemi et al., 2017). In our study, scopolamine pretreatment disrupt spatial acquisition in BM and PA, as might be expected. The rats only treated subchronically with the CB_1 agonist, WIN55,212-2, did not modify spatial memory in BM in the probe trial at the dose of 0.5 mg/kg.

On the contrary, the subchronic WIN55,212-2 (0,5 mg/kg) prevented scopolamine amnesic effect mainly in the spatial learning and memory BM test, but also had some protective effects in the aversive stimulus-associated PA test. It is well established that pretreatment with scopolamine is able to disrupt learning and memory in different memory task, especially in BM and PA (George et al., 2014; Malikowska-Racia et al., 2018). Scopolamine mainly affects to cholinergic transmission at basal forebrain, motor cortex, globus pallidus, hippocampus, perirhinal cortex and amygdala. However, choline acetyltransferase (ChAT) levels seem to be affected only in the hippocampus and amygdala (Ray et al., 1992; Hescham et al., 2014). ACh is a crucial mediator of learning and memory (Blokland, 1995). Scopolamine is able to bring about a decrease of 52 % of cortical and 39% of hippocampal ACh levels (Spignoli et al., 1987). Several

studies showed cholinesterase inhibitors prevent the scopolamine amnesic effect (Sadek et al., 2016b; Pattanashetti et al., 2017; Shin et al., 2018). The specific underlying mechanisms to explain these amnesic effects are not clear, but probably include the blocking of specific postsynaptic muscarinic receptor subtypes. The administration of specific presumable presynaptic M_2/M_4 antagonists can restore the scopolamine amnesic effect (Vannucchi et al., 1997).

The effects promoted in cognition by cannabinoids are a hot topic of discussion. Several studies have shown that WIN55,212-2 causes memory impairment (Lawston et al., 2000; Arguello and Jentsch, 2004; Abush and Akirav, 2012). These entire studies share a point in common, the dosage used. More and more studies show the biphasic effect of the treatments with different cannabinoid compounds, supporting the positive effect of low doses in cognition (Kirschmann, Pollock et al., 2017; Kirschmann, McCalley et al., 2017). Once again, it appears likely that an interaction between cannabinoid and cholinergic system could account for their procognitive effects (Redmer et al., 2003; Kovacs et al., 2012; Rinaldo and Hansel, 2013; Nagode et al., 2014). The details about how this interaction is produced remain unknown. Some studies point to cannabinoids modulating the dose-response effects in acetylcholine release in hippocampus and cortex (Gessa et al., 1997; 1998; Carta et al., 1998; Nava et al., 2001). In that respect, high doses of Δ^9-tetrahydrocannabinol (Δ^9-THC) administration resulted in decreased brain AChE activity and decreased acetylcholine release in the hippocampus. Effects that lead to spatial memory alterations, but the memory was restored following the administration of an AChE inhibitor (Mishima et al., 2002; Abdel-Salam et al., 2016). This data are in concordance with the effect that we observed in cortex and hippocampus, when the subchronic treatment with WIN55,212-2 (0.5 mg/kg) to control rats, that decreased the AChE activity. Curiously, the administration of the CB1 agonist was i.p., but these effects were restricted to these particular brain areas. Other data that support the cannabinoid-cholinergic interaction are the alleviative effects of WIN55,212-2 on cholinergic-induced toxicity (Nallapaneni et al., 2006; 2008). WIN55,212-2 could prevent the spatial memory impairment , but when doses of WIN55,212-2 are low and cholinergic transmission has been altered, then, cannabinoid agonists could prevent the spatial memory impairment.

In contrast, although WIN55,212-2 could modulate ACh release and lead to a beneficial effect in the cognition process, as demonstrated by the spatial learning and memory effect in the BM test, it did not prevent the scopolamine- induced amnesic effects in the PA test. The treatment prevented scopolamine-induce amnesic effect in spatial acquisition but did not in aversive memory. It has been suggested that cannabinoid activation produce different effects in emotional memory formation (extinction learning, evaluated by PA) and non-emotional memories (such as spatial learning, evaluated by BM) (Chhatwal and Ressler, 2007). In this manner, in our study,

the subchronic treatment with WIN55,212-2 (0.5 mg/kg) impaired aversive memory in control rats, resulting in an apparent similar effect to that elicited by the acute scopolamine administration. Moreover, both drugs when administered directly into the dorsal hippocampus (intra-CA_1) have demonstrated their capacity to decrease memory consolidation and induce amnesia in the PA tests (Jamali-Raeufy et al., 2011). However, when the cannabinoid was microinjected into the amygdala improved scopolamine-induced memory consolidation impairment (Nedaei et al., 2016). A different approach was used in our study, where both WIN55,212-2 and scopolamine were administered intraperitoneally, allowing to both drugs the distribution to other brain pathways.

Apart from cognitive effects observed in cognition, cannabinoid compounds also have demonstrated to have effects on the ascending and descending pathways that control pain perception. It should be noted that analgesia is one of the most characterized effects of cannabinoids (Wiley et al., 2014). In particular, WIN55,212-2 is able to decrease neuropathic pain-related behavior via CB_1/CB_2 peripheral receptors (Desroches et al., 2014), and dose-dependently produces antinociception in heat tail-flick test (Pan et al., 2014). Therefore, to correctly interpret our PA test results we had to demonstrate if our subchronic treatment was also altering the pain sensibility, considering that a painful aversive stimulus (weak electrical shock in paws) is used to measure cognitive impairment in PA test. Our results showed that subchronic WIN55,212-2 (0.5 mg/kg) treatment modified pain sensitivity in our animals in two different test analyzing pain perception, probably biasing the learning and memory results obtained in the PA test. We have demonstrated that the followed treatment with WIN55,212-2 was able to increase the pain threshold. The results would suggest that the electrical shock applied during the acquisition phase of the PA test, was not received with the same intensity by the WIN55,212-2-treated animals. Therefore, the analgesia induced by the treatment with the CB_1 agonists could be responsible of the difficulties to measure its pro-cognitive effects using the PA test, making the results obtained during the spatial BM test more reliable. Our subchronic treatment with WIN55,212-2 also was able to modify the animals motor activity. WIN55,212-2-treated animals were slower than vehicle-treated animals. Nevertheless, unchanged total path length during the trainings suggests that motor reduction did not affect spatial acquisition. The cholinergic system is also related to motor activity. Scopolamine-increased motor activity and ACh release in the striatum, hippocampus and frontal cortex correlates with locomotor activity (Day et al., 1991). Moreover, cholinergic denervation of the forebrain causes enhancement of locomotor activity responses related to dopaminergic activity (Mattsson et al., 2002). The reduction in locomotor activity following WIN55,212-2 administration had been previously described (Compton et al., 1992). Synthetic cannabinoids but not Δ^9-THC demonstrated their ability to decrease locomotor activity in the staircase test (Schreiber et al., 2018). In addition, the cannabinoid CB_1 receptor

biphasically modulates motor activity and regulates dopamine release in brain regions involved in reward and locomotion (Polissidis et al., 2013). Together, these results suggest once again, the possible modulation of the cholinergic system by CB_1-mediated signaling.

Low doses of WIN55,212-2 can prevent scopolamine amnesic effects as demonstrated in the spatial learning and memory BM test, but the mechanism of action remains unknown. It seems that the treatment modifies ACh levels. BFCN are not only the most important ACh producers within the brain, but also they control one of the most relevant pathways implicated in the control of learning and memory that is specifically damaged in AD patients. Thus the followed treatment with the CB_1 agonist should be exerting its cognitive enhancing effects in the signaling pathways controlled by these cells. Therefore the next phase of the study was to perform similar treatments and experiments in the BFCN lesion model.

Subchronic WIN55,212-2 administration restores spatial acquisition in the cholinergic lesion model of the basal forebrain in rat

The subchronic treatment with WIN55,212-2 (0.5 mg/kg) to rats with a previous lesion of the BFCN was able to induce a restoration of the cognitive impairment that was induced by 192IgG-saporin. Using the same dose and treatment schedule WIN55,212-2 did not affect spatial acquisition in control rats. In the other hand, the results obtained in the PA test analyzing the learning and memory of an aversive stimulus were comparable to those obtained with the acute pharmacological blockade of the muscarinic signaling with scopolamine. WIN55,212-2 worsened aversive learning and memory of a painful stimulus in control rats and did not restore the deficit of this type of memory in lesion rats, the measured analgesic effects of the followed treatment with the cannabinoid agonist could be responsible of these results obtained in the PA test. In general, cannabinoid administrations, and more specifically, WIN55,212-2, have been described to cause cognition deficit using the PA test (Hasanein and Teimuri Far, 2015). In addition, WIN55,212-2 administration has even been used as a cognitive deficit animal model (Nasehi et al., 2010; Shiri et al., 2017). CB_1 receptor plays a relevant role in the extinction of aversive memories; CB_1 receptor-deficient mice show normal acquisition and consolidation in a fear-conditioning task, but fear extinction is strongly impaired (Marsicano, 2002). This effect has also been observed in other studies where the microinjection of CB_1 antagonists directly in the basolateral amygdala or the CA_1 significantly impairs extinction of inhibitory avoidance (Abush and Akirav, 2010). Against this background and as previously mentioned, 192IgG-saporin lesion was able to induce up-regulation of CB_1 densities in both hippocampus and amygdala, areas also involved in the control of fear and pain perception. If the cannabinoids were able to extinct aversive memory, it would be difficult to discriminate the real contribution for extinction of

aversive memory between CB_1 activation or cholinergic disruption. Therefore, the possible cholinergic restoration by WIN55,212-2 administration is complex to be analyzed using this PA test. In addition we have demonstrated that the followed treatment with WIN55,212-2 shows analgesic effects. In summary, the results that would be obtained using behavior tests associated to a painful stimulus such as the PA to analyze changes in learning and memory elicited by cannabinoid treatments should have all the mentioned reasons in mind for a correct interpretation of the results.

The possible mechanisms of action for the restoring effects of the CB_1 agonist treatment obtained in the spatial learning and memory using the BM test are discussed in next sections in the context of the biochemical data obtained from the brain of these animals. Nevertheless, one of the first possible hypotheses that we considered was related to the previously reported anti-inflammatory effects of some cannabinoid compounds.

Similar brain lesions with 192IgG-saporin have shown microglia activation, a cerebral indicator of neuroinflammation (Rossner et al., 1995; Seeger, G. et al., 1997; Lemke et al., 1998; Moor et al., 1998). The cannabinoid system apparently act on inflammation through different mechanisms from those of nonsteroidal anti-inflammatory drugs and several clinical trials are already trying to explore the potential of the cannabinoid system modulation for the treatment of inflammatory processes (Zurier and Burstein, 2016). Therefore, we decided to compare the efficacy of our subchronic treatment at different post-lesion times, trying to avoid any possibleneuroinflammatory process that would be induced by the lesion. We perform a similar study in rats eight months after the lesion. Firstly, we proved that the learning and memory impairment on our model of cholinergic dysfunction remained until 8 months after lesion. Then, we also could prove that WIN55,212-2 treatment was also able to improve this cognitive impairment in a similar way than 2 weeks post-lesion.

There are only a few reports regarding the time course of similar brain lesions analyzing the development of cholinergic hypofunction and/or a possible recovery (Abdulla et al., 1997). It was described that following similar protocols of lesion of the basal forebrain cognitive deficits persisted for several weeks, and a gradual but not complete recovery eventually occurred; these animals also showed a decrease of cortical AChE and ChAT but had no effect on the density of muscarinic receptors (Bartus et al., 1985). The memory restoration by itself could be a compensatory mechanism involving cholinergic nuclei of basal forebrain areas different than nucleus basalis magnocellularis (Szigeti et al., 2013). The selective administration of 192IgG-saporin could also result in long-term changes of other neurotransmitter systems that could modify the outcome of such compensatory mechanisms (Severino et al., 2007). Together all this results support the idea that the decrease of cortical AChE and/or ChAT levels could not explain by itself

the cognitive dysfunction, perdurable changes in muscarinic receptor signaling may be necessary to obtain persistent memory deficits. Basal forebrain seems to have a huge plasticity capacity to recover the control of learning and memory signaling after less aggressive lesions than the used in our study (Groleau et al., 2018). However, following our lesion protocol the animals remained with the cognitive impairment for up to 8 months, enough time to avoid neuroinflammatory processes to a minimum. Although the significant damage of the cholinergic system that was persistent during months, the subchronic treatment with WIN55,212-2 (0.5 mg/kg) was also able to restore the spatial memory. Moreover, the treatment could also contribute to amplify the memory recovery mechanisms described by other authors following similar but less aggressive basal forebrain cholinergic lesions.

In the other hand, as expected, the cannabinoid agonist treatment had the same effect in locomotion in the cholinergic lesion model than in the pharmacological model of muscarinic antagonism. WIN55,212-2 treated rats moved more slowly than vehicle treated rats. The measured hyperactivity that was induced by the lesion was reduced by the cannabinoid treatment even below the control levels. Both control and lesion rats treated with the cannabinoid agonist moved more pslowly during the BM trainings, although this effect did not affect to the spatial acquisition parameters. As previously was mentioned, the lesion of the BFCNseems to decrease ACh cortical levels that could be counterbanlanced probably by an increase of the dopaminergic signaling resulting in increased motor activity hyperactivity. . Cannabinoids could biphasically modify cortical ACh levels and the results obtained in other studies when analyzing the tetrad of tests used to assess cannabinoid-induced effects (motor activity, ring catalepsy, hypothermia, and analgesia), show that low doses (stimulate) induce opposite effects from high doses (inhibition) in motor activity (Sulcova et al., 1998). All together, data suggest that the subchronic treatment with WIN55,212-2 (0.5 mg/kg) increased cortical ACh above normal level in both groups of rats, lesion and control, that showed a decrease of their motor activity.

Both cannabinoid and cholinergic system Next, neurochemical studies were performed in the brain of rats belonging to all groups of treatment trying to understand the specific mechanisms underlying the behavior modulation, in particular the protective effect of the treatment with WIN55,212-2 (0.5 mg/kg) on the spatial learning and memory induced by the lesion of the BFCN.

Low dose of WIN55,212-2 enhance cholinergic and cannabinoid neurotransmission

In the present study, the lesion of BFCN in rat resulted in a loss of most of the P75 positive neurons in this area, accompanied by reduction of cortical and septal M_2/M_4 receptor activity, up-regulation of CB_1 receptor densities in hippocampus and amygdala, together with a decrease of septal CB_1 activity. All these observed effects contributed to a greater or lesser degree, in a disruption of spatial and aversive learning and memory. As previously explained, the followed subchronic treatment with WIN55,212-2 to lesion rats during the spatial acquisition in the BM test, demonstrated that the animals could perform the probe trial task as well as the control rats. The neurochemical results showed that the cannabinoid treatment did not modify the number of AChE or $p75^{NTR}$ positive cells in nucleus basalis magnocelular, but was able to modulate not only the cannabinoid signaling, but also the cholinergic system including an increase of AChE positive fibers in cortical areas. The sub-chronic i.p. WIN55,212-2 administration with a dose of 0.5 mg/kg during five days decreased M_2/M_4 receptor activity in hippocampus with an up-regulation of both activity and density of CB_1 receptors in this same area. As previously mentioned, both M_2/M_4 receptor and CB_1 receptors could mediate a similar inhibitory signaling in ACh release in hippocampus (Levey, Edmunds, Koliatsos et al., 1995). This results are in concordance with others showing that WIN55,212-2 treatment lead to M_2 decrease in hippocampus (Schulte et al., 2012b). Interestingly, a down-regulation of M_2/M_4 receptors was found in animals with high levels of ACh in hippocampus (du Bois et al., 2005). Besides, the acute treatment with muscarinic antagonist increased the ACh release but inhibited muscarinic autoreceptors in hippocampus mice (Kuribara and Tadokoro, 1983). As mentioned, low doses of WIN55,212-2 are able to enhance ACh release in hippocampus (Tzavara et al., 2003). In addition, cannabinoid system activation in hippocampus regulates different processes of learning and memory acquisition including the production of proteins involved in brain plasticity (Abush and Akirav, 2010). Specifically, WIN55,212-2 could modulated cholinergic activity by CB_1 receptor activation, through mechanisms that regulate the synthesis of plasticity-related proteins (Navakkode and Korte, 2014). These positive effects in cognitive process that are controlled by the hippocampus had been shown in other studies using low doses of THC that were able to restore age-related cognitive dysfunction. In this study, the authors showed that the activation of the cannabinoid system modified proteins and enzymes related with synaptic connectivity or neuroplasticity in the hippocampus, but only in old animals that were able to restore some learning and memory parameters (Bilkei-Gorzo et al., 2017; Sarne et al., 2018). The CA1 region of hippocampus is essential in the spatial memory process. Temporary inactivation of CA1 impairs spatial memory acquisition (Stackman et al., 2016). The memory restoration was only observed when using the spatial BM test, and this test mainly evaluates the septo-hippocampal pathway (Barnes, 1979). Therefore we focused in the changes of both systems, cholinergic and cannabinoid, in CA1

hippocampal region but without overlooking the cortical effects produced by the treatment. Nevertheless, the observed modulation of muscarinic and cannabinoid receptors suggest that they are previous and help to get the WIN55,212-2-mediated protection of spatial acquisition in the BM.

In cortex, WIN55,212-2 administration induced a recovering to control levels in some of the analyzed cholinergic markers. The activation of the cannabinoid system induced an increase of M_2/M_4 receptors activity in cortex that was not attributable to the modulation of the total population of muscarinic. Moreover, the AChE activity was restored to control levels also in cortical areas. No change in total muscarinic receptor density in the cortex was observed after the lesion, but the treatment with WIN55,212-2 induced a decrease in the most internal layers of motor and somatosensory cortices. M_1 is the most abundant subtype of muscarinic receptor that is expressed in cortical areas. Then, M_1 subtype would be the receptor subtype that is contributing to a greater extent to the measured [^{3}H]NMS binding sites in cortex cortex. M_1 overstimulation would deteriorate the maintenance of acetylcholine release in the prefrontal cortex (Vijayraghavan et al., 2018). For these reasons, the measured decrease in MR total population could be indicating a down-regulation of cortical M_1 subtype leading to increased ACh levels and positive effects on learning and memory. Further experiments trying to identify specific cortical regulation of this subtype could demonstrate not only this possibility, but also if the M_1-mediated regulation of PLC could be a link between the eCB and cholinergic systems. Unfortunately one of the limitations of the [^{35}S]GTPγS binding technique is that we can not measure the activity of receptors coupled to Gq proteins subtype, such as the M_1.

The activity mediated by cortical M_2/M_4 receptors was restored after the cannabinoid treatment indicating a possible modulation of M_2 presynaptic autoreceptors in cortical interneurons or the already described postsynaptic M_2 receptors, since most of the BFCN with cortical innervation were eliminated. These cortical M_2 receptors would limit the release of ACh under high neuronal activity conditions, and would not be activated by physiological levels (Moor et al., 1998). In addition, cholinergic stimulators produce bell-shaped dose-response curves in studies of learning and memory (Senda et al., 1998). Then high doses of cholinergic stimulators would activate muscarinic auto-receptors that control endogenous ACh release (Baghdoyan et al., 1998). Therefore, the measured increase of cortical M_2/M_4 receptor activity could be a response to extracellular ACh high levels elicited by the cannabinoid treatment. . The cannabinoid treatment would increase ACh levels in cortex that would also lead to block the amnesic effects in the model of acute muscarinic antagonism with scopolamine, and to restore basocortical cholinergic signaling in the model of basal forebrain lesion.

All these effects in cortex are also related to the down-regulation of the motor activity observed in lesion rats after the cannabinoid treatment, in the context of the cholinergic-dopaminergic equilibrium.

The animals with the basal forebrain lesion showed AChE staining reduction also in the lesion area, that the treatment with the cannabinoid agonist was not able to restore In the basal forebrain most of the ChAT-positive neurons contain also AChE and vice versa (Eckenstein and Sofroniew, 1983). The remaining AChE staining in the lesion area could correspond to fibers of cholinoceptive cells, that may innervate to a few (around 25%) surviving cholinergic cells. The basal forebrain is the principal ACh producer and supplier of all the cortical areas, and a cortical increase of ACh release was measured by B stimulation (Rasmusson et al., 1992). The lesion group would have decreased around a 75% in cortical ACh production. It has also been reported that deep brain stimulation in basal forebrain improved memory in cognitive impaired animals (Liu et al., 2017; 2018). After nucleus basalis cholinergic depletion, surviving cells were stimulated and cognitive improvement was obtained (Lee et al., 2016b). There are studies that suggest that cannabinoid agonists potentiate ACh release in the frontal cortex by activating cannabinoid receptors in brain regions other than the frontal cortex (Verrico et al., 2003). All these result could suggest that in our study the cannabinoid treatment to lesion rats would activate the cannabinoid system acting on cholinergic surviving cells present at the nucleus basalis magnocellularis that could enhance cholinergic release to supply the ACh in cortical areas. This effect would lead to restoration of cortical cholinergic transmission and a cognitive improvement in both models of cholinergic dysfunction the muscarinic acute antagonism and the basal forebrain cholinergic lesion.

Specific activation of CB_1 lead to memory restoration

As above explained, the subchronic WIN55,212-2 administration to the BFCN lesion model in rats was able to restore the learning and memory of spatial acquisition parameters using the BM test. There are studies which describe also the possible role of the CB_2 subtype of cannabinoid receptors in regulating spatial memory (Ronca et al., 2015; Li and Kim, 2016). Moreover, some studies are showing protective effects on memory by synthetic cannabinoids mediated by other receptors different from CB_1 and CB_2 receptor subtypes (Ratano et al., 2017). The results of the present study indicate that memory restoration was by CB_1 activation, but the possible effects of WIN55,212-2 in CB_2 activation or effects in a non-CB_1 receptor mechanism could not be completely discarded. The results showed that although the learning and memory memory effects are mediated by CB_1 receptors, there are neurochemical changes induced by the co-administration of WIN55,212-2 and SR141716A that were not antagonized. When

WIN55,212-2 was administered together with SR141716A the activity mediated by M_2/M_4 receptors only was antagonized in cortical areas These results would suggest the effect on cortex was the responsible of the protective effects on spatial memory measured with the cannabinoid agonist treatment. But it also suggests that SR141716A could have its own effects in cholinergic transmission. A further discussion of these results will be explained in a next section together with the effects induced by the subchronic treatment with SR141716A alone.

Biphasic effect of low (0.5 mg/kg) *versus* higher (3 mg/kg) dose of WIN55,212 in memory

As discussed earlier, cannabinoids effects in memory are usually associated to the dose used; high doses are related to memory impairment, while low doses have protective effect. In the present study a high dose of WIN55,212-2 impaired in control rats both types of analyzed learning and memory tests, spatial and aversive. In contrast, the same treatment with the higher dose assayed (3 mg/kg) was able to enhance spatial memory deficits in lesion rats but with almost the same potency that with the low dose (0.5 mg/kg).

In control animals, the subchronic treatment with the high dose of WIN55,212-2 lead to up-regulation of CB_1 receptor densityin cortex, basal ganglia and hippocampus. On the contrary, the 3 mg/kg dose of the cannabinoid agonist induced a down regulation of muscarinic activity on cortical areas of control group of rats. This result is supported for the extended idea that cannabinoids impair memory affecting cholinergic transmission. High doses of WIN55,212-2 induced deficits in spatial learning but was recovered in the presence of the cholinesterase inhibitor rivastigmine (Robinson et al., 2010). It seems that normalization of overall firing frequency by increase of the ACh available is critical for the recovery of behavioral function. WIN55,212-2 promotes ACh release and inhibits electrically evoked acetylcholine release in hippocampus (Gifford and Ashby 1996; Gifford et al. 1997a,b, (PMID: 9760025). WIN55,212-2 can also inhibit LTP in CA1 (Misner and Sullivan,1999, Terranova et al. 1995, Collins et al. 1994, Nowicky et al,1987), and CB_1 knock-out mice show enhanced LTP in this area (Bohme et al., 2000). Although M_2/M_4 activity was decreased in cortex, it seems that the above-mentioned behavior effects on memory the high dose of the cannabinoid agonist in control rats could be explained by their down-regulation in hippocampus and concretely in CA1, since WIN55,212-2 administration directly into CA1 have a similar impairing effect in the spatial memory to the one that we found in control rats (Suenaga 2008, Abush and Akirav, 2010).

As previously discussed, cannabinoid agonists elicit biphasic effects also in motor activity (Davis et al., 1972). High doses increased the motor activity of the rats, the opposite effect than observed with the low dose. Cortical M_2/M_4 activity recorded in the control rats treated with the

high dose of the cannabinoid agonists was even lower than the recorded for the lesion group. That observation indicates that the cortical ACh levels induced by the high dose in a control animal could be even lower than those induced by the BFCN lesion. In lesion group, high doses of WIN55,212-2 also lead to up-regulation of CB_1 receptor density in most of the recorded brain areas. AChE activity in cortex was restored to control levels in a similar way than that obtained with low dose, but the main difference was that cortical M_2/M_4 and CB_1 activities did not change after high doses. In hippocampus, M_2/M_4-mediated activity was conserved also in CA1 and CA3, areas implicated in spatial memory (Flasbeck et al., 2018). When WIN55,212-2 was administered at low doses, led to decreased M_2/M_4 CA1/CA3 hippocampal activity but CB_1 activity was unchanged. On the contrary, high doses led to decreased CB_1 receptor activity and did not modify M_2/M_4. Both doses lead to restore spatial memory but seems that it could be through different biochemical mechanisms. In hippocampus activation of M_2 and CB_1 receptors could end in the same final inhibitory signaling transmission. Both inhibit ACh release in the synapse but they are in different synapse (Fukudome et al., 2004).

As previously was argued, it is well established that high doses of cannabinoids disrupt memory and that protective effects in cognition are only obtained after low doses. Our results show that cannabinoid agonists can modulate cholinergic transmission, but if the cholinergic transmission works correctly the cannabinoids at medium-high doses could break the inhibitory equilibrium between both systems and lead to memory impairment. However, if the cholinergic transmission is compromised, then cannabinoids would restore it to control levels.

SR141716A impaired memory in control and did not improve completely cognition in lesion rats

The behavioral studies showed that the subchronic co-treatment with WIN55,212-2 (0.5 mg/kg) together with SR141716A (0.5 mg/kg) antagonized the memory positive effects of the agonist alone. Indicating that the protective effects on learning and memory were specifically mediated by CB_1 central receptors. However, controversial data in relation with SR141716A (also called rimonabant) administration have been reported, describing that this compound is able to improve spatial memory (Wolff and Leander, 2003).

In cortex, the co-administration of WIN55,212-2 together with SR141716A decreased M_2/M_4 activity to that recorded in lesion rats. In contrast, AChE activity increased to control levels. Indicating that only the M_2/M_4 cortical activity was antagonized from all the biochemical parameters that were analyzed. The motor activity down-regulation was also antagonized by the co-treatment with the antagonist, suggesting that cortical ACh return to lesion group levels..

Curiously, when SR141716A was administered alone it had no effect in cortical M_2/M_4 activity, but AChE was also restored to control levels when injected to the lesion rats. It was described that high doses of SR141716A increase ACh release in cortex (Gessa et al., 1998). However, rimonabant at a dose that did not affect basal acetylcholine release, was able to prevent the increase of acetylcholine release by WIN55,212-2 (Acquas et al., 2000). This suggest that rimonabant can block WIN55,212-2 effect in both behavior parameters, motor activity and memory improvement, although the restoration of cortical AChE indicates that this cannabinoid antagonist could also modulate ACh levels. Some studies reported that there is no a direct relation between AChE cortex levels and cognition (Schliebs et al., 1996). It is possible that cortical ACh modulation by SR141716A was not enough to improve memory. In other hand, the effect in hippocampus was not antagonized. WIN55,212-2 together with SR141716A and the treatment only with SR141716A, decreased M_2/M_4 activity. SR141716A could also be able to modify the ACh release in hippocampus (Gifford et al., 2000; Degroot et al., 2006). These results suggest that a combination of down-regulation in M_2/M_4 activity together with activation of CB_1 receptors could induce protective effect in the hippocampus.

In summary, the total outcomes from the subchronic treatment with low doses of WIN55,212-2 (around 0.5 mg/kg), show that the cannabinoid system activation in both septo-hippocampal and baso-cortical pathways lead to protection against cholinergic dysfunction independently of the origin, acute muscarinic antagonism or BFCN depletion. Moreover, these effects are specifically mediated by CB_1 cannabinoid receptor activation. These results highlight the importance of the cannabinoid system in the regulation of the cholinergic transmission in the control of memory and learning, contributing to the development of new treatments for irreversible dementias such as the Alzheimer's disease

CONCLUSIONS

1. The loss of basal forebrain cholinergic neurons in nucleus basalis magnocellularis, that causes spatial and aversive memory impairment, leads to decreased cortical and septal M_2/M_4 activity, but increased of CB_1 in hippocampus and amygdala,
2. Low doses of WIN55,212-2 (0.5 mg/kg) prevent scopolamine amnesic effect in Barnes Maze test by activation of the cannabinoid system and increasing M_2/M_4 activity in cortical, septal and hippocampal area.
3. The subchronic treatment with this CB_1 agonist is also inducing analgesic effects that could bias the evaluation of learning and memory associated with aversive painful stimulus.
4. Subchronic low dose of WIN55,212-2 (0.5 mg/kg) is able to restore the spatial learning and memory impairment induced in the rat model of basal forebrain cholinergic lesion with no cognitive effects in control animals. The activation of CB_1 and M_2/M_4 receptors in cortical areas and the decrease of M_2/M_4 activity in hippocampus may be necessary for memory restoration.
5. The protective effects in spatial learning and memory are specifically mediated by CB_1 receptor signaling. The CB_1 antagonist, rimonabant, blocked these protective effects by inactivation of both CB_1 cannabinoid and M_2/M_4 muscarinic cortical receptors to lesion levels.
6. High doses of WIN55,212-2 (3 mg/kg) also restored spatial learning and memory impairment in a rat model of basal forebrain cholinergic lesion, but the same treatment to control rats impaired spatial memory acquisition. The different regulation of muscarinic and cannabinoid receptors compared to the lower dose could explain these effects.
7. The subchronic treatment with rimonabant alone also impaired spatial learning and memory in control rats and improved some parameters of spatial acquisition in lesion rats. However, the activation of CB_1 cannabinoid receptors seems to be necessary for the recovery of spatial learning and memory.

In summary, low doses of cannabinoid agonist are able to modulate the cholinergic system to restore its control on spatial learning and memory when it has been disrupted.

Acronyms and abbreviations

2-AG	2-Arachidonoylglycerol
[^{3}H] NMS	[3H]-N-methylscopolamine
[^{3}H] QNB	[3H]-quinuclidinyl benzilate
5-HT	5-hydroxytryptamine receptor/serotonin receptor
Δ9-THC	(--)-Δ9-tetrahydrocannabinol
Acetyl-CoA	Acetyl coenzyme A
ACh	Acetylcholine
AChE	Acetylcholinesterase
aCSF	Artificial cerebrospinal fluid
AD	Alzheimer´s disease
AEA	Anandamide
AMPA	α-amino-3-hydroxy-5-methyl-4-isoxazolepropionic acid receptor
APP	Amyloid precursor protein
AU	Arbitrary units
Aβ	Amyloid-beta
BDNF	Brain-derived neurotrophic factor
BFCN	Basal forebrain cholinergic neurons
BSA	Bovine serum albumin
cAMP	Cyclic adenosine monophosphate
CB_1 receptor	Subtype one of cannabinoid receptors
CB_2 receptor	Subtype two of cannabinoid receptors
Ch	Choline

ChAT	Choline acetyltransferase
CNS	Central nervous system
CSF	Cerebrospinal fluid
DAG	Diacylglycerol
DAGL	Diacylglycerol lipase
DSE	Depolarization-Induced suppression of excitation
DSI	Depolarization-Induced suppression of Inhibition
DTT	DL-dithiothreitol
eCB	Endocannabinoid
FAAH	Fatty acid amide hydrolase
GABA	Gamma aminobutyric acid
GAD65	Glutamic acid decarboxylase 65kDa
GAD67	Glutamic acid decarboxylase 67kDa
GDP	Guanosine 5′-diphosphate
GFAP	Glial fibrilar acidic protein
GPCR	G protein-coupled receptor
GTPγS	Guanosine 5'-O-(3-thiotriphosphate)
HC-3	Hemicholinium-3
HDB	Horizontal diagonal band of Broca
I.c.v.	Intracerebroventricular
IP3	Inositol trisphosphate
Iso-OMPA	Tetraisopropylpyrophosphoramide
LDTg	Laterodorsal tegmental area
LTD	Long-term depression

mAChR	Muscarinic acetylcholine receptor
MAGL	Monoacylglycerol lipase
MCI	Mild cognitive impairment
mGluR	Metabotropic glutamate receptors
mNGF	Mature nerve growth factor
MRI	Magnetic resonance imaging
MS	Medial septal nucleus/medial septum
nAChR	Nicotinic acetylcholine receptors
NAPE	N-acyl-phosphatidylethanolamines
B	Nucleus basalis magnocellularis
nbM	Nucleus basalis of Meynert
NGF	Nerve growth factor
NMDA	N-methyl D-aspartate
O.D.	Optical density
$p75^{NTR}$	Low affinity nerve-growth factor receptor
PB	Phosphate buffer
PBS	Phosphate-buffered saline
PC	Phosphatidylcholine
PE	Phosphatidylethanolamine
PI	Propidium iodide
PIP2	Phosphatidylinositol 4,5-bisphosphate
PKA	Protein kinase A
PKC	Protein kinase C
PLA1	Phospholipase A1

PLA2	Phospholipase A2
PLC	Phospholipase C
PLD	Phospholipase D
PPTg	Pedunculopontine tegmental area
ProNGF	Precursor nerve growth factor
SAP	192IgG-saporin-treated group
S.c.	Subcutaneous
SDHACU	Sodium dependent-high affinity choline uptake
ST	Sulfatides
STD	Short-term depression
TBS	Tris-buffered saline
T.E.	Tissue equivalent
TM	Transmembrane
VAChT	Vesicular Acetylcholine transporter
VDB	Vertical diagonal band of Broca

REFERENCES

Abdel-Salam OM, Youness ER, Khadrawy YA, et al (2016). Acetylcholinesterase, butyrylcholinesterase and paraoxonase 1 activities in rats treated with cannabis, tramadol or both. Asian Pac J Trop Med 9: 1089-1094.

Abdulla FA, Calaminici M, Gray JA, et al (1997). Changes in the sensitivity of frontal cortical neurones to acetylcholine after unilateral lesion of the nucleus basalis with alpha-amino-3-OH-4-isoxozole propionic acid (AMPA): effects of basal forebrain transplants into neocortex. Brain Res Bull 42: 169-186.

Abush H, Akirav I (2012). Short- and long-term cognitive effects of chronic cannabinoids administration in late-adolescence rats. PLoS One 7: e31731.

Abush H, Akirav I (2010). Cannabinoids modulate hippocampal memory and plasticity. Hippocampus 20: 1126-1138.

Acquas E, Pisanu A, Marrocu P, et al (2001). Delta9-tetrahydrocannabinol enhances cortical and hippocampal acetylcholine release in vivo: a microdialysis study. Eur J Pharmacol 419: 155-161.

Adams NC, Lozsadi DA, Guillery RW (1997). Complexities in the thalamocortical and corticothalamic pathways. Eur J Neurosci 9: 204-209.

Ahmad R, Goffin K, Van den Stock J, et al (2014). In vivo type 1 cannabinoid receptor availability in Alzheimer's disease. Eur Neuropsychopharmacol 24: 242-250.

Aisen P, Touchon J, Amariglio R, et al (2017). EU/US/CTAD Task Force: Lessons Learned from Recent and Current Alzheimer's Prevention Trials. J Prev Alzheimers Dis 4: 116-124.

Aitta-Aho T, Hay YA, Phillips BU, et al (2018). Basal Forebrain and Brainstem Cholinergic Neurons Differentially Impact Amygdala Circuits and Learning-Related Behavior. Curr Biol 28: 2557-2569.e4.

Akinyemi AJ, Oboh G, Oyeleye SI, et al (2017). Anti-amnestic Effect of Curcumin in Combination with Donepezil, an Anticholinesterase Drug: Involvement of Cholinergic System. Neurotox Res 31: 560-569.

Albuquerque EX, Pereira EF, Alkondon M, et al (2009). Mammalian nicotinic acetylcholine receptors: from structure to function. Physiol Rev 89: 73-120.

Angelucci F, Gelfo F, De Bartolo P, et al (2011). BDNF concentrations are decreased in serum and parietal cortex in immunotoxin 192 IgG-Saporin rat model of cholinergic degeneration. Neurochem Int 59: 1-4.

Araujo DM, Lapchak PA, Collier B, et al (1988). Characterization of N-[^{3}H]methylcarbamylcholine binding sites and effect of N-methylcarbamylcholine on acetylcholine release in rat brain. J Neurochem 51: 292-299.

Arendt T, Bigl V, Tennstedt A, et al (1984). Correlation between cortical plaque count and neuronal loss in the nucleus basalis in Alzheimer's disease. Neurosci Lett 48: 81-85.

Arguello PA, Jentsch JD (2004). Cannabinoid CB1 receptor-mediated impairment of visuospatial attention in the rat. Psychopharmacology (Berl) 177: 141-150.

Arnold JC, Hunt GE, McGregor IS (2001). Effects of the cannabinoid receptor agonist CP 55,940 and the cannabinoid receptor antagonist SR 141716 on intracranial self-stimulation in Lewis rats. Life Sci 70: 97-108.

Ashton JC, Glass M (2007). The cannabinoid CB2 receptor as a target for inflammation-dependent neurodegeneration. Curr Neuropharmacol 5: 73-80.

Atwood BK, Mackie K (2010a). CB2: a cannabinoid receptor with an identity crisis. Br J Pharmacol 160: 467-479.

Atwood BK, Mackie K (2010b). CB2: a cannabinoid receptor with an identity crisis. Br J Pharmacol 160: 467-479.

Baghdoyan HA, Lydic R, Fleegal MA (1998). M2 muscarinic autoreceptors modulate acetylcholine release in the medial pontine reticular formation. J Pharmacol Exp Ther 286: 1446-1452.

Bailey AM, Rudisill ML, Hoof EJ, et al (2003). 192 IgG-saporin lesions to the nucleus basalis magnocellularis (nBM) disrupt acquisition of learning set formation. Brain Res 969: 147-159.

Bainbridge NK, Koselke LR, Jeon J, et al (2008). Learning and memory impairments in a congenic C57BL/6 strain of mice that lacks the M2 muscarinic acetylcholine receptor subtype. Behav Brain Res 190: 50-58.

Barker DL, Herbert E, Hildebrand JG, et al (1972). Acetylcholine and lobster sensory neurones. J Physiol 226: 205-229.

Bartus RT (2000). On neurodegenerative diseases, models, and treatment strategies: lessons learned and lessons forgotten a generation following the cholinergic hypothesis. Exp Neurol 163: 495-529.

Bartus RT, Flicker C, Dean RL, et al (1985). Selective memory loss following nucleus basalis lesions: long term behavioral recovery despite persistent cholinergic deficiencies. Pharmacol Biochem Behav 23: 125-135.

Basavarajappa BS, Shivakumar M, Joshi V, et al (2017). Endocannabinoid system in neurodegenerative disorders. J Neurochem 142: 624-648.

Baxter MG (2001). Effects of selective immunotoxic lesions on learning and memory. Methods Mol Biol 166: 249-265.

Baxter MG, Bucci DJ, Gorman LK, et al (2013). Selective immunotoxic lesions of basal forebrain cholinergic cells: effects on learning and memory in rats. Behav Neurosci 127: 619-627.

Baxter MG, Bucci DJ, Gorman LK, et al (1995). Selective immunotoxic lesions of basal forebrain cholinergic cells: effects on learning and memory in rats. Behav Neurosci 109: 714-722.

Baxter MG, Gallagher M (1996). Intact spatial learning in both young and aged rats following selective removal of hippocampal cholinergic input. Behav Neurosci 110: 460-467.

Beltramo M, Stella N, Calignano A, et al (1997). Functional role of high-affinity anandamide transport, as revealed by selective inhibition. Science 277: 1094-1097.

Benito C, Nunez E, Tolon RM, et al (2003). Cannabinoid CB2 receptors and fatty acid amide hydrolase are selectively overexpressed in neuritic plaque-associated glia in Alzheimer's disease brains. J Neurosci 23: 11136-11141.

Berger-Sweeney J, Heckers S, Mesulam MM, et al (1994). Differential effects on spatial navigation of immunotoxin-induced cholinergic lesions of the medial septal area and nucleus basalis magnocellularis. J Neurosci 14: 4507-4519.

Berger-Sweeney J, Stearns NA, Murg SL, et al (2001b). Selective immunolesions of cholinergic neurons in mice: effects on neuroanatomy, neurochemistry, and behavior. J Neurosci 21: 8164-8173.

Biegon A, Greenberger V, Segal M (1986). Quantitative histochemistry of brain acetylcholinesterase and learning rate in the aged rat. Neurobiol Aging 7: 215-217.

Bilkei-Gorzo A, Albayram O, Ativie F, et al (2018). Cannabinoid 1 receptor signaling on GABAergic neurons influences astrocytes in the ageing brain. PLoS One 13: e0202566.

Bilkei-Gorzo A, Albayram O, Draffehn A, et al (2017). A chronic low dose of Delta(9)-tetrahydrocannabinol (THC) restores cognitive function in old mice. Nat Med 23: 782-787.

Bisogno T, MacCarrone M, De Petrocellis L, et al (2001). The uptake by cells of 2-arachidonoylglycerol, an endogenous agonist of cannabinoid receptors. Eur J Biochem 268: 1982-1989.

Blokland A (1995). Acetylcholine: a neurotransmitter for learning and memory? Brain Res Brain Res Rev 21: 285-300.

Bo Y, Zhang X, Wang Y, et al (2017). The n-3 Polyunsaturated Fatty Acids Supplementation Improved the Cognitive Function in the Chinese Elderly with Mild Cognitive Impairment: A Double-Blind Randomized Controlled Trial. Nutrients 9: 10.3390/nu9010054.

Boegman RJ, Jhamandas K, Cockhill J (1992). Differential effect of excitotoxins in the basal forebrain on choline acetyltransferase activity in the cortex and amygdala. Ann N Y Acad Sci 648: 254-255.

Bonner TI, Buckley NJ, Young AC, et al (1987). Identification of a family of muscarinic acetylcholine receptor genes. Science 237: 527-532.

Bouaboula M, Perrachon S, Milligan L, et al (1997). A selective inverse agonist for central cannabinoid receptor inhibits mitogen-activated protein kinase activation stimulated by insulin or insulin-like growth factor 1. Evidence for a new model of receptor/ligand interactions. J Biol Chem 272: 22330-22339.

Brem AK, Ran K, Pascual-Leone A (2013). Learning and memory. Handb Clin Neurol 116: 693-737.

Brown SM, Wager-Miller J, Mackie K (2002). Cloning and molecular characterization of the rat CB2 cannabinoid receptor. Biochim Biophys Acta 1576: 255-264.

Bubser M, Bridges TM, Dencker D, et al (2014). Selective activation of M4 muscarinic acetylcholine receptors reverses MK-801-induced behavioral impairments and enhances associative learning in rodents. ACS Chem Neurosci 5: 920-942.

Bucci DJ, Holland PC, Gallagher M (1998). Removal of cholinergic input to rat posterior parietal cortex disrupts incremental processing of conditioned stimuli. J Neurosci 18: 8038-8046.

Buckley NJ, Bonner TI, Brann MR (1988). Localization of a family of muscarinic receptor mRNAs in rat brain. J Neurosci 8: 4646-4652.

Butt AE, Bowman TD (2002). Transverse patterning reveals a dissociation of simple and configural association learning abilities in rats with 192 IgG-saporin lesions of the nucleus basalis magnocellularis. Neurobiol Learn Mem 77: 211-233.

Bystrowska B, Frankowska M, Smaga I, et al (2018). Effects of Cocaine Self-Administration and Its Extinction on the Rat Brain Cannabinoid CB1 and CB2 Receptors. Neurotox Res.

Calignano A, La Rana G, Giuffrida A, et al (1998). Control of pain initiation by endogenous cannabinoids. Nature 394: 277-281.

Carta G, Nava F, Gessa GL (1998). Inhibition of hippocampal acetylcholine release after acute and repeated Delta9-tetrahydrocannabinol in rats. Brain Res 809: 1-4.

Cass DK, Flores-Barrera E, Thomases DR, et al (2014). CB1 cannabinoid receptor stimulation during adolescence impairs the maturation of GABA function in the adult rat prefrontal cortex. Mol Psychiatry 19: 536-543.

Castaneto MS, Gorelick DA, Desrosiers NA, et al (2014). Synthetic cannabinoids: epidemiology, pharmacodynamics, and clinical implications. Drug Alcohol Depend 144: 12-41.

Caulfield MP (1993). Muscarinic receptors--characterization, coupling and function. Pharmacol Ther 58: 319-379.

Caulfield MP, Birdsall NJ (1998). International Union of Pharmacology. XVII. Classification of muscarinic acetylcholine receptors. Pharmacol Rev 50: 279-290.

Cheng H, Wang M, Li JL, et al (2013). Specific changes of sulfatide levels in individuals with pre-clinical Alzheimer's disease: an early event in disease pathogenesis. J Neurochem 127: 733-738.

Chhatwal JP, Ressler KJ (2007). Modulation of fear and anxiety by the endogenous cannabinoid system. CNS Spectr 12: 211-220.

Cohen BN, Mackey ED, Grady SR, et al (2012). Nicotinic cholinergic mechanisms causing elevated dopamine release and abnormal locomotor behavior. Neuroscience 200: 31-41.

Colgin LL, Kramar EA, Gall CM, et al (2003). Septal modulation of excitatory transmission in hippocampus. J Neurophysiol 90: 2358-2366.

Compton DR, Gold LH, Ward SJ, et al (1992). Aminoalkylindole analogs: cannabimimetic activity of a class of compounds structurally distinct from delta 9-tetrahydrocannabinol. J Pharmacol Exp Ther 263: 1118-1126.

Conner JM, Chiba AA, Tuszynski MH (2005). The basal forebrain cholinergic system is essential for cortical plasticity and functional recovery following brain injury. Neuron 46: 173-179.

Conner JM, Culberson A, Packowski C, et al (2003). Lesions of the Basal forebrain cholinergic system impair task acquisition and abolish cortical plasticity associated with motor skill learning. Neuron 38: 819-829.

Conner JM, Varon S (1992). Distribution of nerve growth factor-like immunoreactive neurons in the adult rat brain following colchicine treatment. J Comp Neurol 326: 347-362.

Cooper-Kuhn CM, Winkler J, Kuhn HG (2004). Decreased neurogenesis after cholinergic forebrain lesion in the adult rat. J Neurosci Res 77: 155-165.

Cravatt BF, Demarest K, Patricelli MP, et al (2001). Supersensitivity to anandamide and enhanced endogenous cannabinoid signaling in mice lacking fatty acid amide hydrolase. Proc Natl Acad Sci U S A 98: 9371-9376.

Cravatt BF, Giang DK, Mayfield SP, et al (1996). Molecular characterization of an enzyme that degrades neuromodulatory fatty-acid amides. Nature 384: 83-87.

Cruz-Martinez AM, Tejas-Juarez JG, Mancilla-Diaz JM, et al (2018). CB1 receptors in the paraventricular nucleus of the hypothalamus modulate the release of 5-HT and GABA to stimulate food intake in rats. Eur Neuropsychopharmacol.

Cummings J, Lee G, Ritter A, et al (2018). Alzheimer's disease drug development pipeline: 2018. Alzheimers Dement (N Y) 4: 195-214.

Dashniani M, Burjanadze M, Beselia G, et al (2009a). Spatial memory following selective cholinergic lesion of the nucleus basalis magnocellularis. Georgian Med News (174): 77-81.

Davies P, Maloney AJ (1976). Selective loss of central cholinergic neurons in Alzheimer's disease. Lancet 2: 1403.

Davis M, O Connell T, Johnson S, et al (2018). Estimating Alzheimer's Disease Progression Rates from Normal Cognition Through Mild Cognitive Impairment and Stages of Dementia. Curr Alzheimer Res 15: 777-788.

Davis WM, Moreton JE, King WT, et al (1972a). Marihuana on locomotor activity: biphasic effect and tolerance development. Res Commun Chem Pathol Pharmacol 3: 29-35.

Day J, Damsma G, Fibiger HC (1991). Cholinergic activity in the rat hippocampus, cortex and striatum correlates with locomotor activity: an in vivo microdialysis study. Pharmacol Biochem Behav 38: 723-729.

Degroot A, Kofalvi A, Wade MR, et al (2006). CB1 receptor antagonism increases hippocampal acetylcholine release: site and mechanism of action. Mol Pharmacol 70: 1236-1245.

DeKosky ST (2031). Neurobiology and molecular biology of Alzheimer's disease. Rev Neurol 35: 752-760.

Delvalle JA, Greengard O (1976). The regulation of phenylalanine hydroxylase in rat tissues in vivo. The maintenance of high plasma phenylalanine concentrations in suckling rats: a model for phenylketonuria. Biochem J 154: 613-618.

Derkinderen P, Toutant M, Burgaya F, et al (1996). Regulation of a neuronal form of focal adhesion kinase by anandamide. Science 273: 1719-1722.

D'Esposito M, Postle BR (2015). The cognitive neuroscience of working memory. Annu Rev Psychol 66: 115-142.

Desroches J, Charron S, Bouchard JF, et al (2014). Endocannabinoids decrease neuropathic pain-related behavior in mice through the activation of one or both peripheral CB(1) and CB(2) receptors. Neuropharmacology 77: 441-452.

Deutsch DG, Chin SA (1993). Enzymatic synthesis and degradation of anandamide, a cannabinoid receptor agonist. Biochem Pharmacol 46: 791-796.

Devane WA, Hanus L, Breuer A, et al (1992). Isolation and structure of a brain constituent that binds to the cannabinoid receptor. Science 258: 1946-1949.

Di Marzo V (2008). Endocannabinoids: synthesis and degradation. Rev Physiol Biochem Pharmacol 160: 1-24.

Di Marzo V, Fontana A, Cadas H, et al (1994). Formation and inactivation of endogenous cannabinoid anandamide in central neurons. Nature 372: 686-691.

Dinh TP, Freund TF, Piomelli D (2002). A role for monoglyceride lipase in 2-arachidonoylglycerol inactivation. Chem Phys Lipids 121: 149-158.

Dobryakova YV, Kasianov A, Zaichenko MI, et al (2018). Intracerebroventricular Administration of (192)IgG-Saporin Alters Expression of Microglia-Associated Genes in the Dorsal But Not Ventral Hippocampus. Front Mol Neurosci 10: 429.

Drachman DA (1977). Memory and cognitive function in man: does the cholinergic system have a specific role? Neurology 27: 783-790.

Drachman DA, Leavitt J (1974). Human memory and the cholinergic system. A relationship to aging? Arch Neurol 30: 113-121.

Du Bois TM, Bell W, Deng C, et al (2005). A high n-6 polyunsaturated fatty acid diet reduces muscarinic M2/M4 receptor binding in the rat brain. J Chem Neuroanat 29: 282-288.

Du X, Wang X, Geng M (2018). Alzheimer's disease hypothesis and related therapies. Transl Neurodegener 7: 2-018.

Dudai Y (2004). The neurobiology of consolidations, or, how stable is the engram? Annu Rev Psychol 55: 51-86.

Easton A, Douchamps V, Eacott M, et al (2012). A specific role for septohippocampal acetylcholine in memory? Neuropsychologia 50: 3156-3168.

Ebert U, Kirch W (1998). Scopolamine model of dementia: electroencephalogram findings and cognitive performance. Eur J Clin Invest 28: 944-949.

Eckenstein F, Sofroniew MV (1983). Identification of central cholinergic neurons containing both choline acetyltransferase and acetylcholinesterase and of central neurons containing only acetylcholinesterase. J Neurosci 3: 2286-2291.

El-Khadragy MF, Al-Olayan EM, Abdel Moneim AE (2014). Neuroprotective effects of Citrus reticulata in scopolamine-induced dementia oxidative stress in rats. CNS Neurol Disord Drug Targets 13: 684-690.

Emre M, Heckers S, Mash DC, et al (1993). Cholinergic innervation of the amygdaloid complex in the human brain and its alterations in old age and Alzheimer's disease. J Comp Neurol 336: 117-134.

Eriksdotter M, Navarro-Oviedo M, Mitra S, et al (2018). Cerebrospinal fluid from Alzheimer patients affects cell-mediated nerve growth factor production and cell survival in vitro. Exp Cell Res 371: 175-184.

Eubanks LM, Rogers CJ, Beuscher AE, et al (2006). A molecular link between the active component of marijuana and Alzheimer's disease pathology. Mol Pharm 3: 773-777.

Fagone P, Jackowski S (2013). Phosphatidylcholine and the CDP-choline cycle. Biochim Biophys Acta 1831: 523-532.

Fantegrossi WE, Wilson CD, Berquist MD (2018). Pro-psychotic effects of synthetic cannabinoids: interactions with central dopamine, serotonin, and glutamate systems. Drug Metab Rev 50: 65-73.

Farkas S, Nagy K, Palkovits M, et al (2012). (1)(2)(5)I]SD-7015 reveals fine modalities of CB(1) cannabinoid receptor density in the prefrontal cortex during progression of Alzheimer's disease. Neurochem Int 60: 286-291.

Fernandez-Ruiz J, Romero J, Ramos JA (2015). Endocannabinoids and Neurodegenerative Disorders: Parkinson's Disease, Huntington's Chorea, Alzheimer's Disease, and Others. Handb Exp Pharmacol 231: 233-259.

Ferrari-DiLeo G, Mash DC, Flynn DD (1995). Attenuation of muscarinic receptor-G-protein interaction in Alzheimer disease. Mol Chem Neuropathol 24: 69-91.

Ferraro L, Tomasini MC, Gessa GL, et al (2001). The cannabinoid receptor agonist WIN 55,212-2 regulates glutamate transmission in rat cerebral cortex: an in vivo and in vitro study. Cereb Cortex 11: 728-733.

Fischer W, Chen KS, Gage FH, et al (1992). Progressive decline in spatial learning and integrity of forebrain cholinergic neurons in rats during aging. Neurobiol Aging 13: 9-23.

Fitz NF, Gibbs RB, Johnson DA (2008). Selective lesion of septal cholinergic neurons in rats impairs acquisition of a delayed matching to position T-maze task by delaying the shift from a response to a place strategy. Brain Res Bull 77: 356-360.

Flasbeck V, Atucha E, Nakamura NH, et al (2018). Spatial information is preferentially processed by the distal part of CA3: Implication for memory retrieval. Behav Brain Res.

Flynn DD, Ferrari-DiLeo G, Levey AI, et al (1995). Differential alterations in muscarinic receptor subtypes in Alzheimer's disease: implications for cholinergic-based therapies. Life Sci 56: 869-876.

Flynn DD, Weinstein DA, Mash DC (1991). Loss of high-affinity agonist binding to M1 muscarinic receptors in Alzheimer's disease: implications for the failure of cholinergic replacement therapies. Ann Neurol 29: 256-262.

Freund TF, Hajos N (2003). Excitement reduces inhibition via endocannabinoids. Neuron 38: 362-365.

Freund TF, Katona I, Piomelli D (2003). Role of endogenous cannabinoids in synaptic signaling. Physiol Rev 83: 1017-1066.

Fukudome Y, Ohno-Shosaku T, Matsui M, et al (2004). Two distinct classes of muscarinic action on hippocampal inhibitory synapses: M2-mediated direct suppression and M1/M3-mediated indirect suppression through endocannabinoid signalling. Eur J Neurosci 19: 2682-2692.

Galve-Roperh I, Rueda D, Gomez del Pulgar T, et al (2002). Mechanism of extracellular signal-regulated kinase activation by the CB(1) cannabinoid receptor. Mol Pharmacol 62: 1385-1392.

Garcia-Alloza M, Zaldua N, Diez-Ariza M, et al (2006). Effect of selective cholinergic denervation on the serotonergic system: implications for learning and memory. J Neuropathol Exp Neurol 65: 1074-1081.

Gelfo F, Petrosini L, Graziano A, et al (2013). Cortical metabolic deficits in a rat model of cholinergic basal forebrain degeneration. Neurochem Res 38: 2114-2123.

George A, Ng CP, O'Callaghan M, et al (2014). In vitro and ex-vivo cellular antioxidant protection and cognitive enhancing effects of an extract of Polygonum minus Huds (Lineminus) demonstrated in a Barnes Maze animal model for memory and learning. BMC Complement Altern Med 14: 161-6882.

Gessa GL, Casu MA, Carta G, et al (1998). Cannabinoids decrease acetylcholine release in the medial-prefrontal cortex and hippocampus, reversal by SR 141716A. Eur J Pharmacol 355: 119-124.

Gessa GL, Mascia MS, Casu MA, et al (1997a). Inhibition of hippocampal acetylcholine release by cannabinoids: reversal by SR 141716A. Eur J Pharmacol 327: R1-2.

Geula C, Mesulam MM, Saroff DM, et al (1998). Relationship between plaques, tangles, and loss of cortical cholinergic fibers in Alzheimer disease. J Neuropathol Exp Neurol 57: 63-75.

Gibbs RB, Johnson DA (2007). Cholinergic lesions produce task-selective effects on delayed matching to position and configural association learning related to response pattern and strategy. Neurobiol Learn Mem 88: 19-32.

Gifford AN, Ashby CR (1996). Electrically evoked acetylcholine release from hippocampal slices is inhibited by the cannabinoid receptor agonist, WIN 55212-2, and is potentiated by the cannabinoid antagonist, SR 141716A. J Pharmacol Exp Ther 277: 1431-1436.

Gifford AN, Bruneus M, Gatley SJ, et al (2000). Cannabinoid receptor-mediated inhibition of acetylcholine release from hippocampal and cortical synaptosomes. Br J Pharmacol 131: 645-650.

Gil-Bea FJ, Garcia-Alloza M, Dominguez J, et al (2005). Evaluation of cholinergic markers in Alzheimer's disease and in a model of cholinergic deficit. Neurosci Lett 375: 37-41.

Giuffrida A, Parsons LH, Kerr TM, et al (1999). Dopamine activation of endogenous cannabinoid signaling in dorsal striatum. Nat Neurosci 2: 358-363.

Glass M, Brotchie JM, Maneuf YP (1997). Modulation of neurotransmission by cannabinoids in the basal ganglia. Eur J Neurosci 9: 199-203.

Gold PE (2003). Acetylcholine modulation of neural systems involved in learning and memory. Neurobiol Learn Mem 80: 194-210.

Gonzalez de San Roman, E, Manuel I, Giralt MT, et al (2017). Imaging mass spectrometry (IMS) of cortical lipids from preclinical to severe stages of Alzheimer's disease. Biochim Biophys Acta 1859: 1604-1614.

Gorelick PB, Furie KL, Iadecola C, et al (2017). Defining Optimal Brain Health in Adults: A Presidential Advisory From the American Heart Association/American Stroke Association. Stroke 48: e284-e303.

Gotti C, Clementi F (2004). Neuronal nicotinic receptors: from structure to pathology. Prog Neurobiol 74: 363-396.

Gotti C, Fornasari D, Clementi F (1997). Human neuronal nicotinic receptors. Prog Neurobiol 53: 199-237.

Gratwicke J, Kahan J, Zrinzo L, et al (2013). The nucleus basalis of Meynert: a new target for deep brain stimulation in dementia? Neurosci Biobehav Rev 37: 2676-2688.

Green RC, Mesulam MM (1988). Acetylcholinesterase fiber staining in the human hippocampus and parahippocampal gyrus. J Comp Neurol 273: 488-499.

Griffiths PD, Perry RH, Crossman AR (1994). A detailed anatomical analysis of neurotransmitter receptors in the putamen and caudate in Parkinson's disease and Alzheimer's disease. Neurosci Lett 169: 68-72.

Gritti I, Mainville L, Jones BE (1994). Projections of GABAergic and cholinergic basal forebrain and GABAergic preoptic-anterior hypothalamic neurons to the posterior lateral hypothalamus of the rat. J Comp Neurol 339: 251-268.

Groleau M, Chamoun M, Vaucher E (2018a). Stimulation of Acetylcholine Release and Pharmacological Potentiation of Cholinergic Transmission Affect Cholinergic Receptor Expression Differently during Visual Conditioning. Neuroscience 386: 79-90.

Grothe M, Heinsen H, Teipel SJ (2012). Atrophy of the cholinergic Basal forebrain over the adult age range and in early stages of Alzheimer's disease. Biol Psychiatry 71: 805-813.

Grzeda E, Schlicker E, Toczek M, et al (2017). CB1 receptor activation in the rat paraventricular nucleus induces bi-directional cardiovascular effects via modification of glutamatergic and GABAergic neurotransmission. Naunyn Schmiedebergs Arch Pharmacol 390: 25-35.

Gupta PP, Pandey RD, Jha D, et al (2015). Role of traditional nonsteroidal anti-inflammatory drugs in Alzheimer's disease: a meta-analysis of randomized clinical trials. Am J Alzheimers Dis Other Demen 30: 178-182.

Gusev PA, Gubin AN (2010). Recent and remote memory recalls modulate different sets of stereotypical interlaminar correlations in Arc/Arg3.1 mRNA expression in cortical areas. Brain Res 1352: 118-139.

Gutierrez H, Gutierrez R, Silva-Gandarias R, et al (1999). Differential effects of 192IgG-saporin and NMDA-induced lesions into the basal forebrain on cholinergic activity and taste aversion memory formation. Brain Res 834: 136-141.

Haga T (1971). Synthesis and release of (14 C)acetylcholine in synaptosomes. J Neurochem 18: 781-798.

Hajos N, Freund TF (2002). Pharmacological separation of cannabinoid sensitive receptors on hippocampal excitatory and inhibitory fibers. Neuropharmacology 43: 503-510.

Hajos N, Katona I, Naiem SS, et al (2000). Cannabinoids inhibit hippocampal GABAergic transmission and network oscillations. Eur J Neurosci 12: 3239-3249.

Hajos N, Ledent C, Freund TF (2001). Novel cannabinoid-sensitive receptor mediates inhibition of glutamatergic synaptic transmission in the hippocampus. Neuroscience 106: 1-4.

Han X, M Holtzman D, McKeel DW, et al (2002). Substantial sulfatide deficiency and ceramide elevation in very early Alzheimer's disease: potential role in disease pathogenesis. J Neurochem 82: 809-818.

Hansen HS, Lauritzen L, Moesgaard B, et al (1998). Formation of N-acyl-phosphatidylethanolamines and N-acetylethanolamines: proposed role in neurotoxicity. Biochem Pharmacol 55: 719-725.

Hanus L, Breuer A, Tchilibon S, et al (1999). HU-308: a specific agonist for CB(2), a peripheral cannabinoid receptor. Proc Natl Acad Sci U S A 96: 14228-14233.

Harkany T, Dobszay MB, Cayetanot F, et al (2005). Redistribution of CB1 cannabinoid receptors during evolution of cholinergic basal forebrain territories and their cortical projection areas: a comparison between the gray mouse lemur (Microcebus murinus, primates) and rat. Neuroscience 135: 595-609.

Harkany T, Hartig W, Berghuis P, et al (2003a). Complementary distribution of type 1 cannabinoid receptors and vesicular glutamate transporter 3 in basal forebrain suggests input-specific retrograde signalling by cholinergic neurons. Eur J Neurosci 18: 1979-1992.

Harmon KM, Wellman CL (2003). Differential effects of cholinergic lesions on dendritic spines in frontal cortex of young adult and aging rats. Brain Res 992: 60-68.

Harrison PJ, Barton AJ, Najlerahim A, et al (1991). Increased muscarinic receptor messenger RNA in Alzheimer's disease temporal cortex demonstrated by in situ hybridization histochemistry. Brain Res Mol Brain Res 9: 15-21.

Hasanein P, Teimuri Far M (2015). Effects of URB597 as an inhibitor of fatty acid amide hydrolase on WIN55, 212-2-induced learning and memory deficits in rats. Pharmacol Biochem Behav 131: 130-135.

Hayes TL, Lewis DA (1992). Nonphosphorylated neurofilament protein and calbindin immunoreactivity in layer III pyramidal neurons of human neocortex. Cereb Cortex 2: 56-67.

Haywood PT, Divekar N, Karalliedde LD (1999). Concurrent medication and the neuromuscular junction. Eur J Anaesthesiol 16: 77-91.

Hebert-Chatelain E, Desprez T, Serrat R, et al (2016). A cannabinoid link between mitochondria and memory. Nature 539: 555-559.

Heckers S, Ohtake T, Wiley RG, et al (1994a). Complete and selective cholinergic denervation of rat neocortex and hippocampus but not amygdala by an immunotoxin against the p75 NGF receptor. J Neurosci 14: 1271-1289.

Heckers S, Ohtake T, Wiley RG, et al (1994b). Complete and selective cholinergic denervation of rat neocortex and hippocampus but not amygdala by an immunotoxin against the p75 NGF receptor. J Neurosci 14: 1271-1289.

Heider M, Schliebs R, Rossner S, et al (1997). Basal forebrain cholinergic immunolesion by 192IgG-saporin: evidence for a presynaptic location of subpopulations of alpha 2- and beta-adrenergic as well as 5-HT2A receptors on cortical cholinergic terminals. Neurochem Res 22: 957-966.

Heifets BD, Castillo PE (2009). Endocannabinoid signaling and long-term synaptic plasticity. Annu Rev Physiol 71: 283-306.

Heinrich JN, Butera JA, Carrick T, et al (2009). Pharmacological comparison of muscarinic ligands: historical versus more recent muscarinic M1-preferring receptor agonists. Eur J Pharmacol 605: 53-56.

Hepler DJ, Olton DS, Wenk GL, et al (1985). Lesions in nucleus basalis magnocellularis and medial septal area of rats produce qualitatively similar memory impairments. J Neurosci 5: 866-873.

Herkenham M, Lynn AB, Little MD, et al (1990). Cannabinoid receptor localization in brain. Proc Natl Acad Sci U S A 87: 1932-1936.

Hernandez-Hernandez A, Adem A, Ravid R, et al (1995). Preservation of acetylcholine muscarinic M2 receptor G-protein interactions in the neocortex of patients with Alzheimer's disease. Neurosci Lett 186: 57-60.

Hescham S, Temel Y, Casaca-Carreira J, et al (2014). A neuroanatomical analysis of the effects of a memory impairing dose of scopolamine in the rat brain using cytochrome c oxidase as principle marker. J Chem Neuroanat 59-60: 1-7.

Hosseini N, Alaei H, Reisi P, et al (2017). The effects of NBM- lesion on synaptic plasticity in rats. Brain Res 1655: 122-127.

Howlett AC (2002). The cannabinoid receptors. Prostaglandins Other Lipid Mediat 68-69: 619-631.

Hrabovszky E, Wittmann G, Kallo I, et al (2012). Distribution of type 1 cannabinoid receptor-expressing neurons in the septal-hypothalamic region of the mouse: colocalization with GABAergic and glutamatergic markers. J Comp Neurol 520: 1005-1020.

Huffman JW, Yu S, Showalter V, et al (1996). Synthesis and pharmacology of a very potent cannabinoid lacking a phenolic hydroxyl with high affinity for the CB2 receptor. J Med Chem 39: 3875-3877.

Hulme EC (1990). Muscarinic acetylcholine receptors: typical G-coupled receptors. Symp Soc Exp Biol 44: 39-54.

Hulme EC, Birdsall NJ, Buckley NJ (1990). Muscarinic receptor subtypes. Annu Rev Pharmacol Toxicol 30: 633-673.

Ikonomovic MD, Abrahamson EE, Isanski BA, et al (2007). Superior frontal cortex cholinergic axon density in mild cognitive impairment and early Alzheimer disease. Arch Neurol 64: 1312-1317.

Jamali-Raeufy N, Nasehi M, Ebrahimi-Ghiri M, et al (2011). Cross state-dependency of learning between WIN55, 212-2 and scopolamine in rat dorsal hippocampus. Neurosci Lett 491: 227-231.

Jeong DU, Chang WS, Hwang YS, et al (2011). Decrease of GABAergic markers and arc protein expression in the frontal cortex by intraventricular 192 IgG-saporin. Dement Geriatr Cogn Disord 32: 70-78.

Jeong DU, Oh JH, Lee JE, et al (2016). Basal Forebrain Cholinergic Deficits Reduce Glucose Metabolism and Function of Cholinergic and GABAergic Systems in the Cingulate Cortex. Yonsei Med J 57: 165-172.

Jones BE, Cuello AC (1989). Afferents to the basal forebrain cholinergic cell area from pontomesencephalic--catecholamine, serotonin, and acetylcholine--neurons. Neuroscience 31: 37-61.

Jung KM, Astarita G, Yasar S, et al (2012). An amyloid beta42-dependent deficit in anandamide mobilization is associated with cognitive dysfunction in Alzheimer's disease. Neurobiol Aging 33: 1522-1532.

Kano M (2014). Control of synaptic function by endocannabinoid-mediated retrograde signaling. Proc Jpn Acad Ser B Phys Biol Sci 90: 235-250.

Kano M, Ohno-Shosaku T, Hashimotodani Y, et al (2009). Endocannabinoid-mediated control of synaptic transmission. Physiol Rev 89: 309-380.

Karlsson M, Contreras JA, Hellman U, et al (1997). cDNA cloning, tissue distribution, and identification of the catalytic triad of monoglyceride lipase. Evolutionary relationship to esterases, lysophospholipases, and haloperoxidases. J Biol Chem 272: 27218-27223.

Kasa P (1986). The cholinergic systems in brain and spinal cord. Prog Neurobiol 26: 211-272.

Kathmann M, Weber B, Zimmer A, et al (2001). Enhanced acetylcholine release in the hippocampus of cannabinoid CB(1) receptor-deficient mice. Br J Pharmacol 132: 1169-1173.

Katona I, Rancz EA, Acsady L, et al (2001). Distribution of CB1 cannabinoid receptors in the amygdala and their role in the control of GABAergic transmission. J Neurosci 21: 9506-9518.

Katona I, Sperlagh B, Sik A, et al (1999). Presynaptically located CB1 cannabinoid receptors regulate GABA release from axon terminals of specific hippocampal interneurons. J Neurosci 19: 4544-4558.

Katona I, Urban GM, Wallace M, et al (2006). Molecular composition of the endocannabinoid system at glutamatergic synapses. J Neurosci 26: 5628-5637.

Kendall DA, Yudowski GA (2017). Cannabinoid Receptors in the Central Nervous System: Their Signaling and Roles in Disease. Front Cell Neurosci 10: 294.

Kim J, Isokawa M, Ledent C, et al (2002). Activation of muscarinic acetylcholine receptors enhances the release of endogenous cannabinoids in the hippocampus. J Neurosci 22: 10182-10191.

Kirschmann EK, McCalley DM, Edwards CM, et al (2017). Consequences of Adolescent Exposure to the Cannabinoid Receptor Agonist WIN55,212-2 on Working Memory in Female Rats. Front Behav Neurosci 11: 137.

Kirschmann EK, Pollock MW, Nagarajan V, et al (2017). Effects of Adolescent Cannabinoid Self-Administration in Rats on Addiction-Related Behaviors and Working Memory. Neuropsychopharmacology 42: 989-1000.

Knox D (2016). The role of basal forebrain cholinergic neurons in fear and extinction memory. Neurobiol Learn Mem 133: 39-52.

Koppel J, Bradshaw H, Goldberg TE, et al (2009). Endocannabinoids in Alzheimer's disease and their impact on normative cognitive performance: a case-control and cohort study. Lipids Health Dis 8: 2-511X.

Kosik KS (2013). Diseases: Study neuron networks to tackle Alzheimer's. Nature 503: 31-32.

Kovacs FE, Knop T, Urbanski MJ, et al (2012). Exogenous and endogenous cannabinoids suppress inhibitory neurotransmission in the human neocortex. Neuropsychopharmacology 37: 1104-1114.

Krishnan S, Cairns R, Howard R (2009). Cannabinoids for the treatment of dementia. Cochrane Database Syst Rev (2):CD007204. doi: CD007204.

Kubo T, Maeda A, Sugimoto K, et al (1986). Primary structure of porcine cardiac muscarinic acetylcholine receptor deduced from the cDNA sequence. FEBS Lett 209: 367-372.

Kuribara H, Tadokoro S (1983). Development of tolerance to ambulation-increasing effect of scopolamine dependent on environmental factors in mice. Jpn J Pharmacol 33: 1041-1048.

Lawston J, Borella A, Robinson JK, et al (2000). Changes in hippocampal morphology following chronic treatment with the synthetic cannabinoid WIN 55,212-2. Brain Res 877: 407-410.

Lee JE, Jeong DU, Lee J, et al (2016). The effect of nucleus basalis magnocellularis deep brain stimulation on memory function in a rat model of dementia. BMC Neurol 16: 6-016.

Lee JH, Agacinski G, Williams JH, et al (2010). Intact cannabinoid CB1 receptors in the Alzheimer's disease cortex. Neurochem Int 57: 985-989.

Lemke R, Hartig W, Rossner S, et al (1998). Interleukin-6 is not expressed in activated microglia and in reactive astrocytes in response to lesion of rat basal forebrain cholinergic system as demonstrated by combined in situ hybridization and immunocytochemistry. J Neurosci Res 51: 223-236.

Lemtiri-Chlieh F, Levine ES (2007). Lack of depolarization-induced suppression of inhibition (DSI) in layer 2/3 interneurons that receive cannabinoid-sensitive inhibitory inputs. J Neurophysiol 98: 2517-2524.

Levey AI, Edmunds SM, Hersch SM, et al (1995). Light and electron microscopic study of m2 muscarinic acetylcholine receptor in the basal forebrain of the rat. J Comp Neurol 351: 339-356.

Levey AI, Kitt CA, Simonds WF, et al (1991). Identification and localization of muscarinic acetylcholine receptor proteins in brain with subtype-specific antibodies. J Neurosci 11: 3218-3226.

Li Y, Kim J (2016). CB2 Cannabinoid Receptor Knockout in Mice Impairs Contextual Long-Term Memory and Enhances Spatial Working Memory. Neural Plast 2016: 9817089.

Little PJ, Compton DR, Johnson MR, et al (1988). Pharmacology and stereoselectivity of structurally novel cannabinoids in mice. J Pharmacol Exp Ther 247: 1046-1051.

Liu AK, Chang RC, Pearce RK, et al (2015). Nucleus basalis of Meynert revisited: anatomy, history and differential involvement in Alzheimer's and Parkinson's disease. Acta Neuropathol 129: 527-540.

Liu R, Crawford J, Callahan PM, et al (2018). Intermittent stimulation in the nucleus basalis of meynert improves sustained attention in rhesus monkeys. Neuropharmacology 137: 202-210.

Liu R, Crawford J, Callahan PM, et al (2017). Intermittent Stimulation of the Nucleus Basalis of Meynert Improves Working Memory in Adult Monkeys. Curr Biol 27: 2640-2646.e4.

Livingston G, Sommerlad A, Orgeta V, et al (2017). Dementia prevention, intervention, and care. Lancet 390: 2673-2734.

Ljubojevic V, Luu P, De Rosa E (2014). Cholinergic contributions to supramodal attentional processes in rats. J Neurosci 34: 2264-2275.

Llorente-Ovejero A, Manuel I, Giralt MT, et al (2017). Increase in cortical endocannabinoid signaling in a rat model of basal forebrain cholinergic dysfunction. Neuroscience 362: 206-218.

Lopez A, Aparicio N, Pazos MR, et al (2018). Cannabinoid CB2 receptors in the mouse brain: relevance for Alzheimer's disease. J Neuroinflammation 15: 158-018.

Lopez JA, Armstrong ML, Piegors DJ, et al (1990). Vascular responses to endothelin-1 in atherosclerotic primates. Arteriosclerosis 10: 1113-1118.

Lopez OL, DeKosky ST (2031). Neuropathology of Alzheimer's disease and mild cognitive impairment. Rev Neurol 37: 155-163.

Lu XR, Ong WY, Mackie K (1999). A light and electron microscopic study of the CB1 cannabinoid receptor in monkey basal forebrain. J Neurocytol 28: 1045-1051.

Lukas RJ, Changeux JP, Le Novere N, et al (1999). International Union of Pharmacology. XX. Current status of the nomenclature for nicotinic acetylcholine receptors and their subunits. Pharmacol Rev 51: 397-401.

Maejima T, Ohno-Shosaku T, Kano M (2001). Endogenous cannabinoid as a retrograde messenger from depolarized postsynaptic neurons to presynaptic terminals. Neurosci Res 40: 205-210.

Mailleux P, Verslijpe M, Vanderhaeghen JJ (1992). Initial observations on the distribution of cannabinoid receptor binding sites in the human adult basal ganglia using autoradiography. Neurosci Lett 139: 7-9.

Malikowska-Racia N, Podkowa A, Salat K (2018). Phencyclidine and Scopolamine for Modeling Amnesia in Rodents: Direct Comparison with the Use of Barnes Maze Test and Contextual Fear Conditioning Test in Mice. Neurotox Res.

Mann DM, Hardy J (2013). Amyloid or tau: the chicken or the egg? Acta Neuropathol 126: 609-613.

Mann DM, Yates PO, Marcyniuk B (1984). Changes in nerve cells of the nucleus basalis of Meynert in Alzheimer's disease and their relationship to ageing and to the accumulation of lipofuscin pigment. Mech Ageing Dev 25: 189-204.

Manuel I, Gonzalez de San Roman, E, Giralt MT, et al (2014). Type-1 cannabinoid receptor activity during Alzheimer's disease progression. J Alzheimers Dis 42: 761-766.

Margulies JE, Hammer RP (1991). Delta 9-tetrahydrocannabinol alters cerebral metabolism in a biphasic, dose-dependent manner in rat brain. Eur J Pharmacol 202: 373-378.

Marisco PC, Carvalho FB, Rosa MM, et al (2013). Piracetam prevents scopolamine-induced memory impairment and decrease of NTPDase, 5'-nucleotidase and adenosine deaminase activities. Neurochem Res 38: 1704-1714.

Marsicano G, Lutz B (1999). Expression of the cannabinoid receptor CB1 in distinct neuronal subpopulations in the adult mouse forebrain. Eur J Neurosci 11: 4213-4225.

Marsicano G, Wotjak CT, Azad SC, et al (2002). The endogenous cannabinoid system controls extinction of aversive memories. Nature 418: 530-534.

Marston HM, West HL, Wilkinson LS, et al (1994). Effects of excitotoxic lesions of the septum and vertical limb nucleus of the diagonal band of Broca on conditional visual discrimination: relationship between performance and choline acetyltransferase activity in the cingulate cortex. J Neurosci 14: 2009-2019.

Martin HG, Bernabeu A, Lassalle O, et al (2015). Endocannabinoids Mediate Muscarinic Acetylcholine Receptor-Dependent Long-Term Depression in the Adult Medial Prefrontal Cortex. Front Cell Neurosci 9: 457.

Martinez-Gardeazabal J, Gonzalez de San Roman, E, Moreno-Rodriguez M, et al (2017). Lipid mapping of the rat brain for models of disease. Biochim Biophys Acta 1859: 1548-1557.

Mash DC, Flynn DD, Potter LT (1985). Loss of M2 muscarine receptors in the cerebral cortex in Alzheimer's disease and experimental cholinergic denervation. Science 228: 1115-1117.

Mash DC, Potter LT (1986). Autoradiographic localization of M1 and M2 muscarine receptors in the rat brain. Neuroscience 19: 551-564.

Mateo Y, Johnson KA, Covey DP, et al (2017). Endocannabinoid Actions on Cortical Terminals Orchestrate Local Modulation of Dopamine Release in the Nucleus Accumbens. Neuron 96: 1112-1126.e5.

Matsuda LA, Bonner TI, Lolait SJ (1992). Cannabinoid receptors: which cells, where, how, and why? NIDA Res Monogr 126: 48-56.

Mattson MP (2008). Glutamate and neurotrophic factors in neuronal plasticity and disease. Ann N Y Acad Sci 1144: 97-112.

Mattsson A, Ogren SO, Olson L (2002). Facilitation of dopamine-mediated locomotor activity in adult rats following cholinergic denervation. Exp Neurol 174: 96-108.

Mattsson A, Pernold K, Ogren SO, et al (2004). Loss of cortical acetylcholine enhances amphetamine-induced locomotor activity. Neuroscience 127: 579-591.

McGaughy J, Sarter M (1998). Sustained attention performance in rats with intracortical infusions of 192 IgG-saporin-induced cortical cholinergic deafferentation: effects of physostigmine and FG 7142. Behav Neurosci 112: 1519-1525.

McGeer E, McGeer PL (1986). Possible destruction of cholinoceptive neurons by overstimulation of cholinergic tracts. Can J Physiol Pharmacol 64: 363-368.

McGeer PL, Kamo H, Harrop R, et al (1986). Comparison of PET, MRI, and CT with pathology in a proven case of Alzheimer's disease. Neurology 36: 1569-1574.

Meck WH, Williams CL (2003). Metabolic imprinting of choline by its availability during gestation: implications for memory and attentional processing across the lifespan. Neurosci Biobehav Rev 27: 385-399.

Meck WH, Williams CL (1997). Simultaneous temporal processing is sensitive to prenatal choline availability in mature and aged rats. Neuroreport 8: 3045-3051.

Meck WH, Williams CL, Cermak JM, et al (2008). Developmental periods of choline sensitivity provide an ontogenetic mechanism for regulating memory capacity and age-related dementia. Front Integr Neurosci 1: 7.

Medalla M, Barbas H (2012). The anterior cingulate cortex may enhance inhibition of lateral prefrontal cortex via m2 cholinergic receptors at dual synaptic sites. J Neurosci 32: 15611-15625.

Mehlhorn G, Loffler T, Apelt J, et al (1998). Glucose metabolism in cholinoceptive cortical rat brain regions after basal forebrain cholinergic lesion. Int J Dev Neurosci 16: 675-690.

Melvin LS, Milne GM, Johnson MR, et al (1993). Structure-activity relationships for cannabinoid receptor-binding and analgesic activity: studies of bicyclic cannabinoid analogs. Mol Pharmacol 44: 1008-1015.

Mendiguren A, Aostri E, Pineda J (2018). Regulation of noradrenergic and serotonergic systems by cannabinoids: relevance to cannabinoid-induced effects. Life Sci 192: 115-127.

Mesulam M (2004). The cholinergic lesion of Alzheimer's disease: pivotal factor or side show? Learn Mem 11: 43-49.

Mesulam MM (2004). The cholinergic innervation of the human cerebral cortex. Prog Brain Res 145: 67-78.

Mesulam MM (1998). Some cholinergic themes related to Alzheimer's disease: synaptology of the nucleus basalis, location of m2 receptors, interactions with amyloid metabolism, and perturbations of cortical plasticity. J Physiol Paris 92: 293-298.

Mesulam MM (1990). Human brain cholinergic pathways. Prog Brain Res 84: 231-241.

Mesulam MM, Geula C (1994). Butyrylcholinesterase reactivity differentiates the amyloid plaques of aging from those of dementia. Ann Neurol 36: 722-727.

Mesulam MM, Geula C (1988). Acetylcholinesterase-rich pyramidal neurons in the human neocortex and hippocampus: absence at birth, development during the life span, and dissolution in Alzheimer's disease. Ann Neurol 24: 765-773.

Mesulam MM, Mufson EJ, Levey AI, et al (1983). Cholinergic innervation of cortex by the basal forebrain: cytochemistry and cortical connections of the septal area, diagonal band nuclei, nucleus basalis (substantia innominata), and hypothalamus in the rhesus monkey. J Comp Neurol 214: 170-197.

Mesulam MM, Mufson EJ, Wainer BH, et al (1983). Central cholinergic pathways in the rat: an overview based on an alternative nomenclature (Ch1-Ch6). Neuroscience 10: 1185-1201.

Michalek H, Fortuna S, Pintor A (1989). Age-related differences in brain choline acetyltransferase, cholinesterases and muscarinic receptor sites in two strains of rats. Neurobiol Aging 10: 143-148.

Millington WR, Wurtman RJ (1982). Choline administration elevates brain phosphorylcholine concentrations. J Neurochem 38: 1748-1752.

Mishima K, Egashira N, Matsumoto Y, et al (2002). Involvement of reduced acetylcholine release in Delta9-tetrahydrocannabinol-induced impairment of spatial memory in the 8-arm radial maze. Life Sci 72: 397-407.

Mohapel P, Leanza G, Kokaia M, et al (2005). Forebrain acetylcholine regulates adult hippocampal neurogenesis and learning. Neurobiol Aging 26: 939-946.

Monory K, Polack M, Remus A, et al (2015). Cannabinoid CB1 receptor calibrates excitatory synaptic balance in the mouse hippocampus. J Neurosci 35: 3842-3850.

Moor E, Schirm E, Jacso J, et al (1998). Effects of neostigmine and atropine on basal and handling-induced acetylcholine output from ventral hippocampus. Neuroscience 82: 819-825.

Mossello E, Ballini E (2012). Management of patients with Alzheimer's disease: pharmacological treatment and quality of life. Ther Adv Chronic Dis 3: 183-193.

Muccioli GG, Stella N (2008). Microglia produce and hydrolyze palmitoylethanolamide. Neuropharmacology 54: 16-22.

Mufson EJ, Counts SE, Perez SE, et al (2008). Cholinergic system during the progression of Alzheimer's disease: therapeutic implications. Expert Rev Neurother 8: 1703-1718.

Mufson EJ, Ginsberg SD, Ikonomovic MD, et al (2003a). Human cholinergic basal forebrain: chemoanatomy and neurologic dysfunction. J Chem Neuroanat 26: 233-242.

Mufson EJ, Ma SY, Dills J, et al (2002). Loss of basal forebrain P75(NTR) immunoreactivity in subjects with mild cognitive impairment and Alzheimer's disease. J Comp Neurol 443: 136-153.

Mufson EJ, Martin TL, Mash DC, et al (1986). Cholinergic projections from the parabigeminal nucleus (Ch8) to the superior colliculus in the mouse: a combined analysis of horseradish peroxidase transport and choline acetyltransferase immunohistochemistry. Brain Res 370: 144-148.

Muir JL, Page KJ, Sirinathsinghji DJ, et al (1993). Excitotoxic lesions of basal forebrain cholinergic neurons: effects on learning, memory and attention. Behav Brain Res 57: 123-131.

Mulder J, Zilberter M, Pasquare SJ, et al (2011). Molecular reorganization of endocannabinoid signalling in Alzheimer's disease. Brain 134: 1041-1060.

Mulugeta E, Chandranath I, Karlsson E, et al (2006). Temporal and region-dependent changes in muscarinic M4 receptors in the hippocampus and entorhinal cortex of adrenalectomized rats. Exp Brain Res 173: 309-317.

Munro S, Thomas KL, Abu-Shaar M (1993). Molecular characterization of a peripheral receptor for cannabinoids. Nature 365: 61-65.

Musella A, Fresegna D, Rizzo FR, et al (2017). A novel crosstalk within the endocannabinoid system controls GABA transmission in the striatum. Sci Rep 7: 7363-017.

Myers CE, Ermita BR, Harris K, et al (1996). A computational model of cholinergic disruption of septohippocampal activity in classical eyeblink conditioning. Neurobiol Learn Mem 66: 51-66.

Nagode DA, Tang AH, Yang K, et al (2014). Optogenetic identification of an intrinsic cholinergically driven inhibitory oscillator sensitive to cannabinoids and opioids in hippocampal CA1. J Physiol 592: 103-123.

Nakamura S, Tani Y, Maezono Y, et al (1992). Learning deficits after unilateral AF64A lesions in the rat basal forebrain: role of cholinergic and noncholinergic systems. Pharmacol Biochem Behav 42: 119-130.

Nallapaneni A, Liu J, Karanth S, et al (2008). Pharmacological enhancement of endocannabinoid signaling reduces the cholinergic toxicity of diisopropylfluorophosphate. Neurotoxicology 29: 1037-1043.

Nallapaneni A, Liu J, Karanth S, et al (2006). Modulation of paraoxon toxicity by the cannabinoid receptor agonist WIN 55,212-2. Toxicology 227: 173-183.

Narushima M, Uchigashima M, Fukaya M, et al (2007). Tonic enhancement of endocannabinoid-mediated retrograde suppression of inhibition by cholinergic interneuron activity in the striatum. J Neurosci 27: 496-506.

Nasehi M, Piri M, Jamali-Raeufy N, et al (2010). Influence of intracerebral administration of NO agents in dorsal hippocampus (CA1) on cannabinoid state-dependent memory in the step-down passive avoidance test. Physiol Behav 100: 297-304.

Nava F, Carta G, Colombo G, et al (2001). Effects of chronic Delta(9)-tetrahydrocannabinol treatment on hippocampal extracellular acetylcholine concentration and alternation performance in the T-maze. Neuropharmacology 41: 392-399.

Navakkode S, Korte M (2014). Pharmacological activation of CB1 receptor modulates long term potentiation by interfering with protein synthesis. Neuropharmacology 79: 525-533.

Navarrete M, Araque A (2008). Endocannabinoids mediate neuron-astrocyte communication. Neuron 57: 883-893.

Nedaei SE, Rezayof A, Pourmotabbed A, et al (2016). Activation of endocannabinoid system in the rat basolateral amygdala improved scopolamine-induced memory consolidation impairment. Behav Brain Res 311: 183-191.

Nieto-Escamez FA, Sanchez-Santed F, de Bruin JP (2002). Cholinergic receptor blockade in prefrontal cortex and lesions of the nucleus basalis: implications for allocentric and egocentric spatial memory in rats. Behav Brain Res 134: 93-112.

Nitsch RM, Slack BE, Wurtman RJ, et al (1992). Release of Alzheimer amyloid precursor derivatives stimulated by activation of muscarinic acetylcholine receptors. Science 258: 304-307.

Nyiri G, Szabadits E, Cserep C, et al (2005). GABAB and CB1 cannabinoid receptor expression identifies two types of septal cholinergic neurons. Eur J Neurosci 21: 3034-3042.

Office P (2017). Correction: Do cognitive interventions improve general cognition in dementia? a meta-analysis and meta-regression. BMJ Open 7: e005247corr1-2014.

Ohara K, Kondo N, Xie D, et al (1994). Normal sequences of muscarinic acetylcholine receptors (m1 and m2) in patients with Alzheimer's disease and vascular dementia. Neurosci Lett 178: 23-26.

Ohno-Shosaku T, Matsui M, Fukudome Y, et al (2003). Postsynaptic M1 and M3 receptors are responsible for the muscarinic enhancement of retrograde endocannabinoid signalling in the hippocampus. Eur J Neurosci 18: 109-116.

Ohno-Shosaku T, Shosaku J, Tsubokawa H, et al (2002). Cooperative endocannabinoid production by neuronal depolarization and group I metabotropic glutamate receptor activation. Eur J Neurosci 15: 953-961.

Okuda T, Haga T (2003). High-affinity choline transporter. Neurochem Res 28: 483-488.

Paban V, Chambon C, Farioli F, et al (2011). Gene regulation in the rat prefrontal cortex after learning with or without cholinergic insult. Neurobiol Learn Mem 95: 441-452.

Paban V, Chambon C, Jaffard M, et al (2005). Behavioral effects of basal forebrain cholinergic lesions in young adult and aging rats. Behav Neurosci 119: 933-945.

Pagani M, Giuliani A, Oberg J, et al (2016). Predicting the transition from normal aging to Alzheimer's disease: A statistical mechanistic evaluation of FDG-PET data. Neuroimage 141: 282-290.

Palazuelos J, Aguado T, Egia A, et al (2006). Non-psychoactive CB2 cannabinoid agonists stimulate neural progenitor proliferation. FASEB J 20: 2405-2407.

Pan JX, Wang ZL, Li N, et al (2014). Analgesic tolerance and cross-tolerance to the cannabinoid receptors ligands hemopressin, VD-hemopressin(alpha) and WIN55,212-2 at the supraspinal level in mice. Neurosci Lett 578: 187-191.

Parent MJ, Cyr M, Aliaga A, et al (2013). Concordance between in vivo and postmortem measurements of cholinergic denervation in rats using PET with [^{18}F]FEOBV and choline acetyltransferase immunochemistry. EJNMMI Res 3: 70-219X.

Parent M, Bedard MA, Aliaga A, et al (2012). PET imaging of cholinergic deficits in rats using [^{18}F]fluoroethoxybenzovesamicol ([^{18}F]FEOBV). Neuroimage 62: 555-561.

Passmore MJ (2008). The cannabinoid receptor agonist nabilone for the treatment of dementia-related agitation. Int J Geriatr Psychiatry 23: 116-117.

Pastotter B, Tempel T, Bauml KT (2017). Long-Term Memory Updating: The Reset-of-Encoding Hypothesis in List-Method Directed Forgetting. Front Psychol 8: 2076.

Pattanashetti LA, Taranalli AD, Parvatrao V, et al (2017). Evaluation of neuroprotective effect of quercetin with donepezil in scopolamine-induced amnesia in rats. Indian J Pharmacol 49: 60-64.

Pellborn LA, Rossner S (1995). 27,800 visitors at the annual meeting of the Swedish Medical Society 1994. Lakartidningen 92: 2190.

Perry EK, Perry RH, Blessed G, et al (1978). Changes in brain cholinesterases in senile dementia of Alzheimer type. Neuropathol Appl Neurobiol 4: 273-277.

Pertwee RG (2010). Receptors and channels targeted by synthetic cannabinoid receptor agonists and antagonists. Curr Med Chem 17: 1360-1381.

Pertwee RG (2008). Ligands that target cannabinoid receptors in the brain: from THC to anandamide and beyond. Addict Biol 13: 147-159.

Pertwee RG (1999). Cannabis and cannabinoids: pharmacology and rationale for clinical use. Forsch Komplementarmed 6 Suppl 3: 12-15.

Piavchenko GA, Shmarkova LI, Nozdrin VI (2015). Changes in the Number of Neurons in the Motor Cortex of Rats and their Locomotor Activity in the Age Aspect. Morfologiia 147: 7-10.

Piomelli D, Beltramo M, Glasnapp S, et al (1999). Structural determinants for recognition and translocation by the anandamide transporter. Proc Natl Acad Sci U S A 96: 5802-5807.

Pisanu A, Acquas E, Fenu S, et al (2006). Modulation of Delta(9)-THC-induced increase of cortical and hippocampal acetylcholine release by micro opioid and D(1) dopamine receptors. Neuropharmacology 50: 661-670.

Pizzo DP, Thal LJ, Winkler J (2002). Mnemonic deficits in animals depend upon the degree of cholinergic deficit and task complexity. Exp Neurol 177: 292-305.

Polissidis A, Galanopoulos A, Naxakis G, et al (2013). The cannabinoid CB1 receptor biphasically modulates motor activity and regulates dopamine and glutamate release region dependently. Int J Neuropsychopharmacol 16: 393-403.

Price DL, Martin LJ, Sisodia SS, et al (1991). Aged non-human primates: an animal model of age-associated neurodegenerative disease. Brain Pathol 1: 287-296.

Prince M, Bryce R, Albanese E, et al (2013). The global prevalence of dementia: a systematic review and metaanalysis. Alzheimers Dement 9: 63-75.e2.

Qiu C, Fratiglioni L (2015). A major role for cardiovascular burden in age-related cognitive decline. Nat Rev Cardiol 12: 267-277.

Quinlivan M, Chalon S, Vergote J, et al (2007). Decreased vesicular acetylcholine transporter and alpha(4)beta(2) nicotinic receptor density in the rat brain following 192 IgG-saporin immunolesioning. Neurosci Lett 415: 97-101.

Quirion R, Aubert I, Lapchak PA, et al (1989). Muscarinic receptor subtypes in human neurodegenerative disorders: focus on Alzheimer's disease. Trends Pharmacol Sci Suppl: 80-84.

Ramanathan D, Tuszynski MH, Conner JM (2009). The basal forebrain cholinergic system is required specifically for behaviorally mediated cortical map plasticity. J Neurosci 29: 5992-6000.

Ramirez BG, Blazquez C, Gomez del Pulgar T, et al (2005). Prevention of Alzheimer's disease pathology by cannabinoids: neuroprotection mediated by blockade of microglial activation. J Neurosci 25: 1904-1913.

Rangel-Lopez E, Colin-Gonzalez AL, Paz-Loyola AL, et al (2015). Cannabinoid receptor agonists reduce the short-term mitochondrial dysfunction and oxidative stress linked to excitotoxicity in the rat brain. Neuroscience 285: 97-106.

Rasmusson DD, Clow K, Szerb JC (1992). Frequency-dependent increase in cortical acetylcholine release evoked by stimulation of the nucleus basalis magnocellularis in the rat. Brain Res 594: 150-154.

Rastogi S, Unni S, Sharma S, et al (2014). Cholinergic immunotoxin 192 IgG-SAPORIN alters subicular theta-gamma activity and impairs spatial learning in rats. Neurobiol Learn Mem 114: 117-126.

Ratano P, Palmery M, Trezza V, et al (2017). Cannabinoid Modulation of Memory Consolidation in Rats: Beyond the Role of Cannabinoid Receptor Subtype 1. Front Pharmacol 8: 200.

Ray CA, Blin J, Chase TN, et al (1992). Effects of cholinergic agonists on regional brain energy metabolism in the scopolamine-treated rat. Neuropharmacology 31: 1193-1199.

Redmer A, Kathmann M, Schlicker E (2003). Cannabinoid CB(1) receptor-mediated inhibition of hippocampal acetylcholine release is preserved in aged mice. Br J Pharmacol 138: 1425-1430.

Reever CM, Ferrari-DiLeo G, Flynn DD (1997). The M5 (m5) receptor subtype: fact or fiction? Life Sci 60: 1105-1112.

Riedel G, Davies SN (2005). Cannabinoid function in learning, memory and plasticity. Handb Exp Pharmacol (168): 445-477.

Rinaldi-Carmona M, Barth F, Heaulme M, et al (1994). SR141716A, a potent and selective antagonist of the brain cannabinoid receptor. FEBS Lett 350: 240-244.

Rinaldi-Carmona M, Barth F, Millan J, et al (1998). SR 144528, the first potent and selective antagonist of the CB2 cannabinoid receptor. J Pharmacol Exp Ther 284: 644-650.

Rinaldo L, Hansel C (2013). Muscarinic acetylcholine receptor activation blocks long-term potentiation at cerebellar parallel fiber-Purkinje cell synapses via cannabinoid signaling. Proc Natl Acad Sci U S A 110: 11181-11186.

Rodriguez-Puertas R, Pascual J, Vilaro T, et al (1997). Autoradiographic distribution of M1, M2, M3, and M4 muscarinic receptor subtypes in Alzheimer's disease. Synapse 26: 341-350.

Ronca RD, Myers AM, Ganea D, et al (2015). A selective cannabinoid CB2 agonist attenuates damage and improves memory retention following stroke in mice. Life Sci 138: 72-77.

Rossner S (1997). Cholinergic immunolesions by 192IgG-saporin--useful tool to simulate pathogenic aspects of Alzheimer's disease. Int J Dev Neurosci 15: 835-850.

Rossner S, Hartig W, Schliebs R, et al (1995). 192IgG-saporin immunotoxin-induced loss of cholinergic cells differentially activates microglia in rat basal forebrain nuclei. J Neurosci Res 41: 335-346.

Rossner S, Schliebs R, Bigl V (1995). 192IgG-saporin-induced immunotoxic lesions of cholinergic basal forebrain system differentially affect glutamatergic and GABAergic markers in cortical rat brain regions. Brain Res 696: 165-176.

Rossor MN, Svendsen C, Hunt SP, et al (1982). The substantia innominata in Alzheimer's disease: an histochemical and biochemical study of cholinergic marker enzymes. Neurosci Lett 28: 217-222.

Roy R, Niccolini F, Pagano G, et al (2016). Cholinergic imaging in dementia spectrum disorders. Eur J Nucl Med Mol Imaging 43: 1376-1386.

Rubboli F, Court JA, Sala C, et al (1994). Distribution of neuronal nicotinic receptor subunits in human brain. Neurochem Int 25: 69-71.

Sabbatini M, Bronzetti E, Felici L, et al (1999). NADPH-diaphorase histochemistry in the rat cerebral cortex and hippocampus: effect of electrolytic lesions of the nucleus basalis magnocellularis. Mech Ageing Dev 107: 147-157.

Sadek B, Khan N, Darras FH, et al (2016). The dual-acting AChE inhibitor and H3 receptor antagonist UW-MD-72 reverses amnesia induced by scopolamine or dizocilpine in passive avoidance paradigm in rats. Physiol Behav 165: 383-391.

Salgado H, Bellay T, Nichols JA, et al (2007). Muscarinic M2 and M1 receptors reduce GABA release by Ca2+ channel modulation through activation of PI3K/Ca2+ -independent and PLC/Ca2+ -dependent PKC. J Neurophysiol 98: 952-965.

Sanchez C, de Ceballos ML, Gomez del Pulgar T, et al (2001). Inhibition of glioma growth in vivo by selective activation of the CB(2) cannabinoid receptor. Cancer Res 61: 5784-5789.

Sani S, Traul D, Klink A, et al (2003). Distribution, progression and chemical composition of cortical amyloid-beta deposits in aged rhesus monkeys: similarities to the human. Acta Neuropathol 105: 145-156.

Sarne Y, Toledano R, Rachmany L, et al (2018). Reversal of age-related cognitive impairments in mice by an extremely low dose of tetrahydrocannabinol. Neurobiol Aging 61: 177-186.

Schlicker E, Gothert M (1998). Interactions between the presynaptic alpha2-autoreceptor and presynaptic inhibitory heteroreceptors on noradrenergic neurones. Brain Res Bull 47: 129-132.

Schliebs R, Feist T, Rossner S, et al (1994). Receptor function in cortical rat brain regions after lesion of nucleus basalis. J Neural Transm Suppl 44: 195-208.

Schreiber S, Bader M, Lenchinski T, et al (2018). Functional effects of synthetic cannabinoids versus Delta(9) -THC in mice on body temperature, nociceptive threshold, anxiety, cognition, locomotor/exploratory parameters and depression. Addict Biol.

Schulte K, Steingruber N, Jergas B, et al (2012). Cannabinoid CB1 receptor activation, pharmacological blockade, or genetic ablation affects the function of the muscarinic auto- and heteroreceptor. Naunyn Schmiedebergs Arch Pharmacol 385: 385-396.

Seeger G, Hartig W, Rossner S, et al (1997). Electron microscopic evidence for microglial phagocytic activity and cholinergic cell death after administration of the immunotoxin 192IgG-saporin in rat. J Neurosci Res 48: 465-476.

Seeger T, Fedorova I, Zheng F, et al (2004). M2 muscarinic acetylcholine receptor knock-out mice show deficits in behavioral flexibility, working memory, and hippocampal plasticity. J Neurosci 24: 10117-10127.

Segal M, Auerbach JM (1997). Muscarinic receptors involved in hippocampal plasticity. Life Sci 60: 1085-1091.

Selden NR, Gitelman DR, Salamon-Murayama N, et al (1998). Trajectories of cholinergic pathways within the cerebral hemispheres of the human brain. Brain 121 (Pt 12): 2249-2257.

Senda T, Matsuno K, Kobayashi T, et al (1998). Ameliorative effect of SA4503, a novel cognitive enhancer, on the basal forebrain lesion-induced impairment of the spatial learning performance in rats. Pharmacol Biochem Behav 59: 129-134.

Severino M, Pedersen AF, Trajkovska V, et al (2007). Selective immunolesion of cholinergic neurons leads to long-term changes in 5-HT2A receptor levels in hippocampus and frontal cortex. Neurosci Lett 428: 47-51.

Shatalin K, Lebreton S, Rault-Leonardon M, et al (1999). Electrostatic channeling of oxaloacetate in a fusion protein of porcine citrate synthase and porcine mitochondrial malate dehydrogenase. Biochemistry 38: 881-889.

Shimizu I, Kawashima K, Ishii D, et al (2003). Urodynamics in a rat neurogenic bladder model with a unilateral electrolytic lesion of the basal forebrain. BJU Int 91: 861-867.

Shin CY, Kim HS, Cha KH, et al (2018). The Effects of Donepezil, an Acetylcholinesterase Inhibitor, on Impaired Learning and Memory in Rodents. Biomol Ther (Seoul) 26: 274-281.

Shire D, Calandra B, Rinaldi-Carmona M, et al (1996). Molecular cloning, expression and function of the murine CB2 peripheral cannabinoid receptor. Biochim Biophys Acta 1307: 132-136.

Shiri M, Komaki A, Oryan S, et al (2017). Effects of cannabinoid and vanilloid receptor agonists and their interaction on learning and memory in rats. Can J Physiol Pharmacol 95: 382-387.

Showalter VM, Compton DR, Martin BR, et al (1996). Evaluation of binding in a transfected cell line expressing a peripheral cannabinoid receptor (CB2): identification of cannabinoid receptor subtype selective ligands. J Pharmacol Exp Ther 278: 989-999.

Singewald GM, Rjabokon A, Singewald N, et al (2011). The modulatory role of the lateral septum on neuroendocrine and behavioral stress responses. Neuropsychopharmacology 36: 793-804.

Singh B, Parsaik AK, Mielke MM, et al (2014). Association of mediterranean diet with mild cognitive impairment and Alzheimer's disease: a systematic review and meta-analysis. J Alzheimers Dis 39: 271-282.

Skaper SD, Buriani A, Dal Toso R, et al (1996). The ALIAmide palmitoylethanolamide and cannabinoids, but not anandamide, are protective in a delayed postglutamate paradigm of excitotoxic death in cerebellar granule neurons. Proc Natl Acad Sci U S A 93: 3984-3989.

Smiley JF, Levey AI, Mesulam MM (1999). M2 Muscarinic Receptor Immunolocalization in Cholinergic Cells of the Monkey Basal Forebrain and Striatum. Neuroscience 90: 803-814.

Smiley JF, Mesulam MM (1999). Cholinergic neurons of the nucleus basalis of Meynert receive cholinergic, catecholaminergic and GABAergic synapses: an electron microscopic investigation in the monkey. Neuroscience 88: 241-255.

Smith G (1988). Animal models of Alzheimer's disease: experimental cholinergic denervation. Brain Res 472: 103-118.

Smith JC, Nielson KA, Woodard JL, et al (2014). Physical activity reduces hippocampal atrophy in elders at genetic risk for Alzheimer's disease. Front Aging Neurosci 6: 61.

Solari N, Hangya B (2018). Cholinergic modulation of spatial learning, memory and navigation. Eur J Neurosci.

Solas M, Francis PT, Franco R, et al (2013). CB2 receptor and amyloid pathology in frontal cortex of Alzheimer's disease patients. Neurobiol Aging 34: 805-808.

Spignoli G, Magnani M, Giovannini MG, et al (1987). Effect of pyroglutamic acid stereoisomers on ECS and scopolamine-induced memory disruption and brain acetylcholine levels in the rat. Pharmacol Res Commun 19: 901-912.

Springer JE, Koh S, Tayrien MW, et al (1987). Basal forebrain magnocellular neurons stain for nerve growth factor receptor: correlation with cholinergic cell bodies and effects of axotomy. J Neurosci Res 17: 111-118.

Stackman RW, Cohen SJ, Lora JC, et al (2016). Temporary inactivation reveals that the CA1 region of the mouse dorsal hippocampus plays an equivalent role in the retrieval of long-term object memory and spatial memory. Neurobiol Learn Mem 133: 118-128.

Stedman E, Stedman E (1937). The mechanism of the biological synthesis of acetylcholine: The isolation of acetylcholine produced by brain tissue in vitro. Biochem J 31: 817-827.

Steffens M, Szabo B, Klar M, et al (2003). Modulation of electrically evoked acetylcholine release through cannabinoid CB1 receptors: evidence for an endocannabinoid tone in the human neocortex. Neuroscience 120: 455-465.

Stella F, Canonici AP, Gobbi S, et al (2011). Attenuation of neuropsychiatric symptoms and caregiver burden in Alzheimer's disease by motor intervention: a controlled trial. Clinics (Sao Paulo) 66: 1353-1360.

Stempel AV, Stumpf A, Zhang HY, et al (2016). Cannabinoid Type 2 Receptors Mediate a Cell Type-Specific Plasticity in the Hippocampus. Neuron 90: 795-809.

Straiker A, Mackie K (2007). Metabotropic suppression of excitation in murine autaptic hippocampal neurons. J Physiol 578: 773-785.

Sugiura T, Kondo S, Sukagawa A, et al (1995). 2-Arachidonoylglycerol: a possible endogenous cannabinoid receptor ligand in brain. Biochem Biophys Res Commun 215: 89-97.

Sulcova E, Mechoulam R, Fride E (1998). Biphasic effects of anandamide. Pharmacol Biochem Behav 59: 347-352.

Sullivan JM (2000). Cellular and molecular mechanisms underlying learning and memory impairments produced by cannabinoids. Learn Mem 7: 132-139.

Sunderland T, Tariot PN, Cohen RM, et al (1987). Anticholinergic sensitivity in patients with dementia of the Alzheimer type and age-matched controls. A dose-response study. Arch Gen Psychiatry 44: 418-426.

Sunderland T, Tariot PN, Weingartner H, et al (1986). Pharmacologic modelling of Alzheimer's disease. Prog Neuropsychopharmacol Biol Psychiatry 10: 599-610.

Szigeti C, Bencsik N, Simonka AJ, et al (2013). Long-term effects of selective immunolesions of cholinergic neurons of the nucleus basalis magnocellularis on the ascending cholinergic pathways in the rat: a model for Alzheimer's disease. Brain Res Bull 94: 9-16.

Tanimura A, Kawata S, Hashimoto K, et al (2009). Not glutamate but endocannabinoids mediate retrograde suppression of cerebellar parallel fiber to Purkinje cell synaptic transmission in young adult rodents. Neuropharmacology 57: 157-163.

Tasker JG, Chen C, Fisher MO, et al (2015). Endocannabinoid Regulation of Neuroendocrine Systems. Int Rev Neurobiol 125: 163-201.

The Bengal Dispensatory and Companion to the Pharmacopoeia, Chiefly Compiled from the Works of Roxburgh, Wallich, Ainslie, Wight and Arnot, Royle, Pereira, Lindley, Richard, Fee, and Including the Results of Numerous Special Experiments. (1843)Br Foreign Med Rev 16: 352-363.

Toledano A, Alvarez MI (2004). Lesions and dysfunctions of the nucleus basalis as Alzheimer's disease models: general and critical overview and analysis of the long-term changes in several excitotoxic models. Curr Alzheimer Res 1: 189-214.

Torres EM, Perry TA, Blockland A, et al (1994). Behavioural, histochemical and biochemical consequences of selective immunolesions in discrete regions of the basal forebrain cholinergic system. Neuroscience 63: 95-122.

Tsang SW, Pomakian J, Marshall GA, et al (2007). Disrupted muscarinic M1 receptor signaling correlates with loss of protein kinase C activity and glutamatergic deficit in Alzheimer's disease. Neurobiol Aging 28: 1381-1387.

Tsou K, Brown S, Sanudo-Pena MC, et al (1998). Immunohistochemical distribution of cannabinoid CB1 receptors in the rat central nervous system. Neuroscience 83: 393-411.

Turkanis SA, Karler R (1981). Excitatory and depressant effects of delta 9-tetrahydrocannabinol and cannabidiol on cortical evoked responses in the conscious rat. Psychopharmacology (Berl) 75: 294-298.

Turnbull MT, Boskovic Z, Coulson EJ (2018). Acute Down-regulation of BDNF Signaling Does Not Replicate Exacerbated Amyloid-beta Levels and Cognitive Impairment Induced by Cholinergic Basal Forebrain Lesion. Front Mol Neurosci 11: 51.

Tzavara ET, Bymaster FP, Davis RJ, et al (2004). M4 muscarinic receptors regulate the dynamics of cholinergic and dopaminergic neurotransmission: relevance to the pathophysiology and treatment of related CNS pathologies. FASEB J 18: 1410-1412.

Tzavara ET, Bymaster FP, Felder CC, et al (2003). Dysregulated hippocampal acetylcholine neurotransmission and impaired cognition in M2, M4 and M2/M4 muscarinic receptor knockout mice. Mol Psychiatry 8: 673-679.

Tzavara ET, Wade M, Nomikos GG (2003). Biphasic effects of cannabinoids on acetylcholine release in the hippocampus: site and mechanism of action. J Neurosci 23: 9374-9384.

Van den Elsen, G A H, Ahmed AIA, Verkes RJ, et al (2015). Tetrahydrocannabinol in Behavioral Disturbances in Dementia: A Crossover Randomized Controlled Trial. Am J Geriatr Psychiatry 23: 1214-1224.

Van den Elsen, G A, Ahmed AI, Verkes RJ, et al (2015). Tetrahydrocannabinol for neuropsychiatric symptoms in dementia: A randomized controlled trial. Neurology 84: 2338-2346.

Van den Elsen, G A, Tobben L, Ahmed AI, et al (2017). Effects of tetrahydrocannabinol on balance and gait in patients with dementia: A randomised controlled crossover trial. J Psychopharmacol 31: 184-191.

Van Sickle MD, Duncan M, Kingsley PJ, et al (2005). Identification and functional characterization of brainstem cannabinoid CB2 receptors. Science 310: 329-332.

Vandenbroucke AR, Sligte IG, Barrett AB, et al (2014). Accurate metacognition for visual sensory memory representations. Psychol Sci 25: 861-873.

Vannucchi MG, Scali C, Kopf SR, et al (1997). Selective muscarinic antagonists differentially affect in vivo acetylcholine release and memory performances of young and aged rats. Neuroscience 79: 837-846.

Verrico CD, Jentsch JD, Dazzi L, et al (2003). Systemic, but not local, administration of cannabinoid CB1 receptor agonists modulate prefrontal cortical acetylcholine efflux in the rat. Synapse 48: 178-183.

Vijayraghavan S, Major AJ, Everling S (2018). Muscarinic M1 Receptor Overstimulation Disrupts Working Memory Activity for Rules in Primate Prefrontal Cortex. Neuron 98: 1256-1268.e4.

Vilaro MT, Palacios JM, Mengod G (1994). Multiplicity of muscarinic autoreceptor subtypes? Comparison of the distribution of cholinergic cells and cells containing mRNA for five subtypes of muscarinic receptors in the rat brain. Brain Res Mol Brain Res 21: 30-46.

Vilaro MT, Wiederhold KH, Palacios JM, et al (1992). Muscarinic M2 receptor mRNA expression and receptor binding in cholinergic and non-cholinergic cells in the rat brain: a correlative study using in situ hybridization histochemistry and receptor autoradiography. Neuroscience 47: 367-393.

Volicer L, Stelly M, Morris J, et al (1997). Effects of dronabinol on anorexia and disturbed behavior in patients with Alzheimer's disease. Int J Geriatr Psychiatry 12: 913-919.

Volpicelli LA, Levey AI (2004). Muscarinic acetylcholine receptor subtypes in cerebral cortex and hippocampus. Prog Brain Res 145: 59-66.

Vorhees CV, Williams MT (2014). Assessing spatial learning and memory in rodents. ILAR J 55: 310-332.

Vos SJ, Verhey F, Frolich L, et al (2015). Prevalence and prognosis of Alzheimer's disease at the mild cognitive impairment stage. Brain 138: 1327-1338.

Waite JJ, Chen AD, Wardlow ML, et al (1994). Behavioral and biochemical consequences of combined lesions of the medial septum/diagonal band and nucleus basalis in the rat when ibotenic acid, quisqualic acid, and AMPA are used. Exp Neurol 130: 214-229.

Waite JJ, Chen AD, Wardlow ML, et al (1995). 192 immunoglobulin G-saporin produces graded behavioral and biochemical changes accompanying the loss of cholinergic neurons of the basal forebrain and cerebellar Purkinje cells. Neuroscience 65: 463-476.

Waite JJ, Thal LJ (1996). Lesions of the cholinergic nuclei in the rat basal forebrain: excitotoxins vs. an immunotoxin. Life Sci 58: 1947-1953.

Walsh TJ, Kelly RM, Dougherty KD, et al (1995). Behavioral and neurobiological alterations induced by the immunotoxin 192-IgG-saporin: cholinergic and non-cholinergic effects following i.c.v. injection. Brain Res 702: 233-245.

Walter L, Franklin A, Witting A, et al (2003). Nonpsychotropic cannabinoid receptors regulate microglial cell migration. J Neurosci 23: 1398-1405.

Walther S, Mahlberg R, Eichmann U, et al (2006). Delta-9-tetrahydrocannabinol for nighttime agitation in severe dementia. Psychopharmacology (Berl) 185: 524-528.

Walther S, Schupbach B, Seifritz E, et al (2011). Randomized, controlled crossover trial of dronabinol, 2.5 mg, for agitation in 2 patients with dementia. J Clin Psychopharmacol 31: 256-258.

Wang HY, Friedman E (1994). Receptor-mediated activation of G proteins is reduced in postmortem brains from Alzheimer's disease patients. Neurosci Lett 173: 37-39.

Watkins BA, Kim J (2015). The endocannabinoid system: directing eating behavior and macronutrient metabolism. Front Psychol 5: 1506.

Weiner DM, Levey AI, Brann MR (1990). Expression of muscarinic acetylcholine and dopamine receptor mRNAs in rat basal ganglia. Proc Natl Acad Sci U S A 87: 7050-7054.

Wellman CL, Sengelaub DR (1991). Cortical neuroanatomical correlates of behavioral deficits produced by lesion of the basal forebrain in rats. Behav Neural Biol 56: 1-24.

Wenk GL, Stoehr JD, Quintana G, et al (1994). Behavioral, biochemical, histological, and electrophysiological effects of 192 IgG-saporin injections into the basal forebrain of rats. J Neurosci 14: 5986-5995.

Wess J (1993). Molecular basis of muscarinic acetylcholine receptor function. Trends Pharmacol Sci 14: 308-313.

Westlake TM, Howlett AC, Bonner TI, et al (1994). Cannabinoid receptor binding and messenger RNA expression in human brain: an in vitro receptor autoradiography and in situ hybridization histochemistry study of normal aged and Alzheimer's brains. Neuroscience 63: 637-652.

Whitehouse PJ, Price DL, Clark AW, et al (1981). Alzheimer disease: evidence for selective loss of cholinergic neurons in the nucleus basalis. Ann Neurol 10: 122-126.

Whitehouse PJ, Struble RG, Clark AW, et al (1982a). Alzheimer disease: plaques, tangles, and the basal forebrain. Ann Neurol 12: 494.

Whitehouse PJ, Struble RG, Clark AW, et al (1982b). Alzheimer disease: plaques, tangles, and the basal forebrain. Ann Neurol 12: 494.

Wiley JL, Marusich JA, Huffman JW (2014). Moving around the molecule: relationship between chemical structure and in vivo activity of synthetic cannabinoids. Life Sci 97: 55-63.

Wilson MA, Fadel JR (2017). Cholinergic regulation of fear learning and extinction. J Neurosci Res 95: 836-852.

Winkler J, Power AE, Ramirez GA, et al (1998). Short-term and complete reversal of NGF effects in rats with lesions of the nucleus basalis magnocellularis. Brain Res 788: 1-12.

Winkler J, Ramirez GA, Thal LJ, et al (2000). Nerve growth factor (NGF) augments cortical and hippocampal cholinergic functioning after p75NGF receptor-mediated deafferentation but impairs inhibitory avoidance and induces fear-related behaviors. J Neurosci 20: 834-844.

Wolff MC, Leander JD (2003). SR141716A, a cannabinoid CB1 receptor antagonist, improves memory in a delayed radial maze task. Eur J Pharmacol 477: 213-217.

Wrenn CC, Wiley RG (1998). The behavioral functions of the cholinergic basal forebrain: lessons from 192 IgG-saporin. Int J Dev Neurosci 16: 595-602.

Xi ZX, Peng XQ, Li X, et al (2011). Brain cannabinoid CB(2) receptors modulate cocaine's actions in mice. Nat Neurosci 14: 1160-1166.

Xing SH, Zhu CX, Zhang R, et al (2014). Huperzine a in the treatment of Alzheimer's disease and vascular dementia: a meta-analysis. Evid Based Complement Alternat Med 2014: 363985.

Younts TJ, Castillo PE (2014). Endogenous cannabinoid signaling at inhibitory interneurons. Curr Opin Neurobiol 26: 42-50.

Zemek F, Drtinova L, Nepovimova E, et al (2014). Outcomes of Alzheimer's disease therapy with acetylcholinesterase inhibitors and memantine. Expert Opin Drug Saf 13: 759-774.

Zemishlany Z, Thorne AE (1991). Anticholinergic challenge and cognitive functions: a comparison between young and elderly normal subjects. Isr J Psychiatry Relat Sci 28: 32-41.

Zhao Y, Tzounopoulos T (2011). Physiological activation of cholinergic inputs controls associative synaptic plasticity via modulation of endocannabinoid signaling. J Neurosci 31: 3158-3168.

Zurier RB, Burstein SH (2016). Cannabinoids, inflammation, and fibrosis. FASEB J 30: 3682-3689.